

CROSS-LINK BETWEEN THE UBIQUITIN-PROTEASOME SYSTEM (UPS) AND
AUTOPHAGY IN THE REGULATION OF MITOPHAGY

by
NUR MEHPARE KOCA TURK

Submitted to the Faculty of Engineering and Natural Sciences
in partial fulfillment of
the requirements for the degree of
Doctor of Philosophy

Sabanci University
July 2018

CROSS-LINK BETWEEN THE UBIQUITIN-PROTEASOME SYSTEM
(UPS) AND AUTOPHAGY IN THE REGULATION OF MITOPHAGY

APPROVED BY:

Prof. Dr Devrim Gözüaçık
(Thesis Supervisor)

Prof. Dr Uğur Sezerman

Asst. Prof. Dr Umut Şahin

Asst. Prof. Dr Öznur Taştan

Asst. Prof. Dr Yavuz Oktay

DATE OF APPROVAL: 26/07/2018

© Nur Mehpare KOCATURK 2018
All Rights Reserved

ABSTRACT

CROSS-LINK BETWEEN THE UBIQUITIN-PROTEASOME SYSTEM (UPS) AND AUTOPHAGY IN THE REGULATION OF MITOPHAGY

NUR MEHPARE KOCATURK

Ph.D. Dissertation, July 2018

Thesis Supervisor: Prof. Devrim Gozuacik

Keywords: Autophagy, Ubiquitin-Proteasome System, UPS, mitochondria, mitophagy, protein-protein interaction, organelle homeostasis

Autophagy and the ubiquitin–proteasome system (UPS) are the two major intracellular protein quality control and recycling mechanisms that are responsible for cellular homeostasis in eukaryotes. Ubiquitylation is utilized as a degradation signal for both systems, however, the two system differ in terms of their mode of actions. The UPS is responsible for the degradation of short-lived proteins and soluble unfolded/misfolded proteins whereas autophagy eliminates rather long-lived proteins, insoluble protein aggregates and even whole organelles (e.g., mitochondria, peroxisomes) and pathogenic invaders (e.g., bacteria). In addition to an indirect connection between the two systems through ubiquitylated proteins, recent data indicate the presence of functional connections and reciprocal regulation mechanisms between these degradation pathways. In this thesis work, we have characterized and analyzed novel and direct links between the UPS and autophagy. Autophagy of mitochondria was chosen as a model to study the interaction and crosstalk between autophagy and the UPS. Functional consequences of these findings will be presented and discussed in detail.

ÖZET

ÜBİKİTİN-PROTEAZOM SİSTEMİ VE OTOFAJİ ARASINDAKİ BAĞLANTILARIN MİTOFAJİDEKİ REGÜLASYONU

Nur Mehpere KOCATÜRK

Doktora Tezi, Temmuz 2018

Tez Danışmanı: Prof. Devrim Gözüaçık

Anahtar Kelimeler: Otofaji, Ubikitin-Proteazom Sistemi, UPS, mitokondri, mitofaji, protein-protein etkileşimi, organel homeostazi

Otofaji ve ubikitin-proteazom sistemi ökartotik hücrelerde, hücre içi homestaza katkıda bulunan iki ana protein kalite control ve geri dönüşüm mekanizmasıdır. Ubikitinasyon, her iki system için de bozulma işareti olarak kullanılır, fakat iki mekanizma birbirinden işleyiş bakımından ayrılırlar. Ubikitin-proteazom sistemi kısa ömürlü proteinlerin ve çözünür haldeki katlanma bozukluğu olan proteinlerin yıkımından sorumlu olurken, otofaji daha uzun ömürlü proteinlerin, protein çökeltilerinin, hatta organellerin (örn., mitokondriler, peroksizomlar) ve patojenik işgalcilerin (örn., bakteriler) ortadan kaldırılmasından sorumludur. Ubikitinlenmiş proteinlerin iki mekanizma tarafından yıkılması sayesinde iki mekanizma arasındaki dolaylı bağlantıya ek olarak, güncel veriler iki mekanizmanın aarsındaki fonksiyonel bağlantıların ve karşılıklı control sistemlerinin olduğunu göstermektedir. Bu doktora tezinde, ubikitin-proteazom ve otofaji mekanizmaları arasındaki yeni ve doğrudan bağlantılar bulunup analiz edilmiştir. Mitokondrilerin otofajisi, ubikitin-proteazom sistemi ve otofaji arasındaki bağlantının çalışılması için model olarak seçilmiştir. Bu buluşların fonksiyonel yansımaları sunulularak detaylıca tartışılacaktır.

“To my family”

ACKNOWLEDGEMENTS

I would like to express my great gratitude to my doctoral supervisor Prof. Dr. Devrim Gozuacik for his endless support, motivation and guidance not only during my doctoral studies but also for the rest of my life.

I would like to thank all former and current Gozuacik Lab members, working environment become full of joy and science with their contribution. Among the members, first place will go for my precious mentor Dr. Karin Eberhart to whom i learned everything. Her genorosity to share her knowledge in science, endless support and warmest feelings meant a lot to me. In this manner, I have to thank one more time Prof. Dr. Gozuacik, he let me to be a part of his lab and i found my given sister.

I would like to express my sincere appreciation to Prof. Joern Dengjel to whom hosted me in his lab for my proteomic experiments and his immense carefulness not only guidance in the experiments but also form y future plans.

I would like to express my gratefulness to TÜBİTAK (The Scientific and Technological Research Council of Turkey), BİDEB 2211 Graduate Scholarship Program for the appreciated financial support during my PhD studies.

My family... Nothing could be possible without knowing that whatever you do is supported by your family without questionaring. I felt so lucky each an every day that i was never ever alone during this long and tough journey. It is difficult to express my indebtness feelings to my family. What i could only do is thanking for the life including me in such a great family.

TABLE OF CONTENTS

1.	INTRODUCTION.....	1
	1.1 UBIQUITIN-PROTEASOME SYSTEM.....	2
	1.1.1 The Conjugation System.....	2
	1.1.2 Proteasomes: Structure and Regulation	4
	1.1.3 Ubiquitin-like Modifiers	6
	1.1.4 PSMA7	7
	1.2 AUTOPHAGY	16
	1.2.1 Upstream Regulation	17
	1.2.2 Initiation and Membrane Nucleation	19
	1.2.3 Membrane Elongation and Closure	20
	1.2.4 Autophagosome-Lysosome Fusion	21
	1.2.5 Autophagy Receptors: Ub Code for Selective Autophagy.....	21
	1.2.6 ATG5	24
	1.3 THE UPS – AUTOPHAGY CONNECTION	29
	1.3.1. Compensatory Mechanisms Between the UPS and Autophagy	29
	1.3.2 Interplay Between the UPS-Autophagy in the Selective Clearance of Cytosolic Proteins ...	33
	1.3.3 Degradation of Proteasomes or Autophagy Components as a Cross Control Mechanism..	36
	1.3.3.1 Control of the Proteasome Abundance by the Autophagy.....	36
	1.3.3.2 Control of Autophagy Components by the UPS	37
	1.3.4 Transcriptional Mechanisms Connecting the UPS and Autophagy.....	39
	1.3.5 Crosstalk and Co-regulatory Mechanisms.....	44
	1.3.5.1 Xenophagy: Removal of Intracellular Invaders	44
	1.3.5.2 Mitophagy: Mitochondrial Turnover	47
	1.3.5.2.1 PINK1/Parkin-dependent Mitophagy.....	48
	1.3.5.2.2 Parkin-independent Mitophagy.....	52
	1.3.5.2.3 Mitophagy During Reticulocyte Maturation	53
	1.3.5.3 Pexophagy: Autophagic Removal of Peroxisomes	54
	1.3.5.4 Autophagic Removal of Ribosomes and Stress Granules.....	58
	1.3.6 Proposed Direct Link Between the UPS and Autophagy: PSMA7, PSMB5, UBA1, UBE2L3 and ATG5	60
2.	MATERIALS AND METHODS	62
	2.1 PLASMIDS, CONSTRUCTS and SIRNAs.....	62
	2.2 YEAST-TWO-HYBRID SCREEN.....	63
	2.3 CELL CULTURE	65
	2.3.1 Cell Line Maintenance	65
	2.3.2 Transfections and Crispr ATG5 cells Generation	66
	2.3.2.1 Calcium-Phosphate Transfection	66
	2.3.2.2 Retrovirus and Lentivirus Production for Mammalian Cell Infection.....	66
	2.3.2.3 Retroviral Infection for Parkin Stable Cell Generation	68
	2.3.2.4 Crispr ATG5 HeLa Cell Generation.....	70
	2.3.2.4 1 Lentiviral vector digestion, oligo annealing and cloning into digested vector	71
	2.3.2.4 2 Lentivirus production of confirmed constructs, lentiviral transduction and monoclonal selection	74
	2.3.3 Mitochondrial Stress and Mitophagy Induction in Cell Culture.....	74
	2.4 PROTEIN ISOLATION AND IMMUNOBLOTTING TESTS	75

2.5	<i>MITOCHONDRIAL ISOLATION</i>	77
2.6	<i>IMMUNOPRECIPITATION TESTS</i>	78
2.7	<i>IMMUNOFLUORESCENCE TESTS</i>	79
2.8	<i>ANTI-DNA STAINING TEST</i>	80
2.9	<i>GEL FILTRATION ANALYSES</i>	81
2.10	<i>SILAC LABELLING AND EXPERIMENTATION</i>	82
2.11	<i>LIQUID CHROMATOGRAPHY, SAMPLE PREPARATION FOR MS/MS</i>	83
2.12	<i>LC-MS/MS and MS DATA ANALYSIS</i>	83
2.13	<i>PROTEASOME ACTIVITY ASSAY MEASUREMENT</i>	84
2.14	<i>ATP ASSAY MEASUREMENT</i>	85
3.	RESULTS	86
3.1	<i>CONFIRMATION AND CHARACTERIZATION OF ATG5-PSMA7 INTERACTION</i>	86
3.1.1	Confirmation of ATG5-PSMA7 interaction in mammalian cells.....	86
3.1.2	ATG5-PSMA7 Interaction Modelling.....	91
3.1.3	Analysis of The Dynamics in ATG5-PSMA7-Parkin Interaction	96
3.1.4	Determination of The Subcellular Localization of ATG5-PSMA7-Parkin Interaction	108
3.1.5	The Functional Role of ATG5-PSMA7 Interaction in Selective Autophagy	118
3.1.6	The Effect of Other Proteasomal Subunits on Mitophagy	158
3.1.7	Target Prediction on Mitochondria for ATG5 Localization	165
3.2	<i>IDENTIFICATION OF OTHER PROTEASOMAL COMPONENTS AS DIRECT INTERACTORS OF ATG5</i>	175
3.2.1	SILAC-Based Screening.....	175
3.2.2	Validation of SILAC-based ATG5 Interaction Partners.....	176
3.3	<i>MITOCHONDRIAL MOTILITY CONTROL THROUGH ATG5 INTERACTORS</i>	184
3.3.1	The Role of PSMA7 on Mitochondrial Motility	184
3.3.2	The Effect of DIAPH1 on Mitochondrial Motility and Mitophagy	187
4.	DISCUSSION	198
5.	CONCLUSION AND FUTURE ASPECTS	206
6.	REFERENCES	208
	APPENDIX A	294
	APPENDIX B	296
	APPENDIX C	297
	PUBLICATIONS	297
	<i>Publication List</i>	298
	<i>Conference Papers</i>	299
	<i>Poster Presentations</i>	300
	<i>Awards</i>	301

LIST OF TABLES

Table 1.1.4 1: Reported PSMA7 interactors.....	9
Table 1.2.6 1: Reported ATG5 interactors.....	26
Table 2.4.1: The recipe of home-made separating gel (LOWER) for SDS-PAGE.....	76
Table 2.4.2: The recipe of home-made stacking gel (UPPER) for SDS-PAGE.....	76
Table 3.1.2 1: Critical residues for ATG5-PSMA7 Interaction.....	92
Table 3.2.2 1: CCCP induced UPS-associated ATG5 Interactome List of HEK/293T..	179
Table 3.2.2 2: CCCP induced UPS-associated PSMA7 Interactome List of HEK/293T.....	180
Table 3.2.2 3: UPS-associated ATG5 Interactome Combined List with Differential Autophagy Inducing Conditions in HEK/293T cells	181
Table 3.2.2 4: CCCP induced UPS-associated Cytoplasmic ATG5 Interactome List of HEK/293T cells.....	182
Table 3.2.2 5: CCCP induced UPS-associated Mitochondrial ATG5 Interactome List of HEK/293T cells.....	183
Table 3.3.2 1: List of Top 4 Significant Hits from SILAC-based ATG5 Interactome Screen in HEK/293T cells.....	187

LIST OF FIGURES

FIGURE 1.1.1 1: THE 3D STRUCTURAL VIEW OF UBIQUITIN MOLECULE.	3
FIGURE 1.1.1 2: THE REPRESENTATIVE SCHEME OF THE UBIQUITIN CONJUGATION SYSTEM AND PROTEASOMAL DEGRADATION.	4
FIGURE 1.1.4 1: THE 3D STRUCTURE OF HUMAN PSMA7 AND ITS LOCATION IN 20S PROTEASOME.	7
FIGURE 1.1.4 2: PSMA7 INTERACTION NETWORK WAS OBTAINED BY USING BIOGRID SOFTWARE.	15
FIGURE 1.2 1: THE SCHEMATIC REPRESENTATION OF SEQUENTIAL STAGES OF AUTOPHAGY MECHANISM.	17
FIGURE 1.2 2: MOLECULAR REGULATORS INVOLVED IN DIFFERENT STAGES OF THE AUTOPHAGY PROCESS.	18
FIGURE 1.2.5 1: AUTOPHAGIC MACHINERY SELECTIVELY DEGRADE CELLULAR TARGETS AND INVADERS.	22
FIGURE 1.2.5. 2: AUTOPHAGY RECEPTORS MAKE BRIDGES BETWEEN SELECTIVE CARGO AND AUTOPHAGIC MACHINERY THROUGH THEIR SPECIALIZED INTERACTION DOMAINS.	23
FIGURE 1.2.6 1: STRUCTURAL VIEW OF ATG5 PROTEIN.	25
FIGURE 1.2.6 2: ATG5 INTERACTION NETWORK WAS OBTAINED BY USING BIOGRID SOFTWARE.	28
FIGURE 1.3.1: SCHEMATIC REPRESENTATION OF COMPENSATORY ACTIONS BETWEEN THE UPS AND AUTOPHAGY.	30
FIGURE 1.3.2 1: INTERPLAY BETWEEN THE UPS AND AUTOPHAGY SYSTEM AGAINST UBIQUITYLATED MISFOLDED PROTEINS.	35
FIGURE 1.3.3.1: THE SCHEMATIC REPRESENTATION OF HOW PROTEASOMES ARE DEGRADED SELECTIVELY BY AUTOPHAGY.	37
FIGURE 1.3.5.1: XENOPHAGY MECHANISMS IN MAMMALS.	46
FIGURE 1.3.5.2: MOLECULAR DETAILS OF MITOPHAGY PATHWAYS IN MAMMALIAN CELLS.	51
FIGURE 1.3.5.3: SCHEMATIC REPRESENTATION OF SELECTIVE REMOVAL OF PEROXISOMES BY AUTOPHAGY MACHINERY.	57
FIGURE 1.3.5.4: SELECTIVE TARGETING OF RIBOSOMES AND STRESS GRANULES FOR DEGRADATION TO THE UPS OR AUTOPHAGY MECHANISMS.	59
FIGURE 2.3.2.3 1: MAP OF THE PMXS-IP HA-PARKIN CONSTRUCT.	69
FIGURE 2.10 1: THE PIPELINE OF TRI-SILAC EXPERIMENTS STARTING FROM LABELLING CELLS WITH GIVEN AMINO ACID CONTAINING MEDIUM TO MS-DERIVED DATA ANALYSIS.	82
FIGURE 3.1.1 1: THE PIPELINE OF VALIDATION METHODS OF ATG5-PSMA7 INTERACTION IN MAMMALS.	86
FIGURE 3.1.1 2: PSMA7 IMMUNOPRECIPITATION EXPERIMENT RESULT OF HEK/293T CELLS.	87
FIGURE 3.1.1 3: ATG5 IMMUNOPRECIPITATION EXPERIMENTS WERE PERFORMED IN HEK/293T CELLS.	88
FIGURE 3.1.1 4: ENDOGENOUS ATG5 IMMUNOPRECIPITATION EXPERIMENTS WERE PERFORMED IN MEF CELLS.	89

FIGURE 3.1.1 5: THE COLOCALIZATION EXPERIMENTS WERE PERFORMED IN HEK/293T (UPPER PART) AND HELA (LOWER PART) CELLS.	90
FIGURE 3.1.2 1: THE PIPELINE OF THE PERFORMED EXPERIMENTS IN ORDER TO ADDRESS THE ATG5-PSMA7 INTERACTION DOMAIN. ...	91
FIGURE 3.1.2 2: COMPUTATIONAL MODELLING OF ATG5 (PDB CODE: 4GDK, BLUE) AND PSMA7	92
FIGURE 3.1.2 3: SCHEMATIC REPRESENTATION OF PSMA7 FRAGMENTS.	93
FIGURE 3.1.2 4: INTERACTION MAPPING EXPERIMENTS IN HEK/293T CELLS.	94
FIGURE 3.1.2 5: COMPETITION TEST BETWEEN FULL LENGTH PSMA7 AND C-TERMINAL FRAGMENT OF THE PROTEIN IN HEK/293T CELLS.	95
FIGURE 3.1.3 1: LIST OF PERFORMED EXPERIMENTS TO ANALYZE STRESS-INDUCED DYNAMIC INTERACTION ATG5-PSMA7 INTERACTION AND INVESTIGATION OF OTHER COMPLEX COMPONENTS.	96
FIGURE 3.1.3 2: PSMA7-IMMUNOPRECIPITATION EXPERIMENTS PERFORMED IN HEK/293T CELLS.	97
FIGURE 3.1.3 3: COLOCALIZATION EXPERIMENTS OF PSMA7 AND ATG5 WITH MITOCHONDRIAL STRESS INDUCERS IN HEK/293T CELLS ANALYZED BY CONFOCAL MICROSCOPY.	98
FIGURE 3.1.3 4: COLOCALIZATION EXPERIMENTS OF PSMA7 AND ATG5 WITH MITOCHONDRIAL STRESS INDUCERS IN HELA CELLS ANALYZED BY CONFOCAL MICROSCOPY.	99
FIGURE 3.1.3 5: SILAC-BASED LC-MS/MS ANALYSIS RESULTS OF HEK/293T CELLS.	100
FIGURE 3.1.3 6: GEL FILTRATION TESTS OF HEK/293T CELL-DERIVED TOTAL LYSATES.....	101
FIGURE 3.1.3 7: THE MOLECULAR WEIGHT MARKER CALIBRATION PEAKS OF THE GEL FILTRATION EXPERIMENTS OVER SUPERDEX 200 COLUMN.....	102
FIGURE 3.1.3 8: REPRESENTATIVE CHROMATOGRAMS OF DMSO TREATED CONTROL CELL LYSATES (LEFT PANEL) AND CCCP TREATED CELL LYSATES (RIGHT PANEL) OF HEK/293T CELLS THROUGH THE FPLC SEPARATION.	102
FIGURE 3.1.3 9: CONFIRMATION OF PSMA7 AND PARKIN INTERACTION BY PERFORMING IMMUNOPRECIPITATION EXPERIMENTS IN HEK/293T CELLS.	103
FIGURE 3.1.3 10: ATG5 IMMUNOPRECIPITATION TESTS FOR PARKIN BINDING IN HEK/293T CELLS.	104
FIGURE 3.1.3 11: COLOCALIZATION EXPERIMENTS OF PSMA7 AND PARKIN WITH CCCP TREATMENT IN HEK/293T CELLS ANALYZED BY CONFOCAL MICROSCOPY.....	105
FIGURE 3.1.3 12: COLOCALIZATION EXPERIMENTS OF PSMA7 AND PARKIN WITH CCCP TREATMENT IN HELA CELLS ANALYZED BY CONFOCAL MICROSCOPY.	106
FIGURE 3.1.3 13: PSMA7 AND PSMB5 ARE NOT THE TARGETS OF AUTOPHAGIC DEGRADATION.	107

FIGURE 3.1.4. 1: EXPERIMENTAL FLOW IN ORDER TO FIGURE OUT THE SUBCELLULAR LOCALIZATION OF THE ATG5-PSMA7 CONTAINING PROTEIN COMPLEXES.	108
FIGURE 3.1.4. 2: PSMA7 FOUND ON MITOCHONDRIA. HELA CELLS	109
FIGURE 3.1.4. 3: ATG5 FOUND ON MITOCHONDRIA HELA CELLS	110
FIGURE 3.1.4 4: THE PRESENCE OF PSMA7 ON MITOCHONDRIA STIMULATED WITH MITOCHONDRIAL STRESS (HELA CELLS).	111
FIGURE 3.1.4 5: THE PRESENCE OF ATG5 ON MITOCHONDRIA STIMULATED WITH MITOCHONDRIAL STRESS (HELA CELLS).	112
FIGURE 3.1.4 6: THE PRESENCE OF ATG5 ON MITOCHONDRIA STIMULATED WITH MITOCHONDRIAL STRESS (HEK/293 CELLS).	113
FIGURE 3.1.4 7: THE PRESENCE OF PARKIN ON MITOCHONDRIA STIMULATED WITH MITOCHONDRIAL STRESS (HELA CELLS).	114
FIGURE 3.1.4 8: SUBCELLULAR FRACTIONATION OF HEK/293T CELLS PROVING THE ENHANCED TRANSLOCATION OF ATG5 AND PSMA7 ONTO MITOCHONDRIA UPON CCCP TREATMENT.	115
FIGURE 3.1.4 9: GEL FILTRATION EXPERIMENT RESULTS OF MITOCHONDRIAL AND CYTOPLASMIC FRACTIONS UNDER BASAL AND CCCP TREATMENT CONDITIONS.	116
FIGURE 3.1.4 10: GEL FILTRATION CHROMOTOGRAMS OF THE CYTOPLASMIC AND MITOCHONDRIAL PROTEIN SAMPLES OVER THE SUPERDEX 200 COLUMN RUN.	117
FIGURE 3.1.5 1: THE GLOBAL EFFECT OF KNOCKOUT ATG5 AND KNOCKDOWN PSMA7 ANALYZED IN TERMS OF SEVERAL DIFFERENT ASPECTS.	118
FIGURE 3.1.5 2: PROTEASOMAL ACTIVITY MEASUREMENT RESULTS OF WT AND ATG5 KO MEF CELLS. WT AND ATG5 KO MEF CELLS.	119
FIGURE 3.1.5 3: ATP ASSAY RESULTS OF WT AND ATG5 KO MEF CELLS IN RESPONSE TO OLIGOMYCIN TREATMENT	120
FIGURE 3.1.5 4: THE SIRNA-MEDIATED KNOCKDOWN EFFECT OF PSMA7 ENHANCED AUTOPHAGIC ACTIVITY IN HEK/293T CELLS.	121
FIGURE 3.1.5 5: THE RESULTS OF PSMA7 KNOCKDOWN ON LC3 DOT FORMATION ANALYSES IN HEK/293T CELLS.	121
FIGURE 3.1.5 6: THE EFFECT OF KNOCKDOWN PSMA7 ANALYZED ON MITOPHAGY IN TERMS OF SEVERAL DIFFERENT ASPECTS.	122
FIGURE 3.1.5 7: THE EFFECT OF KNOCK DOWN PSMA7 ON PARKIN TRANSLOCATION ONTO MITOCHONDRIA IN HEK/293T CELLS.	123
FIGURE 3.1.5 8: THE EFFECT OF KNOCK DOWN PSMA7 ON PARKIN TRANSLOCATION ONTO MITOCHONDRIA IN HELA CELLS.	124
FIGURE 3.1.5 9: WESTERN BLOTTING RESULTS OF SUBCELLULAR FRACTIONATION TESTS FOR THE ANALYSIS OF PSMA7 DEFICIENCY ON PARKIN RECRUITMENT IN HEK/293T CELLS.	125
FIGURE 3.1.5 10: COLOCALIZATION ANALYSES SHOWING THE ROLE OF PSMA7 ON PINK1 AND PARKIN INTERACTION IN HELA CELLS.	126
FIGURE 3.1.5 11: MYC-TAGGED IMMUNOPRECIPITATION RESULTS FOR ANALYZING THE EFFECT OF PSMA7 ON PINK1 AND PARKIN INTERACTION IN HEK/293T CELLS.	127
FIGURE 3.1.5 12: COLOCALIZATION TEST TO CHECH THE EFFECT OF KNOCK DOWN PSMA7 ON MFN2 AND PARKIN INTERACTION IN HEK/293T CELLS.	128

FIGURE 3.1.5 13: THE QUANTIFICATION GRAPHIC OF PARKIN AND MFN2 COLOCALIZATION IN HEK/293T CELLS.	129
FIGURE 3.1.5 14: COLOCALIZATION TEST TO CHECH THE EFFECT OF KNOCK DOWN PSMA7 ON MFN2 AND PARKIN INTERACTION IN HELA CELLS.	130
FIGURE 3.1.5 15: THE QUANTIFICATION GRAPHIC OF PARKIN AND MFN2 COLOCALIZATION IN HELA CELLS.	131
FIGURE 3.1.5 16: EFFECT OF KNOCK DOWN PSMA7 ON MFN2 DEGREDDATION IN HEK/293T CELLS.	132
FIGURE 3.1.5 17: EFFECT OF KNOCK DOWN PSMA7 ON TOM40 DEGREDDATION IN HEK/293T CELLS.	132
FIGURE 3.1.4 18: THE EFFECT OF PSMA7 ON UBIQUITYLATION LEVELS OMM PROTEINS OF HEK/293T CELLS.	133
FIGURE 3.1.5 19: THE EFFECT OF KNOCK DOWN PSMA7 ON MITOCHONDRIA ASSOCIATED GFP-OPTN DOT FORMATION IN HELA CELLS.	135
FIGURE 3.1.5 20: THE QUANTIFICATION OF MITOCHONDRIA ASSOCIATED GFP-OPTN DOT FORMATION IN HELA CELLS.	136
FIGURE 3.1.4 21: THE EFFECT OF KNOCKDOWN PSMA7 ON MITOCHONDRIA ASSOCIATED NDP52 DOT FORMATION IN HELA CELLS.	136
FIGURE 3.1.5 22: THE EFFECT OF SIRNA-MEDIATED KNOCK DOWN OF PSMA7 ON MITOCHONDRIA ASSOCIATED GFP-LC3 DOT FORMATION.	137
FIGURE 3.1.5 23: THE QUANTIFICATION OF MITOCHONDRIA ASSOCIATED GFP-LC3 DOT FORMATION IN HELA CELLS.	138
FIGURE 3.1.5 24: THE EFFECT OF KNOCK DOWN PSMA7 ON MITOCHONDRIA ASSOCIATED GFP-LC3 DOT FORMATION IN HEK/293T CELLS.	139
FIGURE 3.1.5 25: THE QUANTIFICATION OF GFP-LC3 DOT ASSOCIATED MITOCHONDRIA OF HEK/293T CELLS.	140
FIGURE 3.1.5 26: ANTI-DNA STAINING RESULTS OF HELA CELLS TO ANALYZE MITOCHONDRIAL DNA IN HELA CELLS.	141
FIGURE 3.1.5 27: THE QUANTIFICATION OF MITOCHONDRIAL DNA AMOUNT OF HELA CELLS.	142
FIGURE 3.1.5 28: THE EFFECT OF PROTEASOMAL ACTIVITY ON ATG5 RECRUITMENT ONTO MITOCHONDRIA IN PARKIN STABLE HELA CELLS.	143
FIGURE 3.1.5 29: QUANTIFICATION OF MITOCHONDRIA ASSOCIATED ATG5 IN HELA CELLS.	144
FIGURE 3.1.5 30: THE EFFECT OF ATG5 DEFFICIENCY ON MITOPHAGY WAS INVESTIGATED IN DIFFERENT STAGES OF MITOPHAGY.	145
FIGURE 3.1.5 31: THE EFFECT OF SHRNA-MEDIATED KNOCKDOWN OF ATG5 ON MITOPHAGY IN HEK/293T CELLS WAS ANALYZED UNDER CONFOCAL MICROSCOPE.	146
FIGURE 3.1.5 32: THE EFFECT OF SHRNA-MEDIATED KNOCKDOWN OF ATG5 ON MITOPHAGY IN HELA CELLS WAS ANALYZED UNDER CONFOCAL MICROSCOPE.	147

FIGURE 3.1.5 33: THE EFFECT OF SHRNA MEDIATED KNOCK DOWN OF ATG5 ON MITOCHONDRIA ASSOCIATED GFP-OPTN DOT FORMATION IN HELA CELLS.....	148
FIGURE 3.1.5 34: THE QUANTIFICATION OF MITOCHONDRIA ASSOCIATED GFP-OPTN DOT FORMATION IN HELA CELLS.....	149
FIGURE 3.1.5 35: THE EFFECT OF KNOCK DOWN ATG5 ON PARKIN RECRUITMENT TO MITOCHONDRIA IN HELA CELLS.	150
FIGURE 3.1.5 36: THE QUANTIFICATION OF PARKIN TRANSLOCATION ONTO MITOCHONDRIA OF HELA CELLS.....	151
FIGURE 3.1.5 37: SUBCELLULAR FRACTIONATIONS TESTS OF HEK/293T CELLS.	151
FIGURE 3.1.5 38: THE EFFECT OF ATG5 DEFFICIENCY IN MEF CELLS.	152
FIGURE 3.1.5 39: CONFIRMATION OF ATG5-/- HELA CLONES.....	153
FIGURE 3.1.5 40: THE EFFECT OF ATG5 MITOCHONDRIAL PROTEIN LEVELS WAS ANALYSED IN CNT AND ATG5-/- HELA CELLS.....	154
FIGURE 3.1.5 41: THE EFFECT OF ATG5 ON UBIQUITIN PHOSPHORYLATION AS A READOUT OF PINK1 ACTIVITY.	155
FIGURE 3.1.5 42: THE EFFECT OF ATG5 DEFFICIENCY IN PINK1- PARKIN INTERACTION IN HELA CELLS.....	156
FIGURE 3.1.6 1: SILAC-BASED LC-MS/MS ANALYSIS.	158
FIGURE 3.1.6 2: CCCP INDUCES OTHER PROTEASOMAL SUBUNITS TO MITOCHONDRIA.....	159
FIGURE 3.1.6. 3: THE EFFECT OF OTHER PROTEASOMAL SUBUNITS AND OVERALL PROTEASOME ACTIVITY ON MITOPHAGY IN TERMS OF RECRUITMENT OF REGULATORS INVESTIGATED.....	160
FIGURE 3.1.6. 4: THE EFFECT OF SIRNA-MEDIATED KNOCKDOWN OF PSMB5 ON PARKIN RECRUITMENT TO MITOCHONDRIA.....	161
FIGURE 3.1.6 5: SIRNA MEDIATED KNOCKDOWN OF PSMB5 RESULTED IN DECREASE IN CCCP-INDUCED PARKIN TRANSLOCATION ONTO MITOCHONDRIA.....	162
FIGURE 3.1.6 6: THE EFFECT OF PROTEASOME INHIBITION ON PROTEIN RECRUITMENT ONTO MITOCHONDRIA IN HEK/293T CELLS.	163
FIGURE 3.1.6 7: THE EFFECT OF PROTEASOME INHIBITION ON PROTEIN RECRUITMENT ONTO MITOCHONDRIA IN PARKIN STABLE HEK/293T CELLS.	164
FIGURE 3.1.7 1: SILAC-BASED LC-MS/MS ANALYSIS.	165
FIGURE 3.1.7 2: ATG5 IMMUNOPRECIPITATION EXPERIMENTS TO TEST VDAC2 BINDING IN HEK/293T CELLS.	166
FIGURE 3.1.7 3: COLOCALIZATION TESTS OF ENDOGENOUS ATG5 AND VDAC1 BY IMMUNOSTAINING OF HEK/293T CELLS.	167
FIGURE 3.1.7 4: COLOCALIZATION TESTS OF ENDOGENOUS ATG5 AND VDAC1 BY IMMUNOSTAINING OF HELA CELLS.	168
FIGURE 3.1.7 5: MITOCHONDRIAL VDAC1-ATG5 INTERACTION TESTS IN PARKIN STABLE HEK/293T CELLS.....	169
FIGURE 3.1.7 6: VDAC1-ATG5 INTERACTION TEST ON MITOCHONDRIA IN PARKIN STABLE HELA CELLS.....	170
FIGURE 3.1.7 7: TOM40-ATG5 INTERACTION TEST ON MITOCHONDRIA IN PARKIN STABLE HEK/293T CELLS.....	171

FIGURE 3.1.7 8: TOM40-ATG5 INTERACTION TEST ON MITOCHONDRIA IN PARKIN STABLE HELA CELLS.....	172
FIGURE 3.1.7 9: MFN2-ATG5 INTERACTION TEST ON MITOCHONDRIA IN PARKIN STABLE HEK/293T CELLS.	173
FIGURE 3.1.7 10: MFN2-ATG5 INTERACTION TEST ON MITOCHONDRIA IN PARKIN STABLE HELA CELLS.....	174
FIGURE 3.2.1 1: SILAC-BASED LC-MS/MS ANALYSIS.	175
FIGURE 3.2.2 1: CO-IMMUNOPRECIPITATION TEST FOR THE VALIDATION OF PROTEOMIC DATA IN HEK/293T CELLS.....	176
FIGURE 3.2.2 2: SUBCELLULAR LOCALIZATION OF UBA1 AND UBE2L3 ENZYMES IN HEK/293T CELLS.	177
FIGURE 3.2.2 3: DETERMINATION OF THE CELLULAR ATG5-UBA1 AND ATG5-UBE2L3 INTERACTION BY SUBCELLULAR FRACTIONATION FOLLOWED BY IMMUNOPRECIPITATION TESTS IN HEK/293T CELLS.	178
FIGURE 3.3.1 1: THE EFFECT OF CCCP ON MITOCHONDRIAL MOTILITY ANALYZED IN HELA CELLS.....	184
FIGURE 3.3.1 2: THE EFFECT OF SIRNA-MEDIATED KNOCKDOWN OF PSMA7 AND PSMB5 ON MITOCHONDRIAL MOTILITY ANALYZED IN HELA CELLS.	185
FIGURE 3.3.1 3: THE EFFECT OF SIRNA-MEDIATED KNOCKDOWN OF PSMA7 ON MITOCHONDRIAL MOTILITY ANALYZED IN HELA CELLS.	186
FIGURE 3.3.2 1: DIAPH1 REGULATED MITOCHONDRIAL REPOSITIONING IN CELLS.....	188
FIGURE 3.3.2 2: CONFIRMATION OF ATG5 AND DIAPH1 INTERACTION BY IMMUNOPRECIPITATION TESTS IN HEK/293T CELLS.....	189
FIGURE 3.3.2 3: ENDOGENOUS ATG5 BINDING TEST FOR DIAPH1 PROTEIN IN HEK/293T CELLS.....	190
FIGURE 3.3.2 4: ENDOGENOUS ATG5 BINDING TEST FOR DIAPH1 PROTEIN IN HELA CELLS.....	190
FIGURE 3.3.2 5: DIAPH1 WAS FOUND ON MITOCHONDRIA UPON CCCP TREATMENT IN HEK/293T CELLS.	191
FIGURE 3.3.2 6: THE EFFECT OF KNOCKDOWN DIAPH1 ON MITOPHAGY IN HEK/293T CELLS.	192
FIGURE 3.3.2 7: THE EFFECT OF KNOCKDOWN DIAPH1 ON MITOPHAGY IN HELA CELLS.	193
FIGURE 3.3.2 8: THE EFFECT OF KNOCKDOWN DIAPH1 ON MITOCHONDRIA AND CYTOSKELETON CONNECTION IN HELA CELLS.	194
FIGURE 3.3.2 9: IMMUNOPRECIPITATION EXPERIMENTS TO CHECK THE EFFECT OF PSMA7 ON ATG5 AND DIAPH1 INTERACTION PERFORMED IN HEK/293T CELLS.	195
FIGURE 3.3.2 10: IMMUNOPRECIPITATION EXPERIMENTS TO TEST ENDOGENOUS PSMA7 AND DIAPH1 BINDING IN HEK/293T CELLS.	196
FIGURE 3.3.2 11: MITOCHONDRIAL MOTILITY CONTROL BY PSMA7 AND DIAPH1.	197
FIGURE 4.1: PROPOSED INTERACTION MODEL FOR CCCP-INDUCED PROTEIN COMPLEX FORMATION ONTO MITOCHONDRIA.	202

FIGURE 4.2: DETAILED MODEL-1 FOR PROPOSED HYPOTHESIS IN THE REGULATION OF MITOPHAGY.....	202
FIGURE 4.3: DETAILED MODEL-2 FOR PROPOSED HYPOTHESIS IN THE REGULATION OF MITOPHAGY.....	203

LIST OF ABBREVIATIONS

UPS: Ubiquitin-proteasome system

Ub: Ubiquitin

Ubl: Ubiquitin-like modifiers

SUMO: Small Ubiquitin-like modifier

STUBLs: SUMO-targeted ubiquitin ligases

HECT: Homologous to E6-AP carboxyterminal domain

RING domain: Really interesting new gene domain

DUBs: Deubiquitinating enzymes

ATG: Autophagy-related genes

CMA: Chaperone mediated autophagy

PAS: Phagophore assembly site

AMPK: AMP activated protein kinases

mTOR: Mammalian target of rapamycin

PI3K: Class-III-Phosphatidylinositol-3-Kinase

PI3P: Phosphatidylinositol-3-phosphate

LC3: Microtubule-associated protein 1 light chain 3

MAPK: Mitogen-activated protein kinases

BECN1: Beclin1

FIP200: Focal adhesion kinase-family interacting protein of 200 kDa

p70S6K: 70 kDa polypeptide 1 ribosomal protein S6 kinase

WIPI1/2: WD-repeat protein interacting with phospholipids

DFCP1: Double FYVE-containing protein

Alfy: Autophagy linked FYVE protein

PE: Phosphatidylethanolamine

PINK1: PTEN Induced Putative Kinase 1

BNIP3L: BCL2/adenovirus E1B-interacting protein 3-like

OPTN: Optineurin

NDP52: Nuclear dot protein 52

OMM: Outer mitochondrial membrane

IMM: Inner mitochondrial membrane

PARL: Presenilin Associated Rhomboid Like

MPP: Mitochondria processing protease

DMEM: Dulbecco's modified eagle medium

GFP: Green fluorescent protein

YFP: Yellow fluorescent protein

DMSO: Dimethyl sulfoxide

CCCP: Carbonyl cyanide 3-chlorophenylhydrazone

STAURO: Staurosporine

PBS: Phosphate-buffered saline

HBS: Hepes-buffered saline

K: Lysine, Lys

S: Serine, Ser

Pro: Proline

Cys: Cysteine

Ile: Isoleucine

Arg: Arginine

XIAP: X-Linked inhibitor of apoptosis

SIAH1: Seven in absentia homolog 1

GP78: Glycoprotein 78

MUL1: Mulan, Mitochondrial ubiquitin ligase activator of NF κ B 1

MITOL: MARCH5, Membrane Associated Ring-CH-Type Finger 5

MDM2: E3 ubiquitin-protein ligase Mdm2

TRIM21: Tripartite Motif Containing 21

TRIM28: Tripartite motif-containing protein 28

USPs: Ubiquitin specific proteases

NBR1: Neighbor of BRCA1 gene 1 protein

pVHL: von Hippel-Lindau tumor suppressor protein

HIF1 α : Hypoxia inducible factor 1 alpha subunit

HAF: Hypoxia-associated factor

SEN1: SUMO1/sentrin specific peptidase 1

AIMs: ATG8-interacting motifs

UIMs: Ubiquitin-interacting motifs

LIR: LC3-interacting region

FAO: Fatty acid oxidation

ROS: Reactive oxygen species

RNS: Reactive nitrogen species

PEXs: Peroxins, Peroxisome biogenesis factors

PMPs: Peroxisomal membrane proteins

ATM: Ataxia telangiectasia mutated ser/thr kinase

1. INTRODUCTION

The ubiquitin–proteasome system (UPS) and macroautophagy (hereafter referred as autophagy) are major cellular catabolic pathways conserved from yeast to man. The degradation of short-lived proteins through the UPS required substrate modification through sequential addition of ubiquitin molecules (Finley, 2009; Hershko, 1983, 2005). Polyubiquitin modified substrates are then recognized by the subunits of multicatalytic protease complexes called proteasomes (Hershko and Ciechanover, 1998; Schwartz and Ciechanover, 2009).

Proteasomes are highly efficient structures that are mainly responsible for the degradation of short-lived proteins, soluble unfolded or misfolded proteins as well as polipeptides. On the other hand, rather long-lived proteins, accumulations of insoluble protein aggregates and damaged whole organelles such as dysfunctional mitochondria and Endoplasmic Reticulum are eliminated by the autophagy-lysosome system (Groll and Huber, 2003, 2004; Klionsky, 2007). Autophagy is characterized by the formation of double-membrane structures called autophagosomes, which later on fuse with lysosomes, becoming autolysosomes in order to degrade autophagosomal contents through the action of hydrolytic enzymes.

The UPS and autophagy are independent but interconnected systems, and inhibition of one system could have a positive influence on the activity of the other. There is growing evidence in the literature about these indirect connections between the two degradative system (Collins and Goldberg, 2017; Mizushima, 2018; Yu et al., 2018). In this study, I will first briefly summarize the two systems, and then discuss in detail various examples of coordination and crosstalk between them. And finally, i will introduce the novel and the first proposed direct link between the UPS and autophagy system.

1.1 UBIQUITIN-PROTEASOME SYSTEM

Ubiquitin-Proteasome system is involved in the regulation of various cellular signaling process, including protein quality control, transcription, cell cycle progression, DNA repair, cell stress response and apoptosis. For instance during cell cycle regulation, timely progression of each phase of the cycle based on sequential transcription and degradation of cell cycle proteins, such as cyclins (Benanti, 2012; Glotzer et al., 1991).

1.1.1 The Conjugation System

Ubiquitylation, the covalent conjugation of small and globular ubiquitin molecule to other proteins, is a special post translational modification, in addition to serving as an essential degradation signal for proteins or it may alter their localization, function or activity based on the added number of ubiquitin molecules to the substrates.

Binding of ubiquitin to the substrate occurs through a three-step cascade mechanism: *(i)* First, Ub is linked to a cysteine residue with its terminal glycine to an activating enzyme, E1, in an ATP-dependent manner. *(ii)* Second, the activated ubiquitin is then transferred to a conjugating enzyme, E2, by energy-rich thiol ester bond at a cysteine residue. *(iii)* Third, ubiquitin is finally attached to the destined substrate protein that is specifically bound to one member of the E3 ubiquitin ligase family (Hershko and Ciechanover, 1998). Up to now, there have been identified 2 E1 encoding genes, more than 40 genes E2 encoding genes, and over 1000 E3 encoding genes in the human genome (Clague et al., 2015; Pickart and Eddins, 2004). In cells, each E1 enzyme exhibits different preference for E2, and during the association of E2 and E3 enzymes, providing further complexity. The biochemical details of ubiquitylation are determined by the involved E3 enzymes. E3 enzymes can be divided into two major groups that are namely

HECT-domain E3s and RING-finger E3s (Huang et al., 1999). HECT type E3s form thiolester intermediate products with ubiquitin through their conserved cysteine residue, as in the case of E1 and E2 enzymes. However, RING-finger E3s, instead of forming thiolester intermediates act as a scaffold proteins which brings into a close proximity both a Ub-E2 intermediate and a substrate. Therefore, through a conformational change Ub directly transferred to the substrate from E3 enzyme (Ciechanover, 2012; Petroski and Deshaies, 2005).

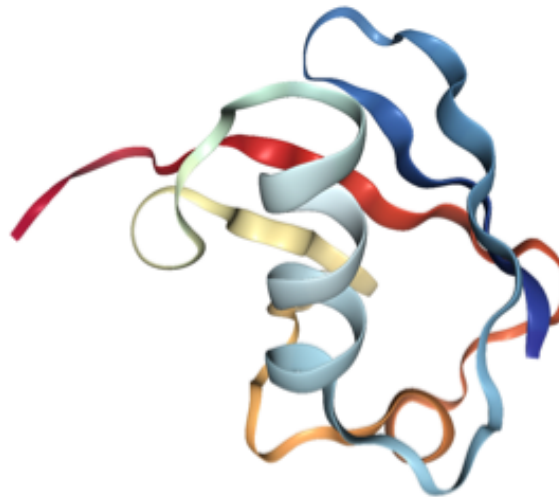


Figure 1.1.1 1: The 3D structural view of ubiquitin molecule. PDB Code: 1UBQ (retrieved from (Vijay-Kumar et al., 1987)).

Based on the lysine (K) residues are involved in polyubiquitin chain formation, the polyubiquitin linkages are characterized and given names as K6, K11, K27, K29, K33, K48, or K63 chains. Following discovery, K48-linked polyubiquitin chain was first characterized as the signal to target proteins for proteasomal degradation. Conversely, K11- or K63- linked polyubiquitin chains and even single ubiquitin molecule conjugations, termed as monoubiquitinylation were considered as signals for nonproteolytic functions (Behrends and Harper, 2011). These non-proteolytic chain types are involved in regulation of several processes such as gene transcription, DNA repair, cell cycle progression, apoptosis, and receptor endocytosis (Welchman et al., 2005). However, recent reports have demonstrated that all types of ubiquitin chains as well as monoubiquitinylation can target substrates for degradation via autophagy.

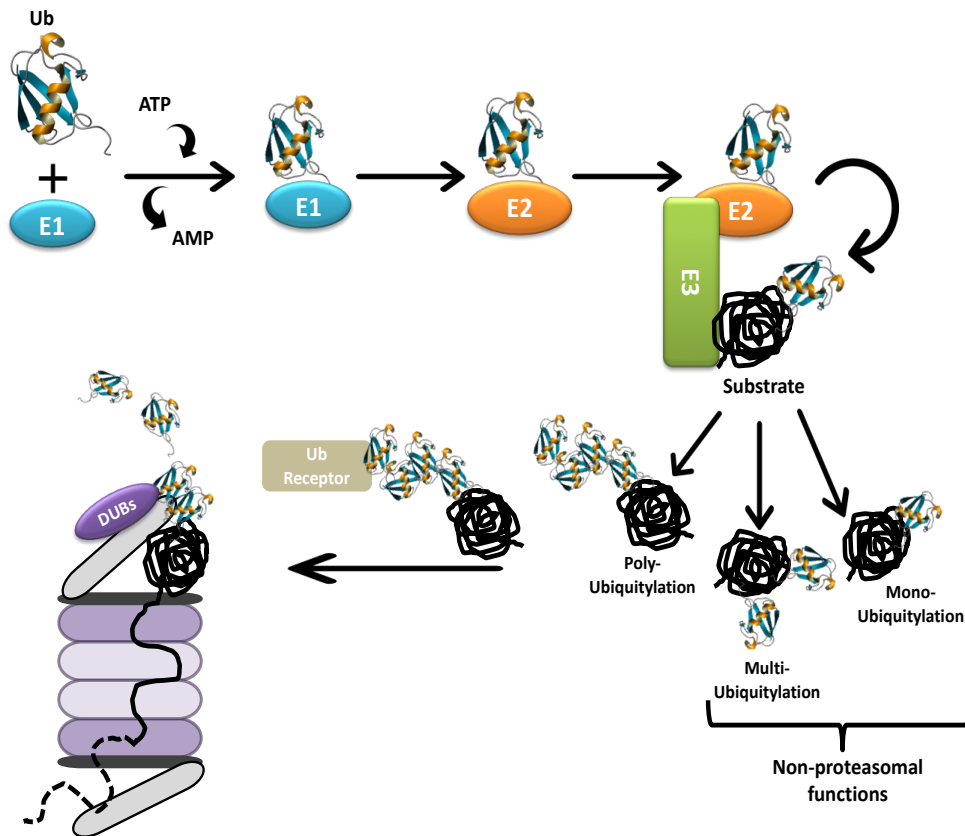


Figure 1.1.1 2: The Representative Scheme of the Ubiquitin Conjugation System and Proteasomal Degradation.

1.1.2 Proteasomes: Structure and Regulation

The 26S proteasome is a multicatalytic, ATP-dependent protease complex, which consists of a proteocatalytic, core particle (20S proteasome) and a regulatory particle (19S proteasome) is found as attached to one or two end-rings of the 20S proteasome. Barrel-shaped structure, the 20S proteasome composed of 28 distinct subunits. The two end rings of 20S proteasome contain seven different α subunits. These α rings are responsible for serving as template for the β subunit incorporation. The two middle rings of 20S proteasome contain seven different β subunits. β subunits are the critical elements for the differential catalytic activity of the 20S proteasomes whereas α subunits serve as gate for the unfolded proteins for degradation. 20S proteasome exhibits trypsin-like, caspase-like, and chymotrypsin-like activities, by the catalytic preferences of the major components:

β 1, β 2 and β 5 subunits respectively. All the catalytic subunits have different active sites on the interior surface of the core particle providing differential preferences for the cleavage of the peptides (Heinemeyer et al., 2004). Prior to the degradation, substrate experiences several steps. These steps could be listed as, getting unfolded and translocated into the catalytic chamber with the guidance of α subunits. The size of the released range between 3-25 amino acid residues and these peptides experience further cleavage into single amino acids by peptidases (Tomkinson and Lindås, 2005). So that proteasomal degradation generates essential amino acids for the reuse of the cells. Therefore as a major side-effect proteasomal inhibition, deleterious shortage of amino acids resulted in increased cellular lethality (Suraweera et al., 2012).

In addition to constitutive proteasomes, in mammals, there are also alternative proteasomes known as immunoproteasomes and these proteasomes are differentiated by the incorporation of alternative β 1i, β 2i, and β 5i subunits instead of other constitutive subunits. The immunoproteasomes are stimulated with γ -interferon and specifically shown to generate peptides for antigen presentation (Griffin et al., 1998).

Base and the lid domains of the 19S proteasome functions in differentiating ubiquitinated substrates and internalizing them in 20S proteasome for further degradation (Lander et al., 2012). The key part of the 19S base consists of six AAA ATPases (Rpt1–Rpt6) that form a hexameric Rpt ring and maintain several crucial functions: (1) They link the 19S to the heptameric α -ring of the 20S proteasomes and (2) provide a force for the 20S proteasome become open position. (3) They unfold proteins in an energy dependent manner which was generated from ATP hydrolysis and (4) translocate unfolded substrates into the 20S proteasome (Smith et al., 2007). Base subdomain also contains non-ATPase proteins including Rpn10 and Rpn13. Rpn10 and Rpn13 contain ubiquitin-binding domains and therefore could have function as receptors for ubiquitin modified substrates (Finley, 2009).

Recent findings revealed that ubiquitylation is a reversible modification. Deubiquitinating enzymes (DUBs) are proteases are able to remove ubiquitin or ubiquitin-like molecules from substrates and disassociates polyubiquitin linkages. Therefore DUBs are critical players to modulate the UPS-mediated degradation based on the cellular conditions (Turcu Francisca E. Reyes, Ventii Karen H., 2010). There have

been identified 90 DUBs encoded by the human genome and are classified into seven different groups including ubiquitin specific processing proteases (USPs) (He et al., 2016; Pinto-Fernandez and Kessler, 2016). There are three deubiquitinases (DUBs) Poh1, Usp14 and Uch37 shown to be associated with 19S proteasome and these DUBs through physical interaction remove ubiquitin chains from the substrates, stimulates ATP hydrolysis for 20S proteasomal gate opening (Peth et al., 2009). Free ubiquitin pool in cells is tightly regulated by: DUBs allow recycling and reuse of ubiquitin molecules and are also responsible for processing of newly synthesized ubiquitin precursors (Collins and Goldberg, 2017; Grou et al., 2015; Komander et al., 2009; Lee et al., 2011).

1.1.3 Ubiquitin-like Modifiers

SUMO, NEDD8, FAT10, Ufm1 and ISG15 are some of the identified and characterized other molecules known as ubiquitin-like modifiers (Ubls) (Hendriks et al., 2014; Wang et al., 2017; Yau and Rape, 2016). These modifiers are very similar to ubiquitin in terms of structure and their way of conjugation to other biomolecules in cells. The attachment to the substrate is maintained by the carboxyl group of the glycine, likewise in ubiquitylation (Hochstrasser, 2009).

Among these Ubls, SUMO can be conjugated to various ubiquitin linkages generated on substrates, such as K6, K11, K27, K48, and K63, forming a ubiquitin–SUMO hybrids (Hendriks et al., 2014). Eventhough there have been identified more than 1000 substrates, the sumoylation process is maintained by a single E1, a single E2, and a few E3 enzymes (Hendriks and Vertegaal, 2016). The SUMO isopeptidases could reversible remove SUMO molecules from SUMO modified substrates (also known as ULP, SENP, and SUSP) in the same manner with DUBs (Pichler et al., 2017). Various cellular pathways such as DNA damage response, transcriptional regulation, and stress responses are regulated by sumoylation. Interestingly, recent studies uncovered that SUMO-targeted ubiquitin ligases (STUBLs) can conjugate ubiquitin to SUMO molecules on substrates (Hendriks et al., 2014; Sriramachandran and Dohmen, 2014; Szargel et al., 2015). Ubiquitylation of SUMO moieties can induce substrate degradation by the

proteasome and therefore regulate the metabolic stabilities of SUMO-conjugated substrates.

1.1.4 PSMA7

Among the α subunits, $\alpha 4$ (also known as PSMA7, RC6-1 or XACP7), is one of the best characterized proteasomal subunit. PSMA7 composed of eight α -helices and eleven β -stranded sheets in its 3D structure (Figure 1.1.4 1, A.) and located at the two end rings of 20S proteasome (Figure 1.1.4 1, B and C) having a regulatory role rather than exhibiting catalytic activity.

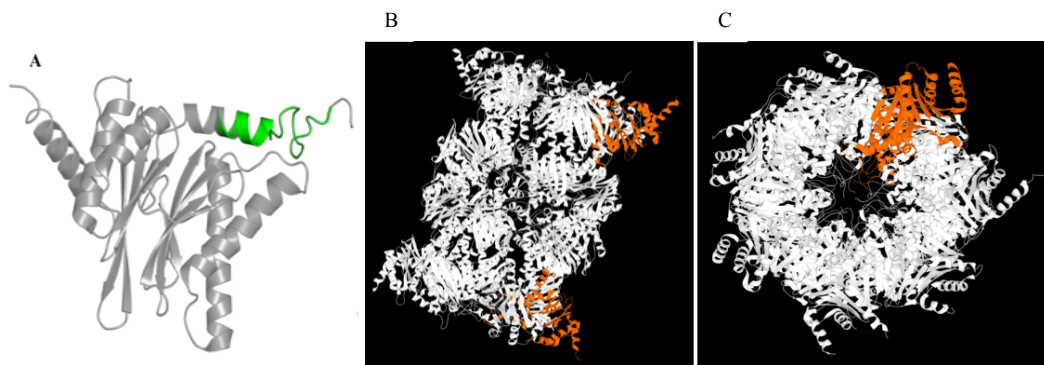


Figure 1.1.4 1: The 3D structure of human PSMA7 and its location in 20S proteasome. (PDB code: 5lf1.C). A. PSMA7 (N-Terminus in Green), B. Side view of 20S proteasome, C. Top view of 20S proteasome, and PSMA7 shown in Orange (Schrader et al., 2016).

During proteasome assembly, first α rings are formed and then they provide a landing path for incorporation of β subunits. In vitro and in vivo experiments revealed that PSMA7 N-terminal region was critical for binding many of the other α subunits, suggesting its involvement of the half proteasomes (Apcher et al., 2004). The cellular non-proteasomal PSMA7 level is also controlled by proteasomal degradation through ubiquitylation by BRCA1. Non-receptor kinase family proteins c-Abl-Arg complex-mediated phosphorylation of PSMA7 at Y106 residue prevented PSMA7 from proteasomal degradation. PSMA7 subunit level regulated by c-Abl and tightly correlated with

proteasome abundance in cells (Li et al., 2015). Not only the proteasome abundance, but also PSMA7 is critical subunit for the activity of proteasomes. Tyr153 phosphorylation of PSMA7 by the c-Abl-Arg complex compromised proteasomal degradation. Non-phosphorylation Y153F mutant of PSMA7 failed to proceed in G1/S phase in cell cycle implicating the another critical role in PSMA7 and its regulation for cellular homeostasis (Liu et al., 2006).

HIF1 α , reactive oxygen responsive transcription factor, is tightly regulated by proteasomal degradation under basal condition. HIF1 α contains two transactivation domains at its N-terminal region: 531-575 amino acid and 786-826 amino acid residues. PSMA7 identified an interaction partner of HIF1 α and inhibited HIF1 α transactivation therefore its function in both normoxia and hypoxia by inducing its proteasomal degradation (Cho et al., 2001). As an additional level of PSMA7-mediated control of cellular HIF1 α level involved Calcineurin. Calcineurin binding to PSMA7 attenuated HIF1 α transactivation (Li et al., 2011).

An endocytic membrane transport protein, RAB7 was identified as binding partner of PSMA7 through its C-terminal region. PSMA7-RAB7 interaction suggested a central regulatory role of PSMA7 in RAB7-associated endocytic membrane recruitment and transport regardless from proteasomal function of PSMA7 (Dong et al., 2004).

In addition to its core structure that participates in the structure of the 20S proteasome, PSMA7 contains a protruding C-terminus that is available for protein-protein interactions. Giving the high variety of the identified interaction partners, PSMA7 shown to be involved in various cellular processes. Table 1.1.4 1 summarizes the identified interaction partners of PSMA7 by using various techniques.

Table 1.1.4 1: Reported PSMA7 interactors.

Interactor	Experimental System	Reference
ABL1	Affinity Capture-Western	(Liu et al., 2006)
ABL1	Co-fractionation	(Liu et al., 2006)
ABL1	Affinity Capture-Western	(Liu et al., 2006)
ABL1	Biochemical Activity	(Liu et al., 2006)
ABL1	Affinity Capture-Western	(Li et al., 2015)
ABL2	Affinity Capture-Western	(Liu et al., 2006)
ABL2	Biochemical Activity	(Liu et al., 2006)
ADRM1	Co-fractionation	(Wan et al., 2015)
AIMP1	Affinity Capture-Western	(Tandle et al., 2009)
AMBRA1	Affinity Capture-MS	(Antonioli et al., 2014a)
AMFR	Affinity Capture-MS	(Christianson et al., 2012)
AP3M1	Co-fractionation	(Kristensen et al., 2012)
APP	Reconstituted Complex	(Oláh et al., 2011)
BAG3	Affinity Capture-MS	(Chen et al., 2013)
BARD1	Two-hybrid	(Woods et al., 2012)
BRCA1	Affinity Capture-Western	(Li et al., 2015)
BRCA1	Far Western	(Li et al., 2015)
BRCA1	Biochemical Activity	(Li et al., 2015)
BRCA1	Affinity Capture-MS	(Ertych et al., 2016)
CAPN10	Two-hybrid	(Wang et al., 2011)
CEP85	Affinity Capture-MS	(Blomen et al., 2015)
COPS5	Affinity Capture-MS	(Bennett et al., 2010)
CUL1	Reconstituted Complex	(Bloom et al., 2006)
CUL1	Affinity Capture-MS	(Bennett et al., 2010)
CUL3	Affinity Capture-Western	(Shen et al., 2007)
CYLD	Affinity Capture-MS	(Elliott et al., 2016)
ECSCR	Affinity Capture-Western	(Ikeda et al., 2009a)
ECSCR	Affinity Capture-Western	(Ikeda et al., 2009a)
EGFR	PCA	(Deribe et al., 2009)
ERRF1	Two-hybrid	(Ying et al., 2010)
EXOSC9	Co-fractionation	(Wan et al., 2015)
FKBP8	Affinity Capture-MS	(Nakagawa et al., 2007)
FN1	Affinity Capture-MS	(Humphries et al., 2009)
HECW2	Affinity Capture-MS	(Lu et al., 2013)
HIF1A	Reconstituted Complex	(Cho et al., 2001)
HIF1A	Affinity Capture-Western	(Cho et al., 2001)

HIF1A	Affinity Capture-Western	(Yi et al., 2008)
HUWE1	Affinity Capture-MS	(Thompson et al., 2014)
IKBKE	Affinity Capture-MS	(Ewing et al., 2007)
INSIG1	Reconstituted Complex	(Ikeda et al., 2009b)
INSIG2	Reconstituted Complex	(Ikeda et al., 2009b)
IQCB1	Affinity Capture-MS	(Sang et al., 2011)
ISG15	Affinity Capture-MS	(Zhao et al., 2005)
ITGA4	Affinity Capture-MS	(Byron et al., 2012)
MAPK4	Affinity Capture-MS	(Varjosalo et al., 2013)
MAPK6	Affinity Capture-MS	(Varjosalo et al., 2013)
MAVS	Affinity Capture-Western	(Jia et al., 2009)
MAVS	Affinity Capture-Western	(Jia et al., 2009)
MCM2	Affinity Capture-MS	(Drissi et al., 2015)
MDM2	Co-fractionation	(Kulikov et al., 2010)
MDM2	Affinity Capture-Western	(Kulikov et al., 2010)
MDM2	Affinity Capture-Western	(Sdek et al., 2005)
MRPS16	Co-fractionation	(Havugimana et al., 2012)
MYC	Affinity Capture-MS	(Koch et al., 2007)
NEDD8	Affinity Capture-MS	(Norman and Shiekhattar, 2006)
NME2	Affinity Capture-MS	(Ewing et al., 2007)
NOD1	Affinity Capture-Western	(Yang et al., 2013)
NOD1	Affinity Capture-Western	(Yang et al., 2013)
NOS2	Affinity Capture-MS	(Foster et al., 2013)
NTRK1	Affinity Capture-MS	(Emdal et al., 2015)
P4HB	Co-fractionation	(Wan et al., 2015)
PARK2	Affinity Capture-MS	(Sarraf et al., 2013)
PLK1	Affinity Capture-MS	(Feng et al., 2001)
PLK1	Affinity Capture-Western	(Feng et al., 2001)
POMP	Co-fractionation	(Fricke et al., 2007)
POMP	Two-hybrid	(Fricke et al., 2007)
POMP	Affinity Capture-Western	(Hirano et al., 2006)
PPP3R1	Two-hybrid	(Li et al., 2011)
PPP3R1	Affinity Capture-Western	(Li et al., 2011)
PPP3R1	Affinity Capture-Western	(Li et al., 2011)
PR39	Affinity Capture-Western	(Gao et al., 2000)
PR39	Affinity Capture-Western	(Gao et al., 2000)
PSMA1	Two-hybrid	(Apcher et al., 2004)
PSMA1	Affinity Capture-Western	(Apcher et al., 2004)
PSMA1	Affinity Capture-Western	(Apcher et al., 2004)
PSMA1	Two-hybrid	(Jayarapu and Griffin, 2004)
PSMA1	Co-fractionation	(Tipler et al., 1997)
PSMA1	Two-hybrid	(Fricke et al., 2007)
PSMA1	Co-fractionation	(Havugimana et al., 2012)

PSMA1	Co-fractionation	(Kristensen et al., 2012)
PSMA1	Affinity Capture-MS	(Huttlin et al., 2015)
PSMA1	Co-fractionation	(Wan et al., 2015)
PSMA1	Affinity Capture-MS	(Huttlin et al., 2017)
PSMA2	Two-hybrid	(Vinayagam et al., 2011)
PSMA2	Affinity Capture-MS	(Claverol et al., 2002)
PSMA2	Two-hybrid	(Apcher et al., 2004)
PSMA2	Affinity Capture-Western	(Apcher et al., 2004)
PSMA2	Affinity Capture-MS	(Bousquet-Dubouch et al., 2009)
PSMA2	Two-hybrid	(Fricke et al., 2007)
PSMA2	Co-fractionation	(Havugimana et al., 2012)
PSMA2	Co-purification	(Froment et al., 2005)
PSMA2	Affinity Capture-MS	(Froment et al., 2005)
PSMA2	Co-fractionation	(Kristensen et al., 2012)
PSMA2	Co-fractionation	(Wan et al., 2015)
PSMA3	Two-hybrid	(Vinayagam et al., 2011)
PSMA3	Two-hybrid	(Apcher et al., 2004)
PSMA3	Affinity Capture-Western	(Apcher et al., 2004)
PSMA3	Affinity Capture-Western	(Apcher et al., 2004)
PSMA3	Affinity Capture-Western	(Nandi et al., 1997)
PSMA3	Two-hybrid	(Fricke et al., 2007)
PSMA3	Co-fractionation	(Havugimana et al., 2012)
PSMA3	Two-hybrid	(Wang et al., 2011)
PSMA3	Co-fractionation	(Kristensen et al., 2012)
PSMA3	Co-fractionation	(Wan et al., 2015)
PSMA4	Two-hybrid	(Apcher et al., 2004)
PSMA4	Affinity Capture-Western	(Apcher et al., 2004)
PSMA4	Affinity Capture-Western	(Apcher et al., 2004)
PSMA4	Co-fractionation	(Apcher et al., 2004)
PSMA4	Two-hybrid	(Jayarapu and Griffin, 2004)
PSMA4	Affinity Capture-Western	(Nandi et al., 1997)
PSMA4	Two-hybrid	(Fricke et al., 2007)
PSMA4	Co-fractionation	(Havugimana et al., 2012)
PSMA4	Co-fractionation	(Kristensen et al., 2012)
PSMA4	Co-fractionation	(Wan et al., 2015)
PSMA5	Affinity Capture-Western	(Apcher et al., 2004)
PSMA5	Co-fractionation	(Havugimana et al., 2012)
PSMA5	Co-fractionation	(Kristensen et al., 2012)
PSMA5	Co-fractionation	(Wan et al., 2015)
PSMA6	Two-hybrid	(Apcher et al., 2004)
PSMA6	Two-hybrid	(Apcher et al., 2004)
PSMA6	Affinity Capture-Western	(Apcher et al., 2004)
PSMA6	Affinity Capture-Western	(Apcher et al., 2004)

PSMA6	Two-hybrid	(Jayarapu and Griffin, 2004)
PSMA6	Two-hybrid	(Fricke et al., 2007)
PSMA6	Two-hybrid	(Fricke et al., 2007)
PSMA6	Co-fractionation	(Havugimana et al., 2012)
PSMA6	Co-fractionation	(Kristensen et al., 2012)
PSMA6	Co-fractionation	(Wan et al., 2015)
PSMA6	Reconstituted Complex	(Ishii et al., 2015)
PSMA7	Two-hybrid	(Fricke et al., 2007)
PSMA8	Co-fractionation	(Havugimana et al., 2012)
PSMB1	Two-hybrid	(Jayarapu and Griffin, 2007)
PSMB1	Co-fractionation	(Havugimana et al., 2012)
PSMB1	Co-fractionation	(Kristensen et al., 2012)
PSMB1	Affinity Capture-Western	(Yuan et al., 2013)
PSMB1	Co-fractionation	(Wan et al., 2015)
PSMB1	Affinity Capture-MS	(Huttlin et al., 2017)
PSMB2	Co-fractionation	(Havugimana et al., 2012)
PSMB2	Co-fractionation	(Kristensen et al., 2012)
PSMB2	Co-fractionation	(Wan et al., 2015)
PSMB2	Affinity Capture-MS	(Huttlin et al., 2017)
PSMB3	Co-fractionation	(Havugimana et al., 2012)
PSMB3	Co-fractionation	(Kristensen et al., 2012)
PSMB3	Co-fractionation	(Wan et al., 2015)
PSMB3	Affinity Capture-MS	(Huttlin et al., 2017)
PSMB4	Co-fractionation	(Havugimana et al., 2012)
PSMB4	Co-fractionation	(Kristensen et al., 2012)
PSMB4	Affinity Capture-MS	(Huttlin et al., 2015)
PSMB4	Co-fractionation	(Wan et al., 2015)
PSMB4	Affinity Capture-MS	Hein MY (2015)
PSMB4	Affinity Capture-MS	(Huttlin et al., 2017)
PSMB5	Co-fractionation	(Havugimana et al., 2012)
PSMB5	Co-fractionation	(Kristensen et al., 2012)
PSMB5	Co-fractionation	(Wan et al., 2015)
PSMB5	Affinity Capture-MS	(Hein et al., 2015)
PSMB6	Co-fractionation	(Havugimana et al., 2012)
PSMB6	Co-fractionation	(Kristensen et al., 2012)
PSMB6	Co-fractionation	(Wan et al., 2015)
PSMB7	Co-fractionation	(Havugimana et al., 2012)
PSMB7	Co-fractionation	(Kristensen et al., 2012)
PSMB7	Affinity Capture-MS	(Huttlin et al., 2015)
PSMB7	Co-fractionation	(Wan et al., 2015)
PSMB7	Affinity Capture-MS	(Huttlin et al., 2017)
PSMB8	Co-fractionation	(Havugimana et al., 2012)
PSMB8	Co-fractionation	(Wan et al., 2015)
PSMB9	Two-hybrid	(Jayarapu and Griffin, 2007)

PSMB9	Two-hybrid	(Fricke et al., 2007)
PSMB9	Affinity Capture-MS	(Huttlin et al., 2015)
PSMB9	Co-fractionation	(Wan et al., 2015)
PSMB9	Affinity Capture-MS	(Huttlin et al., 2017)
PSMC1	Co-fractionation	(Havugimana et al., 2012)
PSMC1	Co-fractionation	(Wan et al., 2015)
PSMC2	Co-fractionation	(Havugimana et al., 2012)
PSMC2	Co-fractionation	(Wan et al., 2015)
PSMC3	Co-fractionation	(Havugimana et al., 2012)
PSMC3	Co-fractionation	(Wan et al., 2015)
PSMC4	Co-fractionation	(Havugimana et al., 2012)
PSMC4	Co-fractionation	(Wan et al., 2015)
PSMC5	Co-fractionation	(Havugimana et al., 2012)
PSMC5	Co-fractionation	(Wan et al., 2015)
PSMC6	Co-fractionation	(Havugimana et al., 2012)
PSMC6	Co-fractionation	(Wan et al., 2015)
PSMD1	Co-fractionation	(Garrett et al., 2004)
PSMD1	Co-fractionation	(Havugimana et al., 2012)
PSMD1	Co-fractionation	(Wan et al., 2015)
PSMD11	Co-fractionation	(Havugimana et al., 2012)
PSMD11	Co-fractionation	(Wan et al., 2015)
PSMD12	Co-fractionation	(Havugimana et al., 2012)
PSMD12	Co-fractionation	(Wan et al., 2015)
PSMD13	Affinity Capture-MS	(Ewing et al., 2007)
PSMD13	Co-fractionation	(Havugimana et al., 2012)
PSMD13	Co-fractionation	(Wan et al., 2015)
PSMD14	Co-fractionation	(Havugimana et al., 2012)
PSMD14	Affinity Capture-MS	(Wang et al., 2007)
PSMD2	Co-fractionation	(Havugimana et al., 2012)
PSMD2	Co-fractionation	(Wan et al., 2015)
PSMD3	Co-fractionation	(Havugimana et al., 2012)
PSMD4	Co-fractionation	(Hamazaki et al., 2007)
PSMD4	Co-fractionation	(Liu et al., 2006)
PSMD4	Co-fractionation	(Havugimana et al., 2012)
PSMD4	Co-fractionation	(Wan et al., 2015)
PSMD5	Co-fractionation	Havugimana PC (2012)
PSMD5	Co-fractionation	(Wan et al., 2015)
PSMD6	Co-fractionation	Thompson HG (2004)
PSMD6	Co-fractionation	(Havugimana et al., 2012)
PSMD6	Co-fractionation	(Wan et al., 2015)
PSMD7	Co-fractionation	Thompson HG (2004)
PSMD7	Co-fractionation	(Havugimana et al., 2012)
PSMD7	Co-fractionation	(Wan et al., 2015)
PSMD8	Co-fractionation	(Havugimana et al., 2012)

PSME1	Co-fractionation	(Havugimana et al., 2012)
PSME3	Co-fractionation	(Havugimana et al., 2012)
PSME4	Co-fractionation	(Kristensen et al., 2012)
PSMF1	Two-hybrid	(Wang et al., 2011)
PSMG1	Affinity Capture-Western	(Hirano et al., 2006)
PSMG3	Affinity Capture-Western	(Hirano et al., 2006)
PYCR1	Co-fractionation	(Kristensen et al., 2012)
RAB7A	Affinity Capture-Western	(Dong et al., 2004)
RAB7A	Affinity Capture-Western	(Dong et al., 2004)
RAD23A	Affinity Capture-MS	(Scanlon et al., 2009)
RB1	Affinity Capture-Western	(Sdek et al., 2005)
RBM3	Co-fractionation	(Havugimana et al., 2012)
RMND5B	Affinity Capture-MS	(Boldt et al., 2016)
RNF185	Affinity Capture-MS	(Iioka et al., 2007)
SAMD1	Co-fractionation	(Havugimana et al., 2012)
SHFM1	Affinity Capture-MS	(Wei et al., 2008)
SLX1B	Affinity Capture-MS	(Svendsen et al., 2009)
SNRPA1	Co-fractionation	(Havugimana et al., 2012)
SPTBN1	Co-fractionation	(Havugimana et al., 2012)
SYVN1	Affinity Capture-MS	(Christianson et al., 2012)
TAT1	Affinity Capture-Western	(Apcher et al., 2003)
TBXA2R	Affinity Capture-Western	(Sasaki et al., 2007)
TBXA2R	Two-hybrid	(Sasaki et al., 2007)
TBXA2R	Two-hybrid	(Nakahata et al., 2007)
TERF1	Affinity Capture-MS	(Giannone et al., 2010)
TIMP2	Affinity Capture-MS	(Ewing et al., 2007)
TSC22D2	Two-hybrid	(Li et al., 2016)
UBC	Affinity Capture-MS	(Matsumoto et al., 2005)
UBQLN1	Affinity Capture-Western	(Lim et al., 2009)
UCHL5	Affinity Capture-MS	(Yao et al., 2008)
UCHL5	Co-fractionation	(Wan et al., 2015)
VCAM1	Affinity Capture-MS	(Humphries et al., 2009)
VCP	Two-hybrid	(Wang et al., 2011)

The network of PSMA7 and its reported interactors underlines that PSMA7 has mainly involved in proteasome complex. However, it was also reported to interacted with various proteins showing that has key role in differential cellular mechanisms. The PSMA7 interaction network was depicted in Figure 1.1.4 2 using BioGRID software.

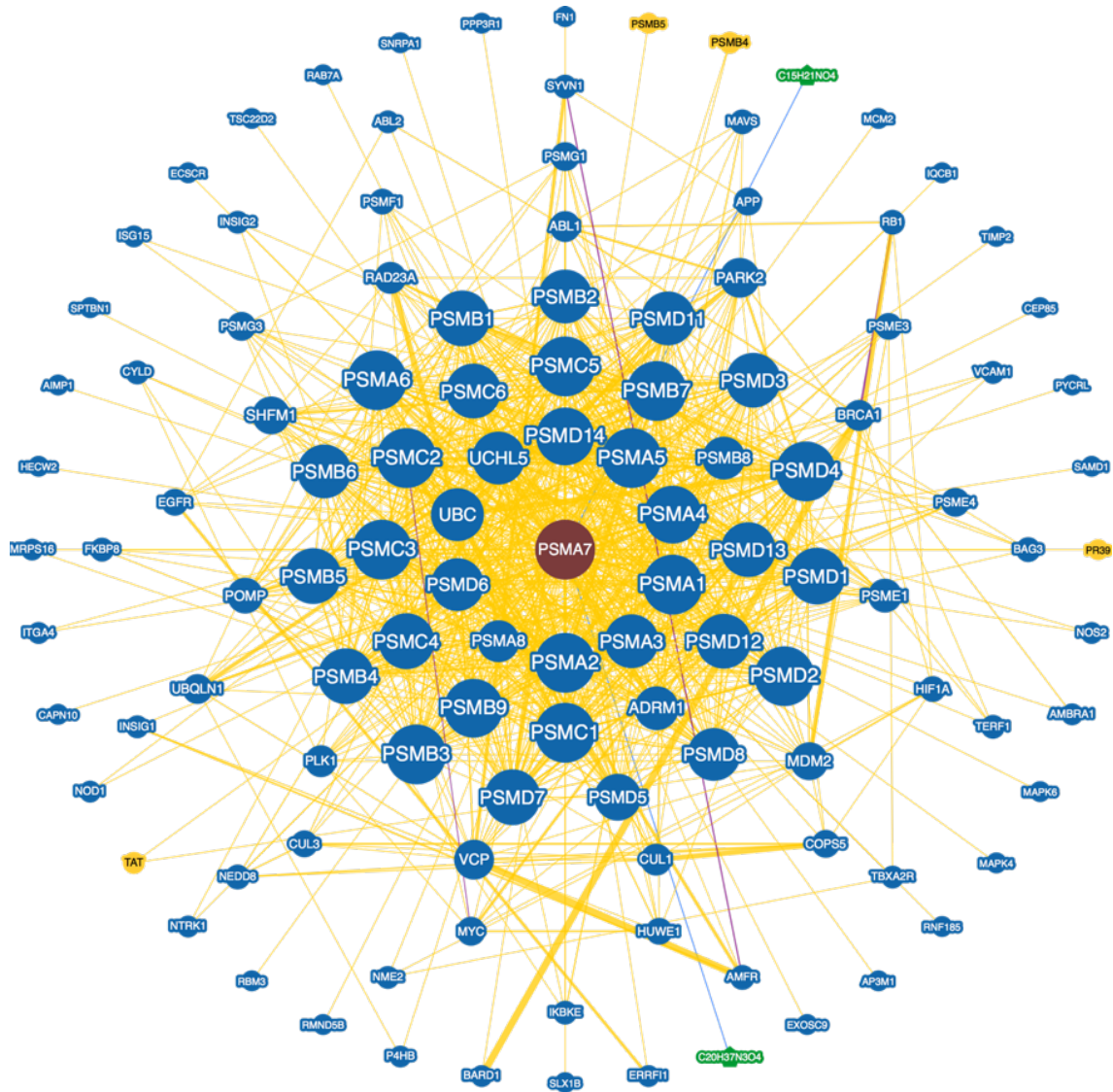


Figure 1.1.4 2: PSMA7 interaction network was obtained by using BioGRID software.

Due to its involvement of various cancer types ranging from the lung cancer to colorectal cancer, as well as its critical role in innate immunity it is emerging to understand the molecular details behind the interaction of PSMA7 and its partners under different cellular and environmental conditions.

1.2 AUTOPHAGY

Autophagy classified in three main types: that are macroautophagy, microautophagy and chaperon-mediated autophagy (CMA). These three different types of autophagy share common feature as final step of degradation targets are carried to the lysosomes but they differ in the process of delivery to the lytic organelles.

In CMA, cytosolic proteins are recognized through their pentapeptide signature motif (KFERQ) by a well known chaperon protein called heat shock 70 kDa protein (HSC70). After recognition, HSC70 protein binds to lysosomal-associated membrane protein 2A (LAMP2A). The degradation targets subsequently gets unfolded and translocated to the lysosomal lumen for degradation (Susmita Kaushik and Ana Maria Cuervo, 2013). During microautophagy, following direct engulfment of cargo, the cytosolic content is sequestered by a small invagination of the lysosomal membrane that pinches off into lumen (Li et al., 2012). The best studied type of autophagy is macroautophagy (hereafter called autophagy). Autophagy is characterized by the engulfment of differential degradation targets by a double-membrane structure (also called as isolation membrane) as a portion of cytoplasm that enclosed to form autophagosomes (Lamb et al., 2013). Mature autophagosomes fuse with lytic organelles to form autolysosomes as a consequence degradation occurs by the action of hydrolases. Following degradation, autophagy provides molecular building blocks and supply energy during cellular stress conditions.

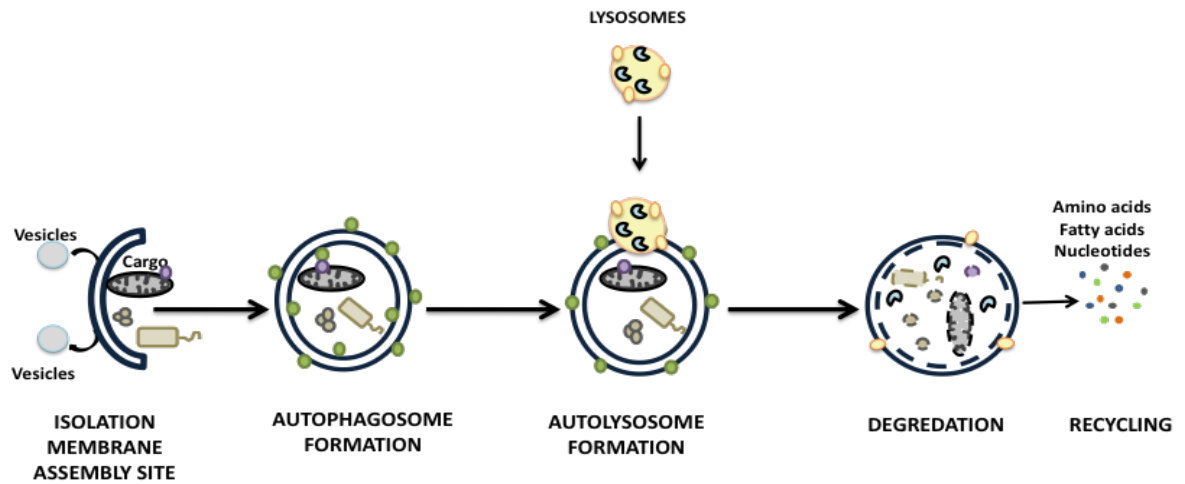


Figure 1.2 1: The schematic representation of sequential stages of autophagy mechanism.

Unraveling the molecular mechanisms of autophagy process has gained acceleration following the initial discovery of approximately 35 autophagy-related (ATG) genes from genetic studies in yeast (Nakatogawa et al., 2007). Later on, it is understood that mammals have orthologs for most of the yeast ATG proteins, as well as producing some additional factors specific to higher eukaryotes. The autophagic cascade has been divided into distinct stages: Upstream regulation, initiation/nucleation, elongation and closure, and autophagosome-lysosome fusion (Detailed representation given in Figure 1.2 1 and Figure 1.2 2).

1.2.1 Upstream Regulation

The regulation of autophagy is central to the understanding of its mechanisms and related diseases. Two main kinase systems known to regulate the autophagic pathway: the mTOR–ULK1 and the BECN1 complex. mTOR, or target of rapamycin (TOR in nonmammalian species), belongs to the family of phosphoinositide-3-kinase related kinase (PIKKs) (Sengupta et al., 2010). mTOR is so-called because it gives response to treatment with rapamycin and other kinase inhibitors that have been widely used to induce autophagy, even under nutrient-rich conditions (Hara et al., 1998). mTOR was found in

two different complexes, as complex 1 (mTORC1) and complex 2 (mTORC2). mTORC2 is less sensitive to rapamycin. These two complexes contain several proteins in common (Deptor, GβL, and PRAS40), but other components are specific to mTORC1 (Raptor) or mTORC2 (Rictor, SIN1, and Protor).

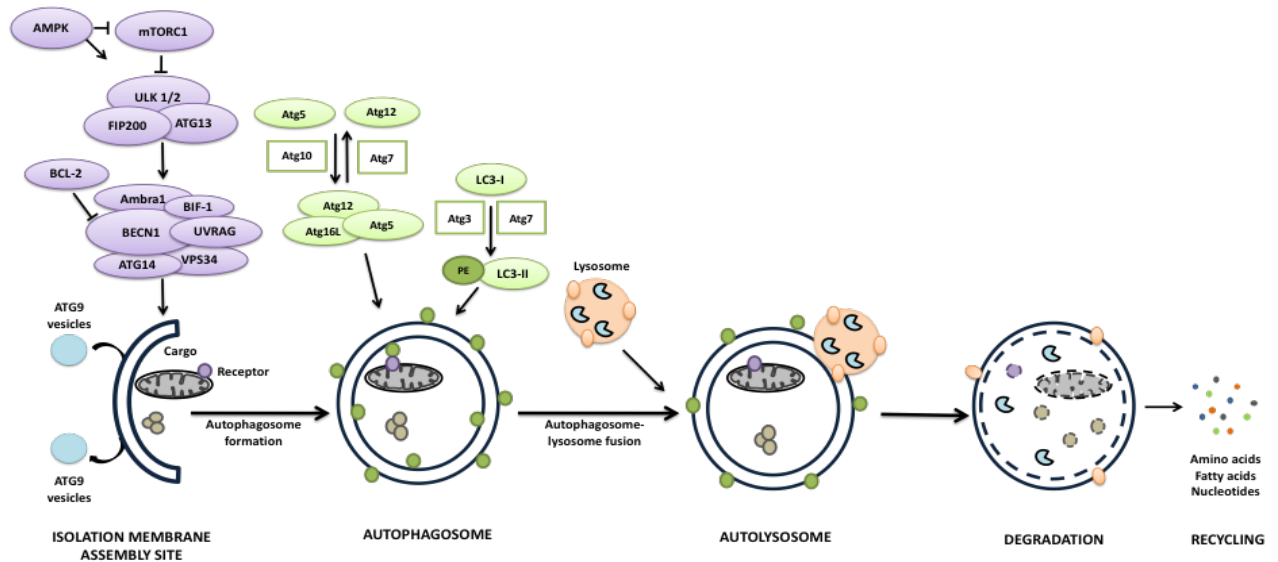


Figure 1.2 2: Molecular regulators involved in different stages of the autophagy process.

The serine-threonine kinase TOR is key factor for integrating signaling pathways that regulate cellular homeostasis, by coordinating anabolic and catabolic processes upon nutrients, energy and oxygen availability, as well as growth factor signaling (Kroemer et al., 2010). When mTOR is activated in the presence of nutrients or growth factors, the mTORC1 complex gets associated with the ULK1/2 complex and hyperphosphorylates its ATG13 subunit. This hyperphosphorylation results in its inactivation and subsequent down-regulation of autophagy. The ULK complex contains the ULK1 or ULK2 kinase, ATG13, FIP200 (focal adhesion kinase-family interacting protein of 200 kDa) and ATG101, an ATG13-binding protein in mammals. When activated, mTORC1 favors cell growth by promoting translation via the phosphorylation of p70S6K (70 kDa polypeptide 1 ribosomal protein S6 kinase) and of 4E-BP1, an inhibitor of translation initiation, therein inactivating it (Chen and Klionsky, 2011).

However when nutrient and growth factors are limiting in the environment mTORC1 is downregulated and gets disassociated from the ULK1/2 complex. This disassociation causes its subsequent dephosphorylation and its activation. Due to its autophosphorylation ability, the activated ULK1/2 phosphorylates itself and ATG13 and FIP200 to activate autophagy in cells. The active ULK1/2 remains attached to the isolation membrane during nutrient deprivation. Eventhough the exact mechanism in which ULK1/2 activate downstream effectors and components of autophagic machinery is vogue, but it is shown that ULK1/2 can phosphorylate AMBRA1 (activating molecule of BECN1-regulated autophagy 1) which is a component of the VPS34 associated BECN1 complex (Mehrpour et al., 2010).

1.2.2 Initiation and Membrane Nucleation

The nascent membrane, called the “isolation membrane”, wraps around a portion of cytoplasm that may contain soluble proteins, organelles, or aggregates to be degraded. Due to its crescent-shaped structure is also called the “phagophore” or “omegasome”, which is assembled at the phagophore assembly site (PAS). The source of the isolation membrane is still under debate, and both the ER, mitochondria, plasma membrane, and the Golgi apparatus have been implicated (Weidberg et al., 2011). A complex of class III phosphatidylinositol 3-kinases (PI3K) controls the nucleation step and the assembly of the initial phagophore formation. The core components of PI3K complex are also responsible for the catalytic activity of the complex and these are VPS34 (vacuolar protein sorting 34), VPS15, and a positive regulatory unit BECN1 (ATG6 in yeast). The cellular autophagy level in mammals mainly determined by the activity of this complex and is tightly regulated by positive and negative regulators. Mammalian cells host BECN 1-binding proteins, including positive regulator ATG14L [also known as Barkor (BECN1-associated ATG Key regulator)], Bif-1 and UVRAG, and negative regulators, Bcl-2, and Rubicon (Funderburk et al., 2010). Phosphatidylinositol-3-phosphate (PtdIns3P) is generated by VPS34 and constitutes an essential membrane component of the elongating isolation membrane. In mammalian cells, PtdIns3P molecules function as recruiting point for several autophagy-related proteins to the isolation membrane. WIPI1/2 (orthologous to yeast ATG18), DFCP1, and Alfy are recruited by PtdIns3P to the isolation membrane.

Subsequently, WIPI1/2 attenuates membrane rearrangements and positioning that ultimately facilitate the formation of autophagosomes by an unknown molecular mechanism (Mauthe et al., 2011). ATG9 (mATG9 or ATG9L1 in mammals) is the only transmembrane ATG protein. ATG9L1 functions in trafficking between the *trans*-Golgi network and endosomal systems in normal cells. However, as a response to starvation, it localizes to autophagic vacuoles. ATG9L1 was shown to carry lipids or to prepare a kind of platform for recruiting effectors to the phagophore (Young, 2006).

1.2.3 Membrane Elongation and Closure

Elongation of the isolation membrane relies on two ubiquitin-like conjugation reactions. In the first system, basically ATG12 protein is conjugated to ATG5 protein resulting in the formation of an oligomeric ATG5-ATG12 complex which then recruits ATG16L protein to promote elongation and the closure of the autophagosomes. ATG5-ATG12 complex formation requires E1- and E2-like activities. ATG7 (an E1-like enzyme) protein activates ATG12 and the activated ATG12 then transferred to ATG10 (E2-like enzyme) and then finally conjugated to ATG5 (Hanada et al., 2007). The ATG12-ATG5 conjugate then associates with ATG16L (ATG16 in yeast) by a non-covalent binding similar to an E3-like enzyme.

The other system contains the ATG8 (in yeast) proteins. Mammalian ATG8 homologues are grouped into three subfamilies, that are, the LC3 subfamily (LC3A, B, and C), the GABARAP subfamily (GABARAP and GABARAPL1/GEC1), and GABARAPL2/GATE-16 (Shpilka et al., 2011). In mammals, LC3B functions as the main ATG8 homolog (Tanida et al., 2004). These LC3B proteins are synthesized as precursors and are critical components of autophagosome formation. ATG4 protein is involved in the LC3 processing steps. A cysteine protease ATG4 cleaves LC3 from its C-terminus and a glycine residue is exposed. Cleaved form of LC3 then activated by ATG7 (E1-like enzyme), activated LC3 transferred to ATG3 (E2-like enzyme), and finally through covalent binding linked to an amino group of phosphatidylethanolamine (PE). These LC3 associated PE (LC3-PE) is utilized for major membrane phospholipid during autophagy by the ATG5-ATG12-ATG16L complex (Hanada et al., 2007). Conjugation of LC3-PE

to both sides of the isolation membrane enables them to act as surface receptors for the specific recruitment of other proteins. Lipidated LC3 proteins are also involved in membrane biogenesis of autophagosomes via their membrane fusion activity (Nakatogawa et al., 2007). ATG4 is also capable of cleaving LC3-PE therein by deconjugation, controls the active LC3 level as well as the size of the autophagosomes in cells. The autophagosomal closure results in a typical double-membraned vacuole formation and following closure ATG12-ATG5-ATG16L complex leaves the autophagosome, autophagosomal membrane associated LC3-PE molecules are placed in the cytosolic surface and PE molecules are cleaved by ATG4 for recycling (Kabeya, 2004).

1.2.4 Autophagosome-Lysosome Fusion

Following autophagosome formation, PE-LC3B protein attached to the outer membrane of the autophagosome is subjected to a cleavage reaction by ATG4 and released back to the cytosol for reuse (Kirisako et al., 2000). In mammalian cells, autophagosome and lysosome fusion event require the lysosomal membrane protein LAMP-2, several SNARE proteins and the small GTPase Rab7 (Jager, 2004; Tanaka et al., 2000). After fusion, the degradation of engulfed materials is mediated by a series of lysosomal acid hydrolases (Tanida et al., 2004). Then small molecule products of hydrolytic cleavage after degradation, particularly amino acids are transported back to the cytosol in order to be involved in protein synthesis and therein to support cellular functions during stress conditions.

1.2.5 Autophagy Receptors: Ub Code for Selective Autophagy

In the last decade, emerging evidence revealed that autophagy process is able to distinguish and direct specific cargo molecules to the lysosomes for further degradation steps. Based on the differences in the degradation targets, different autophagy terms were coined to distinguish the mechanisms (Figure 1.2.5. 1). The best studied processes are

mitophagy: the selective removal of mitochondria (Okamoto et al., 2009), aggrephagy: removal of misfolded aggregates (Lamark and Johansen, 2012), xenophagy: the selective autophagy of pathogenic intracellular invaders (Wileman, 2013), and pexophagy: removal peroxisome by autophagy (Till et al., 2012). Basically, the selective autophagy is ensured mainly by specific adaptor proteins for each identified processes. Additionally, direct interactions between the core autophagy machinery and target molecules have been observed.

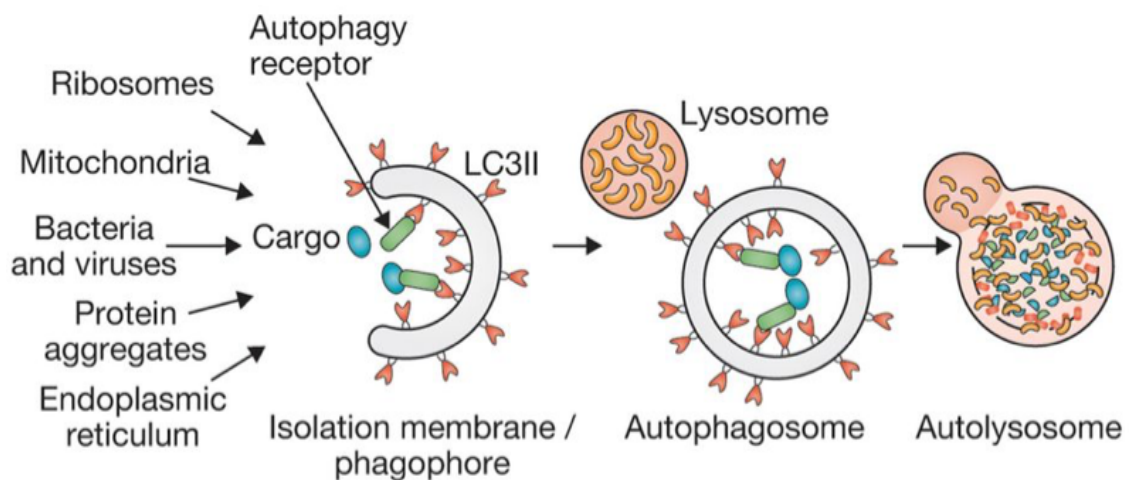


Figure 1.2.5 1: Autophagic machinery selectively degrade cellular targets and invaders.(retrieved from (Stolz et al., 2014)).

Recent findings in the field of ubiquitin, revealed that ubiquitin has a fundamental role in selective autophagy (Kirkin et al., 2009; Rogov et al., 2014). Degradation targets of autophagy might be specifically labelled with ubiquitin. The recognition of ubiquitinated proteins during autophagy or the proteasome is mediated by ubiquitin receptors that are interacting with ubiquitin through non covalent binding by their ubiquitin-binding domains (UBD).

p62/SQSM1 (hereafter p62), is the first protein reported to have such an adaptor function (Pankiv et al., 2007) and observed in ubiquitin associated protein aggregates (Moscat and Diaz-Meco, 2009), was originally discovered as a scaffold in signaling

pathways regulating cell growth and proliferation. P62 contains a C-terminal ubiquitin-binding domain (UBD) (Ciani et al., 2003) and a short LIR (LC3-interacting region) sequence responsible for LC3 interaction (Pankiv et al., 2007). Mice and Drosophila knockout studies revealed that p62 is an essential protein for proper aggregation of ubiquitin labelled proteins. Therefore play essentials role in the autophagic clearence of those aggregates (Komatsu et al., 2007; Nezis et al., 2008).

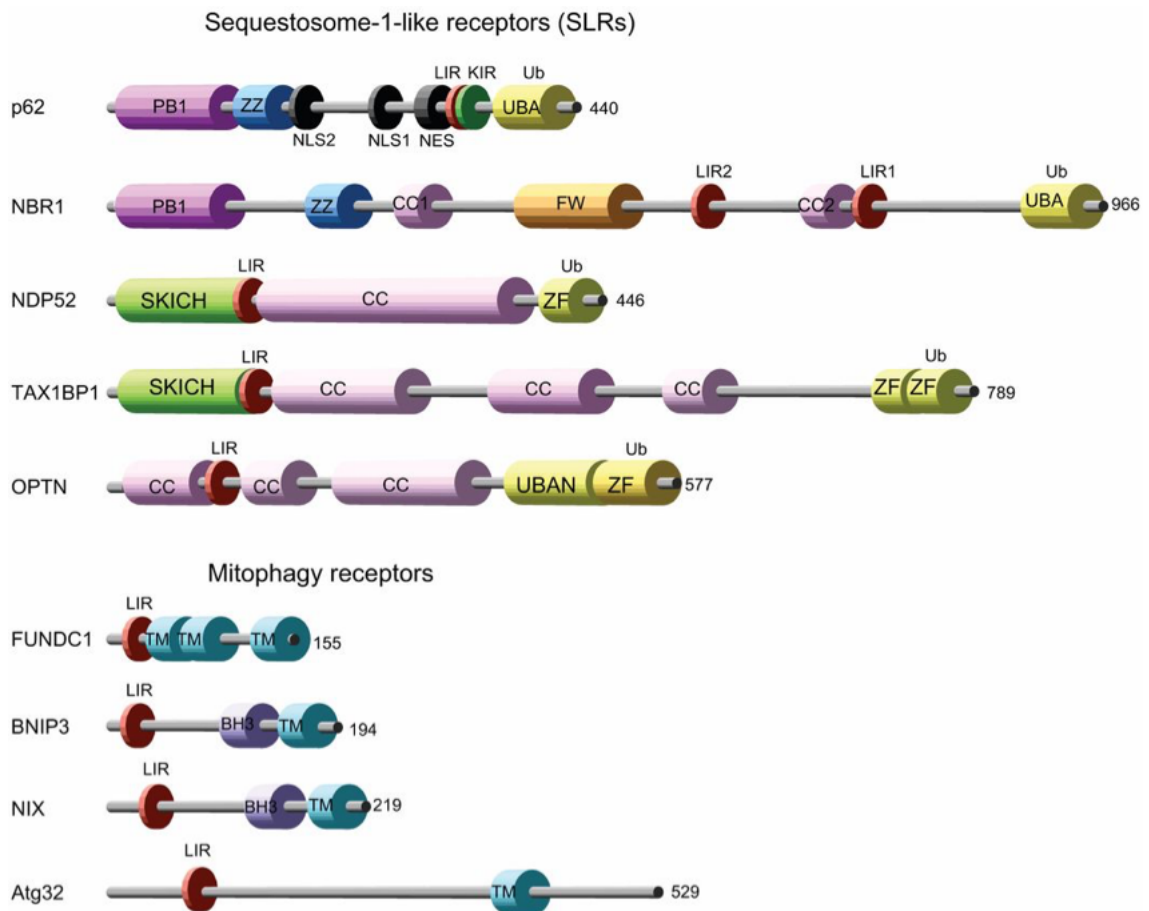


Figure 1.2.5. 2: Autophagy receptors make bridges between selective cargo and autophagic machinery through their specialized interaction domains. (retrived from (Birgisdottir et al., 2013)).

Similarly selective autophagy relies on its own recognition and binding capacity of autophagy receptors to intracellular ubiquitinated aggregates (p62, NBR1, OPTN, TOLLIP) (Kirkin et al., 2009; Korac et al., 2013; Lu et al., 2014; Pankiv et al., 2007),

bacterial invaders (p62, OPTN, NDP52) (Thurston, 2009; Wild et al., 2011; Zheng et al., 2009), peroxisomes (NBR1) (Deosaran et al., 2013), mitochondria (OPTN, NDP52, Tax1BP1) (Lazarou et al., 2015; Sarraf et al., 2013; Wong and Holzbaur, 2014), or proteasomes (RPN10) (Marshall et al., 2015), and the material directed to autophagosomal membranes (Figure 1.2.5. 2). Importantly, based on the length and the type of the Ub chains, ubiquitinated proteins tend to form aggregates, and thus become autophagy substrates (Meier et al., 2012; Morimoto et al., 2015). However, genetic disruption of the essential autophagy genes ATG5 or ATG7 results in the accumulation of Ub chains of different topology, indicating that any ubiquitin linkage type could serve as a degradation signal for autophagy (Riley et al., 2010).

1.2.6 ATG5

The discovery of ATG5 protein based on yeast studies. The mammalian homologue of the protein characterized as an essential component of the autophagy pathway due to its involvement in autophagosomal membrane formation. It has been also identified that rather than membrane formation, calpain-cleaved short fragment of ATG5 implicated in non-autophagic but pro-apoptotic functions suggesting that ATG5 is a key regulator between autophagy and apoptosis in the regulation of cell fate (Codogno and Meijer, 2006; Yousefi et al., 2006). ATG5, a core autophagy protein, involves five β -sheets and two α -helices structurally. ATG5 is 275 amino acid long and composed of Ubiquitin like domain 1 (Ub A) and 2 (Ub B), helix rich domain (HR) and N-terminal alpha helix domain (Matsushita et al., 2007) (shown in Figure 1.2.6 1). The involvement of ATG5 in autophagy pathway is strongly associated with its non-covalent binding to another autophagy protein, ATG12 at K130 residue of ATG5. This ATG5-ATG12 complex is further bound to ATG16L through N-terminal region of ATG5 (Ohsumi and Mizushima, 2004).

Not only the ATG12 and ATG16 proteins, but also other autophagy proteins identified as ATG5 partners in the regulation of autophagy. For example, selective autophagy receptor proteins OPTN (Bansal et al., 2018) and p62 (Fracchiolla et al., 2016), LC3 and TECPR1 (Behrends et al., 2010) pointing out that, ATG5 plays a central role due to its involvement in different stages of autophagy process.

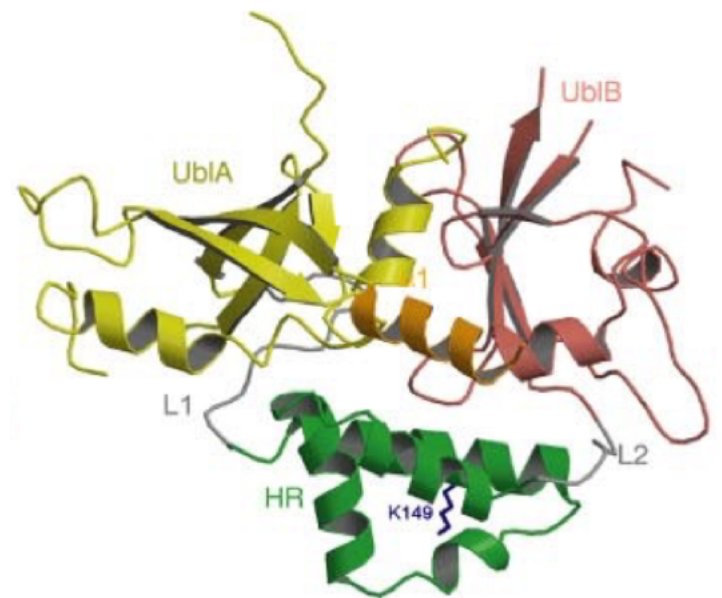


Figure 1.2.6 1: Structural view of ATG5 protein (retrieved from (Matsushita et al., 2007) and modified).

Various knockout and knockdown studies in both *in vitro* and *in vivo* showed that ATG5 deficiency resulted in physiological and neurological defects further supported the essential role of ATG5 cellular and organismal homeostasis. ATG5 protein is one of the key protein through direct interaction regulating various cellular processes as well as involving different stages of autophagy by interacting various other autophagy proteins. Table 1.2.6 1 summarizes the identified interaction partners of ATG5 by using various techniques ranging from yeast-two-hybrid to MS.

Table 1.2.6 1: Reported ATG5 interactors.

Interactor	Experimental System	Reference
ATG12	Affinity Capture-MS	(Ewing et al., 2007)
ATG12	Affinity Capture-MS	(Behrends et al., 2010)
ATG12	Affinity Capture-MS	(Behrends et al., 2010)
ATG12	Affinity Capture-MS	(Chen et al., 2012)
ATG16L1	Affinity Capture-MS	(Behrends et al., 2010)
ATG16L1	Affinity Capture-MS	(Behrends et al., 2010)
ATG16L1	Affinity Capture-MS	(Chen et al., 2012)
ATG16L1	Co-purification	(Chen et al., 2012)
ATG16L1	Affinity Capture-Western	(Ravikumar et al., 2010)
ATG16L1	Reconstituted Complex	(Itoh et al., 2008)
ATG16L1	Co-fractionation	(Kristensen et al., 2012)
ATG16L1	Affinity Capture-MS	(Gammoh et al., 2013)
ATG16L1	Co-crystal Structure	(Otomo et al., 2013)
ATG16L1	Co-fractionation	(Wan et al., 2015)
ATG16L1	Co-crystal Structure	(Kim et al., 2015)
ATG16L1	Two-hybrid	(Kim et al., 2015)
ATG16L1	Reconstituted Complex	(Kim et al., 2015)
ATG3	Affinity Capture-MS	(Behrends et al., 2010)
ATG3	Reconstituted Complex	(Qiu et al., 2013)
ATG3	Affinity Capture-MS	(Huttlin et al., 2017)
BCL10	Affinity Capture-Western	(Paul et al., 2012)
BCL2L1	Affinity Capture-Western	(Yousefi et al., 2006)
BSN	Affinity Capture-Western	(Okerlund et al., 2018)
CALCOCO2	Reconstituted Complex	(Fracchiolla et al., 2016)
CAPN1	Biochemical Activity	(Yousefi et al., 2006)
CAPN2	Biochemical Activity	(Yousefi et al., 2006)
CAV1	Affinity Capture-Western	(Chen et al., 2014)
CAV1	Affinity Capture-Western	(Chen et al., 2014)
CCHCR1	Two-hybrid	(Rolland et al., 2014)
ELAVL1	Affinity Capture-RNA	(Abdelmohsen et al., 2009)
EXOC4	Affinity Capture-Western	(Bodemann et al., 2011)
FADD	Reconstituted Complex	(Pyo et al., 2005)
FADD	Affinity Capture-Western	(Pyo et al., 2005)
FADD	Co-localization	(Pyo et al., 2005)
GNBL2	Co-localization	(Erbil et al., 2016)
GNBL2	Affinity Capture-Western	(Erbil et al., 2016)
GNBL2	Affinity Capture-MS	(Erbil et al., 2016)
GNBL2	Two-hybrid	(Erbil et al., 2016)
HTT	Affinity Capture-Western	(Filimonenko et al., 2010)

IKBIP	Affinity Capture-MS	(Huttlin et al., 2017)
IMPDH2	Affinity Capture-MS	(Ewing et al., 2007)
KEAP1	Two-hybrid	(Rolland et al., 2014)
MAP1LC3B	Affinity Capture-MS	(Behrends et al., 2010)
MAP1LC3C	Affinity Capture-MS	(Behrends et al., 2010)
MEOX2	Two-hybrid	(Rolland et al., 2014)
OPTN	Reconstituted Complex	(Fracchiolla et al., 2016)
OPTN	Affinity Capture-Western	(Bansal et al., 2018)
OPTN	Reconstituted Complex	(Bansal et al., 2018)
RB1CC1	Affinity Capture-Western	(Gammoh et al., 2013)
SIRT1	Affinity Capture-Western	(Lee et al., 2008)
SQSTM1	Reconstituted Complex	(Fracchiolla et al., 2016)
SQSTM1	Affinity Capture-Western	(Fracchiolla et al., 2016)
TAB2	Co-localization	(Takaesu et al., 2012)
TAB3	Co-localization	(Takaesu et al., 2012)
TECPR1	Affinity Capture-MS	(Behrends et al., 2010)
TECPR1	Affinity Capture-MS	(Behrends et al., 2010)
TECPR1	Affinity Capture-MS	(Chen et al., 2012)
TECPR1	Affinity Capture-MS	(Chen et al., 2012)
TECPR1	Affinity Capture-Western	(Chen et al., 2012)
TECPR1	Affinity Capture-Western	(Chen et al., 2012)
TECPR1	Co-localization	(Chen et al., 2012)
TECPR1	Co-purification	(Chen et al., 2012)
TECPR1	Co-crystal Structure	(Kim et al., 2015)
TECPR1	Two-hybrid	(Kim et al., 2015)
TECPR1	Reconstituted Complex	(Kim et al., 2015)
TEKT4	Two-hybrid	(Rolland et al., 2014)
TKT	Affinity Capture-MS	(Behrends et al., 2010)
VCP	Two-hybrid	(Rolland et al., 2014)
WDFY3	Affinity Capture-Western	(Filimonenko et al., 2010)
WDFY3	Reconstituted Complex	(Filimonenko et al., 2010)
WIPI2	Affinity Capture-Western	(Dooley et al., 2014)
WIPI2	Affinity Capture-MS	(Huttlin et al., 2015)
WIPI2	Affinity Capture-MS	(Huttlin et al., 2017)
XPO1	Affinity Capture-MS	(Kırlı et al., 2015)

The network of ATG5 and its reported interactors underlines that ATG5 has a key position in the hearth of autophagy regulation by direct interaction with OPTN, p62,

1.3 THE UPS – AUTOPHAGY CONNECTION

The ubiquitin-proteasome system and autophagy are major and evolutionarily conserved intracellular catabolic pathways and recycling systems from yeast to man. The molecular details behind the two systems revealed that their mode of actions are not interdependent. However, recent studies also showed that there are identified several direct and indirect connections and crosstalks between the two degradative systems. Mitophagy is a good biological example in interdependency between the two system is obvious and best studied. Rather than that, there are other various examples of overlap and communication in cells. In the following chapter, I will explain these connections and communications and summarize the molecular fine-details behind them.

1.3.1. Compensatory Mechanisms Between the UPS and Autophagy

Initial observations about the understanding of possible links between the ubiquitin-proteasome system and autophagy showed that inhibition of one system allowed the compensatory upregulation for the other degradative system. By this way, cellular homeostasis is maintained. Accumulation of potentially toxic cellular materials following inhibition of one degradative system required to be removed by the other system. In this section, I will compile the literature and give examples where functional compensatory mechanisms are observed (represented in Figure 1.3.1).

Proteasomal activity blockage by utilization of various chemicals, including MG132, bortezomib and lactacystine (Fan et al., 2018; Selimovic et al., 2013; Wu et al., 2008) or by genetic approaches (Demishtein et al., 2017) enhanced cellular autophagy levels. For instance, bortezomib-induced proteasome activity inhibition resulted an

upregulation of several autophagy genes such as ATG5 and ATG7, and therefore induced autophagy in various different cell types: prostate cancer cells and mouse embryonic fibroblasts (MEFs). Interestingly, phosphorylation of eukaryotic translation initiation factor-2 alpha (eIF2 α) was suggested as a key modification in which autophagy gene upregulation relies on an ER stress-dependent pathway (Zhu et al., 2010).

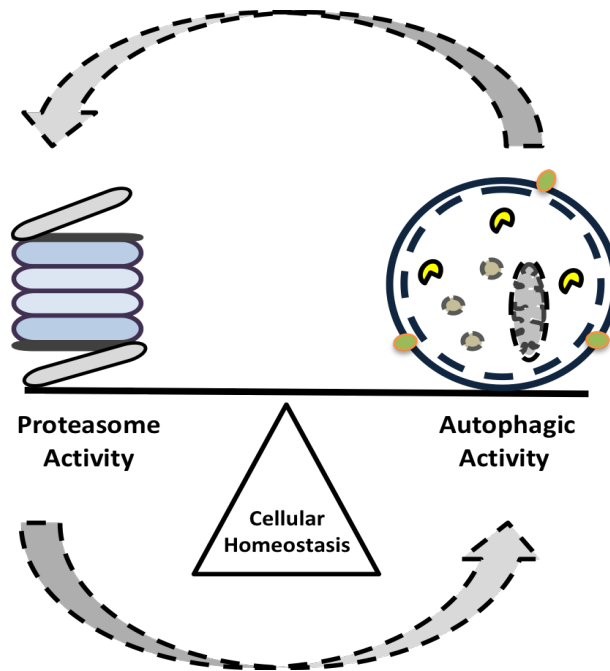


Figure 1.3.1: Schematic representation of compensatory actions between the UPS and autophagy.

In the same direction by the others, proteasome inhibition regulated autophagy gene expression was linked Nrf1-dependent and -independent pathways as an alternative for the ER-stress dependent pathways. Inhibition of proteasome activity was correlated with the p62 and GABARAPL1 protein upregulation prior to autophagy activation in SH-SY5Y neuroblastoma cells through Nrf1-dependent and -independent pathways (Sha et al., 2018). By using MG132 as a proteasome inhibitor, in human SHG-44 glioma cells, decreased cell proliferation, cell cycle arrest at G2/M phase and enhanced autophagic activity through increased Beclin1 and LC3 protein levels were observed (Ge et al., 2009).

Proteasomal activity impairment was also associated with AMPK activation-mediated enhanced autophagic activity. There are accumulating evidence supporting that AMPK and mTORC1 are the two sensors for proteasomal activity loss. In various cell types including, immun macrophages, skin epithelial and endothelial cells, chemical-stimulated proteasome inhibition resulted in AMPK activation (Jiang et al., 2015b; Xu et al., 2012). AMPK activity is controlled by the upstream modulators glycogen synthase kinase-3 β (GSK-3 β) and CaMKK β in cancer cells. Loss of proteasome activity in some cancer cells resulted deregulation of GSK-3 β activity and subsequently upregulation of AMPK activity and autophagy (Sun et al., 2016). On the other hand, Torin-1- or rapamycin-mediated inhibition of mTORC1 stimulated long lived protein degradation through activation of both UPS and autophagy (Zhao et al., 2015; Zhao and Goldberg, 2016). As another example, in retina pigment epithelial cells, lactasistin and epoxomicin-induced proteasome inhibition resulted in blockage of the AKT-mTOR pathway and autophagy induction (Tang et al., 2014).

Conversely, decrease in cellular autophagy levels associated with the enhanced proteasome activity. By utilizing inhibitors and genetical modification of ATG genes, cellular autophagy level is restricted in colon cancer cells. This attenuated autophagic activity enhanced protein expression of proteasomal subunits, including one of the catalytic subunit, PSMB5 and consequently upregulated proteasome activity (Wang et al., 2013). In line with this observation, 3-MA-stimulated inhibition of autophagy resulted in enhanced chymotrypsin-like activity of proteasomes in cultured neonatal rat ventricular myocytes (Tannous et al., 2008). Proteasomes can be also selective degradation targets for autophagic machinery. Autophagic degradation of proteasomes is called proteophagy and will be explained in detail in the following sections. Autophagy-inhibition regulated gain in the proteasomal peptidase activity could be linked to the accumulation of proteasomes (Cuervo et al., 1995; Marshall et al., 2015). On the other hand, in several different cases, following autophagy impairment linked to the accumulation of ubiquitylated substrates. In several independent work, it was observed that ubiquitylated materials were accumulated in especially brain and the liver of the ATG5 or ATG7 knockout mice (Hara et al., 2006; Komatsu et al., 2005, 2006; Riley et al., 2010). Supporting data also came from other experimental animal models such as *Drosophila*

(Nezis et al., 2008). In the similar direction, siRNA-mediated knockdown of ATG7 and ATG12 in HeLa cells resulted in the accumulation of ubiquitylated UPS substrates such as p53 and β -catenine as an indication of UPS impairment (Korolchuk et al., 2009a).

Due to being degradation targets of ubiquitylated substrates for both the UPS and autophagy, ubiquitylation is a key and common component by directing modified substrates to the destined degradation system and therefore granted to the crosstalk between the two system (Dikic, 2017; Korolchuk et al., 2010). Based on this hypothesis, the type of the polyubiquitin chains are the key determinants. For instance, substrates that are conjugated with the K48-linked polyubiquitin chains are predominantly degraded by the proteasomes. In contrast, substrates that are conjugated to K63-linked polyubiquitin chains are degraded by the autophagic membranes. As another ubiquitin associated link between the UPS and autophagy is p62 protein due to its binding capacity to ubiquitylated targets. P62 protein can bind to the both K48- and K63-linked polyubiquitin linkages, yet p62 exhibits higher preference for K63-linked polyubiquitin chains is (Long et al., 2008; Tan et al., 2008; Wooten et al., 2008). Giving the importance of dual binding capacity of p62, it has a potent inhibitory effects on proteasomes. In addition to p62, another key determinant for the faith of the protein is p97/VCP which is involved in UPS and ERAD-related pathways. P97/VCP overexpression deregulated p62 binding to the ubiquitylated materials suggesting that the two proteins are in competition for ubiquitin binding. From another perspective, autophagy inhibition resulted in p62 accumulation and sequestration of the proteins that are p97/VCP targets (Korolchuk et al., 2009a, 2009b).

To conclude, if there is a defect in one of the two degradation mechanisms, the other system is upregulated in order to compensate failure in the elimination of ubiquitylated protein substrates. As explained above, the success rate of compensatory mechanism mostly variable from one cell type to the other as well as cellular conditions.

1.3.2 Interplay Between the UPS-Autophagy in the Selective Clearance of Cytosolic Proteins

Folding and unfolding cycle and 3 dimensional structure of the proteins are the main characteristics for the function of proteins. Newly synthesized proteins with the help of chaperone and co-chaperone proteins, including Hsp40, Hsp70, Hsp90 and Cdc37 become folded. Several stress sources such as heat shock, organellar stress, oxidative stress might result in the accumulation of unfolded/misfolded proteins. These kind of folding problems were linked to several disease-related mutations in the proteins. Hsp40-Hsp70 are responsible for the control of the protein folding at early stages and in contrast Hsp90 has role in later steps. Any potential defects in refolding process of the proteins cause dysfunctional or malfunctioning, therefore potentially toxic aggregates, responsible for the upregulation of stress-related pathways, including cell death. These toxic protein accumulations are controlled by the active removal processes.

Chaperone proteins recognize misfolded or unfolded proteins and direct them proteasomal degradation if they exhibit soluble characteristic feature. These chaperone proteins can also interact with E3 ligases to regulated ubiquitylation pattern of the aggregates. For example Hsp70 and Hsp90 can bind CHIP and stimulates formation of K48-linked polyubiquitin linkages onto unfolded or misfolded proteins. Additionally, BAG family proteins are also in the decision system for degradation of the proteins with folding problems. BAG1 protein shown to bind Hsp70 chaperone complex and stimulates proteasomal degradation of the targets.

On the other hand, to be become removed, insoluble and/or aggregate-prone proteins form aggresomes in cells. There have been identified several E3 ligases including CHIP, Parkin, HRD1 and TRIM50 (Mao et al., 2017; Mishra et al., 2009; Olzmann et al., 2007; Zhang and Qian, 2011) involved in the ubiquitylation cascade, and then ubiquitin-modified aggregated proteins are transported to microtubule organizing centers (MTOC) in order to form aggresomes (Johnston et al., 1998; Kopito, 2000). Formation of aggresome is complex and regulated process. HDAC6 protein was shown to be one of the key regulator of aggresome formation (Matthias et al., 2008). HDAC6 can bind directly to K63-linked polyubiquitin linkages and at the same time dynein proteins (Olzmann et al., 2007). By bridging ubiquitylated aggregates with dynein, HDAC6 stimulates dynein-

mediated transport of ubiquitinated substrates to the aggresome, and therefore critical for the clearance of aggresomes by autophagy (Iwata et al., 2005; Kawaguchi et al., 2003). HDAC6 has an important role in the autophagosome formation besides its role in in aggresome formation providing a link between K63-based ubiquitylated aggregates and dynein to facilitate dynein-mediated transport towards MTOC (Lee et al., 2010; Matthias et al., 2008; Olzmann et al., 2007). These autophagosomes contain ubiquitinated proteins, demonstrating a role for HDAC6 in the maturation of autophagosomes involved in selective autophagy of misfolded proteins. The role of HDAC6 in this process is to regulate the actin cytoskeleton (Lee et al., 2010; Yao, 2010) ISG15 has recently been shown to bind to HDAC6 and p62, and to promote degradation of aggregated proteins via autophagy (Nakashima et al., 2015).

Aggregation could also be important for function of a protein such as p62 which is found in almost all protein aggregates and continuously degraded by autophagy though direct interaction with LC3B (Ichimura et al., 2008; Lamark and Johansen, 2012). Through direct interaction with both ubiquitylated aggregates and LC3B, serve as autophagy receptor to facilitate autophagic clearance. ALFY (autophagy-linked FYVE protein), and NBR1 (neighbor of BRCA1 gene) similarly to p62, are general contents of protein inclusions and are believed to be there because they are involved in both their construction and their degradation by autophagy (Clausen et al., 2010; Filimonenko et al., 2010).

Alternatively, chaperone protein Hsp70 can cooperate with BAG3 and CHIP proteins for aggresome formation (Zhang and Qian, 2011). As in the case of HDAC6, BAG3 can binds to dynein provide transportation of substrates to aggresomes. But differentially, BAG3-dependent aggresome formation is dispensible for CHIP ligase activity. Because BAG3 does not require ubiquitylation of the substrates for their transportation (Gamerding et al., 2011; Zhang and Qian, 2011). On the other hand, BAG3-dependent system requires E3 ligases for autophagic clearance of aggresomes.

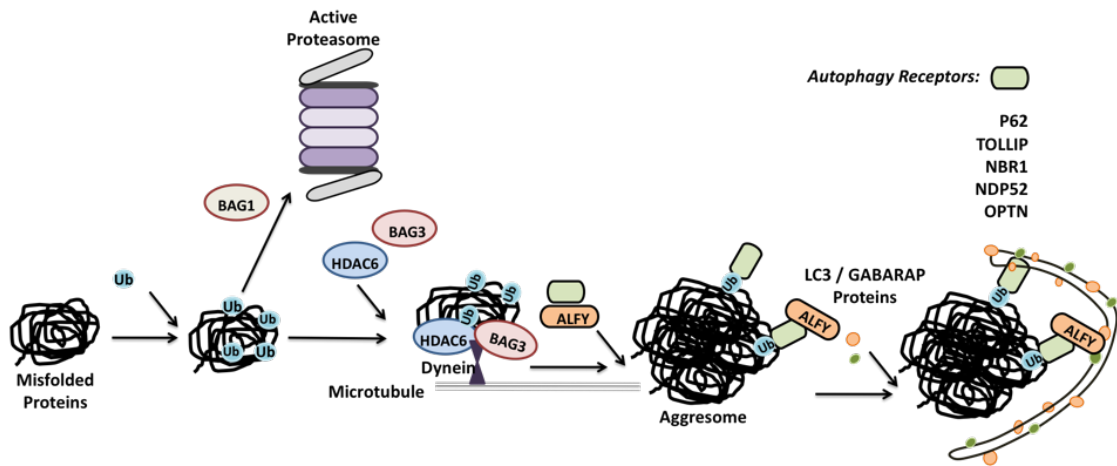


Figure 1.3.2 1: Interplay between the UPS and autophagy system against ubiquitylated misfolded proteins.

Recent findings about the molecular details of neurodegenerative diseases supplemented various examples showing the interplay between the UPS and autophagy in the removal of disease-causing abnormal proteins (Juenemann et al., 2013). One of the best examples is Huntington Disease (HD). Poly-glutamine expansions in a protein called Huntingtin (Htt) are the cause of the HD. These poly-glutamine expansions result in abnormal organization and aggregation of the Htt protein. Htt protein can be modified by both K48- or K63-linked polyubiquitin chains (Bhat et al., 2014). Therefore, based on its ubiquitylation pattern, both UPS and autophagy systems can eliminate mutant Htt in different conditions. For instance, K63-linked polyubiquitin decorated mutant Htt aggregates predominantly cleared by autophagy (Menzies et al., 2015; Renna et al., 2010). On the other hand, ectopic expression of K48-specific E3 ligase Ube3a, drives mutant proteins for proteasomal degradation. In line with this, organismal E3 ligase level is deregulated with age. Therefore the attenuated level of E3 ligases in older experimental conditions favors for autophagic removal through enhanced accumulation of K63-linked polyubiquitins. Another molecular switch in the same context between the UPS and autophagy requires CHIP stimulating proteasomal degradation (Bhat et al., 2014; Jana et al., 2005). Furthermore, as another the switch between the UPS and selective autophagy is the availability of the cellular free ubiquitin pool through both synthesis and recycling (Clague et al., 2015).

1.3.3 Degradation of Proteasomes or Autophagy Components as a Cross Control Mechanism

Along with this introduction part of the thesis, so far, UPS and autophagy were considered as independent, yet functionally complementary systems. However it is also possible that components of one system can be proteolytically degraded by the other system. For instance, there are a huge number of autophagy related proteins are regulated by the UPS in terms of stability, transcriptional regulation and function. On the other hand, autophagic membranes can engulf whole dysfunctional proteasomes spesifically. In this section, I will give examples about the cross control mechanisms that also contributes to the crosstalk and the interplay between the UPS and autophagy.

1.3.3.1 Control of the Proteasome Abundance by the Autophagy

Initial studies showed the localization of the proteasomes in lysosomes as an indication lysosome-associated degradation of proteasomes (Cuervo et al., 1995). Follow up studies in plant studies revealed that, 26S proteasomes can be degraded by lysosomal enzymes in the process of a specific form of selective autophagy, proteaphagy (Marshall et al., 2015). In plants, RPN10 protein was suggested as selective proteaphagy receptor for the recruitment of ATG8-associated membranes. However, RPN10 protein in yeast and mammalian cells did not recruit autophagic membranes. Instead of RPN10, Cue5 protein in the yeast and its human ortholog TOLLIP protein were able to recruit autophagic membranes therefore suggested as selective proteaphagy receptors (Lu et al., 2014). Additionally, p62 was also included in the proteaphagy receptor list (Cohen-kaplan et al., 2016). For instance, nutrient deprivation significantly enhanced ubiquitylation of 19S proteasome components, including RPN1, RPN10, RPN13, and stimulated their engulfment by autophagic membranes in a p62-dependent manner (Cohen-kaplan et al., 2016) (Please see Figure 1.3.3.1).

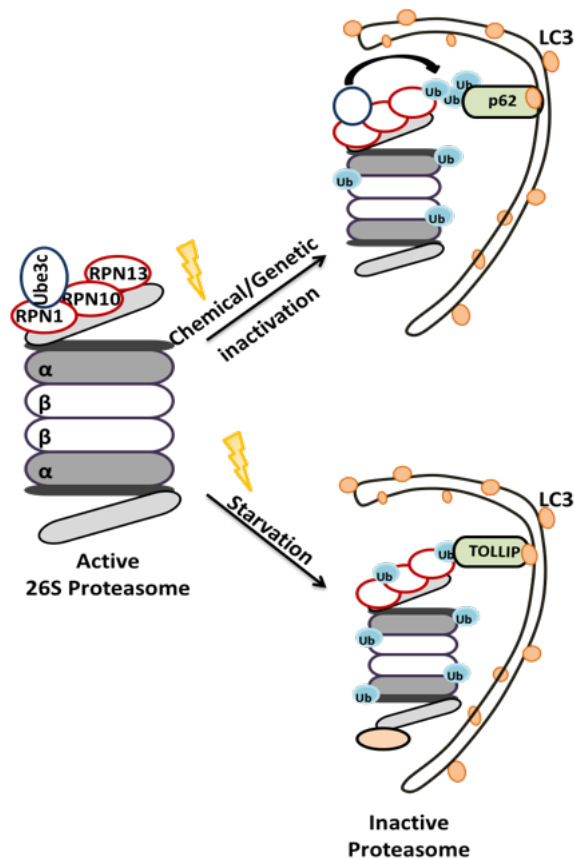


Figure 1.3.3.1: The schematic representation of how proteasomes are degraded selectively by autophagy.

These recent and critical findings highlight the importance of the autophagic degradation of proteasomes in order to control the cellular abundance of the proteasomes as well as proteasomal activities in cells.

1.3.3.2 Control of Autophagy Components by the UPS

Modulation of the half-life of some proteins in the autophagy pathway by the UPS serves as a mean to control cellular autophagic activity. For instance, LC3 protein was shown to be processed in a stepwise manner by the 20S proteasome, a process that was inhibited by p62 binding (Gao et al., 2010). E3 ligase NEDD4-mediated K11-linked ubiquitylation of BECN1 and prevented its binding to VPS34 and led to its degradation (Platta et al., 2012). Another E3 ligase, RNF216 ubiquitylated BECN1 through K48-linked chain

formation (Xu et al., 2014). BECN1 ubiquitylation resulted in autophagy blockage in both cases. Conversely, reversal of BECN1 ubiquitylation by the DUB protein USP19 stabilized the protein under starvation conditions and promoted autophagy (Jin et al., 2016). USP10 and USP13 as well as USP9X were characterized as other DUBs that regulated autophagy through control of BECN1 stability (Jin et al., 2016; Liu et al., 2011).

BECN1 is not the only autophagy protein that is targeted by the UPS in a controlled manner. G-protein-coupled receptor (GPCR) ligands and agonists were reported to regulate cellular ATG14L levels, and therefore autophagy, through ZBTB16-mediated ubiquitylation of the protein (Zhang et al., 2015b). In this system, serum starvation increased GSK3 β -mediated phosphorylation of ZBTB16, resulting in its degradation and subsequent stabilization of ATG14L and restoration of autophagy. AMBRA1 is another UPS-controlled autophagy protein. Cullin-4 was identified as a responsible E3 ligase for the ubiquitylation of AMBRA1 driving it for degradation under nutrient-rich conditions where autophagy should be inhibited. (Antonioli et al., 2014b). The PI3K complex subunit p85b is another example. Ubiquitylation of these signaling component by the E3 ligase SKP1 negatively controlled its cellular levels in order to stimulate autophagic activity (Kuchay et al., 2013).

Ubiquitylation of some autophagy proteins did not result in their immediate proteasomal degradation, yet provided an extra layer of control over the autophagy pathway. For instance, autophagy receptor OPTN was ubiquitylated as a target of the E3 ligase HACE1, and K48-linked ubiquitylation regulated the interaction of the protein with p62 (Liu et al., 2014). TRAF6, a central E3 ligase of the NF- κ B pathway, participated controlled ULK1 activity through K63-linked ubiquitylation. Under nutrient-rich conditions, mTOR phosphorylated AMBRA1 leading to its inactivation. When nutrients were limiting, mTOR inhibition resulted in AMBRA1 dephosphorylation, stimulating its interaction with TRAF6 to facilitate ULK1 K63-linked ubiquitylation (Nazio et al., 2013). Ubiquitylated ULK1 was stabilized the protein, dimerized and regulated its kinase function. Another ubiquitin-dependent regulation mechanism involves AMBRA1-Cullin-5 interaction in the regulation of mTOR complex component DEPTOR. Above-mentioned AMBRA1-Cullin-4 complex dissociated under autophagy-inducing conditions. Upon autophagy stimulation, AMBRA1 dissociated from Cullin-4 and allowing AMBRA1 to bind another E3 ligase, Cullin-5. This newly formed complex was

shown to stabilize DEPTOR and induce mTOR inactivation, providing a negative feedback loop in the control of autophagy (Antonioli et al., 2014b). In another study, TLR4 signaling triggered autophagy through BECN1 ubiquitylation and stabilization. TLR4-associated TRAF6 protein was identified as the E3 ligase responsible for K63-linked ubiquitylation of BECN1 at its BH3 domain. This modification blocked inhibitory BCL-2 binding to the BH3 domain, activated autophagy (Shi and Kehrl, 2010). On the other hand, the deubiquitynating enzyme A20 reversed TRAF6-mediated ubiquitylation of BECN1, resulting in autophagy inhibition (Shi and Kehrl, 2010). Another K63-linked ubiquitylation event on BECN1 was promoted by AMBRA1 and increased BECN1/VPS34 association. In the same context, the WASH protein interacted with BECN1 and suppressed AMBRA1-mediated BECN1 ubiquitylation, and suppressed autophagy (Xia et al., 2013). LC3 and p62 were also subjected to regulatory ubiquitylation. E3 ligase NEDD4 was identified as the E3 ligase in these reactions. NEDD4 was reported to interact with LC3 (Sun et al., 2017) and p62 (Lin et al., 2017). In this system, NEDD4 was essential for stress-induced autophagy activation. LC3 binding to NEDD4 stimulated its ubiquitin ligase activity on the p62 protein (Sun et al., 2017). NEDD4 deficient cells exhibited aberrant p62 containing inclusions, indicating the defect in aggresome clearance (Lin et al., 2017).

1.3.4 Transcriptional Mechanisms Connecting the UPS and Autophagy

Several transcription factors that are regulated by the UPS, including p53, NF κ B, HIF1 α and FOXO, have been implicated in the control of autophagy. In general, these factors were directly activating transcription of key autophagy genes under stress conditions. Some autophagy proteins such as LC3 are consumed in the lysosome following delivery, and during prolonged stress, cellular levels of these proteins are sustained by mechanisms, including transcription. On the other hand, regulation of the transcriptional activity NRF2 involves a special crosstalk between the two systems. In this section, we will summarize molecular details of transcription regulation by the UPS and autophagy.

P53 is one of the well-known transcriptional regulators that has a dual role in autophagy depending on its intracellular localization. P53, a guardian of the genome, was

introduced as a regulator of autophagy. In the absence of stress, cellular active p53 levels are controlled by the E3 ligase HDM2/MDM2 and the UPS. Under DNA damage inducing stress conditions, p14/p19/ARF protein binds, sequesters and inactivates HDM2/MDM2, stabilizing p53. Accumulating p53 protein activates transcription of several stress- and death-related genes, including autophagy-related genes *PRKAB1*, *PRKAB2*, *TSC2*, *ATG2*, *ATG4*, *ATG7*, *ATG10*, *ULK1*, *BNIP3*, *DRAM1* and *SESN2* (Budanov and Karin, 2009; Crighton et al., 2006; Feng et al., 2007; Kenzelmann Broz et al., 2013). On the other hand, a cytosolic form of p53 led to the inhibition of AMPK and activation of the mTOR pathway. In this context, non-genotoxic stress by autophagy-inducing agents such as rapamycin, tunicamycin and nutrient deprivation favored HMD2/MDM2-dependent p53 degradation by the UPS (Tasdemir et al., 2008a, 2008b). Interestingly, HMD2/MDM2 stability and activity were also regulated by E3 ligases SMURF1/2 which in turn determined the stability of p53. SMURF1/2-mediated ubiquitylation increased MDM2-MDMX heterodimerization, decreasing autoubiquitylation of MDM2, therefore stabilized the protein (Nie et al., 2010). Additionally, another E3 ligase, NEDD4-1 was shown to control MDM2 stability and p53 activation (Xu et al., 2015). In addition to MDM2, another E3 ligase, PIRH2, was able to ubiquitylate p53 to control its cellular stability (Shloush et al., 2011).

NF- κ B is a well studied transcriptional regulator of autophagy. As a result of its association with I κ B, NF- κ B is found in an inactive state in the cytosol. In response to agonists, I κ α and I κ β -mediated phosphorylation of I κ B induced its ubiquitylation and subsequent degradation by the UPS. Following I κ B degradation, NF- κ B is free to migrate to the nucleus of the cell and induces transcription of target genes, including Beclin1 and p62 (Copetti et al., 2009; Ling et al., 2012). Regulation of NF- κ B by external signals involve phosphorylation of I κ B by upstream kinases of the IKK complex (IKK α , IKK β , IKK γ /NEMO). Phosphorylated I κ B recruits the E3 ligase SCF- β TRCP, leads to degradation and allows the NF κ B activation (Orian et al., 2000). Another level of regulation involves TNF- α receptor. Binding of TNF- α to TNFR1 leads to the recruitment of TRADD and RIPK1 to the receptor, promoting TRAF- and cIAP-mediated K63 and/or K11 linked ubiquitylation of the RIPK1. Ubiquitylated RIPK1 recruits NEMO and TAB-TAK1 complex for IKK activation. Additionally, RIPK1 might also be modified with K48-linked poly-ubiquitin chains by A20 sending it for proteasomal degradation (Kravtsova-ivantsiv et al., 2015).

However, TNF- α -induced NF- κ B activation was reported to inhibit autophagy (Djavaheri-Mergny et al., 2006). Additionally, TNF- α -induced activation of IKK α or IKK β led to the phosphorylation TSC1/2 and activated mTOR and led to similar outcome (Dan and Baldwin, 2008; Lee et al., 2007). Furthermore, RIPK1 was responsible for suppression of autophagy and its silencing activated autophagy under both basal and stress condition (Yonekawa et al., 2015). RIPK1 was reported to be a target of p62-mediated selective autophagy (Goodall et al., 2016). Moreover, autophagy was responsible for the degradation of NF- κ B activator NIK and IKK complex subunits indicating the presence of a tight cross-regulation of the NF- κ B pathway by the UPS and autophagy (Qing et al., 2007).

Another transcription factor that was controlling the autophagic outcome was HIF1 α . Hypoxia induced HIF1 α transcriptionally regulated various hypoxia response genes, including *GLUT1* (Chen et al., 2001), *NOX2* (Yuan et al., 2011), and *PDK1* (Kim et al., 2006) as well as autophagy genes, including *BNIP3*, *BNIP3L*, *ATG5* and *BECN1* to stimulate autophagy, mitophagy and pexophagy (Bellot et al., 2009; Walter et al., 2014; Zhang et al., 2008). HIF1 α itself was regulated in a UPS-dependent manner. Under normoxia, specific prolyl hydroxylases (PHDs) hydroxylated HIF1 α (Jaakkola et al., 2014). Hydroxylation functions as recognition signal for UbcH5, an E2 enzyme and von Hippel-Lindau protein (the pVHL), E3 ligase complex containing Elongin B and C, Cullin-2, and Rbx1 allowing K48 linked ubiquitination of HIF1 α and its proteasomal degradation (Ohh et al., 2000). In contrast, during hypoxia, PHDs are inhibited and HIF1 α stabilized. SCF E3 ligase complex was also shown to play a role in HIF1 α stability in response to GSK3 β -mediated phosphorylation of the protein (Cassavaugh et al., 2011; Flugel et al., 2012a). Another E3 ligase for HIF1 α which facilitates HIF1 α degradation is HAF (also known as SART1₈₀₀). Unlike pVHL, HAF-mediated ubiquitylation of HIF1 α was not depend on the oxygen levels, suggesting an alternative proteasome-associated HIF1 α regulation mechanism (Koh et al., 2008). Stability of PHD proteins were also controlled by the UPS. For example, SIAH1/2 was shown to direct PHDs for proteasomal degradation under hypoxic stress (Nakayama et al., 2004). Moreover several DUBs were implicated in HIF1 α regulation, including USP20 (Li et al., 2002b), USP28 (Flugel et al., 2012b) and USP33 (Li et al., 2002a).

FOXO family of transcription factors (FOXOs) were associated with various cellular pathways, including autophagy (Zhao et al., 2007). The activity of FOXOs are regulated by their phosphorylation status and following activation, FOXOs translocate to the nucleus and trigger the expression of a number of genes associated with different stages of the autophagy pathway, including *ATG4*, *ATG12*, *BECN1*, *ULK1*, *PIK3C3*, *MAP1LC3* and *GABARAP* (Mammucari et al., 2007; Sanchez et al., 2012; Zhao et al., 2007). There are several connections between FOXOs and autophagy. Activation of the AKT pathway inhibited FOXO3 activity, led to a decrease in LC3 and BNIP3 expression, therefore blocked autophagy (Mammucari et al., 2007; Stitt et al., 2004). On the other hand, AMPK activation led to the phosphorylation of FOXO3a and ULK1, inducing *MAP1LC3*, *GABARAP* and *BECN1* expression and subsequent autophagy activation (Sanchez et al., 2012). Another FOXO family protein FOXK1/2, a negative regulator of FOXO3, was associated with a decrease in autophagy by removing Sin3A/HDAC complex from histone H4 to diminish its acetylation. In this context, nuclear localization of FOXK1/2 was mTOR-dependent and showed an inhibitory effect on autophagy gene expression under basal conditions (Bowman et al., 2014). Moreover, JNK deficiency in neurons increased autophagic activity through FOXO1 mediated BNIP3 upregulation and BECN1 disassociation from BCL-XL (Xu et al., 2011). Another example of a link between FOXOs autophagy involved ATG14. Liver specific knockout of FOXOs resulted in the downregulation of ATG14 and this event was associated with high levels of triglycerides in the liver and serum of mice (Xiong et al., 2012). Additionally, GATA-1 shown to directly regulate FOXO3-mediated activation of LC3 genes to facilitate autophagic activity (Kang et al., 2012).

Activation of various protein kinases, including AKT, IKK and ERK, phosphorylates FOXO proteins and result in their ubiquitylation by E3 ligases, suggesting a critical role of the UPS in the regulation of FOXOs activity (Huang and Tindall, 2011). AKT-mediated phosphorylation of FOXO1 provided a signal for its recognition by the SKP protein, an SCF E3 ligase complex component, followed by FOXO1 ubiquitylation and degradation (Huang et al., 2005). COP1 was also identified as an E3 ligase that regulates FOXO protein stability. COP1 ubiquitylates FOXO1 and promotes its proteasomal degradation. This type of regulation might be important in the glucose metabolism of hepatocytes, and possibly in autophagy modulation under this conditions (Kato et al., 2008). Another FOXO regulating E3 ligase is MDM2 that is specifically

responsible for FOXO1 and FOXO3A ubiquitylation and degradation. MDM2-mediated ubiquitylation was activated by the phosphorylation of FOXOs by AKT. Due to its role in p53 regulation, MDM2 could be part of a more complex regulatory mechanism which could link the UPS, transcriptional regulation and autophagic activity (Fu et al., 2009).

Oxidative stress is also a signal for HIF1 α stabilization. Mitophagy activation under these conditions ensures a decrease in the mitochondrial mass, resulting in the elimination of ROS-producing mitochondria and limiting the oxidative burden. On the other hand, NRF2-KEAP1-P62 pathway was defined as another major oxidative stress response mechanism involving an interplay between the UPS and autophagy. NRF2 is a transcription factor and when activated upregulates antioxidant and metabolic enzymes, including *TXNRD1* (Suvorova et al., 2009), *HMOX1* (Reichard et al., 2007), *GPX2* (Banning et al., 2005a), *GBE1*, *PHK1* (Banning et al., 2005b), and downregulates proinflammation-related genes such as *IL6*, *IL1B* (Kobayashi et al., 2016). KEAP1 is an adaptor protein of the E3 ligase Cullin-3 and plays a role in substrate recognition. Under normal conditions, transcription factor NRF2 is found in association with KEAP1-Cullin-3 E3 ligase complex, that catalyzes its ubiquitylation and rendering it a substrate for proteasomal elimination. P62 was shown to compete with NRF2 for KEAP1 binding, following which NRF2 migrated to the nucleus and accumulated therein, activating cytoprotective and stress-related genes (Kobayashi et al., 2004) (Komatsu et al., 2010). When cells experience oxidative stress, KEAP1-Cullin-3 complex loses affinity for NRF2, NRF2 migrates to the nucleus and accumulates therein, activating cytoprotective and stress-related genes (Kobayashi et al., 2004). P62 binding to KEAP1 promoted its elimination by selective autophagy (Ishimura et al., 2014). Additionally, the NRF2-KEAP1 pathway provides a positive feedback loop for autophagy. P62 was characterized as a direct transcriptional target of activated NRF2 (Jain et al., 2010). KEAP1 regulation by p62 was modulated by the E3 ligase TRIM21. NRF2 activation was negatively affected by TRIM21-mediated K63 linked ubiquitylation of p62 (Pan et al., 2016).

1.3.5 Crosstalk and Co-regulatory Mechanisms

The most prominent link between the UPS and autophagy is the capacity of both system to degrade ubiquitylated substrates. Therefore when one system is impaired, the other degradative system to some extent eliminates the target in order to prevent potential toxicity caused by aggregated proteins (Fuertes et al., 2003; Long et al., 2008). These findings suggest that there is an indirect connection in the two degradation systems in terms of regulating cellular ubiquitin levels and recycling. This crosstalk and co-regulation mechanisms involves mostly the selective autophagy processes including, aggrephagy, xenophagy, mitophagy, pexophagy and ribophagy which will be introduced in the following sections.

1.3.5.1 Xenophagy: Removal of Intracellular Invaders

Autophagy was shown to target a range of pathogens, including group *A. streptococcus*, *Mycobacterium tuberculosis* and *Shigella flexneri* (Gutierrez et al., 2004; Kirkegaard et al., 2004; Ogawa et al., 2005). Identification and targeting of pathogens to autophagy was termed xenophagy. Elimination of invaginated bacteria are ubiquitylated and subsequently degraded by autophagy as an innate immune response. The mechanism by which cells target pathogens to autophagy is analogous to other types of selective autophagy, namely tagging the cargo with modifiers such as ubiquitin (but not exclusively), followed by their recognition by autophagic receptors. Both K63- and K48-linked Ub chains and seven M11-linked mono-ubiquitins were shown to mediate the recognition of different pathogens, but interestingly independent from ATG5 (Collins et al., 2009; Randow and Youle, 2014). Several identified selective autophagic receptors were also implicated in xenophagy, such as p62, OPTN and NDP52 (Thurston, 2009; Wild et al., 2011; Zheng et al., 2009). Eventhough there are identified various E3 ligases involved in labelling intracellular pathogens with ubiquitin chains such as parkin ubiquitylates *Mycobacterium tuberculosis* and Lrsm1 (leucine-rich repeat and sterile alpha motif 10 Trends containing 1) ubiquitylates *Salmonella enterica* (Huett et al., 2012; Manzanillo et al., 2013), however there is no identified protein target for ubiquitylation on pathogens.

Recent studies showed that, bacterial outer membrane-associated and integral outer membrane proteins were targets of ubiquitylation (Fiskin et al., 2016). E3 ligases such as Parkin, RNF166, ARIH1, HOIP and LRSAM1 were implicated in the ubiquitylation reactions prior to autophagic removal of pathogens (Franco et al., 2017; Heath et al., 2016; Huett et al., 2012; Lobato-Márquez and Mostowy, 2017; Manzanillo et al., 2013). For instance, Mycobacterium could be decorated with both K48- and K63-linked ubiquitin chains and the E3 ligase Parkin shown to be responsible for the K63-linked ubiquitylation on Mycobacterium (Collins et al., 2009; Manzanillo et al., 2013).

Alternatively, intracellular *Salmonella* Typhimurium shown to be coated with directly ubiquitin molecules from its endosome-free parts. Linear M1-linked ubiquitin chains formation by the action of LUBAC complex E3 ligase, HOIP on these ubiquitins contributed to the autophagic removal of the pathogens (Noad et al., 2017). p62, OPTN, NDP52 and NBR1 were included in the xenophagy field as selective xenophagy receptor proteins (Thurston, 2009; Wild et al., 2011; Zheng et al., 2009). In addition to the need of selective autophagy receptor utilization, it has also shown that Salmonella carrying endosomes are ubiquitylated which in turn involved in interaction of Ub with one of the autophagy core complex ATG5-12-16L through direct binding with ATG16L (Fujita et al., 2013). Endogenous nucleotide 8-nitroguanosine 3'-5'-cyclic monophosphate (8-nitro-cGMP) has been reported to induce xenophagy. 8-nitro-cGMP promotes S-guanylation of bacterial proteins and subsequently triggers ubiquitylation of those proteins and autophagic removal of ubiquitin-labelled bacteria (Ito et al., 2013). Glycans that were exposed upon disruption of endosomes were a target of Galectin-8 in the cytosol. Direct binding of the galectin to glycans on one side and to the autophagy receptor NDP52 on the other side provided a bridge between autophagosomes and bacteria carrying endosomes (Li et al., 2013). In addition to NDP52, autophagy receptors OPTN and p62 were also reported to bind pathogen- and/or endosome-associated ubiquitin, and direct them to autophagic membranes (Richter et al., 2016; Wild et al., 2011) (Schematic representation is shown in Figure 1.3.5.1).

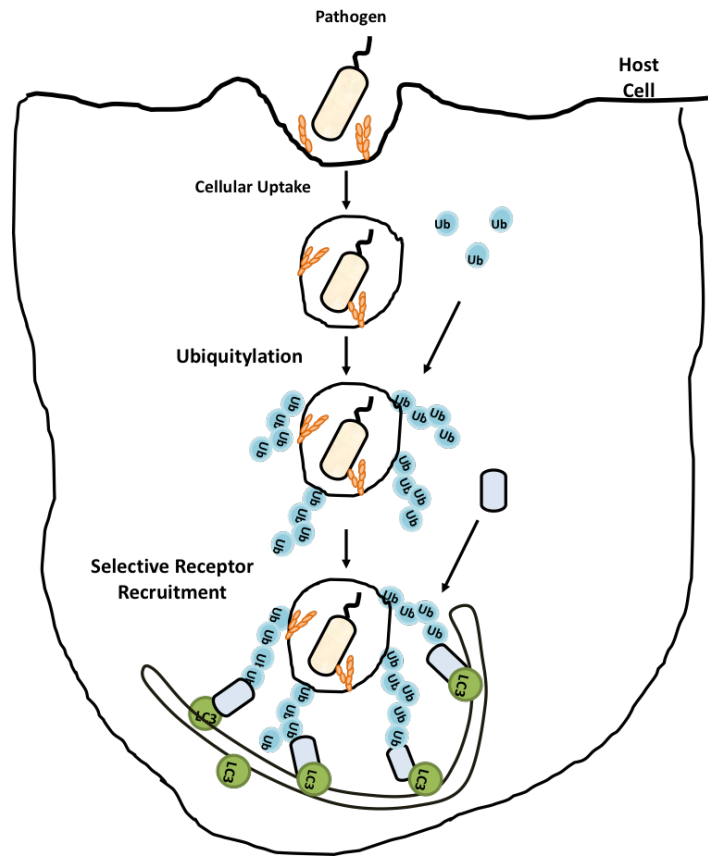


Figure 1.3.5.1: Xenophagy mechanisms in mammals.

Type I interferons are shown to upregulate Ub Like modifiers FAT10 and ISG15, suggesting that these UBLs could essentially involved in cellular immune responses. In line with this, in cytoplasm *Salmonella typhimurium* is surrounded by FAT10 after escaping from vacuolar rupture. However, cells lacking FAT10 do not exhibit restricted bacterial replication defect in their phenotype. Interestingly, NRAMP1 (natural resistance-associated macrophage protein 1) transgenic mice that are deficient for FAT10 are much more susceptible to *S. Typhimurium* than corresponding controls, indicating that FAT10 could be important for antibacterial immunity *in vivo* (Spinnenhirn et al., 2014). Moreover, Usp18, an ISG15 DUB-like peptidase deactivating mutation carrying mice showed accumulation of ISG15 and susceptibility to *Salmonella* infection. *Salmonella* elimination was rescued by deletion of ISG15 in a Usp18 mutant background, suggesting that ISG15 inhibits cellular immune pathways implicated in antibacterial resistance (Bogunovic et al., 2012; Zhang et al., 2015c).

It is speculated that the steady state level of autophagy is sufficient for xenophagy of all the invading bacteria, and that the pathogens have to interfere with autophagy in order to survive. For example, infection by *Listeria*, *Salmonella* and *Shigella* were all shown to induce amino acid starvation through GCN2 phosphorylation, ATF3 induction and mTOR inhibition and subsequently activating autophagic response (Tattoli et al., 2012, 2013). But it is also possible that infectious organisms are able to escape from the cellular defence mechanisms. *Listeria* uses its phospholipases, PlcA and PlcB, in order to escape from autophagic elimination in host cells by reducing PI3P levels and subsequently autophagic flux (Tattoli et al., 2013). After infecting host cells, *M. tuberculosis* (Mtb) can stay dormant for decades and survive inside macrophages due to its ability to escape from autophagic degradation. Following activation by IFN- γ , macrophages can bypass autophagic inhibition by Mtb, leading to the clearance of the pathogen. This process is mediated, at least in part, through the interaction of the shuttling protein ubiquitin-1 with Mtb proteins, and the subsequent recruitment of the autophagic machinery (Sakowski et al., 2015). This complex interplay between ubiquitylation and autophagy achieves the important task of keeping host cells pathogen-free and providing a intracellular innate immune defense mechanism against invaders.

1.3.5.2 Mitophagy: Mitochondrial Turnover

Mitochondria are highly dynamic, double-membrane surrounded organelles that involve in a variety of cellular functions within eukaryotic cells and have ancient bacterial origin. The known major function of mitochondria is energy production for the cells. Within cells, they are involved in amino acid synthesis, fatty acid production, heme synthesis, calcium signaling and as well as innate immunity and cell death processes. Mitochondria have their own genome which is approximately 16 kilobases and encodes 13 oxidative phosphorylation (OXPHOS) complex subunits in addition to both transfer RNAs and ribosomal RNAs. Due to the needs of cells and type of the cells, there can be hundreds copy of a mitochondrial genome in one cell. This raises the importance of maintaining the mitochondrial homeostasis and eliminating dysfunctional mitochondria for a single cell as well as a whole organism.

The removal of a dysfunctional and no more needed whole mitochondria is maintained by a cargo selective type of autophagy, termed as mitophagy (Lemasters, 2005). Eventhough mitophagy shares many of the general autophagy modifiers and steps, the selectivity of autophagosomes for mitochondria requires unique stress triggers and protein reulators.

1.3.5.2.1 PINK1/Parkin-dependent Mitophagy

Parkin/PINK1-dependent mitophagy is one of the best studied form of mitophagy. In different experimental models including mammalian cells, flies and *C.elegans* predominantly mitophagy is maintained by two famous genes their loss-of function mutations are linked to early-onset of Parkinson Disease's: PTEN-induced putative kinase 1 (PINK1), encodes for a mitochondrially localized kinase, and PARK2, encodes a cytosolic E3 ubiquitin ligase (Narendra et al., 2008).

Under normal conditions, after being synthesized as precursor in cytoplasm PINK1 is imported to mitochondria by its N-terminal mitochondria targeting sequence (MTS) through translocase of the outer membrane (TOM) and translocase of the inner membrane (TIM) complexes. When PINK1 is imported, it is post translationally modified within mitochondria by mitochondrial proteases. PINK1 is first cleaved through its N-terminal matrix targeting sequence (MTS) by matrix processing peptidases (MPP) and this cleavage followed by another cleavage by Presenilin-associated rhomboid-like protease (PARL) in matrix (Deas et al., 2011; Jin et al., 2010). PARL-mediated N-terminal cleavage results in destabilizing Phe104 residue and therefore as soon as retranslocated from mitochondria to cytoplasm therein degraded by proteasome through recognition of its N-terminus (Yamano and Youle, 2013).

Under stress conditions, PINK1 import to mitochondria is blocked and therefore is stabilized on the OMM in TOMM complex that composed of several different TOM proteins (Hasson et al., 2013; Lazarou et al., 2012). Two PINK1 protein on OMM get dimerized and this dimerization is necessary for autophosphorylation events therefore the activity of PINK1 dimer. Stabilized PINK1 and its kinase activity is prerequisite event

for recruitment of cytoplasmic E3 ligase Parkin protein to mitochondria (Lazarou et al., 2012). In addition to recruitment of Parkin, PINK1 is shown to enhance the E3 ligase activity of Parkin by phosphorylating its Ser65 residue of ubiquitin-like domain (Ubl) (Kondapalli et al., 2012; Shiba-Fukushima et al., 2012). Further studies on the understanding of structure and the E3 ligase activity of Parkin revealed that either RING1 or unique Parkin domain (UPD) of the protein interfere with the accessibility of the catalytic residue and therefore Parkin is present as autoinhibited form within the cells (Trempe et al., 2013). PINK1-mediated phosphorylation of Parkin at Ser65 changes the conformation of the protein so that allowing to access its catalytic residues to perform ligase activity (Wauer and Komander, 2013). Interestingly, PINK1 also phosphorylates preexisting ubiquitin molecules at Ser65 residue homologous to Ser65 phosphorylation of Parkin and both ubiquitin and Parkin phosphorylation strongly correlates with tethering Parkin to damaged mitochondria and fulfillment E3 ligase activity of Parkin therein allow ubiquitin modification OMM proteins for further PINK1/Parkin-dependent mitophagy steps (Kane et al., 2014; Kazlauskaitė et al., 2014; Koyano et al., 2014; Shiba-Fukushima et al., 2014).

AMBRA1 is ubiquitously expressed in adult midbrain and found in complex with Parkin but is not an ubiquitylation target of Parkin. The Parkin and AMBRA1 interaction is enhanced during mitochondrial depolarization in HEK293 cells, SH-SY5Y cells, and adult mouse brain. Eventhough AMBRA1 has no effect on Parkin recruitment to mitochondria, its activatory effect on PI3K suggested to be critical for PINK/Parkin-mediated mitophagy (Van Humbeek et al., 2011). Through its LIR domain, AMBRA1 itself can bind to LC3 on autophagosomes in Parkin- and p62-independent but LC3-dependent manner (Strappazon et al., 2015). All of these observations suggest that AMBRA1 is a key mitophagy regulator that allows proper mitochondrial clearance in both Parkin-dependent and independent cases (Cianfanelli et al., 2015; Strappazon and Cecconi, 2015).

Autophagy receptor proteins are attached to the ubiquitin labelled cargo through their ubiquitin-binding domains (UBD) and links them to the autophagosome to promote autophagy. p62 a well known autophagy receptor which also binds to ubiquitylated substrates introduced to be a receptor for damaged mitochondria and a linker protein between damaged mitochondria and LC3 that is associated with autophagosomes (Geisler

et al., 2010). However further studies revealed that p62 is not functioning as mitophagy receptor but is essential for clustering of damaged mitochondria in perinuclear region of the cells (Narendra et al., 2010; Okatsu et al., 2010). Rather than p62, four receptor proteins were associated with selective autophagy that are namely NBR1, NDP52, optineurin (OPTN) and TAX1BP1. In order to understand which receptors are required for specifically mitophagy, a cell line which does not express any of those five receptors called penta-knockout (penta KO) generated. Penta KO cells failed to progress elimination of damaged mitochondria and with rescue experiments its seen that NDP52 and OPTN are essential for mitophagy (Lazarou et al., 2015). PINK1 kinase activity as well as Parkin mediated ubiquitin and phospho-ubiquitin conjugates are required for recruitment of NDP52 and OPTN, and their involvement is followed by the recruitment of ULK1, DFCP1 and WIPI1 to the close proximity of mitochondria suggesting that they function as upstream regulators of LC3. In PINK1/Parkin mediated mitophagy, damage enhances TBK1 phosphorylation at Ser172 so that its kinase activity (Lazarou et al., 2015). The increased activity of TBK1, stimulates recruitment and subsequent phosphorylation of selective autophagy receptors OPTN, NDP52 and p62 through physical interaction. TBK phosphorylation on OPTN on Ser473 and Ser513 residues promotes TBK activation and ubiquitin binding to OPTN and following OPTN retention to mitochondria providing a positive feedback mechanism for maintaining successful mitophagy (Heo et al., 2015).

In mitophagy, major receptor for both Parkin and autophagy receptor proteins is phosphorylated ubiquitin (phospho-Ub). Upon depolarization, phospho-Ub recruited to mitochondrial surface therein several proteins get activated. First Parkin is activated by the phospho-Ub and active PINK1 which is generator of phospho-Ub also and then OPTN and NDP52 are activated by TBK1 mediated phosphorylation and ubiquitin binding promoting amplification signals. Due to the critical role of ubiquitin and phospho-ubiquitin in the substrate recognition, Parkin activation and signal amplification.

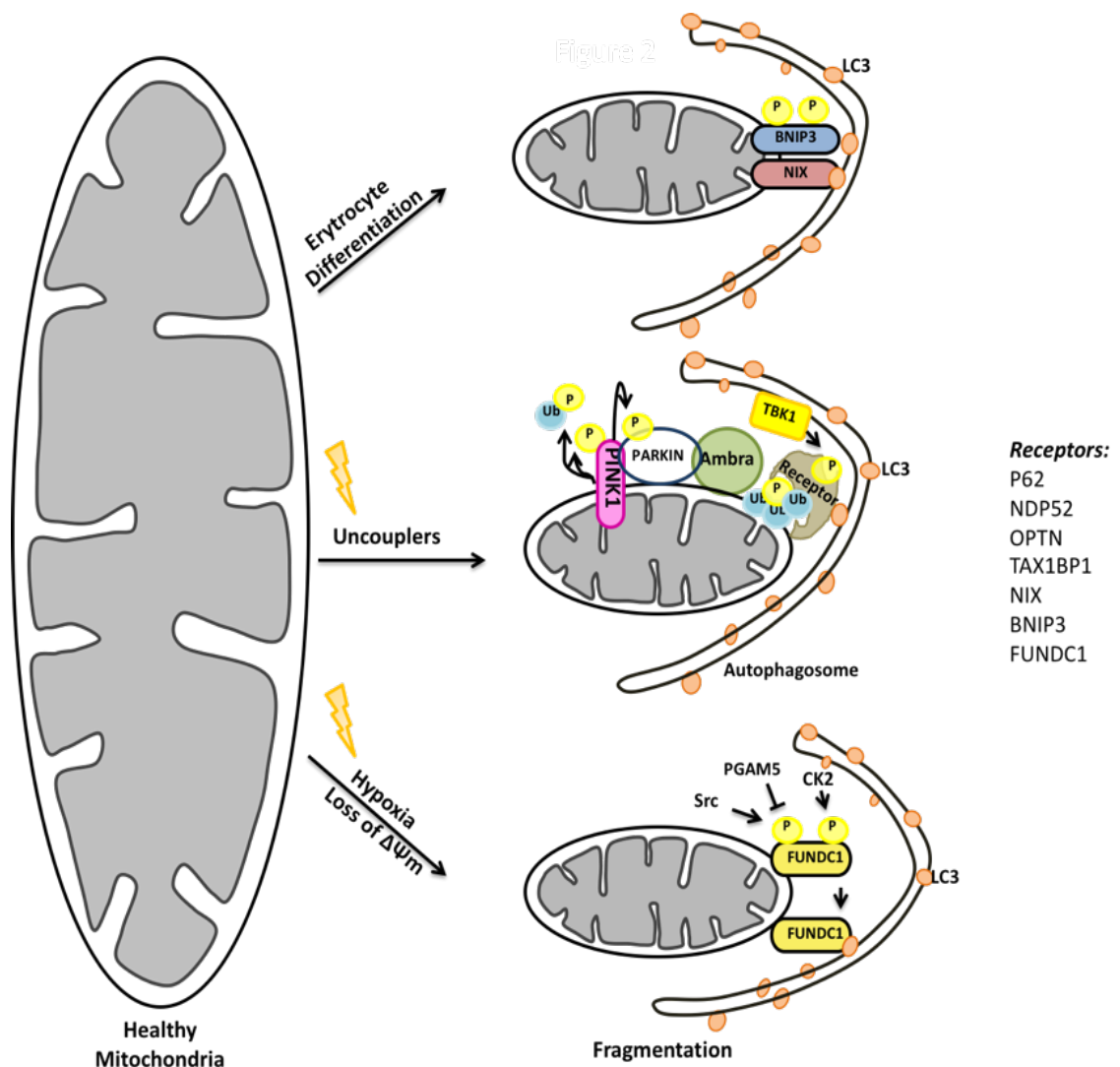


Figure 1.3.5.2: Molecular details of mitophagy pathways in mammalian cells.

Maintenance of these regulation is emerging due to the involvement of mitophagy defects in neurodegeneration. Ubiquitin modification are reversible covalent modifications which are reversed by DUBs. There are several DUBs identified as both positive and negative regulators of mitophagy (Dikic and Bremm, 2014; Wang et al., 2015). USP8/UBPY is a member of ubiquitin-specific protease family recently introduced as a novel controller of mitochondrial quality. USP8, reported to remove K6-linked ubiquitin chains from Parkin specifically (Durcan et al., 2014; Durcan and Fon, 2015). USP8 mediated deubiquitylation of Parkin is important for its recruitment to dysfunctional mitochondria and subsequently proper mitochondrial elimination. USP15, another ubiquitin-specific protease family member of DUBs is highly expressed in brain

and other organs. USP15 mediated deubiquitynation has an inhibitory effect on Parkin-mediated mitophagy but not related to the ubiquitylation level and translocation of Parkin.

It is most likely opposes Parkin-mediated ubiquitylation. Deficiency in USP15, results in rescued mitophagy defects in PD-derived fibroblasts that are carrying PARK2 mutations correlating decreased Parkin expression (Cornelissen et al., 2014). Similar observations also obtained from Parkin deficient flies which have mitochondrial and behavioral defects in their phenotype. Loss of Parkin caused defects in flies were restored by knockdown of DUB CG8334, the closest homolog of USP15 in *Drosophila*. USP30 and USP35 are both mitochondria localized DUBs. USP30 is another identified mitophagy antagonist and localized on mitochondria. In neuronal cells, USP30 shown to remove ubiquitin molecules from proteins on damaged mitochondria that are ubiquitinated by E3 ligase activity of Parkin and therefore inhibits mitophagy (Bingol et al., 2014). Knockdown effect of USP30 is strongly correlated with the Parkin recruitment to damaged mitochondria. However, USP35 has no effect on Parkin translocation. USP35 has differential effect on Parkin-dependent mitophagy, due to its disassociation from mitochondria upon uncoupling suggesting its mitophagy-inhibitory effect taking place in cytoplasm (Wang et al., 2015). USP30 knockdown restored mitophagy defects and improved mitochondrial integrity in Parkin- or PINK1-deficient flies (Bingol et al., 2014).

1.3.5.2.2 Parkin-independent Mitophagy

Expression of Parkin is restricted to a few cell types, including dopaminergic neurons. Consequently, Parkin null animals showed prominent mitophagy defects only in selected brain regions (Lee et al., 2018). In other cell types and tissues, mitophagy proceeds in a Parkin-independent manner. Alternative E3 ligases were found to play a role in mitophagy in these contexts.

Mulan (MUL1) is an E3 ubiquitin ligase that is located on the OMM and plays a role in Parkin-independent mitophagy in different model organisms, including *C.elegans*, *Drosophila* and mammalian cells (Ambivero et al., 2014; Yun et al., 2014). Mulan stabilized DRP1, led to degradation of MFN2 and shown to interact with GABARAP

(Ambivero et al., 2014; Braschi et al., 2009). Another E3 ligase that was associated with mitophagy is GP78 (Christianson et al., 2012). Over expression of GP78 induced MFN1/2 ubiquitylation and degradation followed by mitochondrial fragmentation and mitophagy in mammalian cells lacking Parkin (Fu et al., 2013). Synphilin-1-dependent recruitment of the E3 ligase Siah1 to mitochondria resulted in mitochondrial protein ubiquitylation and mitophagy in a PINK1-dependent but Parkin-independent manner (Szargel et al., 2015). Conversely, another OMM E3 ligase, MITOL (MARCH5), was reported to ubiquitylate FIS1, DRP1 (Yonashiro et al., 2006) and MFN2 (Nakamura et al., 2006), yet inhibit hypoxia-induced and Parkin-independent mitophagy through ubiquitylation and degradation of FUNDC1 (Chen et al., 2017). All these findings underline the fact that mitophagy might proceed in cells which do not express Parkin. Further studies are required to unravel the molecular mechanisms of Parkin-independent mitophagy in different tissues and cell types.

1.3.5.2.3 Mitophagy During Reticulocyte Maturation

During differentiation, in order to increase hemoglobin-bound oxygen loading capacity, reticulocytes lose their organelles, including mitochondria, and become mature red blood cells (Dzierzak and Philipsen, 2013). During this maturation process, a protein called NIX (also known as BNIP3L) is upregulated (Aerbajinai et al., 2003). Characterization of NIX-deficient mice showed a decrease in mature erythrocyte numbers and anemia, as well as accumulation of immature erythrocytes. NIX-deficient erythrocytes failed to eliminate their mitochondria revealing a critical role for NIX in mitophagy (Sandoval et al., 2008; Schweers et al., 2007).

NIX is a C-terminally anchored outer mitochondrial membrane (OMM) protein that contains a LC3-interacting region (LIR) at its cytoplasmic N-terminal part. Through its LIR domain, interact with autophagy protein LC3, enabling engulfment of mitochondria by autophagosomes (Novak et al., 2010). Interestingly, NIX-dependent mitophagy does not require ATG5 or ATG7 proteins, but requires ULK1 (Honda et al., 2014; Kundu et al., 2008). Indeed, ULK1 deficiency led to the accumulation of morphologically abnormal mitochondria in hepatocytes and increased mitochondrial

mass in fibroblasts (Egan et al., 2011; Kundu et al., 2008). Although NIX-dependent mitophagy was predominantly studied in reticulocytes, NIX-deficient mice derived retina revealed increase in mitochondrial mass and reduction in glycolytic enzymes and subsequently delayed neuronal differentiation suggesting it has broader impact in other cell types. In line with this, NIX-dependent mitophagy shown to be involved in the removal of mitochondria during macrophage differentiation (Esteban-Martínez et al., 2017). Recent studies showed that ubiquitylation of NIX/BNIP3L by a PINK1/Parkin-independent mechanism was crucial for mitophagy in different experimental models. In some studies it was also reported that ubiquitylated NIX/BNIP3L colocalized with other selective autophagy receptors such as NBR1 and p62, and it was necessary for mitochondrial stress-induced mitophagy (Ding et al., 2010; Gao et al., 2015; Palikaras et al., 2015) (Figure 1.3.5.2). Therefore, the role of NIX/BNIP3L seems to be more general than previously thought and beyond the developmental context, and stress-induced mitochondrial elimination by autophagy might also require NIX/BNIP3L in different cell and organism types.

In addition to its role in reticulocyte maturation, NIX and especially its homolog BNIP3 were implicated in hypoxia-induced mitophagy (Tracy et al., 2007). In this context, HIF1 α transcriptionally upregulated both NIX and BNIP3 levels (Sowter et al., 2001). As in the case of NIX, BNIP3 also has N-terminal LIR domain, and physically interacted with LC3 and GABARAP to recruit autophagosomes. The interaction between BNIP3, LC3 and GABARAP was regulated by the phosphorylation events on Ser17 and Ser24 residues which defines the LIR domain of the protein (Zhu et al., 2013).

1.3.5.3 Pexophagy: Autophagic Removal of Peroxisomes

Peroxisomes are abundant organelles found in almost all eukaryotes. Peroxisomes maintain a number of cellular functions including fatty acid oxidation (FAO), purine metabolism and phospholipid synthesis (Wanders et al., 2016). A variety of peroxisomal enzymes are involved in redox regulation due to their dual functions in the generation and scavenging of reactive oxygen and nitrogen species (ROS and RNS) therefore cellular dynamics of peroxisomes both biogenesis and degradation must be

tightly regulated in order to maintain cellular needs in terms of peroxisome sizes, numbers and functions (Du et al., 2015; Honsho et al., 2016). Pexophagy is a selective degradation process of peroxisomes by autophagic machinery is identified in yeast and recently in mammals.

Autophagy of peroxisomes, pexophagy, is a selective degradation process of peroxisomes during which the UPS and autophagy mechanisms work in collaboration. Peroxisomes are responsible of a number of cellular functions, including fatty acid oxidation, purine metabolism and phospholipid synthesis (Wanders et al., 2016). Several peroxisomal enzymes are involved in redox regulation due to their dual functions in the generation and scavenging of reactive oxygen and nitrogen species. Therefore, peroxisomes biogenesis and degradation must be tightly regulated in order to control peroxisome size, abundance and function (Du et al., 2015; Honsho et al., 2016). Moreover under stress conditions such as hypoxia, oxidative stress, starvation or conditions causing UPS defects, pexophagy is upregulated.

The understanding of selective autophagy have suggested that ubiquitin is a key actor of selective degradation of membrane proteins of associated organelles as well as aggregates (Kwon and Ciechanover, 2017; Shaid et al., 2013). Consistently, during pexophagy, peroxisomal membrane proteins (PMPs) become highly ubiquitylated (Kim et al., 2008). This ubiquitin modification and Ub-sensing adaptor proteins direct peroxisomes for degradation to autophagosomal membranes. For example, PMP34 and PEX3 induce pexophagy when only associated with Ub through their cytoplasmic parts (Kim et al., 2008; Yamashita et al., 2014). In addition to PEX3, mono-ubiquitylation of PEX5 is also identified as positive regulator of pexophagy under more specific conditions (Wang and Subramani, 2017; Zhang et al., 2015a). In response to ROS, through physical interaction PEX5 recruits ataxia-telangiectasia mutated (ATM) protein to peroxisomes. This kinase therein inactivates mTORC1 and activates ULK1, subsequently induces autophagy. The specificity of pexophagy is mediated by ATM dependent phosphorylation of PEX5 at Ser141 which in turn attenuates mono-ubiquitylation of PEX5 at Lys209. Lys209 mono-ubiquitylation of PEX5 is recognized by receptor protein p62 and peroxisomes are directed to autophagosomes (Tripathi et al., 2016; Zhang et al., 2015a). In addition to Lysine mono-ubiquitylation, PEX5 is also become mono-ubiquitylated through a rare thio-ester bond at its N-terminal cysteine residues for recycling of the

protein. N-terminal cysteine mono-ubiquitylation of PEX5, requires PEX22 associated PEX4 as major E2 enzyme and a complex of PEX2, PEX10 and PEX12, the three E3 ligases in mammalian cells (Platta et al., 2009; Wang and Subramani, 2017). Cysteine mono-ubiquitylation of PEX5, expedites its extraction from peroxisomes through AAA ATPase complex (AAA-complex); PEX1, PEX6, PEX26 (Carvalho et al., 2007; Law et al., 2017; Okumoto et al., 2011).

Pexophagy is also stimulated upon macroautophagy induction such as nutrient deprivation and rapamycin treatment. Starvation and rapamycin mediated mTOR inhibition upregulates PEX2 in HeLa and MEF cells (Sargent et al., 2016). Moreover, ectopically induction of PEX2 leads ubiquitylation of PEX5, NBR1 and another peroxisomal membrane protein 70 kDa, PMP70 and subsequent peroxisome degradation (Sargent et al., 2016).

The involvement of selective autophagy receptors in selective autophagy studied extensively and reviewed above (Chen et al., 2016; Kirkin et al., 2009; Lazarou et al., 2015; Marshall et al., 2015; Okatsu et al., 2010). Till now among all identified cargo specific and ubiquitin-binding receptors proteins, only p62 and NBR1 shown to be involved in pexophagy (Deosaran et al., 2013). Structurally, p62 and NBR1 are very similar therefore they act in the same pathway for pexophagy. Interestingly, NBR1 function is independent from p62 but p62 could increase the efficiency of NBR1-dependent pexophagy. Another pexophagy regulators, PEX13 and PEX14 are also imported through PEX5 to peroxisomes (Lee et al., 2017; Schell-Steven et al., 2005). Under starvation, PEX14 through direct binding to LC3 facilitates pexophagy and under this condition NBR1 is also found to attached to PEX14 in peroxisomes (Jiang et al., 2015a).

During the process of pexophagy, a number of peroxisomal membrane proteins, including peroxins and PMP70 become ubiquitylated (Kim et al., 2008). PEX2-PEX10-PEX12 complex serves as an E3 ligase at least for two well studied peroxisome proteins, PEX5 and PMP70. Ubiquitylation of peroxisome proteins result in the recruitment of p62 and/or NBR1 autophagy receptors, directing these organelles for autophagic degradation. For example, PEX2 overexpression or amino acid starvation activated the ubiquitylation of PEX5, and another peroxisomal membrane protein, PMP70, and led to peroxisome

degradation (Sargent et al., 2016). Moreover in response to oxidative stress, ATM was recruited onto peroxisomes through physical interaction with PEX5 and promote its ubiquitylation. Inactivation of mTORC1 in a TSC2-dependent manner and stimulation of ULK1 phosphorylation by ATM, potentiated pexophagy (Wang and Subramani, 2017; Tripathi et al., 2016; Zhang et al., 2015a). On the other hand, AAA ATPase complex (PEX1, PEX6, PEX26) was shown to extract ubiquitylated PEX5 from peroxisomal membranes and regulate pexophagy (Carvalho et al., 2007; Law et al., 2017; Okumoto et al., 2011) (Figure 1.3.5.3). Although overexpression of ubiquitin-fused constructs of peroxisomal membrane protein PMP34 or PEX3 was reported to induce pexophagy, ubiquitylation of these proteins might not be a prerequisite for the progression of pexophagy since ubiquitylation defective form of PEX3 was able to induce peroxisome ubiquitylation and autophagy (Kim et al., 2008; Yamashita et al., 2014). Both NBR1 and p62 were shown to be recruited onto peroxisomes during pexophagy. Yet, NBR1 was a major pexophagy receptor in a number of contexts, and p62 increased the efficiency of NBR1-dependent pexophagy through direct interaction with the latter (Deosaran et al., 2013; Sargent et al., 2016; Zhang et al., 2015a). Altogether, these findings underline the importance of ubiquitylation for the selective degradation of peroxisomes by autophagy.

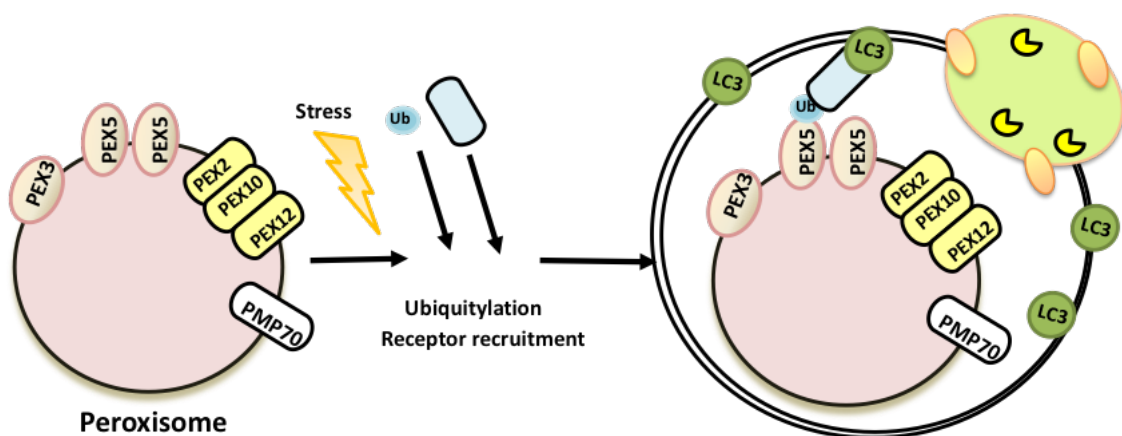


Figure 1.3.5.3: Schematic representation of selective removal of peroxisomes by autophagy machinery.

1.3.5.4 Autophagic Removal of Ribosomes and Stress Granules

In addition to major cellular organelles, autophagy was implicated in the clearance of ribosomes. Although ribosomes can be degraded in a non-specific manner during non-selective autophagy, a special form of selective autophagy is activated under various stress conditions, ribosomal autophagy or ribophagy. On the other hand, mRNA protein complexes that are stalled in translation form stress granules and cleared by both the UPS and autophagy.

Ribophagy was first described in the yeast during nutrient stress and was shown to involve ubiquitylation of the Rpl25 of the 60S ribosome subunit by the ubiquitin ligase Ltn1/Rkr1 and maybe by Rsp5 regulated the activity of Ubp3/Bre5p (Kraft et al., 2008; Kraft and Peter, 2008; Ossareh-Nazari et al., 2014). In the mammalian system, in addition to mTOR inhibition, oxidative stress, induction of chromosomal mis-segregation following MPS1 inhibition or translation inhibition and stress granule formation following sodium arsenite treatment were all shown to induce ribophagy (An and Harper, 2018). Ubiquitylation of ribosomes was observed under ER stress-inducing conditions, and considering the involvement of ubiquitylation in the yeast, it is likely that ribosome ubiquitylation is involved in ribophagy (Higgins et al., 2015). Moreover, p97/VCP that binds to ubiquitylated proteins and that functions in the delivery of these substrates to proteasome was necessary for ribophagy both in yeast and mammalian cells (An and Harper, 2018; Verma et al., 2013). Yet, individual ribosomal proteins were indeed shown to be a target of the UPS (Wyant et al., 2018). Recently, NUFIP1-ZNHIT3 proteins were identified as novel ribophagy receptors that directly connected ribosomes to LC3 and autophagy, but the role of ubiquitylation in this process is not clear to date (Wyant et al., 2018) (Figure 1.3.5.4).

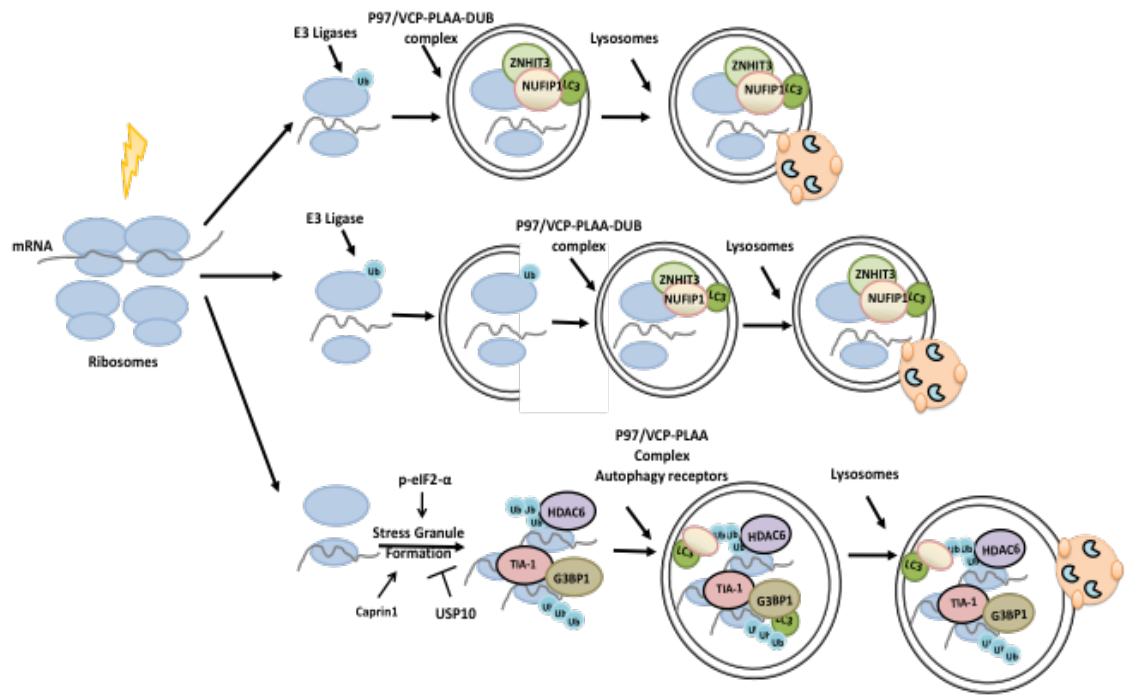


Figure 1.3.5.4: Selective targeting of ribosomes and stress granules for degradation to the UPS or autophagy mechanisms.

On the other hand stress granules are composed of actively accumulated non-translating mRNA ribonucleoprotein complexes (Protter and Parker, 2016). Proteins that accumulated in the stress granules, include stalled 40S ribosomal units and various translation initiation factors (e.g., eIF4E, eIF4G, eIF3, eIF2 and poly(A)-binding protein (PABP)) (Kedersha et al., 2005; Reineke and Lloyd, 2013). A subunit of the eIF2, eIF2- α is phosphorylated under various stress conditions, leading to the blockage of cap-dependent translation. GCN2 is one of the eIF2- α kinases and both proteins were involved in stress granule formation (Farny et al., 2009; Mazroui et al., 2007). G3BP1 and TIA-1 are also among the proteins that contribute to stress granule formation (Kedersha et al., 2000; Tourrière et al., 2003; Waris et al., 2014). Additionally, an interplay between G3BP1, Caprin1 and the DUB protein USP10 was shown to regulate stress granule formation, USP10 having a negative and Caprin1 having a positive on G3BP1-mediated granule condensation (Kedersha et al., 2016) HDAC6 was a component of stress granules as well, and HDAC6 and bound to G3BP1 protein (Seguin et al., 2014). Accumulating data indicate that clearance of stress granules was regulated by both the UPS and

autophagy mechanisms, and the p97/VCP protein is a key component in both processes. For example, inhibition of autophagy or p97/VCP deficiency were linked to decreased stress granule removal (Buchan et al., 2013). Co-factors of p97/VCP determine target selectivity of the protein. In this context, while the association of p97/VCP with the co-factor UFD1L led to the degradation of defective ribosomal products and dysfunctional 60S ribosomes by the UPS (Fujii et al., 2012; Ju et al., 2008; Verma et al., 2013), HDAC6 containing p97/VCP and PLAA associated granules were made a target of ribophagy (Ossareh-Nazari et al., 2010). Therefore depending on the co-factor of choice, p97/VCP has a decisive role in the choice of the degradative pathway through which ribonuclear substrates are eliminated.

1.3.6 Proposed Direct Link Between the UPS and Autophagy: PSMA7, PSMB5, UBA1, UBE2L3 and ATG5

In this Phd study, previously unidentified, novel and direct links between the UPS and autophagy mechanisms were investigated under basal and mitochondrial stress-inducing conditions through direct binding of proteasomal components to core autophagy protein ATG5. Along with this thesis, PSMA7 and ATG5 interaction was verified in multiple and independent technics, including Yeast-Two-Hybrid, immunoprecipitation tests and colocalization analysis as well as gel filtration tests. The functional role of the interaction was investigated by knockdown studies using siRNAs and knockout cells are utilized. Based on omic studies performed during this Phd work, PSMB5, UBA1 and UBE2L3 were suggested as ATG5 interactors. These initial screening data further confirmed with biochemical tests suggesting that ATG5 is multifunctional protein and upon differential stress stimuli provide differential interactome profile regulating cellular homeostasis. And even the same stimuli provided different interaction hits based on the subcellular localization of the protein.

These novel interactions could suggest an extra layer of importance for understanding of the crosstalks between the degradation systems and co-regulation in the elimination of common substrates, especially mitochondria. As well as, potential different roles of the interaction in terms of localization: cytoplasm and mitochondria. Findings

derived from this thesis would be utilized for the therapeutic approaches of mitochondrial defects-causing diseases, including neurodegenerative disorders.

2. MATERIALS AND METHODS

2.1 PLASMIDS, CONSTRUCTS and SIRNAs

Myc-ddk-tagged PSMA7 (RC201169), human PSMA7 (SC319465) and Myc-ddk-tagged human ATG5 (RC235557) plasmids obtained from ORIGENE. Mito-dsRed (#87379), pm-Turquoise2-mito (#36208), YFP-tagged MFN2 (#28010), YFP-tagged Parkin (#23955), mCherry-tagged Parkin (#23956), MYC-tagged Parkin (#17612), N-GFP-tagged PINK1 (#13315), C-GFP-tagged PINK1(#13316), N-MYC-tagged PINK1(#13313), C-MYC-tagged PINK1 (#13314), psPAX2 (#12260), pMD2.G (#12259) and pMXs-IP HA-tagged Parkin (#38248) plasmids obtained from Addgene. pEGFP-tagged LC3, and human ATG5 plasmids were generous gift from Noboru Mizushima, pmCherry-tagged ATG5 plasmid from Jae-Won Soh. For knock down experiments, Smart pool siRNA PSMA7 (M-004209-00-0020 20), siRNA PSMB5 (M-004522-00-0020 20) and Control siRNA (D-001210-01-20) were purchased from Dharmacon. Flag-tagged PSMA7 vector exposed to restriction enzyme cut with *EcoRI* and *XhoI* afterwards ligated into pEGFP-N3 empty vector (Clontech) following *EcoRI* and *SalI* in order to generate pEGFP-tagged PSMA7 construct. Flag-tagged PSMA7 fragments, N-terminal (F1) and C-terminal (F2) were generated by PCR-based cloning using Myc-ddk-PSMA7 as template and primers listed below and then PCR products inserted into pCMV-3Tag-6-Flag empty vector.

The primers used for PSMA7 fragment generation:

PSMA7-F1 Fwd 5' ataggatccagctacgaccgcgccaac 3' TM 65.2

PSMA7-F1 Rev 5' atactcgagtcactccaggaactcgcg 3' TM 62.9

PSMA7-F2 Fwd 5' ataggatccgcccaccaagaactatactgacgaag 3' TM 66.1

PSMA7-F2 Rev 5' tatctcgagtcgatgatgctttctttgt 3' TM 55.5

BamHI: GGATCC

XhoI: CTCGAGT

2.2 YEAST-TWO-HYBRID SCREEN

(by Former students)

For yeast-two-hybrid screening, while pGBKT7-ATG5 construct was used as bait, and a thymus cDNA library in the pACT2 vector was used as prey (Clontech). Screening procedures were followed according to the manuals provided by manufacturers. To cut along story in short, AH109 yeast strain used for transformation of the constructs and potential interactions were observed on selective solid media (leucine, tryptophan, histidine, and/or adenine) without containing plates for 3 to 5 days. After selection, inserts coming from grown colonies were subjected to colony PCR based amplification reaction and subsequently, PCR products were sequenced and characterized. Following colony PCR protocol was followed in order to amplify the plasmid inserts in grown bacteria:

PCR Mix Protocol:

(Reaction Volume 50 μ l)

10X Tag Buffer (Thermo Fischer, B38): 6,5 μ l

MgCl₂: 4,5 μ l

dNTP mix (Thermo Fischer, R0192, 10mM): 2 μ l

Tag Polymerase (Thermo Fischer, 10342020, 1 u/ μ l): 1 μ l

Primer 5' pACT2 (10mM): 1 μ l

Primer 3' (10mM): 1 μ l

Selected colony dissolved in 0,2 M NaOH: 10 μ l

dd H₂O: 39 μ l

PCR Reaction Program:

Step 1: 94 °C for 3 mins.

Step 2: 2x Repeat the cycle

- i. 94 °C for 30 s
- ii. 60 °C for 30 s
- iii. 70 °C for 3 mins

Step 3: 2x Repeat the cycle

- i. 94 °C for 30 s
- ii. 59 °C for 30 s
- iii. 70 °C for 3 mins

Step 4: 2x Repeat the cycle

- i. 94 °C for 30 s
- ii. 58 °C for 30 s

iii. 70 °C for 3 mins

Step 5: 70 °C for 10 mins

When PCR cycles have been terminated, samples were run through 1% agarose DNA gel. During this electrophoretic run, Mass Ruler DNA ladder mix (Thermo Fischer, SM0403) was used as a molecular weight marker. Compare to molecular weight with the amplified samples which show amplification only at around one size of the band were sent for sequencing for further validation and blast-based characterization of the colonies.

2.3 CELL CULTURE

2.3.1 Cell Line Maintenance

HEK293T, HeLa and MEF cells were cultured in DMEM (Dulbecco's modified Eagle's medium; PAN, P04-03500) supplemented with 10% (v/v) fetal bovine serum (FBS; PAN Biotech., P30-3302) and antibiotics (100 units/mL penicillin and 100 µg/mL streptomycin; Biological Industries, BI03-031-1B) and 1% L-glutamine (Biological Industries, BI03-020-1B) under 5% CO₂ in a humidified incubator. In the case of cells that are stably expressing gene of interests or crispr cells, regular media described above was supplemented with mammalian selection marker puromycin according to determined doses for each cell type. All cell types used in this study were adherent. Therefore, in every two days cells when reached to a 80-90% confluency, cells were splitted into new passages. During cell passaging, the media in which celss were growing removed. Cells were washed once with sterile, cell culture grade 1xPBS (PAN Biotech., P04-36500) and PBS was removed. In order to detach cells from plate surface, Trypsin (Biological Industries, BI03-050-1A) was used. Cells were incubated with trypsin for 5 to 7 mins

based on the cell types at 37 °C in 5% CO₂ humidified incubator. After incubation, trypsin was inactivated with 2x volume of complete DMEM. 1 to 10 volume of cell suspension was placed in new plates for further growth.

2.3.2 Transfections and Crispr ATG5 cells Generation

In order to transiently express genes of interest in HEK/293T and HeLa cells, calcium phosphate precipitation used according to given protocol below. For Parkin stable HEK/293T and HeLa cells and Crispr ATG5 HeLa cells, viral transduction protocols followed described below.

2.3.2.1 Calcium-Phosphate Transfection

16 h prior to transfection, 1.5 million HEK/293T and HeLa cells plated in 10 cm² in diameter sterile cell culture plates (all values were doubled for cells grown in 15 cm² plates). In one transfection tube 300 µl of 2X HBS (280mM NaCl, 1.5 mM Na₂HPO₄, 50 mM HEPES, 10 mM KCL, 12 mM D-glucose Monohydrate; pre-heated to 37°C) per condition was added. In the second tube, based on the cellular expression levels of the constructs, 5-10 µg of plasmid DNAs together with the ratio of 1/10 pE-GFP plasmid added. The final volume of the second tube filled up to 270 µl with pre-heated ddH₂O. Next, 30 µl of pre-heated 2.5 M CaCl₂ was added into the second tube and the two tubes were mixed on the vortex to initiate the reaction. The mixed solution was incubated for 15 minutes at RT. When the incubation time was over, transfection mix was added onto cells drop-by-drop and cells continued to grow with transfection mix. 8 h after transfection, cells were washed with 5 ml PBS for three times and plates fullfilled with fresh pre-heated medium. 24 h after transfection, the transfection efficiency was controlled by the GFP expression under fluorescence microscope.

2.3.2.2 Retrovirus and Lentivirus Production for Mammalian Cell Infection

All retrovirus and lentivirus related experiments performed under the biosafety level-2 cell culture cabinets. In order to produce lentiviruses for, using HEK/293T cells as host, plated in 10 cm² plated 16 h prior to transfection. HEK/293T using calcium-phosphate precipitation method psPAX2, pMD2G constructs together with target gene transfected. The detailed transfection recipe given below. 8 h after transfection, cell media refreshed as described in detail above. 24 h and 48 h after transfection, lentivirus containing media collected and centrifugated for 5 min at 300xg. Then, supernatant filtered through 0.45 µm filter unit and stored at -80°C until further need for transduction.

Transfection Protocol:

HBS: 300 µl

Water: 250 µl

Target gene: 10 µg

psPAX2: 8 µg

pMD2.G: 2 µg

CaCl₂: 30 µl

In order to use retroviral constructs for mammalian cell infection, the specific host cell requirements occur. Platinum A cells were used as host which are derivative of 293T cells but contain gag, pol and env genes as default therefore with a single construct transfection allowing efficient retrovirus production. 1.5 million of Platinum A cells plated 16 h prior to transfection. Calcium-Phosphate precipitation method with a given recipe below was also used for retrovirus production for further mammalian cell infection.

Transfection Protocol:

HBS: 300 μ l

Water: 260 μ l

Target gene: 10 μ g

CaCl₂: 30 μ l

8 h after transfection, the media of Platinum A cells renewed. 24 h and 48 h after transfection, retrovirus containing media collected. Right after centrifugation and filtration, retroviruses used for transduction in order to prevent the loss of infection efficiency.

2.3.2.3 Retroviral Infection for Parkin Stable Cell Generation

Due to the lack of endogenous Parkin expression, the need of Parkin stable cell generation raised. The retroviral HA-tagged Parkin construct used for stable cell generation (For map of the plasmid, please see Figure 2.3.2.3 1).

2.3.2.4 Crispr ATG5 HeLa Cell Generation

Crispr ATG5 cell generation required several steps: 1) Construction and validation of constructs, 2) Lentiviral Crispr vector production, 3) Infection of target cells and validation of polyclones, 3) monoclonal selection.

Crispr gRNAs for ATG5 gene were determined by using Optimized Crispr Design tool provided by MIT (crispr.mit.edu). The human genome was selected as target genome and the target gRNA was determined with a high score rate and low off-target gene numbers among the given list. At least two different target guide RNA sequences used for primer design. Human ATG5 Crispr primers used in Crispr cell generation listed below:

Human ATG5-1 Fwd 5' - CACCGAACTTGTTTCACGCTATATC -3'

Human ATG5-1 Rev 5' - AAACGATATAGCGTGAAACAAGTTC-3'

Human ATG5-2 Fwd 5' - CACCGTGATATAGCGTGAAACAAGT -3'

Human ATG5-2 Rev 5' - AAACACTTGTTTCACGCTATATCAC -3'

Human CNT Fwd 5' - CACCGGTAGCGAACGTGTCCGGCGT -3'

Human CNT Rev 5' - AAACACGCCGGACACGTTTCGCTACC -3'

Desalted Crispr human ATG5 and control (non-gene targeting) oligos were solubilized in sterile molecular biology grade water (GE Lifesciences, HyCLONE, SH30221.10) according to manufacturers instructions with a final oligo concentration of 100 μ M.

2.3.2.4 1 Lentiviral vector digestion, oligo annealing and cloning into digested vector

1) pLenti CRISPR-V2 empty vector was exposed to restriction enzyme cut by using a single enzyme *BsmB1* with a given protocol below. Lentiviral vector was digested at 37°C for 16 h.

Digestion Protocol

(Reaction Volume 50 µl)

10X Tango Buffer: 5 µl

DTT (20 mM): 2,5 µl

DNA Template (5ng): 5 µl

BsmB1: 1 µl

ddH₂O: 36,5 µl

2) Digested lentiviral vector extracted from the gel.

Following restriction digestion, *BsmB1* cut and as negative control uncut vectors were separated through 1% agarose gel for 45 minutes. *BsmB1* cut vector extracted from the gel by using Gel extraction and PCR clean up kit (Macherey- Nagel, REF: 740609.50) according to manufacturers instructions. Extracted DNA purity and concentrations determined by nanodrop measurement.

3) Human ATG5 targeting primer pairs were annealed according to given protocol below and performed in a PCR machine.

Annealing Mix

(Reaction Volume 10 μ l)

GRNA oligo Rev (100 μ M): 1 μ l
10X T4 Ligase reaction buffer: 1 μ l
ATP (25 mM): 0,4 μ l
T4 polynucleotide ligase: 0,5 μ l
DdH₂O: 6,1 μ l

Annealing Protocol

Step 1: 37°C for 30 mins.

Step 2: 95°C for 5 mins.

Step 3: Allow the oligos return to RT (5°C/min decrease)

Annealed primers were diluted in ddH₂O with 1:200 ratio for further ligation steps.

4) Annealed primers were inserted into digested lentiviral vector according to following protocol at 16 °C for 16 h:

Ligation Protocol

(Reaction Volume 10 μ l)

10X reaction buffer: 1 μ l
Digester vector: 1 μ l
Annealed primers (diluted): 1 μ l
T4 DNA ligase: 0,5 μ l
ddH₂O: 6,5 μ l

5) Transformation into Stbl3 bacterial strain.

Ligation products were diluted in 1:100 with molecular biology grade water. 10 µl of diluted ligation product used for further transformation step. Heat-shock mediated transformation was performed by using Stbl3 competent bacterial strain. Transformed bacteria were spreaded on ampicillin containing LB agar plates at 37°C for overnight incubation.

6) Colony selection and DNA isolation.

16 h after transformation, 10 single colonies were selected by using toothpick or pipet tip and grown for further 8 hours in ampicillin containing LB broth by shaking with 200 rpm at 37°C. The inserted dna construct were extracted by using mini prep protocol according to manufacturers instructions (Macherey-Nagel, REF:740412.10).

7) Validation of constructs by sequencing

Plasmid DNAs from selected colonies were sent for sequencing (Molecular Cloning Laboratories, USA) for validation of inserted gRNA oligos into the pLenti-V2 vector without mutation. The sequences were analyzed by using tool suggested by the sequencing company.

2.3.2.4 2 Lentivirus production of confirmed constructs, lentiviral transduction and monoclonal selection

Following sequencing-based confirmation, the confirmed colonies were grown overnight in ampicillin supplemented LB broth by shaking with 200 rpm at 37°C. Next, grown bacteria were pelleted with centrifugation at 4°C, 5000g for 30 minutes. In order to use for further infection steps, plasmid DNAs were isolated by using midi prep kit according manufacturers instructions (Macherey-Nagel, REF: 740412.10).

As described in detail above, also for Crispr ATG5 vector containing lentivirus production HEK/293T cells used. Both HEK/293T and HeLa cells used for transduction. Duction of target cells done in 6-well plates and 72 h posttransduction puromycin mediated selection has began. Polyclones were tested in terms of their ATG5 protein levels. Positive clones were then splitted into 96-well plate to have 1 cell per well for monoclonal selection. After reaching enough cell population, each monoclones were tested according to their ATG5 protein level and their response to autophagy. Best clones determined, and following experiments performed bu using these monoclones.

2.3.3 Mitochondrial Stress and Mitophagy Induction in Cell Culture

Mitochondrial stress was stimulated by adding two different chemicals in cell culture media of grown cells. Staurosporine (STAURO; Sigma, S5921) is a general PKC inhibitor, was dissolved in DMSO (Sigma, VWRSAD2650) (2 mM) and used at a final concentration of 1 µM for 12 h. Other chemical which is a protonophore, CCCP (Sigma, C2759) was also dissolved in DMSO (20 mM), mitophagy inducing concentration determined as 10 µM for 12 h.

2.4 PROTEIN ISOLATION AND IMMUNOBLOTTING TESTS

Following the end of the transfection and treatment periods, cells were harvested with PBS and collected in tubes. Continuous centrifugation steps were used to get rid of media remnants from cell pellets. Cell pellets were dissolved in complete protease inhibitors (Sigma, P8340) and 1 mM PMSF (Sigma, P7626) supplemented RIPA buffer (25 mM Tris, 125 mM NaCl, 1% Nonidet P-40, 0.1% SDS, 0.5% sodium deoxycholate, 0.004% sodium azide, pH 8.0) according to their volumes. Then, in every 5 minutes cell pellets mixed by vortexing for 10 sec and incubated on ice for 30 minutes. Afterwards, cell lysate was cleared for 15 minutes centrifugation at 12.000 rpm, 4°C. Cell lysates placed into new tubes and protein concentrations were measured by using the Bradford assay (Sigma, B6916). For further immunoblotting experiments, protein samples were denaturated in 3X protein loading dye (6% SDS, 30% Glycerol, 16% β -Mercaptoethanol and 0.1% Bromophenol blue in 1 M Tris-HCl pH 6.8) by boiling at 95°C for 10 minutes.

Denaturated protein samples were separated in home-made Tris-glycine gels with 10-15% acrylamide (for self-made SDS gel please see Table 2.4.1 and 2.4.2), then gels transferred onto nitrocellulose membrane (GE Healthcare, A10083108) with constant 250 mA for 75 minutes. Following transference, membranes were blocked with 5% non-fat milk (Applichem, A0830,0500) in PBST (0.05% Tween 20 in PBS; 3.2 mM Na_2HPO_4 , 0.5 mM KH_2PO_4 , 1.3 mM KCl, 135 mM NaCl, pH 7.4) for 1 h at RT on the shaker. Then the membranes were washed with PBST 3 times for about 5 minutes on shaker. Then the membranes were incubated with a differential working concentrations of primary antibodies diluted in red solution (5% BSA Cohn V Fraction, 0.02% Sodium Azide in PBST, pH 7.5, Phenol red) and incubated either at RT for 1 h or at 4°C for overnight. After primary antibody incubation, membranes were washed with PBST three times and membranes were incubated with HRP-conjugated secondary antibody diluted with 1:10000 ratio in 5% non-fat milk solution at RT for 1 h. Afterwards, membranes washed 3 times with PBST and homemade ECL solution (25 mM luminol, 9 mM coumeric acid, 70 mM Tris-HCl pH 8.8) prepared. As soon as 3 μl of H_2O_2 was added into the solution the chemical reaction began and the membranes wettened with working solution. Then in order to detect the signal, membranes and blue films (Fujifilm, Blue Sensitive film 47410

19289) on top of the membranes, placed into cassettes for 20 minutes incubation in dark room. At the end of 20 minutes, the signal on the films were developed and fixed using manuel developer and fixer solutions sequentially in dark room.

Due to the need for detection more than 1 protein with the same or close molecular weights, after chemiluminescence detection membranes were incubated with stripping buffer (25mM Tris- HCl, 1% SDS pH 2.0) for 30 minutes at 60°C by shaking in every 5 minutes. Following stripping step, membranes required to be blocked and incubated for desired primary antibodies afterwards.

Table 2.4.1: The recipe of home-made separating gel (LOWER) for SDS-PAGE.

LOWER GEL	15%			12%			10%		
	5ml	10ml	20ml	5ml	10ml	20ml	5ml	10ml	20ml
DdH₂O	850 µl	1.75 ml	3.5 ml	1.35 ml	2.75 ml	5.5 ml	1.7 ml	3.4 ml	6.8 ml
50% Glycerol	400 µl	750 µl	1.5 ml	400 µl	750 µl	1.5 ml	400 µl	750 µl	1.5 ml
Lower Buffer	1.25 ml	2.5 ml	5 ml	1.25 ml	2.5 ml	5 ml	1.25 ml	2.5 ml	5 ml
Bis/Acrylamide	2.5 ml	5 ml	10 ml	2 ml	4 ml	8 ml	1.65 ml	3.35 ml	6.7 ml
10% APS	50 µl	100 µl	200 µl	50 µl	100 µl	200 µl	50 µl	100 µl	200 µl
Temed	5 µl	10 µl	20 µl	5 µl	10 µl	20 µl	5 µl	10 µl	20 µl

Table 2.4.2: The recipe of home-made stacking gel (UPPER) for SDS-PAGE.

UPPER GEL	2.5ml	5ml	7.5ml	12.5ml
DdH₂O	1.62 ml	3.25 ml	4.88 ml	8.13 ml
Upper Buffer	625 µl	1.25 ml	1.87 ml	3.12 ml
Bis/Acrylamide	250 µl	500 µl	750 µl	1.25 ml
10% APS	20 µl	40 µl	60 µl	100 µl
Temed	5 µl	10 µl	15 µl	25 µl

Immunoblots were achieved by using specific antibodies against PSMA7 (Enzo Lifesciences, PW8120), PSMB5 (Enzo Lifesciences, PW8895), Parkin (Santa Cruz Biotech., Sc-32282), TOMM40 (Santa Cruz Biotech., Sc-11414), Flag (Sigma, F3290), ATG5 (Sigma, AO856), LC3 (Novus, 2331), MFN2 (Sigma, M6444), β -Actin (Sigma, A5441), p62 (BD Transduction Lab., 610832), VDAC1 (Millipore, AB10527), Tim23 (BD Transduction, 611222), PINK1 (Novus, BC100-494), ATP5A (Santa Cruz Biotech., sc-58613), UB (PD41, Santa Cruz Biotech., sc-8017), Ser65 phospho-UB (EMD Millipore, ABS1513-I), OPTN (Abcam, ab23666). Following primary antibody incubation, HRP conjugated anti-mouse IgG (Jackson Immuno., 115035003) or anti-rabbit IgG (Jackson Immuno., 1110305144) were selected according to host organism of primary antibody and used with a 1:10.000 dilution in 5% milk in PBST. In order to quantify the band intensities, ImageJ software was used.

2.5 MITOCHONDRIAL ISOLATION

In order to obtain highly purified mitochondria, 30 million cells were cultured for each condition. Cells were harvested and washed with PBS three times by a series of centrifugation. The resulting cell pellet was resuspended in isolation buffer (600 mM sucrose, 10 mM TRIS-HCl pH7.4, 1 mM EDTA pH8.0) supplemented with 0.1 % (v/v) protease inhibitor cocktail, 1 mM NaF (Fluka, 71527), 0.2 mM NaVO₃ (Sigma, 450243) and 0.1 mM PMSF and centrifuged at 500 g and 4°C for 5 min. After dissolving pellets in 1 ml of isolation buffer, transferred into a glass hand-homogenizer. Mechanical disruption was achieved by 25 strokes in the glass potter and maintained always on ice. Following a serial centrifugation steps, first remaining intact cells and nuclei were separated from cytoplasm and then, crude mitochondria from cytoplasm. Crude mitochondria pellet was resuspended in MOPS buffer (250 mM sucrose, 10 mM MOPS (Calbiochem, 475898), 1 mM EDTA pH 8.0, pH 7.2) supplemented with 0.1% (v/v) protease inhibitor cocktail, 1 mM NaF, 0.2 mM NaVO₃ and 0.1 mM PMSF and loaded on top of the precooled sucrose density gradient consisting of 4 distinct sucrose layers with 60, 32, 23 and 15% sucrose solutions, respectively. After ultracentrifugation (Beckman Coulter, Optima Max-XP) at 134.000×g and 4 °C for 1 h the mitochondrial

fraction was visible as a yellowish pellet between 60% and 32% sucrose layers. The mitochondrial fraction was collected with glass pipet and washed with MOPS buffer to remove remaining sucrose solution. Resulting pellet was dissolved in protease inhibitor cocktail and 1 mM PMSF containing RIPA buffer and mitochondrial protein isolation was performed as described above. Bradford assay was used to measure protein concentrations. Purity control of the isolated mitochondria was achieved by immunoblotting of 50-100 μ g mitochondrial fractions and blotting with antibodies against mitochondrial and cytoplasmic proteins.

2.6 IMMUNOPRECIPITATION TESTS

To analyze protein-protein interactions in cells or more specifically on mitochondria, protein lysates were incubated with either Flag-beads (Anti-Flag M2 affinity gel; Sigma A2220) or protein-A/G agarose beads (Santa Cruz Biotech., sc-2001 and sc-2002) that are precoupled with specific antibodies for immunoprecipitation experiments. 25 μ l of beads for each condition were used and washed once with 250 μ l of PBS, once with 250 μ l of RIPA buffer and once with 250 μ l of protease inhibitor supplemented RIPA buffer by centrifugation at 4°C, 6000g for 1 min. 1 mg for overexpressed proteins and 2.5 mg of endogenous proteins were loaded onto the prewashed beads and the total volume filled up to 250 μ l with protease inhibitor containing RIPA buffer. 100 μ g of protein samples was boiled with 3X loading dye as input control. Samples were allowed over-night rotation at 4°C. Then, unbound proteins were washed away by 6 repeats of centrifugation steps with 500 μ l of homemade protease inhibitor (500X) and 1 mM PMSF containing RIPA buffer. After last wash, bead pellets were boiled with 3X loading dye in order to elute bound proteins. Elutes and input controls of each condition were separated in 12% tris-glycine gels.

2.7 IMMUNOFLUORESCENCE TESTS

For immunofluorescence tests, HeLa cells were cultured directly on cover slips in 12-well plates. 25.000 HeLa cells were plated per well. For HEK/293T cells, cover slips were pre-coated with 0.01 % poly-L-lysine (Sigma, P8920). Sterile cover slips were placed in 10 cm² plates and 100 µl of 0.01 % poly-L-lysine solution added onto each cover slips and incubated for 10 mins at RT. Poly-L-lysine solution was removed from the top of the cover slips and cover slips air-dried. Then, slides were washed once with sterile PBS and placed into 12-well plates. 30.000 HEK/293T cells splitted into each well that contains cover slips inside drop by drop.

Following desired transfections and treatments, growth media was removed and washed once with sterile filtered PBS. Cells were fixed with 4% paraformaldehyde ph 7.4 (PFA; Sigma, P6148) for 30 minutes in dark and at RT under the chemical hood due to the toxicity of the chemical. Next, PFA is removed and cells were washed with PBS three times. If the cells were readily suitable for visualization of fluorescence-tagged proteins, 10 µl of mounting solution [50% glycerol (Appllichem, A4453) in filtered PBS] added on microscopy slides and cover slips were placed as the cell containing surface would meet the mounting solution. The excessive amount of mounting solution was removed with the help of dust-free papers and the edges of the cover slips were sealed with nail polish. After becoming dried, the slides were analysed under the confocal microscope with and 63x oil objective (Carl Zeiss, LSM710). If not, after fixation, cells were placed in parafilm covered wells of 6-well plate and therein incubated with 100 µl of blocking reagent [PBS with 0.1% BSA (Sigma, A4503) and 0.1% saponin (Sigma, 84510)] in order to permeabilize the sample for 30 minutes at 4°C by shaking. Following removal of blocking reagent, samples were incubated with 50 µl of primary antibodies diluted (with 1:100-1:200 ratio depending on the efficiency of each antibody) in blocking solution for 1 h, at RT on the shaker. Following primary antibody incubation, solution was removed and washed with PBS for 3 times and samples were incubated for further 1 h with fluorescent-tagged secondary antibodies diluted in blocking solution (1:500 ratio) at RT. Based on the host organisms of the primary antibodies following secondary antibodies were utilized. For primary antibodies produced in mouse host, Alexa Fluor 488 goat anti-

mouse IgG (Thermo Fisher Scientific, 982245), Alexa Fluor 594 goat anti- mouse IgG (Thermo Fisher Scientific, 927075), Alexa Fluor 568 goat anti-mouse IgG (Thermo Fisher Scientific, A11004) and Alexa Fluor 405 goat anti-mouse (Thermo Fisher Scientific, A31553) were used. For primary antibodies produced in rabbit host, Alexa Fluor 488 goat anti- rabbit IgG (Thermo Fisher Scientific, 948490), Alexa Fluor 594 goat anti- rabbit IgG (Thermo Fisher Scientific, 982384), Alexa Fluor 405 goat anti-rabbit IgG (Thermo Fisher Scientific, A31556), and Alexa Fluor 568 goat anti-rabbit IgG (Thermo Fisher Scientific, A11011) were used as secondary antibodies. Next, cover slides were washed, mounted on the slides and analyzed under confocal microscopy.

2.8 ANTI-DNA STAINING TEST

Cellular mitochondrial DNA amount was determined by using anti-DNA (Progen, Cat. No. 61014) staining according to manufacturers instructions and analyzed as described in (Lazarou et al., 2015). Briefly, cells were grown as described in the section 2.7. Following desired transfection and treatments, cells were fixed with 4% PFA and permeabilized by using BSA/Saponin solution. Following permeabilization, coverslides were incubated with 40 μ l of anti-DNA antibody overnight at 4°C with a 1:100 dilution in BSA/Saponin solution. Then Alexa Fluor 488 goat anti- mouse IgG (Thermo Fisher Scientific, 982245) used for secondary antibody incubation with 1:500 dilution. In the last wash of PBS, nuclear DNA was stained by using DAPI with a 1:10⁶ dilution for 5 minutes at RT. Slides were analyzed under confocal microscope.

For analysis, cellular green and blue signals were measured by using IMAGE J software. For mitochondrial DNA, nuclear blue signal was excluded from the green signal. And mtDNA over nuclear DNA ratio was calculated for at least 50-100 cells per condition. Statistical analyses were performed.

2.9 GEL FILTRATION ANALYSES

Gel filtration is fast protein liquid chromatography (FPLC)-based method used for separation of molecules according to their molecular sizes through an automated gradient control and peak collection. In gel filtration experiments, a porous matrix assisted separation was maintained by using a Superose™ 6 10/300 GL column (GE Healthcare, 17-5172-01) with a separation range of 5–5000 kDa or a Superdex-200 10/300 GL (GE healthcare, 17-5175-01) with a separation range of 10-600 kDa. The separation column was connected to the AKTA Prime FPLC system (GE Amersham Pharmacia AKTA FPLC UPC900/P920 System/Frac 900 fraction collector, US). Then first, the column was washed with sonicated 36 ml of deionized water (3 fold greater than of column bed volume) and [(1:1) 0,05% glycerol/RIPA buffer (without protease inhibitors)] until all the parameters (pressure: 1.5 MPa, flow rate: 0,5 ml/min., fraction volume: 0,5 ml, sample loop volume: 500 µl) become stable which were followed real-time on the UNICORN™ software of the AKTA system. Before loading protein samples to the column, the column was washed with 24 ml of sonicated protease inhibitors supplemented RIPA buffer and marker calibration was performed by using 250 µl of molecular weight marker as sample (Sigma, MWGF-1000).

Following marker calibration, 500 µl of samples cellular lysates, cytoplasmic or mitochondrial fractions which approximately contain 5-10mg protein were loaded and fractions were collected in every 0.5 ml volume. Between different samples, the column was re-calibrated with sonicated water, equilibration buffer and protease inhibitor containing RIPA buffer. 250 µl of 3X loading dye was added into each fraction. Samples were boiled and stored at -20°C until use for SDS-PAGE. Electrophoresis and following western blot analysis were performed as explained in detail above.

2.10 SILAC LABELLING AND EXPERIMENTATION

Stable isotope labelling with amino acids in cell culture (SILAC) is a method where during cell division, stable carbon, hydrogen or nitrogen isotopes [Heavy (Arg^{10} , Lys^8), Medium (Arg^6 , Lys^8), and Light (Arg^0 , Lys^0)] were incorporated into cellular proteins while growing cells in SILAC medium (Dengjel et al., 2007, 2012). These differential medium usages enabled relative comparisons between three different experimental conditions (represented in Figure 2.9 1). Cells were grown in indicated SILAC medium for at least 6 cell doubling period prior to settle up experiment.

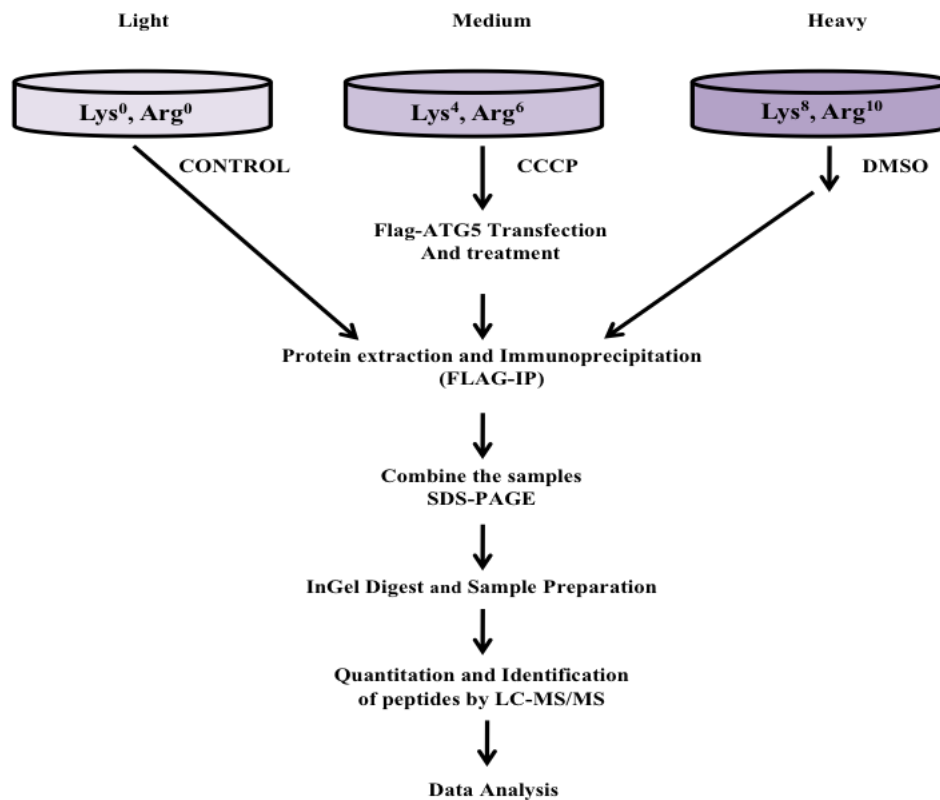


Figure 2.10 1: The pipeline of Tri-SILAC experiments starting from labelling cells with given amino acid containing medium to MS-derived data analysis.

Following cell labelling with stable isotopes, based on the requirements of the experimental plan, cells transfected and treated. Protein samples were extracted or cytoplasmic and mitochondrial fractions isolated. BCA assay was used for measurement

of protein concentrations. 1 - 1.5 mg of protein samples were used for immunoprecipitation experiments (Flag-IPs).

2.11 LIQUID CHROMATOGRAPHY, SAMPLE PREPARATION FOR MS/MS

Elutes were mixed and separated through a pre-cast SDS gel. SDS gels were stained with colloidal blue by using kit according to manufacturers instructions (Invitrogen, LC6025) in order to observe the immunoprecipitated proteins on the gel in correlation with expected molecular weights. The proteins in the gel were cut by scalper into 10 pieces and each pieces placed in one separate tube for further steps. In each tube, in-gel digestion was assessed using trypsin. After trypsin digest and serial vashing steps obtained peptides were analyzed by LC-MS/MS and data interpretation was achieved (Antonioli et al., 2017).

2.12 LC-MS/MS and MS DATA ANALYSIS

AGILENT HP 1200 HPLC series system connected a Q ExactiveTM Hybrid Quadrupole-Orbitrap Mass Spectrometer (Thermo Scientific, IQLAAEGAAPFALGMAZR) was utilized for LC-MS/MS analysis. Through the AGILENT system, HPLC was maintained with the use of a 15 cm silica emitting microcolumn (SilicaTip PicoTip; New Objective) self-packed with reverse-phase ReproSil-Pur C18-AQ beads (the size of 3,5 µm with a 20 µm inner diameter, Dr. Maisch, GmbH, Germany).

Through a linear gradient flow of a 10-30% acetonitrile in 0.5% acetic acid, peptides were allowed for separation with a 250 nl/min flow rate. In FT-MS, under the automated gain control value of 106 with a 60,000 resolution at m/z 400, full-scan mode acquired. 1000 counts and a upper filling limit of 100 ms were adjusted as tresholds for

repetitive MS/MS in the five samples exhibiting highest intensities varying in every sampling and automatic gain control (AGC) target value was determined as 5000 ions. Broad band selection was activated with a $q=0.25$ value for 30 ms over a uniform 35% of collision capacity. Ions that are single charged or unassigned were extracted a dynamic exclusion mode to eliminate ions from sequential MS/MS for 45 s.

The raw data obtained from LC-MS/MS, first subjected to a MaxQuant software run which allows large set of data interpretation with the given criteria. Following corrections in the MaxQuant run, MS-derived peptide peaks were converted into peptide sequences and these peptides were identified in an organism specific database. In our case, MaxQuant 1.4.0.8 version was used for peptide search with default parameters through human Uniprot database. Identified peptides having false discovery rate (FDR) below than 1% were omitted through forward-decoy searches and matches were facilitated between each run. Next, the identified protein list subjected to a several significance tests, including: Benjamini Hochberg and p-value tests by using Perseus software in order to obtain significant hits as interaction partner in at least two different biological replicates.

2.13 PROTEASOME ACTIVITY ASSAY MEASUREMENT

Proteasome activity assay is performed as described in (Liggett et al., 2010). But briefly, Suc-LLVY-AMC, Bz-VGR-AMC and Z-LLE-AMC substrates were solubilized in Assay buffer with a composition of 20 mM Tris-Cl pH 7.5, 1 mM EDTA, 1 mM NaN₃, 1 mM DTT in order to have final concentration of each 10 mM of substrate assay solution. The activity of 20S proteasomes were determined with the help of standard AMC calibration curve with a specific substrate consisting of a differentially increasing concentrations obtained by serial dilutions (0.125 μ M, 0.25 μ M, 0.5 μ M, 1 μ M, 2 μ M, 4 μ M, 8 μ M and 16 μ M).

Substrate assay buffer and Assay buffer with 1:1 ratio used as blank in duplicate wells with 40 μ l total volume per well. Substrates were incubated with cell lysates with 1:1 ratio in final 100 μ l, for 30 mins in water bath (37°C). At the end of 30 mins, each 40 μ l of samples from each tube pipetted into duplicate wells in dark-plate. The reaction then terminated with the addition of 200 μ l of 100 mM sodium chloroacetate dissolved in 30 mM sodium acetate, 70 mM acetic acid, pH 4.3. As soon as terminating solution added, plate is placed into fluorometer and measurement performed with the filters set for 360 nm and 460 nm wave lengths for excitation and emission respectively.

2.14 ATP ASSAY MEASUREMENT

Cellular ATP level was measured according to manufacturers instructions (ATP Bioluminescence Assay Kit HS II; Roche, Cat. No. 11 699 709 001). But in short, cellular ATP levels are determined by comparing the luciferase intensities of lysates with ATP standards. Cells are grown in 6 well plates prior to measurement. Following treatment, cells are harvested and diluted with a concentration of 10^5 to 10^8 cells/ml in 50 μ l in tubes or 25 μ l in microplates. Lysis buffer is added onto the samples and standards. Following 5 minutes incubation at RT, 50 μ l of samples placed into the wells of dark microplate and 50 μ l of luciferase reagent is added per each well. Right after luminometric measurement performed and blank values are extracted from raw data.

3. RESULTS

3.1 CONFIRMATION AND CHARACTERIZATION OF ATG5-PSMA7 INTERACTION

3.1.1 Confirmation of ATG5-PSMA7 interaction in mammalian cells.

The initial Y2H screen was performed in the establishment of the lab by former students. According to Y2H screen, PSMA7 was identified as one of the candidates interacting with ATG5 (for sequence analysis please see Appendix B.1).

In order to validate the Y2H screen in mammalian cells, various immunoprecipitation experiments performed. The experimental set ups in order to confirm the ATG5 and PSMA7 interaction in mammalian cells represented in the pipeline (Figure 3.1.1 1).

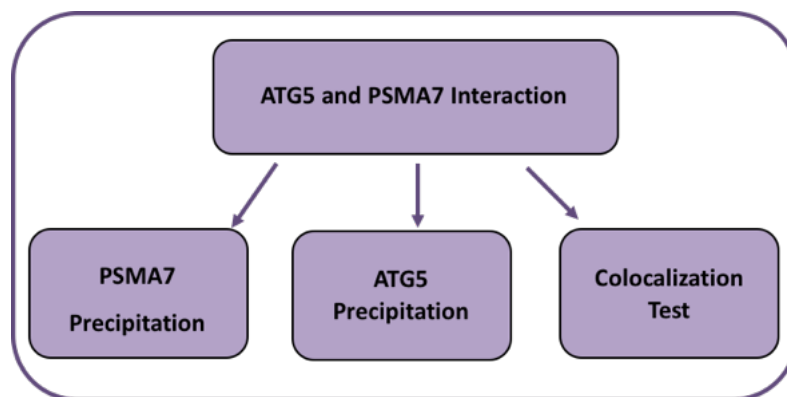


Figure 3.1.1 1: The pipeline of validation methods of ATG5-PSMA7 interaction in mammals.

Utilizing the high protein productivity of HEK/293T cells, following co-transfection experiments of both ATG5 and PSMA7 constructs, PSMA7 immunoprecipitation experiments were performed and ATG5 binding to PSMA7 was observed. The western blots following immunoprecipitation experiment shown in Figure 3.1.1 2.

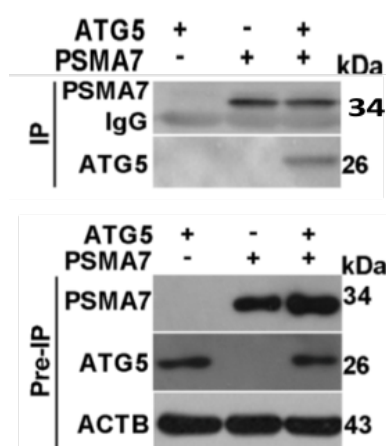


Figure 3.1.1 2: PSMA7 immunoprecipitation experiment result of HEK/293T cells. HEK/293T cells were transfected with Flag-tagged PSMA7, non-tagged human ATG5 or co-transfected with both of the plasmids. 48 h after transfection, cells were harvested and proteins isolated. Following concentration measurement, proteins were incubated with FLAG-beads for immunoprecipitation tests overnight at 4°C. For immunoblotting experiments, ATG5, FLAG and β -ACTIN antibodies were used. *Pre-IP*, Total protein lysates; *IgG*, Immunoglobulin G. β -ACTIN was used as loading control. N=3 independent experiments were performed and one of them shown as representative.

In other way around, immunoprecipitation of ATG5 could also co-precipitate PSMA7 as shown in Figure 3.1.1 3.

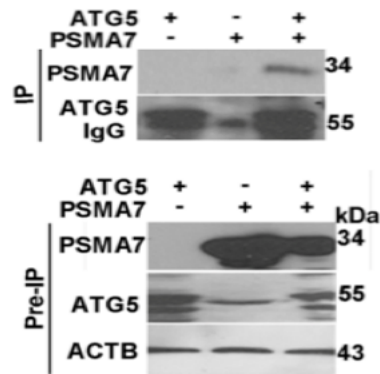


Figure 3.1.1 3: ATG5 immunoprecipitation experiments were performed in HEK/293T cells. HEK/293T cells were transfected with Flag-tagged PSMA7, pmCherry-tagged ATG5 or co-transfected with Flag-tagged PSMA7 and pmCherry-tagged ATG5 constructs. Following 48 h of transfections, cell lysates were incubated with ATG5 antibody coupled protein G agarose beads overnight at 4°C. Immunoprecipitated proteins were analyzed by immunoblotting experiments using FLAG, ATG5 and β -ACTIN antibodies. *Pre-IP*, Total protein lysates; *IgG*, Immunoglobulin G. β -ACTIN was used as loading control. N=3 independent experiments were performed and one of them shown as representative.

The interaction between endogenous proteins rather than overexpressed versions were tested by using mouse embryonic fibroblast (MEF) cells. Related result was shown in Figure 3.1.1 4. In endogenous immunoprecipitation experiments also PSMA7 and ATG5 protein interactions were verified.

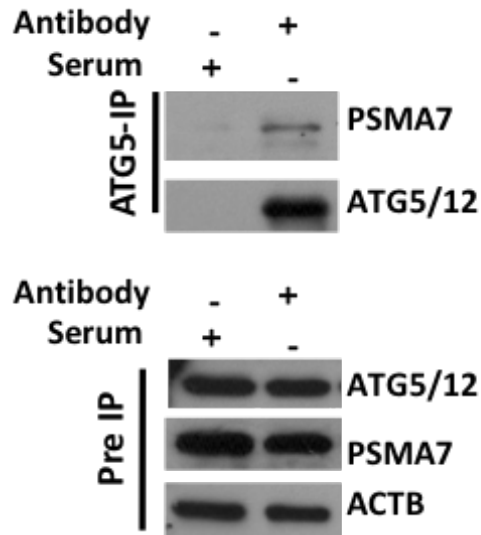


Figure 3.1.1 4: Endogenous ATG5 immunoprecipitation experiments were performed in HEK/293T cells. HEK/293T cells were cultured until they become confluent for 48-72 h. Cell lysates were used for immunoprecipitation with ATG5 antibody coupled protein G plus agarose beads. *Serum*, Rabbit serum for negative control; *Pre-IP*, Total protein lysates; *IgG*, Immunoglobulin G. β -ACTIN was used as loading control. N=3 independent experiments were performed and one of them shown as representative.

As an additional way of to test protein-protein interactions, colocalization of ATG5 and PSMA7 was analyzed by using confocal microscopy. According to data shown in Figure 3.1.1 5, under basal, nutrient rich conditions fluorescent-tagged both proteins were partially colocalized around perinuclear area of the cells.

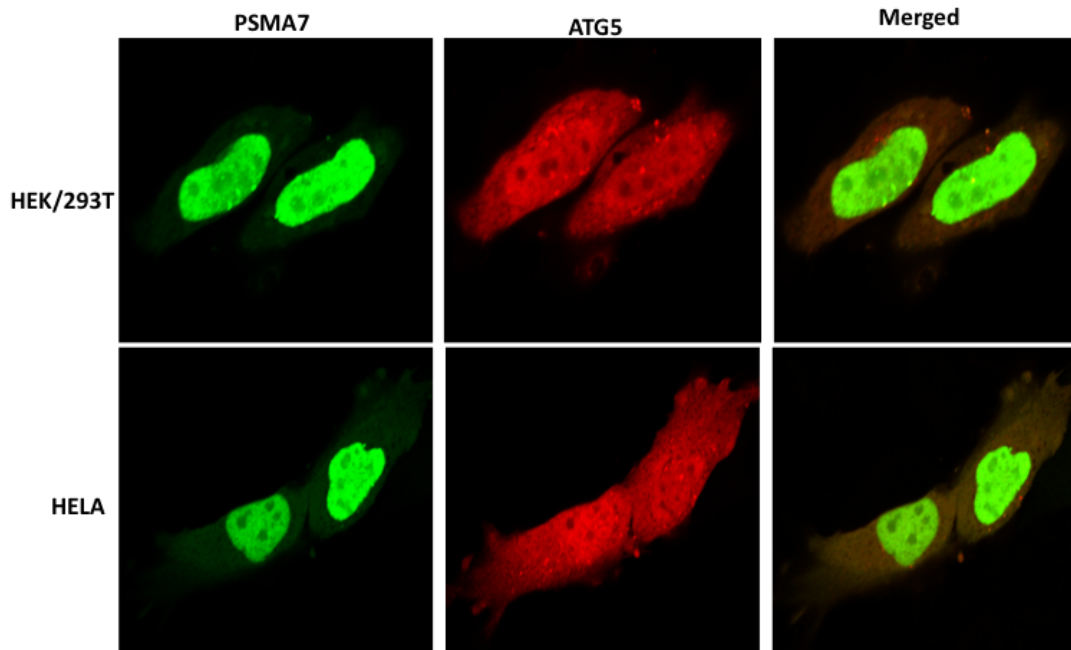


Figure 3.1.1 5: The colocalization experiments were performed in HEK/293T (Upper part) and HELA (Lower part) cells. Cells were cultured on cover slips and co-transfected with pEGFP-tagged PSMA7 (Green) and pmCherry-tagged ATG5 (Red). Following 48 h of post transfection, cells were fixed with 4% PFA and analyzed under confocal microscope. *Merge*, the overlay of Green and Red signals of the cells. N=3 independent experiments performed.

Conclusively, several immunoprecipitation experiments and colocalization tests were all indicated that PSMA7 is a novel interaction partner of ATG5. This interaction is very important due to the being first direct interaction shown between the UPS and autophagy systems.

3.1.2 ATG5-PSMA7 Interaction Modelling

Next, we would like to map the interaction between ATG5 and PSMA7 proteins in order to understand the critical parts of the PSMA7 for ATG5 binding. In order to map the ATG5 and PSMA7 proteins several computational and biochemical tests were performed as described in the pipeline (Figure 3.1.2 1).

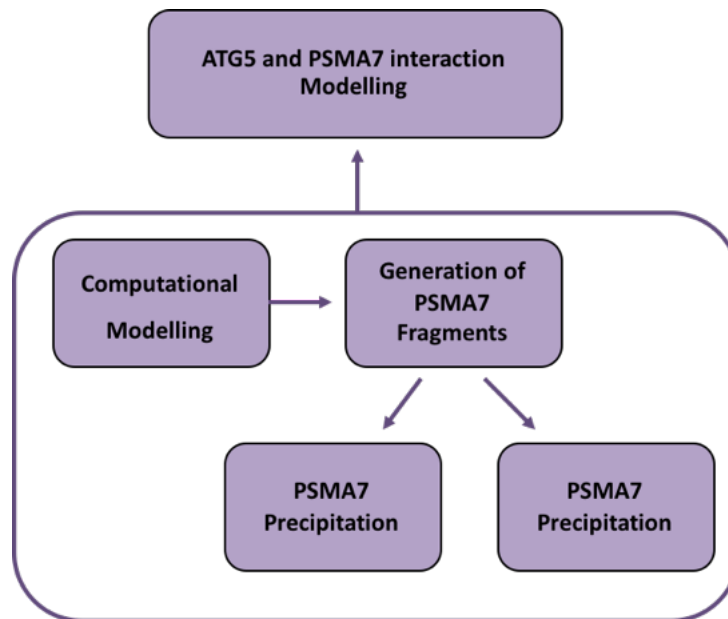


Figure 3.1.2 1: The pipeline of the performed experiments in order to address the ATG5-PSMA7 interaction domain.

By computational modelling performed by Sezerman group (Figure 3.1.2 1), it is suggested that C-terminal part of the PSMA7 especially is important for the protein-protein interaction through salt bridges (Figure 3.1.2 2).

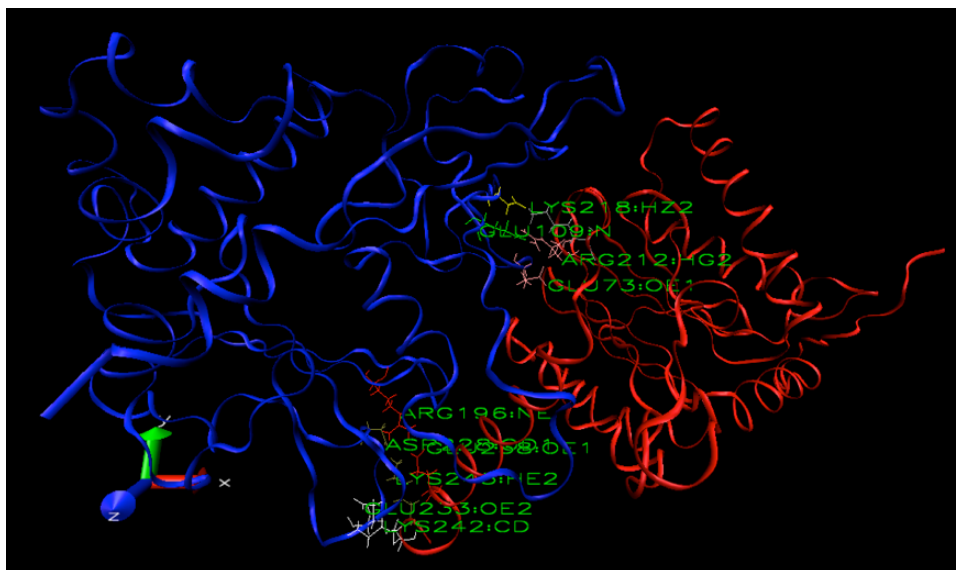


Figure 3.1.2 2: Computational Modelling of ATG5 (PDB Code: 4GDK, Blue) and PSMA7 (PDB Code: 1IRU, Red) (Performed by Sezerman Group).

Table 3.1.2 1: Critical residues for ATG5-PSMA7 Interaction

Important Residues For ATG5-PSMA7 Interaction
ARG196_ATG5-GLU238_PSMA7
ARG30_ATG5-ASP67_PSMA7
ASP111_ATG5-ARG212_PSMA7
ASP111_ATG5-LYS218_PSMA7
ASP228_ATG5-LYS243_PSMA7
ASP231_ATG5-LYS243_PSMA7
GLU109_ATG5-ARG212_PSMA7
GLU109_ATG5-LYS218_PSMA7
GLU233_ATG5-LYS242_PSMA7
GLU71_ATG5-ARG212_PSMA7
GLU71_ATG5-ARG213_PSMA7
GLU73_ATG5-ARG212_PSMA7
LYS201_ATG5-GLU235_PSMA7
LYS201_ATG5-GLU238_PSMA7

According to modelling, all important residues in terms of the interaction is listed in the Table 3.1.2 1. According to this list, it is seen that C-terminal part of the PSMA7 and N- and C-terminal part of the ATG5 protein could be involved in the protein-protein interaction. Based on this finding, using PCR-based cloning strategies, Flag-tagged N- and C-terminal fragments of PSMA7 were generated. F1 represents N-terminal fragment of the protein, F2 represents C-terminal fragment of the protein which also corresponds the Y2H sequence as well as important residues according to modelling (Figure 3.1.2 3).

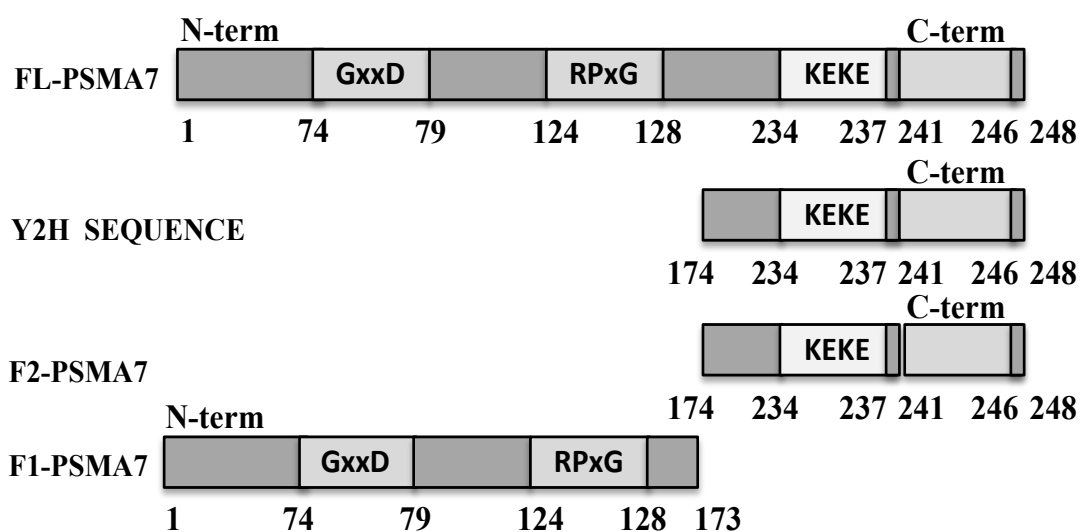


Figure 3.1.2 3: Schematic representation of PSMA7 fragments.

In order to map the interaction between ATG5 and PSMA7, Flag-tagged PSMA7 constructs were immunoprecipitated and co-precipitated ATG5 levels analyzed. According to data shown in Figure 3.1.2 4, F2 fragment showed more affinity to bind ATG5 than F1 fragment proving that C-terminal part is critical for ATG5 interaction.

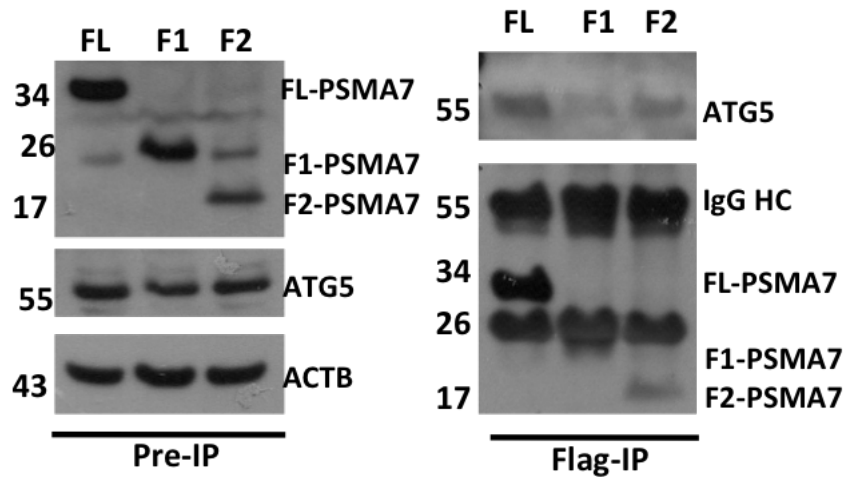


Figure 3.1.2 4: Interaction mapping experiments in HEK/293T cells. HEK/293T cells grown in 10 cm² plates with a 1.5x10⁶ cells per plate. Following 16 h of passaging, cells were transfected with Flag-tagged full length, N-terminal or C-terminal fragments of PSMA7. 48 h of porttransfection, cells were harvested, and protein lysates were incubated with Flag-beads. Immunoprecipitated proteins were eluted in 3x loading dye and samples separated through 12 % SDS-PAGE. For immunoblots, FLAG and ATG5 antibodies are used. ACTB, β -Actin is used for loadig control. Pre-IP, lysate control; Flag-IP, Flag Immunoprecipitation; FL, Full length; F1, N-terminal fragment and F2, C-terminal fragment (n=6 independent experiments performed in HEK/293T cells).

Additionally, we checked potential inhibitory effect of C-terminal fragment of PSMA7 on full length PSMA7 for ATG5 binding. To test this, ATG5 protein was precipitated and co-precipitating PSMA7 fragments were analyzed. According to data shown in Figure 3.1.2 4, full length PSMA7 and C-terminal fragments bind to ATG5. Yet, when the two constructs co-expressed, their individual binding for ATG5 decreased.

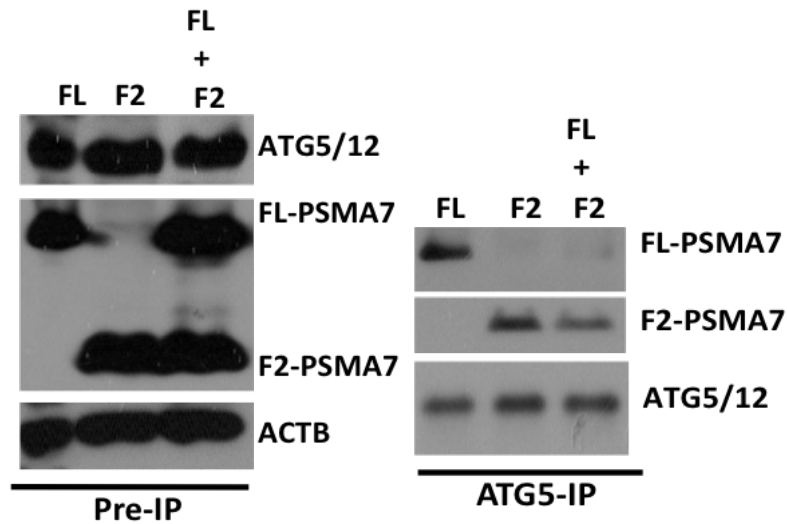


Figure 3.1.2 5: Competition test between full length PSMA7 and C-terminal Fragment of the protein in HEK/293T cells. HEK/293T cells were grown in 10 cm² in a cell density of 1.5x10⁶ per plate. Cells were transfected with Flag-tagged full length PSMA7 or C-terminal fragment of PSMA7 or both fragments were co-transfected. 48 h of post-transfection, cells were harvested and proteins out of them isolated. Cell lysates were incubated with ATG5 antibody coupled-beads overnight at 4°C. Immunoprecipitated proteins were eluted in protein sample buffer by heating for 10 minutes at 95°C. Denaturated samples were separated through 12 % SDS-PAGE. For immunoblotting, FLAG and ATG5 antibodies were used. *ACTB*, β -Actin was used for protein loading control. *Pre-IP*, cell lysate control; *ATG5-IP*, ATG5 Immunoprecipitation; *FL*, Full length and *F2*, C-terminal fragment of PSMA7.

3.1.3 Analysis of The Dynamics in ATG5-PSMA7-Parkin Interaction

In order to understand the dynamic nature of the interaction, under various stress conditions the affinity of the proteins for binding was evaluated. Several different experimental approaches were utilized as represented in the Figure 3.1.3 1.

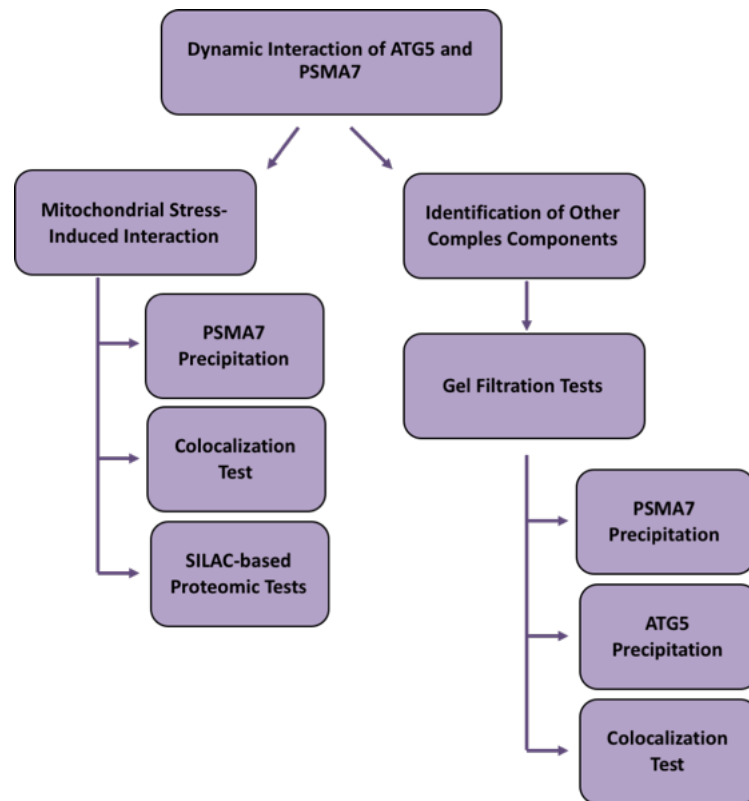


Figure 3.1.3 1: List of performed experiments to analyze stress-induced dynamic Interaction ATG5-PSMA7 interaction and investigation of other complex components.

One of the first observations about colocalization in perinuclear area of the cells had directed us to stimulate cells with mitochondrial stress inducers, including CCCP and staurosporine.

PSMA7 immunoprecipitation experiments showed almost two-fold increased ATG5 binding after CCCP and staurosporine treatments compare to DMSO treated control conditions (Figure 3.1.3. 2).

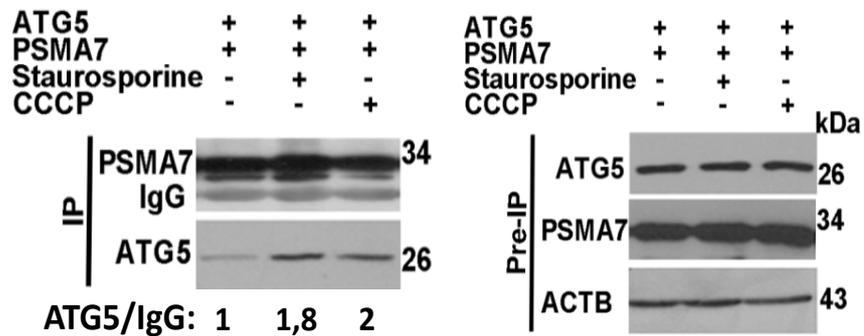


Figure 3.1.3 2: PSMA7-Immunoprecipitation experiments performed in HEK/293T cells. Flag-PSMA7 overexpressed cells exposed to Staurosporine (1 μ M for 12 h), CCCP (10 μ M for 12 h) and DMSO as control. Cell lysates were incubated with FLAG-beads for overnight at 4°C. Protein-protein interactions were analyzed by immunoblotting following SDS-PAGE experiments. *Pre-IP*, lysate control; *IP*, Immunoprecipitation; *IgG*, Immunoglobulin G; *kDa*, kilodaltons. For blotting experiments, ATG5 and PSMA7 antibodies used. β -ACTIN was used as loading control for lysates. The band intensities were measured by using Image J software.

Colocalization experiments in HEK/293T cells showed increased accumulation of ATG5 and PSMA7 dots around nucleus which were confirming increased interaction between ATG5 and PSMA7 upon mitochondrial stress (Figure 3.1.3 3).

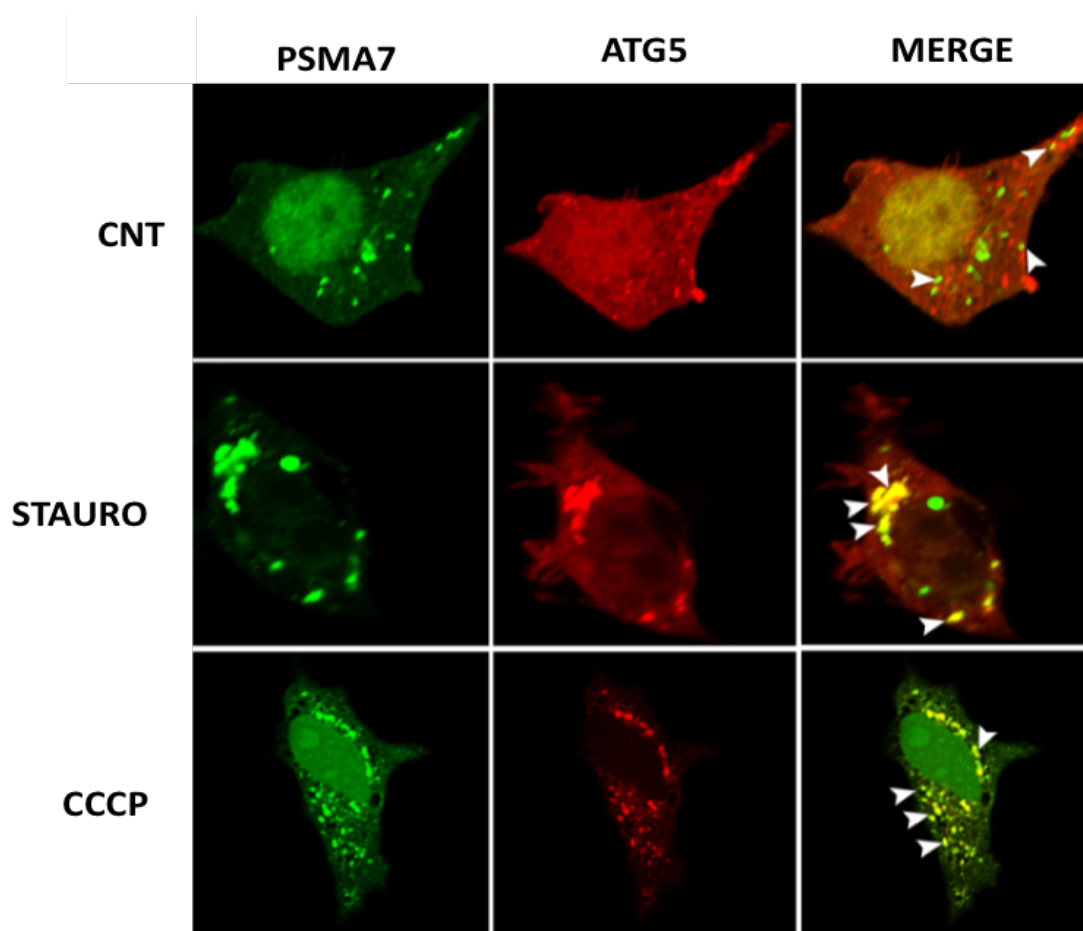


Figure 3.1.3 3: Colocalization experiments of PSMA7 and ATG5 with mitochondrial stress inducers in HEK/293T cells analyzed by confocal microscopy. HEK/293T cells were grown on Poly-L-lysine coated cover slips and following 48 h post-transfection, cells were treated with Staurosporine (1 μ M, 12 h), CCCP (10 μ M, 12 h) and DMSO as treatment control. Following treatment, cells were fixed with 4% PFA and analyzed by using confocal microscopy.

Similar colocalization tests were performed in HELA cells and according to data shown in Figure 3.1.3 4, mitochondrial stress increased PSMA7 and ATG5 colocalization.

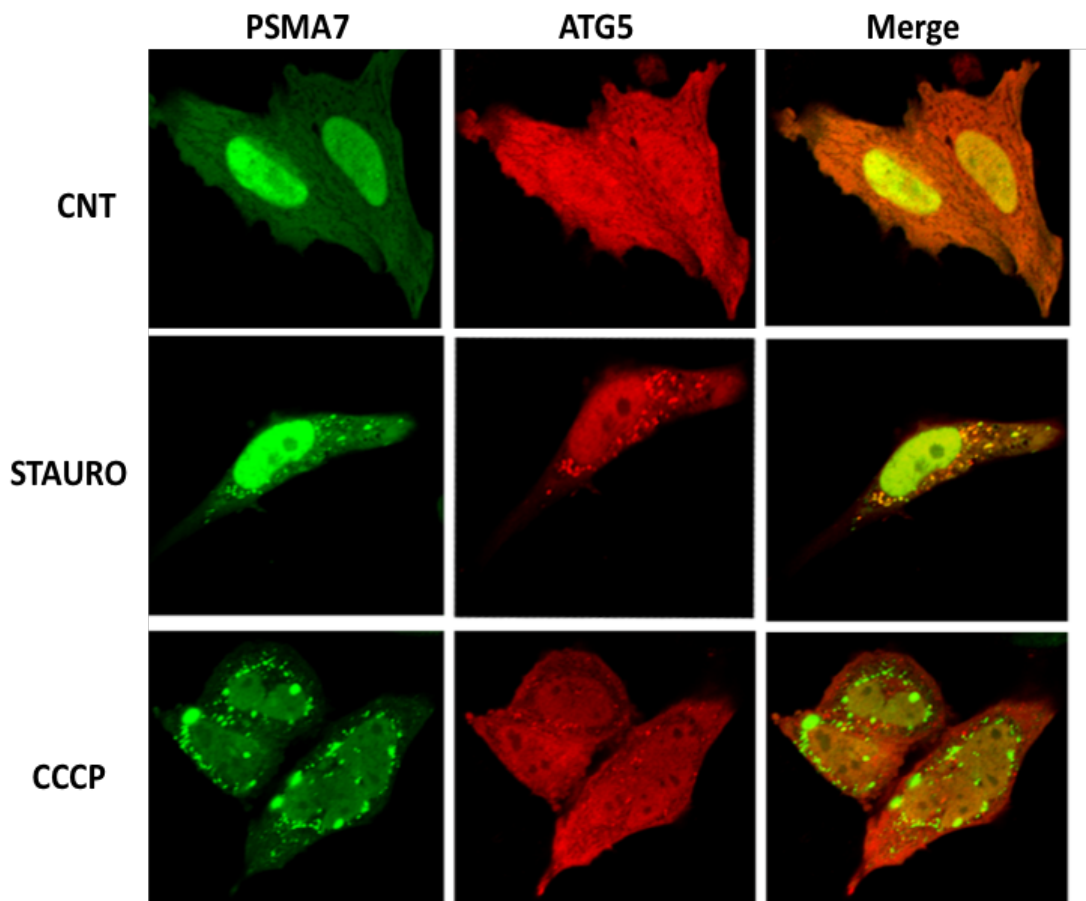


Figure 3.1.3 4: Colocalization experiments of PSMA7 and ATG5 with mitochondrial stress inducers in HELA cells analyzed by confocal microscopy. HELA cells were splitted on coverslides and 16 h after splitting co-transfected with pmCherry-tagged ATG5 and pEGFP-tagged PSMA7. Following 12 h of treatment (Stauro, 1 μ M; CCCP 10 μ M), cells were fixed with 4%PFA and visualized under confocal microscope.

The dynamic interaction between the proteins were further analyzed with a SILAC-based quantitative proteomics in HEK/293T cells. HEK/293T cells were cultured for two weeks prior to experimentation with three different SILAC labels containing cell culture medium. SILAC labelled cells were used for FLAG immunoprecipitation and further LC-MS/MS experiments. By utilizing this method, the mitochondria stress-induced increased ATG5-PSMA7 interaction was confirmed. In Figure 3.1.3 5, the increased ATG5 and PSMA7 complex formation was shown in graphical illustration.

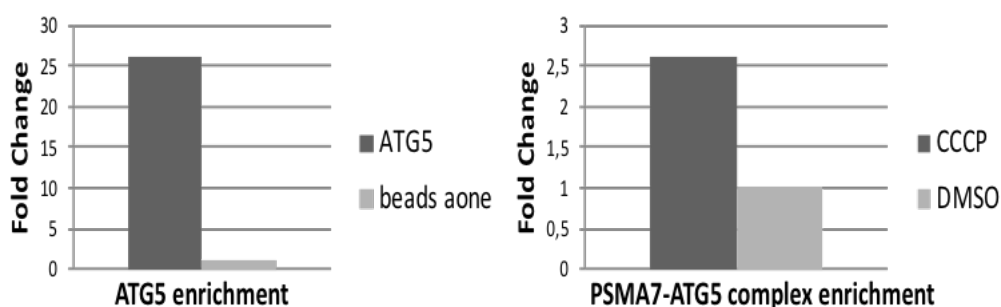


Figure 3.1.3 5: SILAC-based LC-MS/MS analysis results of HEK/293T cells. SILAC labelled cells were transfected with Myc-ddk-tagged ATG5 construct for 48 h. Following 12 h of CCCP (10 μ M) treatment, cell lysates were used for FLAG immunoprecipitation tests. After mixing all conditions, following gel electrophoresis, samples were prepared for LC-MS/MS. The fold change graphs were compared with beads alone (left); enrichment of PSMA7-ATG5 complex under CCCP conditions were compared with DMSO control condition (right) (n=1).

In order to further analyze the protein complexes in a closest to native structure, size exclusion chromatography-based gel filtration experiments were performed. HEK/293T cells were treated with DMSO and mitochondrial stress inducers used as autophagy triggering factors. Cellular lysates were separated through a Superdex 200 column with a separation range of 10 to 600 kDA. According to representative data shown in Figure 3.1.2 5, it was observed that there have been two different protein complexes containing ATG5, PSMA7, PARKIN and PINK1 proteins. The components of the first complex are ATG5-12, PARKIN and PINK1. On the other hand, the second complex was composed of PARKIN, PSMA7 and additionally decreased overlapping fractions of ATG5-12 protein.

As it could be interpreted in the graphical illustrations of Figure 3.1.2 5, PSMA7 and PINK1 were differentially contributed to the ATG5-PARKIN containing protein complexes to generate bigger complexes. Another observation obtained from gel filtration experiments was an indication of a disassociation of a protein with CCCP

treatment due to the protein band shifts at the fraction number 3. Additionally, in line with the previous results, CCCP induced the formation of the ATG5 and PSMA7 containing complex (please see the fraction numbers 4, 5 and 6 in Figure 3.1.3 6).

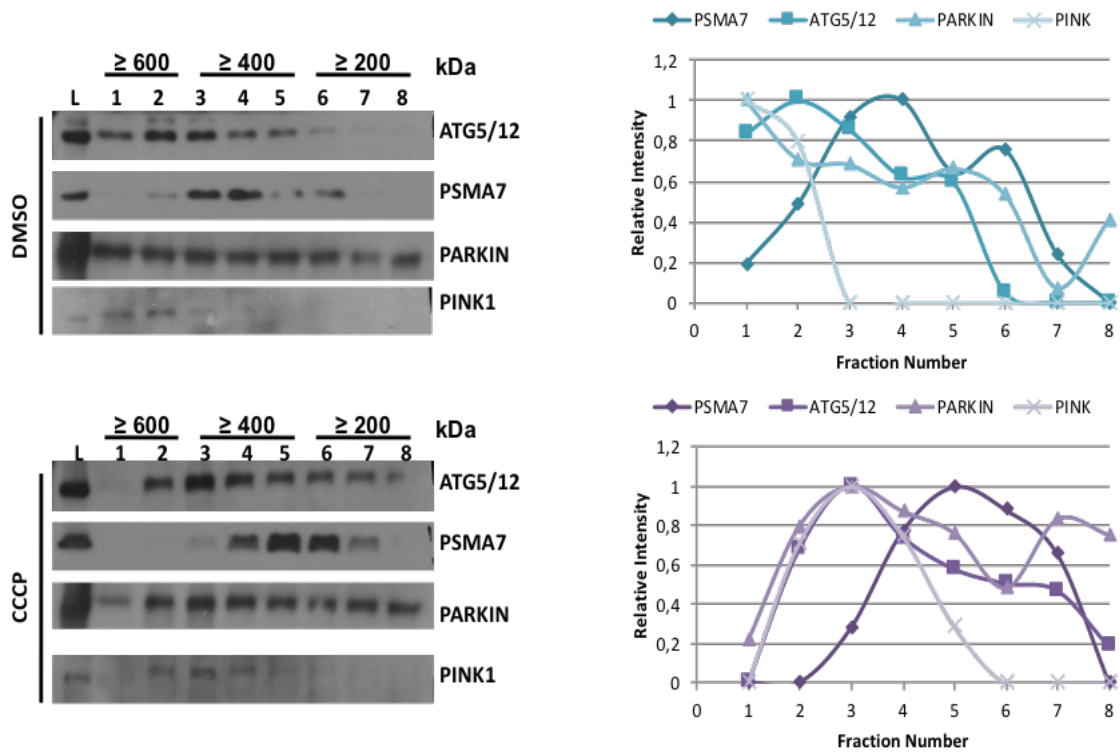


Figure 3.1.3 6: Gel filtration tests of HEK/293T cell-derived total lysates. HEK/293T cells were transfected with Myc-tagged Parkin construct for 48 h. Following treatment with CCCP (10 μ M), 5-10 mg of total cell lysates were applied to the calibrated Superdex 200 10/300 GL (GE Healthcare, 17-5175-01) and 20 fractions collected for each condition. Fractions were separated through SDS-PAGE and ATG5, PSMA7, PARKIN and PINK1 antibodies used for immunoblotting. *L*, Lysate control and *kDa*, kilodaltons (left panel). The graphics were prepared based on the band intensities of the western blots (right panel). The normalization of the bands was performed according to the lysate intensities and the highest intensity of each protein type was set to 1.

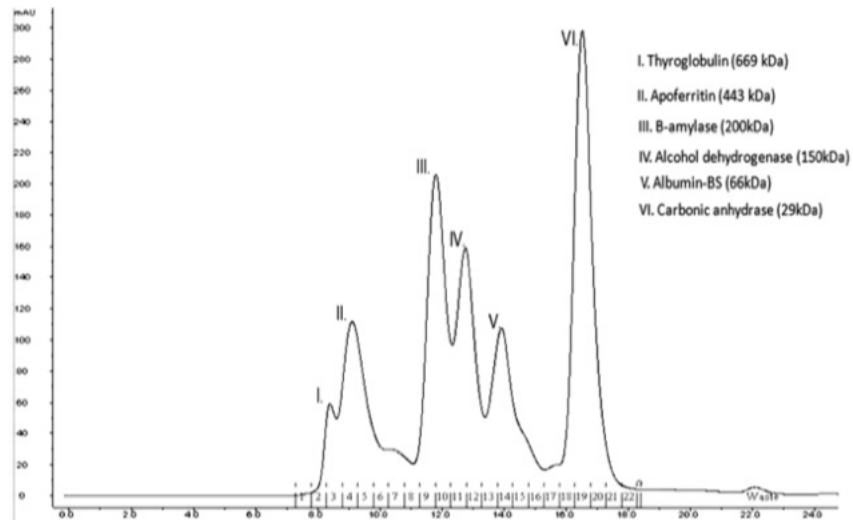


Figure 3.1.3 7: The molecular weight marker calibration peaks of the gel filtration experiments over Superdex 200 column.

Prior to loading protein samples, commercially available molecular marker mix (Sigma, MWGF1000) was separated through the column and the proteins included in the mix was observed in different peaks related to chromatogram.

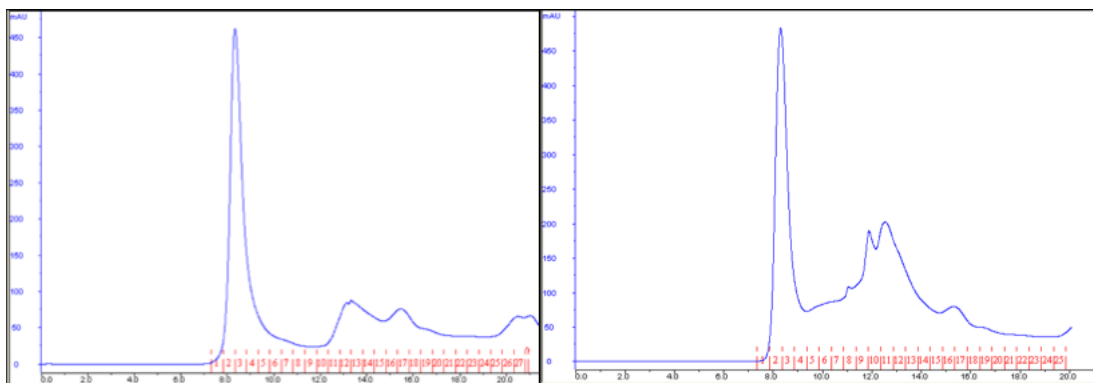


Figure 3.1.3 8: Representative chromatograms of DMSO treated control cell lysates (left panel) and CCCP treated cell lysates (right panel) of HEK/293T cells through the FPLC separation.

Based on the observations derived from gel filtration experiments, PSMA7 immunoprecipitations were performed in order to prove the formation of the different complexes in HEK/293T cells. By immunoprecipitating PSMA7, we could observed Parkin binding and with CCCP and Staurosporine the binding affinity of Parkin to PSMA7 enhanced (Figure 3.1.3 9).

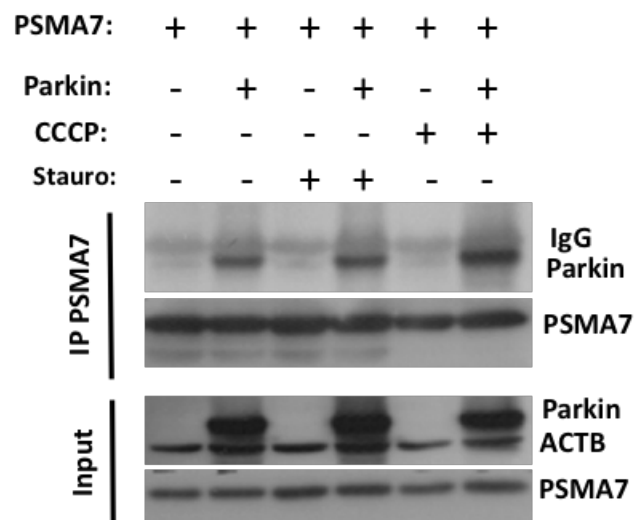


Figure 3.1.3 9: Confirmation of PSMA7 and PARKIN interaction by performing immunoprecipitation experiments in HEK/293T cells. Cells were harvested after 48 h of Flag-tagged PSMA7 and Myc-tagged PARKIN cotransfection and 12 h of Staurosporine (1 μ M) and CCCP (10 μ M) treatment. Following protein extraction and concentration measurement, lysates were incubated with Flag-beads for 16 h at 4°C. Precipitants were eluted and used for further SDS-PAGE and immunoblotting experiment. *Input*, lysate control; *IgG*, Immunoglobulin G; *ACTB*, β -Actin. For blotting, PSMA7 and Parkin antibodies were used. β -Actin antibody was used as loading control.

After proving the CCCP mediated dynamic interaction between PSMA7 and Parkin, the interaction between ATG5 and Parkin also analyzed in HEK/293T cells with ATG5 immunoprecipitation experiments. Under basal conditions, there were no or difficult to detect interaction between ATG5 and Parkin. However, with CCCP treatment the binding of Parkin to ATG5 significantly enhanced proving the formation of ATG5-Parkin-PSMA7 complex in cells (Figure 3.1.3 10).

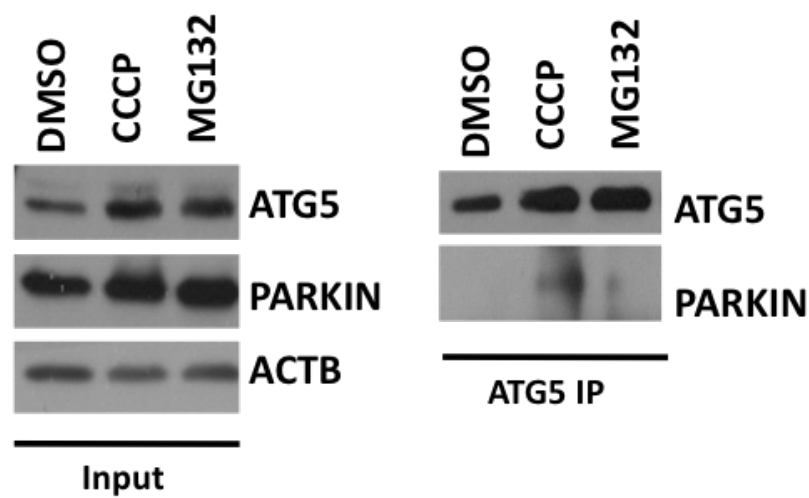


Figure 3.1.3 10: ATG5 immunoprecipitation tests for Parkin binding in HEK/293T cells. HEK293T cells were transfected with YFP-tagged Parkin construct for 48 h. Following CCCP (10 μ M, 12 h) and MG132 (30 μ M, 3 h), lysates were incubated with ATG5 antibody coupled protein A plus agarose beads overnight. Immunoprecipitants after elution used for SDS-PAGE. ATG5, Parkin and β -Actin antibodies were used for blotting. *Input*, lysate control; *ACTB*, β -Actin. β -Actin antibody was used as loading control.

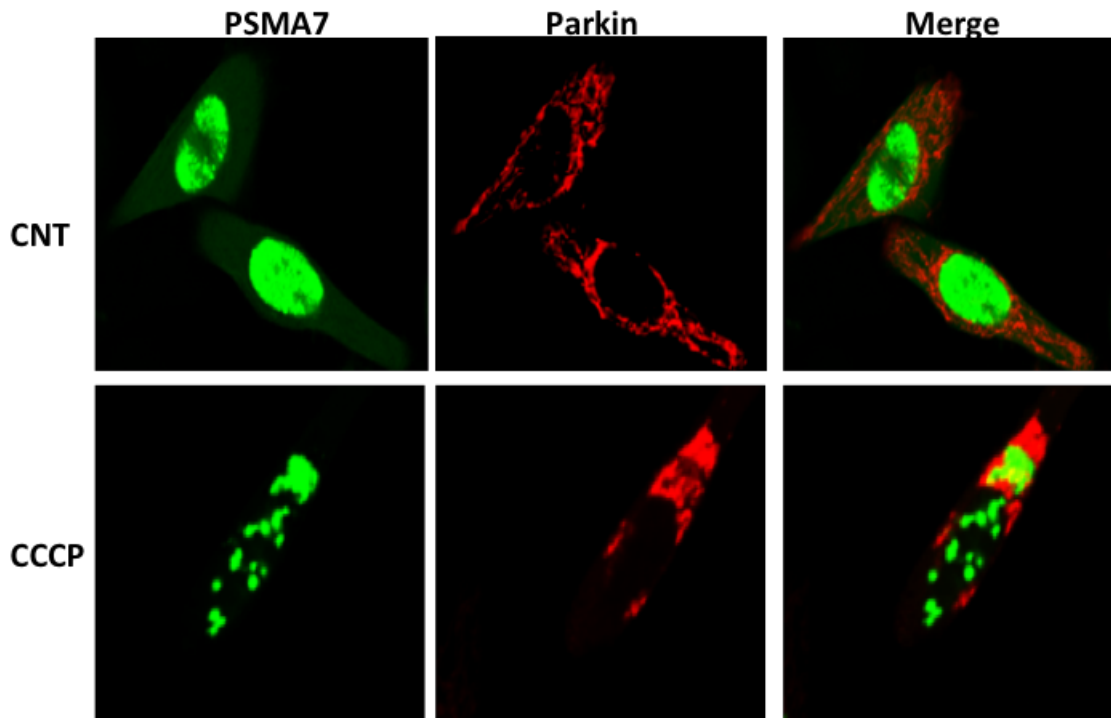


Figure 3.1.3 11: Colocalization experiments of PSMA7 and PARKIN with CCCP treatment in HEK/293T cells analyzed by confocal microscopy. HEK/293T cells were cotransfected with pEGFP-tagged PSMA7 (Green) and mCherry-tagged Parkin (Red) constructs. Following 12 h of CCCP treatment, cells were fixed and analyzed by confocal microscopy. *Merge*, overlay of green and red signals coming from the cells.

Furthermore, to support gel filtration and immunoprecipitation experiments, colocalization tests were also performed in HEK/293T and HELA cells.

As illustrated in Figure 3.1.3 11 and 3.1.3 12, respectively in HEK/293T and HELA cells, CCCP induced PSMA7 and Parkin colocalization in a similar trend of PSMA7 and ATG5 colocalization in accumulated form around perinuclear area.

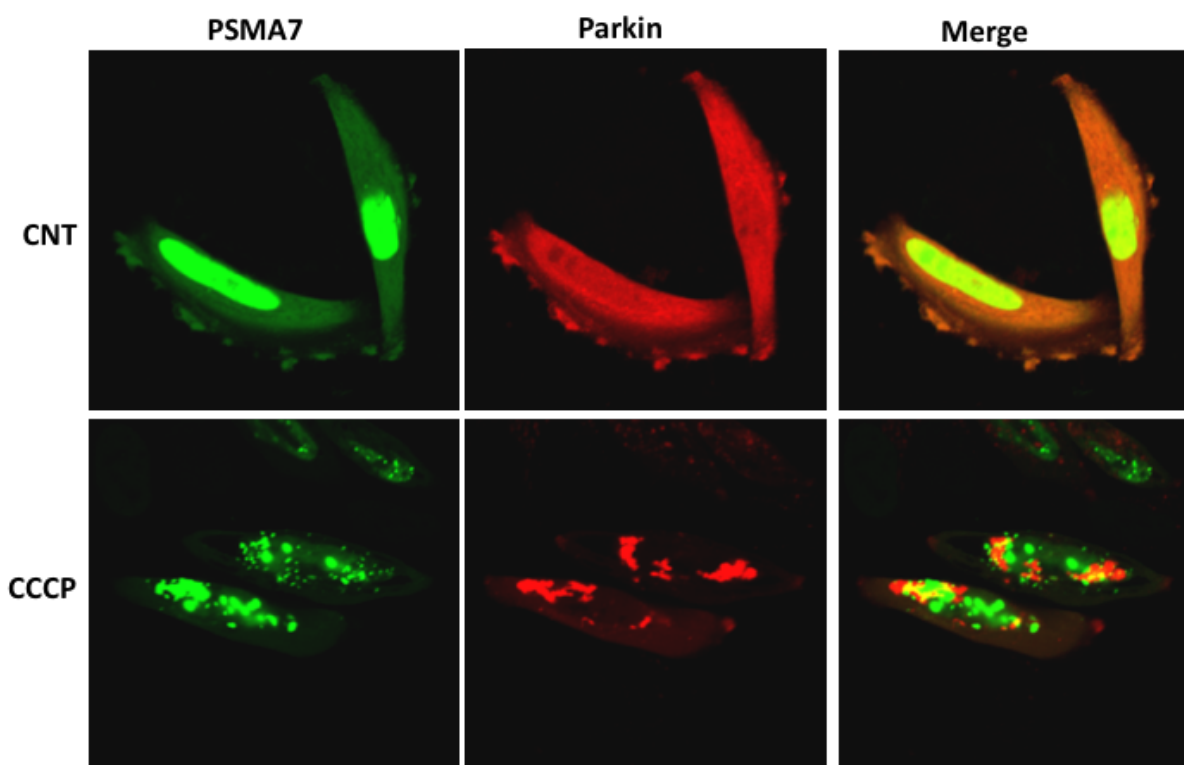


Figure 3.1.3 12: Colocalization experiments of PSMA7 and PARKIN with CCCP treatment in HELA cells analyzed by confocal microscopy. HELA cells were co-transfected with pEGFP-tagged PSMA7 (Green) and pmCherry-tagged Parkin (Red) constructs. Following 12 h of CCCP treatment, cells were fixed with 4% PFA and analyzed by using confocal microscopy. *Merge*, the overlay of the green and red signals coming from the cells.

In order to test the observed CCCP-induced increased interaction between ATG5 and PSMA7 was due to the potential of autophagic degradation of PSMA7 or even whole proteasomes, we checked protein levels upon drug treatments. Regardless from Parkin, Staurosporine and CCCP did not cause any significant decrease in cellular PSMA7 and PSMB5 levels (Figure 3.1.3 13).

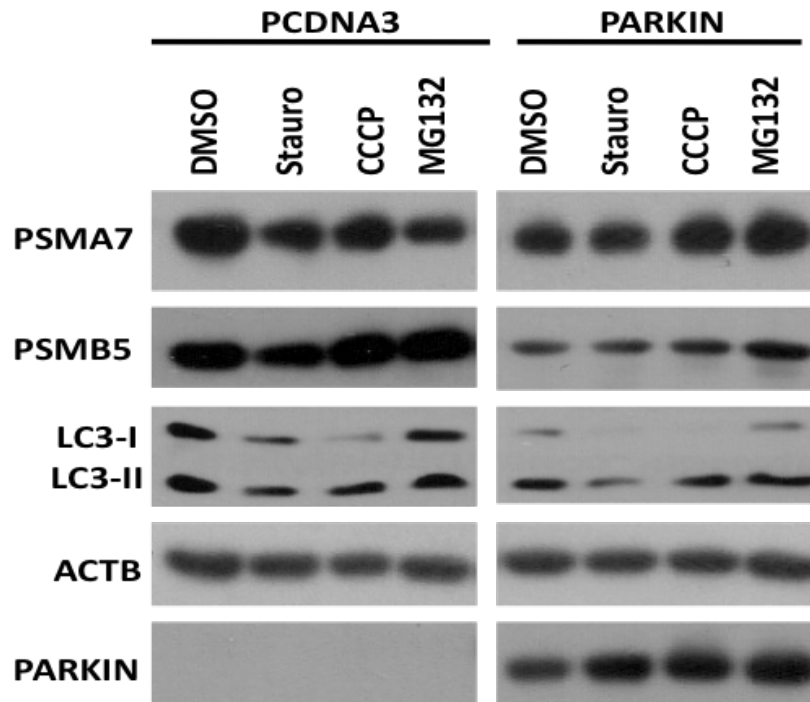


Figure 3.1.3 13: PSMA7 and PSMB5 are not the targets of autophagic degradation. HEK/293T cells were either transfected with YFP-tagged Parkin or pcDNA3.1 empty vector for 48 h. Cells were treated with CCCP (10 μ M, 12 h), Staurosporine (1 μ M, 12 h), MG132 (30 μ M, 3 h) and DMSO as control. Cell lysates used for further western blotting experiments. PSMA7, PSMB5, LC3 and Parkin antibodies were used for specific detection. *ACTB*, β -ACTIN was used for loading control.

All of these data, so far showed that CCCP induced more than one protein complex formation at certain fractions sharing constant proteins (ATG5 and Parkin) and differing with dispensable proteins (PSMA7 and PINK1). This increased interaction was not correlated with autophagic degradation of the proteasomal subunits. CCCP treatment, in all cases resulted in the similar aggregated protein localization at perinuclear area as a hint of organeller deffect most likely the mitochondria.

3.1.4 Determination of The Subcellular Localization of ATG5-PSMA7-Parkin Interaction

Due to the mitochondrial stress stimulated abnormal protein accumulation in the perinuclear region and the involvement of Parkin protein in the clearance of mitochondria by autophagy, we aimed to analyze the subcellular localization of the observed interactions in order to analyze the effect of the presence of ATG5-PSMA7 on mitochondrial autophagy.

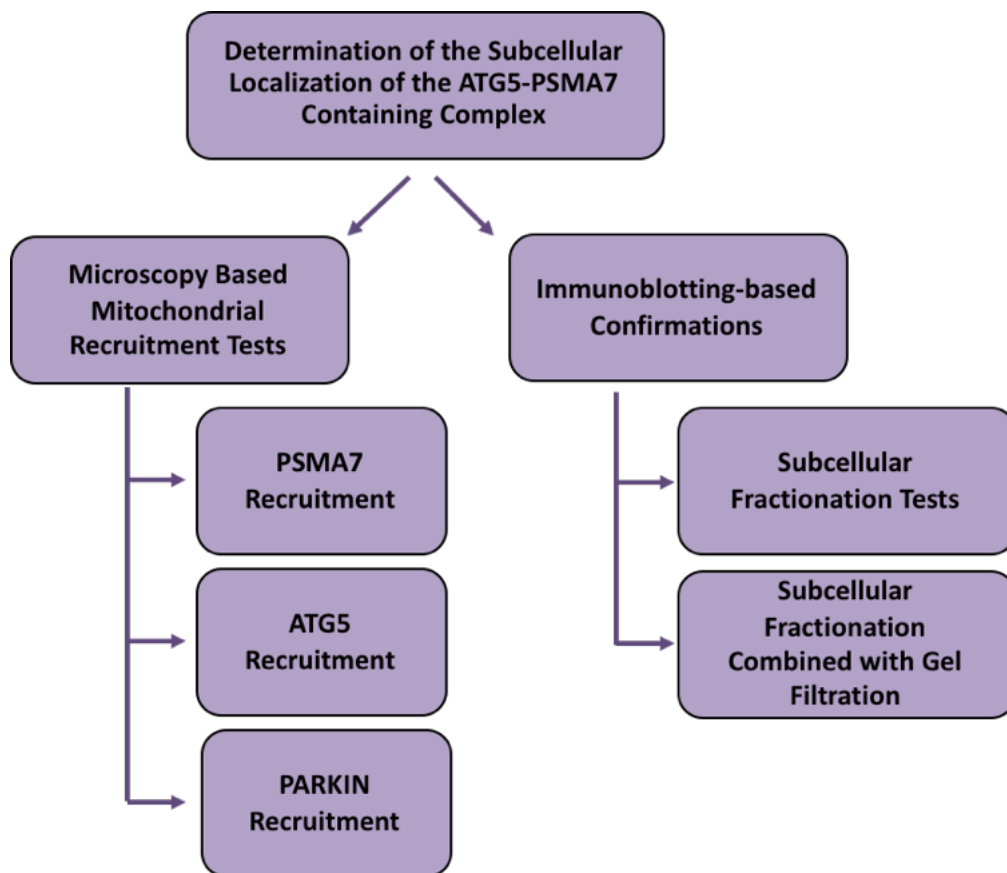


Figure 3.1.4. 1: Experimental flow in order to figure out the subcellular localization of the ATG5-PSMA7 containing protein complexes.

To start with in HELA cells confocal microscopy analysis were performed. In Figure 3.1.4 2, the partial localization of PSMA7 on mitochondria was observed under basal conditions.

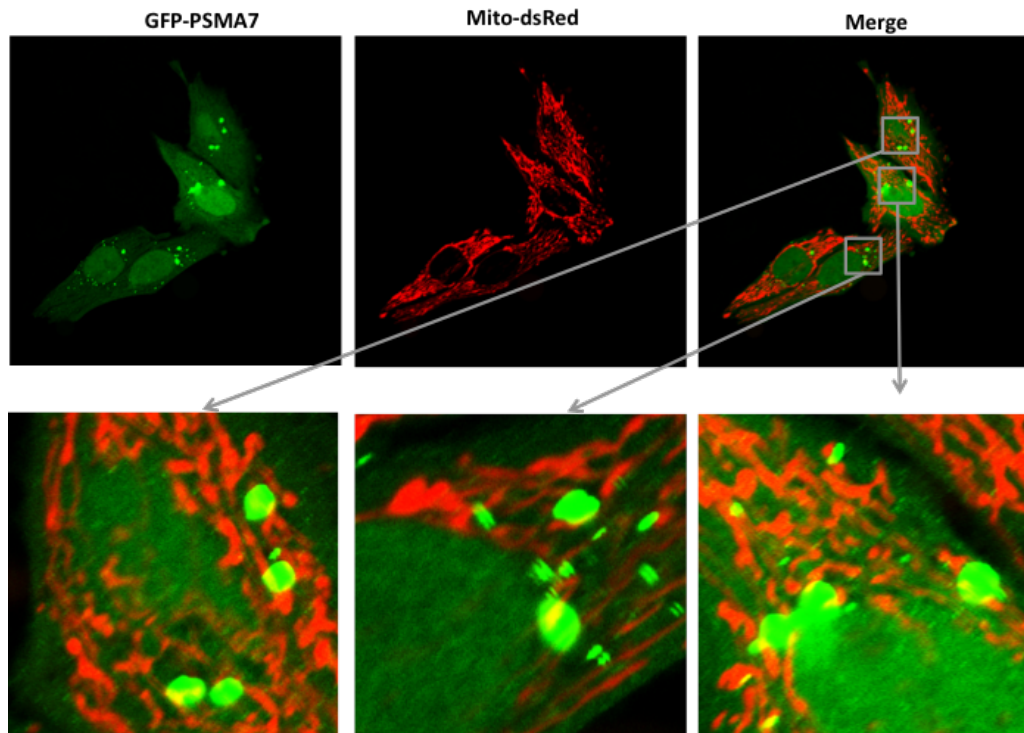


Figure 3.1.4. 2: PSMA7 found on mitochondria. HELA cells were transfected with pEGFP-tagged PSMA7 (Green) and mito-dsRed (Red) constructs for 48 h. Then, 4% PFA fixed cells analyzed under confocal microscope. *Merge*, the overlay of the red and green signals originating from the cells. Representative image of n=3 independent experiments.

Similarly, when the localization of ATG5 protein was checked on mitochondria, the partial colocalization of ATG5 was observed on mitochondria (Figure 3.1.4 3).

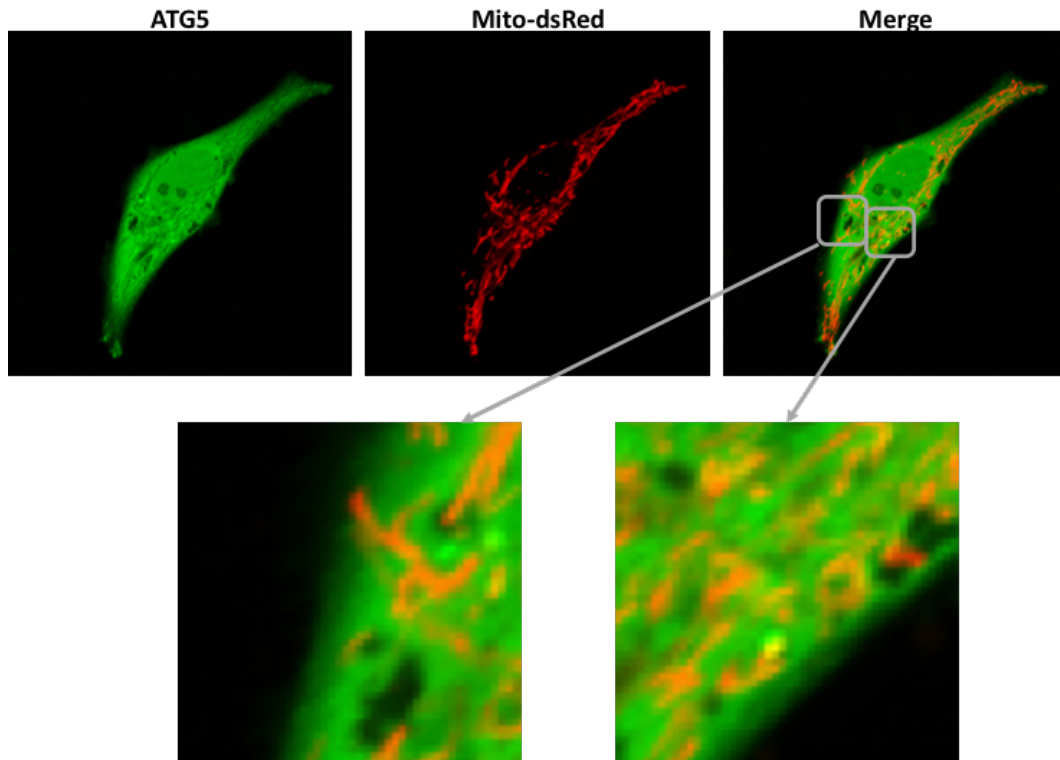


Figure 3.1.4. 3: ATG5 found on mitochondria HELA cells were grown on cover slips and co-transfected with ATG5 (Green) and mito-dsRed (Red) constructs for 48 h. After 4% PFA fixation, cells were analyzed under confocal microscope. *Merge*, The overlay of the Red and Green signals. Representative of n=3 independent experiments.

In order to test the effect of mitochondrial stress on the subcellular colocalization of the ATG5-PSMA7 complex, first confocal microscopy analyses were performed in HELA cells. The mitochondrial stress inducers, Staurosporine and CCCP, enhanced mitochondrial localization of PSMA7 (please see Figure 3.1.4 4) in HELA cells.

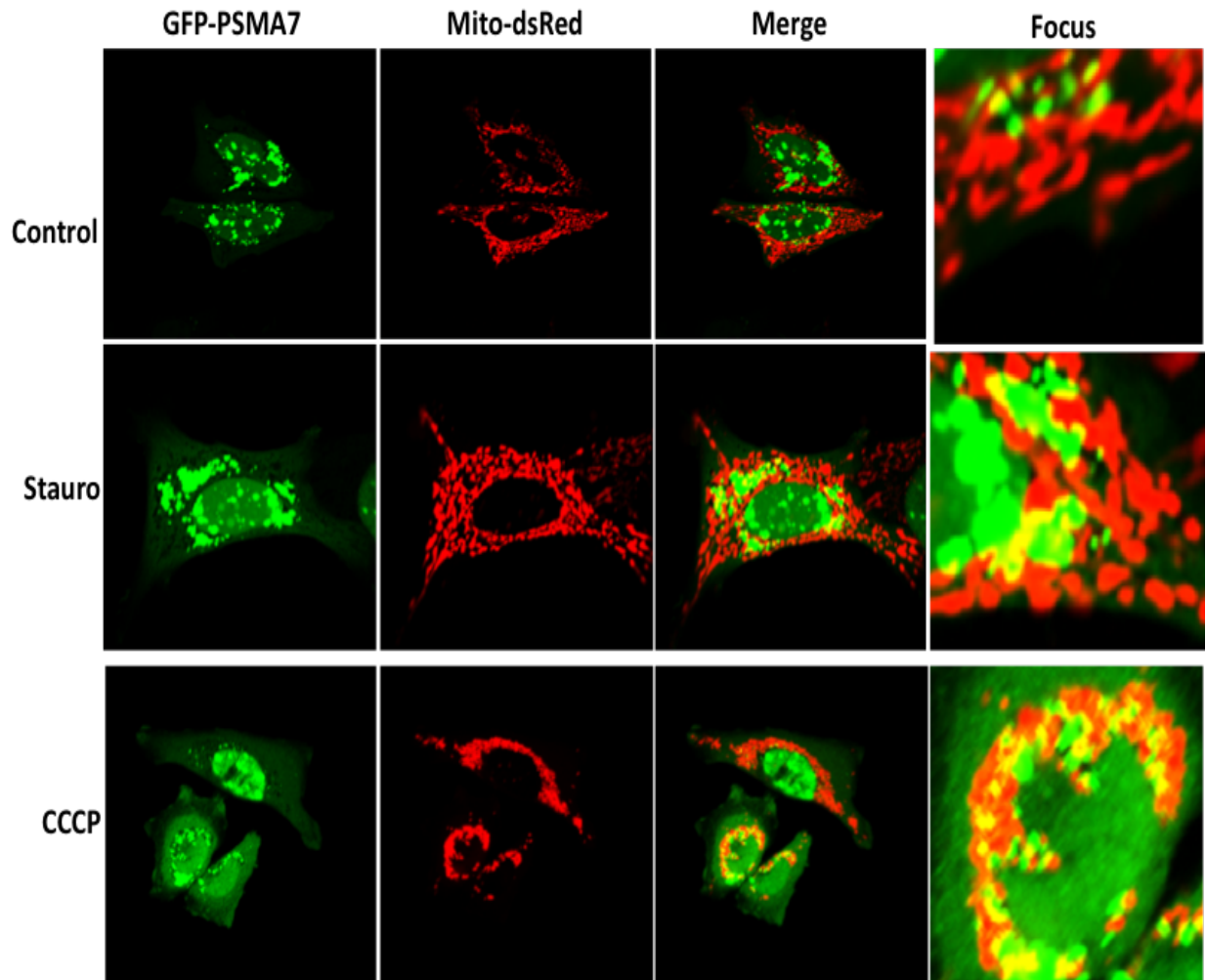


Figure 3.1.4 4: The presence of PSMA7 on mitochondria stimulated with mitochondrial stress (HELA cells). HELA cells were grown on cover slides and co-transfected with pEGFP-tagged PSMA7 (Green) and mito-dsRed (Red) constructs and treated with CCCP (10 μ M, 12 h) and Staurosporine (1 μ M, 12 h). Following 48 h of post transfection and 12 h of treatment, cells were fixed and analyzed under confocal microscope. *Merge*, The overlay of the Red and Green signals. *Focus*, zoomed in area of colocalization. Representative of n=3 independent experiments.

In line with PSMA7, CCCP-induced increased ATG5 translocation onto mitochondria in HELA (please see Figure 3.1.4 5) and HEK/293T cells (Figure 3.1.4 6) was also verified.

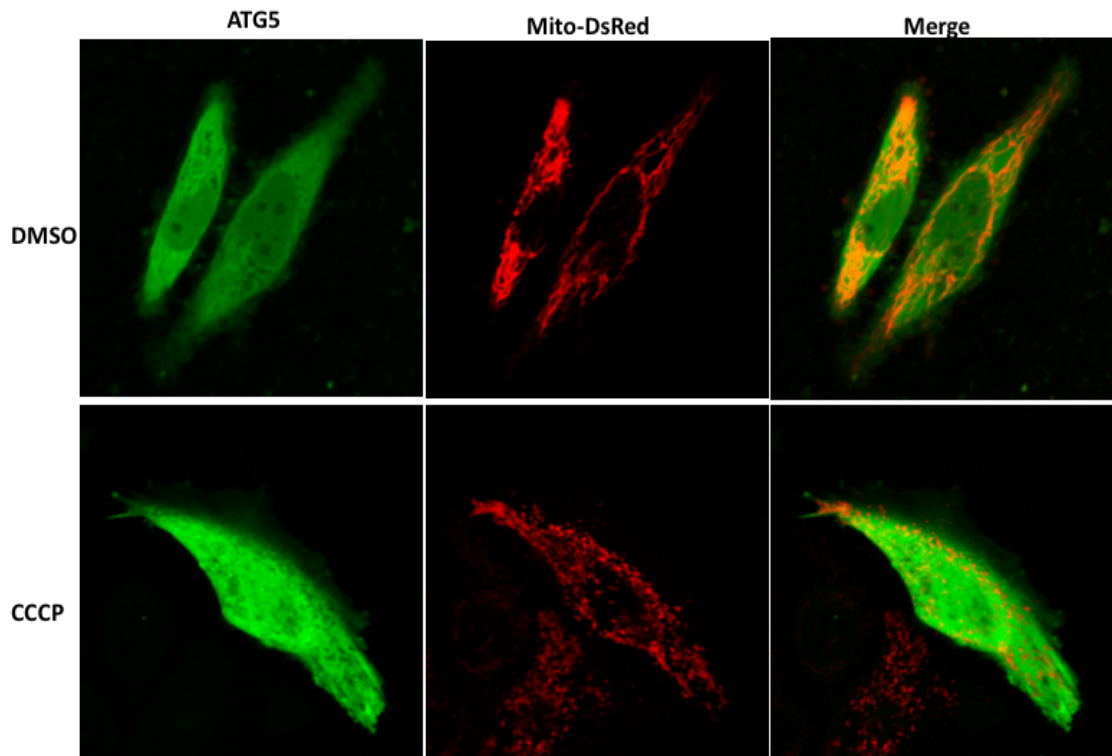


Figure 3.1.4 5: The presence of ATG5 on mitochondria stimulated with mitochondrial stress (HELA cells). HELA cells were cultured on cover slides and co-transfected with YFP-tagged ATG5 (Green) and mito-dsRed (Red) constructs and treated with CCCP (10 μ M, 12 h) and Staurosporine (1 μ M, 12 h). Following 48 h of post transfection and 12 h of treatment, cells were fixed and analyzed under confocal microscope. *Merge*, The overlay of the Red and Green signals. Representative of n=3 independent experiments.

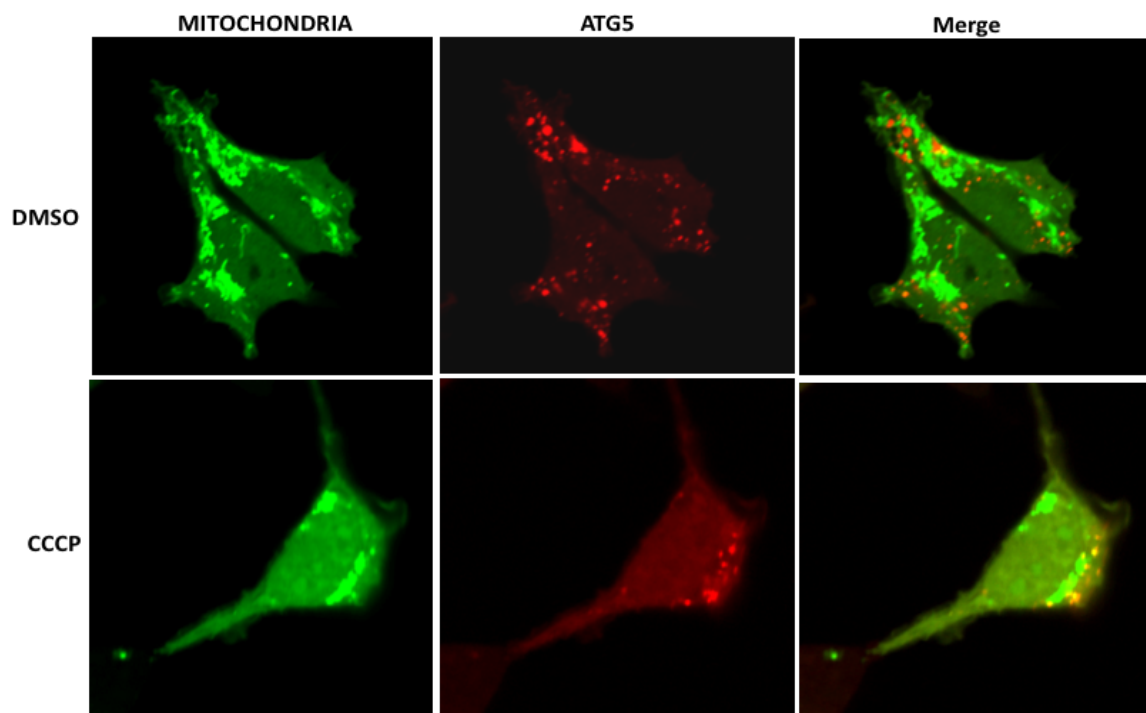


Figure 3.1.4 6: The presence of ATG5 on mitochondria stimulated with mitochondrial stress (HEK/293 cells). HEK/293 cells were cultured on cover slides and co-transfected with pmTurquoise-Mito (Green) and pmCherry-tagged ATG5 constructs and and treated with CCCP (10 μ M, 12 h) and Staurosporine (1 μ M, 12 h). Following 48 h of post transfection and 12 h of treatment, cells were fixed and analyzed under confocal microscope. *Merge*, The overlay of the Red and Green signals. Representative of n=3 independent experiments.

In addition to the increased localization of ATG5 and PSMA7 on mitochondria, subcellular translocation of Parkin was also assessed because of the observed interaction between both PSMA7 and ATG5 and as an indication of mitophagy due to CCCP treatment. In HELA cells, upon CCCP treatment almost all Parkin protein in cells translocated to mitochondria in line with literature (Figure 3.1.4 7).

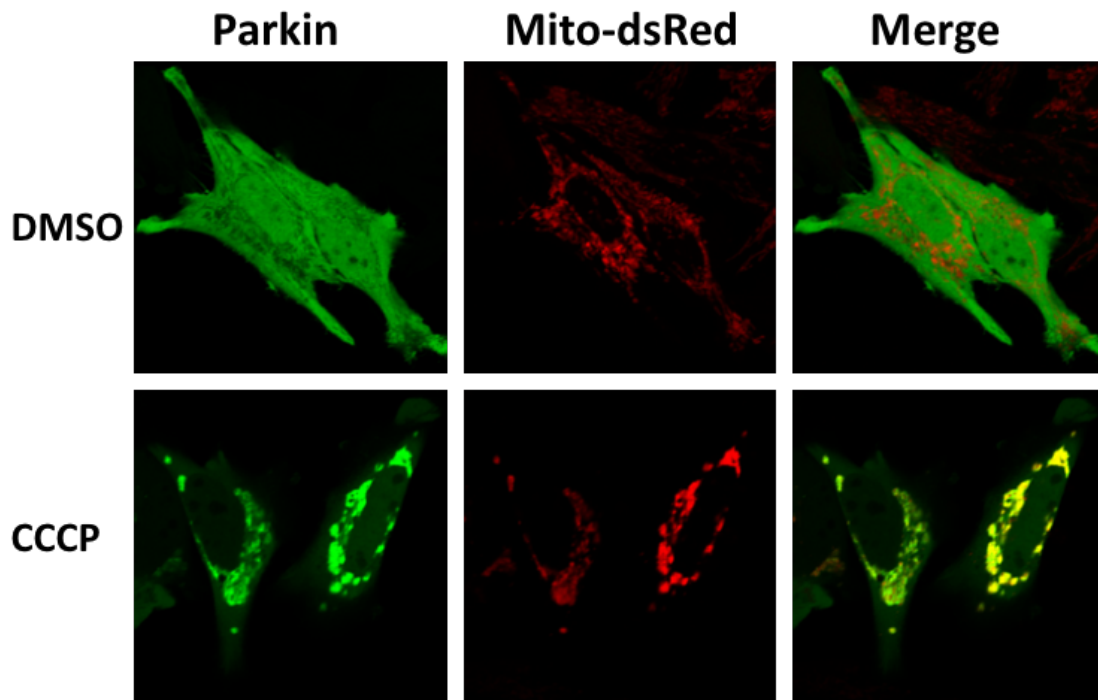


Figure 3.1.4 7: The presence of Parkin on mitochondria stimulated with mitochondrial stress (HELA cells). HELA cells were cultured on coverslides and co-transfected with YFP-tagged Parkin (Green) and mito-dsRed (Red) constructs and treated with CCCP (10 μ M, 12 h) and Staurosporine (1 μ M, 12 h). Following 48 h of post transfection and 12 h of treatment, cells were fixed and analyzed under confocal microscope. *Merge*, The overlay of the Red and Green signals. Representative of n=3 independent experiments.

As an additional way of analyzing the translocation of proteins namely PSMA7 and ATG5 on mitochondria was assessed by performing subcellular fractionation of HEK/293T and HELA cells. Subcellular cytoplasmic and mitochondrial fractions were separated from grown cells. According to western blotting results of subcellular fractions derived from HEK/293T cells in Figure 3.1.4 8, CCCP treatment, increased Parkin, PSMA7 and ATG5 recruitment to mitochondria as an indication of PSMA7 and ATG5 are important for Parkin-dependent mitophagy.

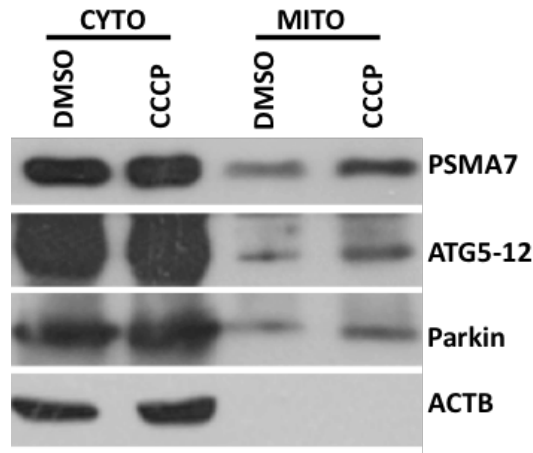


Figure 3.1.4 8: Subcellular fractionation of HEK/293T cells proving the enhanced translocation of ATG5 and PSMA7 onto mitochondria upon CCCP treatment. HEK/293T cells following MYC-tagged Parkin transfection, treated with CCCP (10 μ M, 12 h) or DMSO as control. Cells were harvested and mitochondrial isolation protocol was followed (Please see, Material and Method section). Cytoplasmic and mitochondrial proteins were separated through 12% polyacrylamide gels and subjected to immunoblotting with ATG5, PSMA7, PARKIN and ACTIN antibodies. *ACTB*, β -ACTIN used as cytoplasmic control to check the purity of isolation. *Cyto*, cytoplasm and *Mito*, mitochondria.

Furthermore, gel filtration experiments of cellular cytoplasmic and mitochondrial proteins were performed to better understand the localization of the complexes under basal conditions and CCCP-induced translocation of the proteins from cytoplasm onto mitochondria (Figure 3.1.4 9). Under basal and CCCP treated conditions, short (processed or cleaved) PINK1, Parkin, ATG5-12 and PSMA7 were found as a big molecular complex in cytoplasm (Figure 3.1.4 9, left panel). However, in the case of mitochondrial fractions of the cells things become more complex due to the involvement of the proteins in more than one complexes. Under basal condition, Parkin, PINK1 and ATG5-12 as complex I (Fraction number 3) and Parkin, PSMA7 and decreasing levels of ATG5 gathering as another complex (Fraction number 4-5). When cells exposed CCCP treatment, there have been still two different fractions on mitochondria but the interaction between the proteins to form these observed complexes increased.

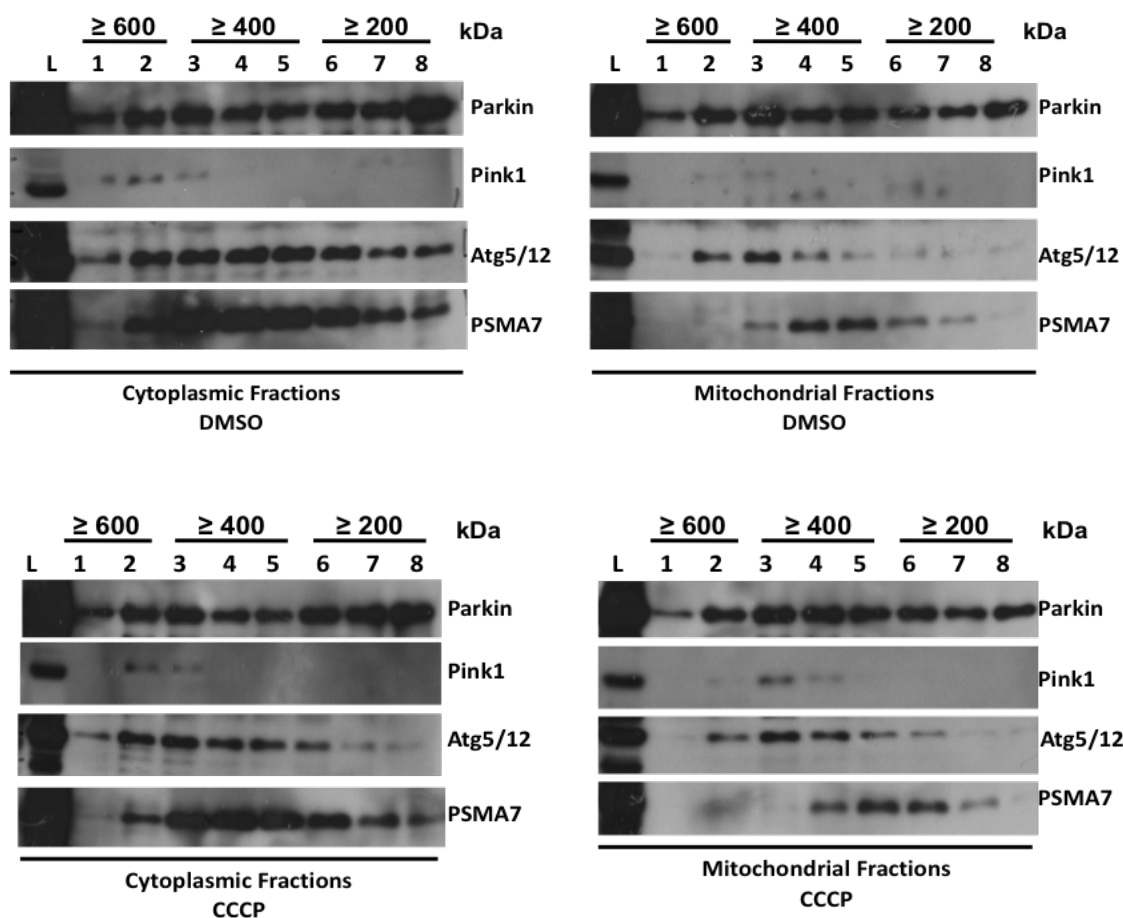


Figure 3.1.4 9: Gel filtration experiment results of mitochondrial and cytoplasmic fractions under basal and CCCP treatment conditions. HEK/293T cells with a 4×10^6 cells were plated into each 15 cm² plates and for each condition of DMSO and CCCP, 10 plates of cells cultured. HEK/293T cells were transfected with YFP-tagged Parkin construt for 48 h. Following 12 h of treatment, cells were collected and subcellular fractionation was performed as described in the method section. 5 mg of both cytoplasmic and mitochondrial protein for each condition were separated through FPLC column. 20 fractions were collected for each condition and denaturated fractions further separated through 12% SDS-PAGE. For immunoblotting, PINK1, ATG5, PSMA7 and Parkin antibodies were used. *L*, lysate control: for cytoplasm, cytoplasmic lysate and for mitochondria, mitochondrial lysate; *kDa*, kilo Dalton.

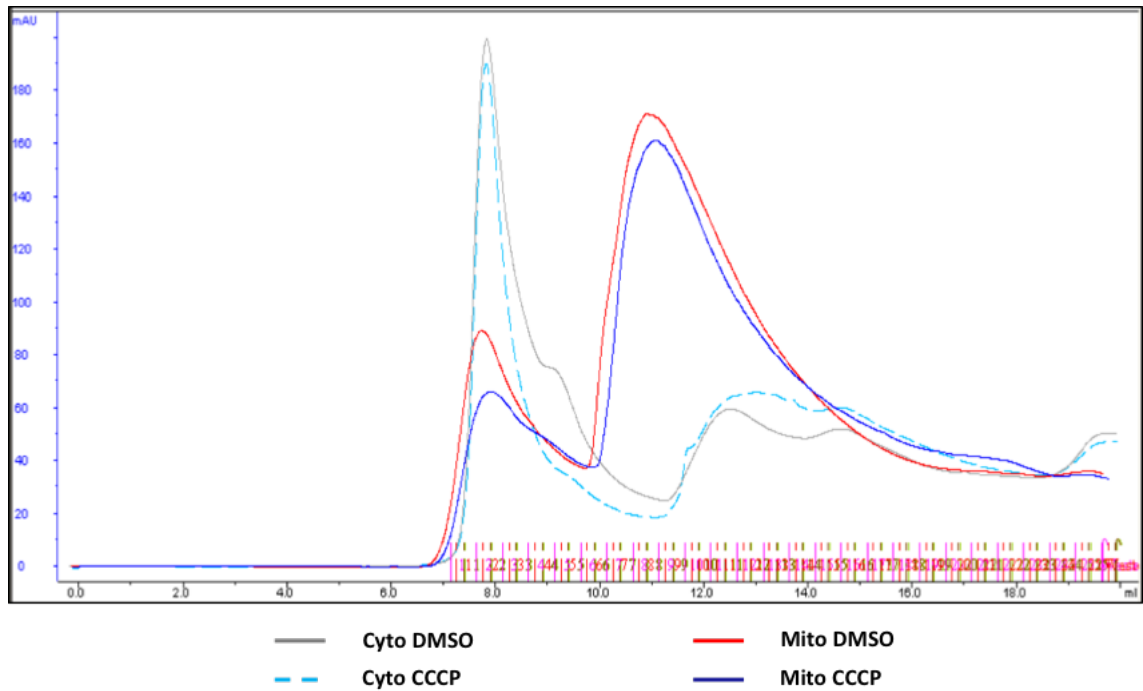


Figure 3.1.4 10: Gel filtration chromatograms of the cytoplasmic and mitochondrial protein samples over the Superdex 200 column run. Cyto, cytoplasm; Mito, mitochondria.

All these data suggested that, PSMA7, ATG5-12, Parkin and PINK1 proteins constitute a various protein complexes in cytoplasm and mitochondria. CCCP treatment enhanced the recruitment of mitochondrial translocation of ATG5-12 and PSMA7 complexes. Due to the involvement of the proteins as a big complex in cytoplasm under basal and treated conditions, and partial disassociation of PSMA7 from the higher molecular weight complex to smaller molecular weight complex, it could be interpreted that PSMA7 has critical role for recruitment of proteins from cytoplasm to mitochondria in order to maintain the mitochondrial homeostasis.

3.1.5 The Functional Role of ATG5-PSMA7 Interaction in Selective Autophagy

In order to better understand the functional role of the proteins contributing to these protein complexes several siRNA, shRNA mediated knockdown experiments and genetically modified knock out cells were utilized. The global effect of deficiency in each protein was investigated in terms of several layers as described in the Figure 3.1.5 1.

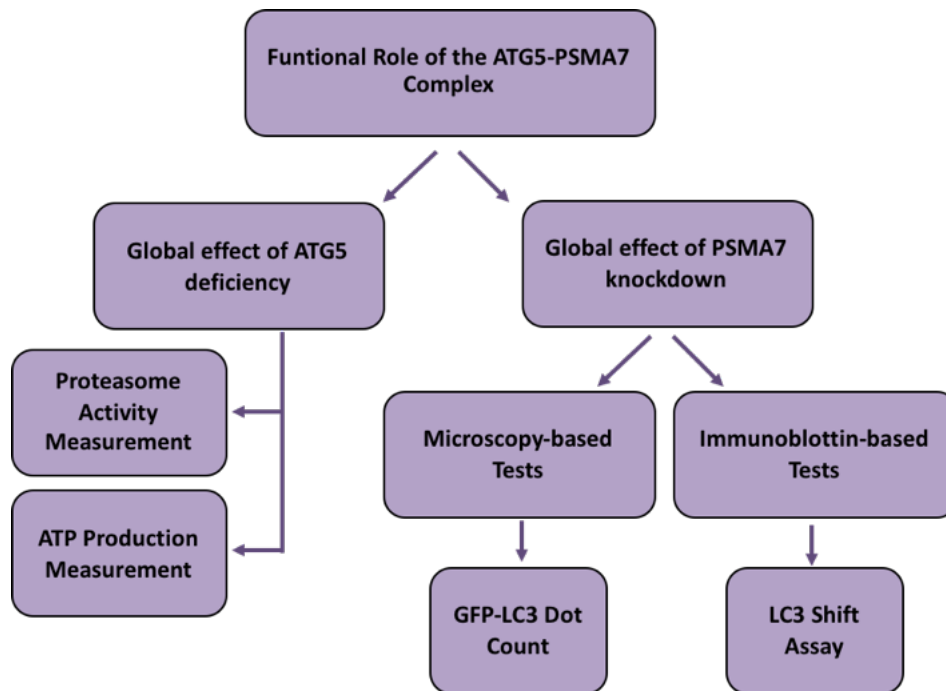


Figure 3.1.5 1: The global effect of knockout ATG5 and knockdown PSMA7 analyzed in terms of several different aspects.

The effect of ATG5 deficiency on proteasomal activity in MEF cells was analyzed (Figure 3.1.5 2). In accordance with the literature, ATG5 deficiency resulted in increased proteasomal activity compare to wild type MEF cells with an increasing time points.

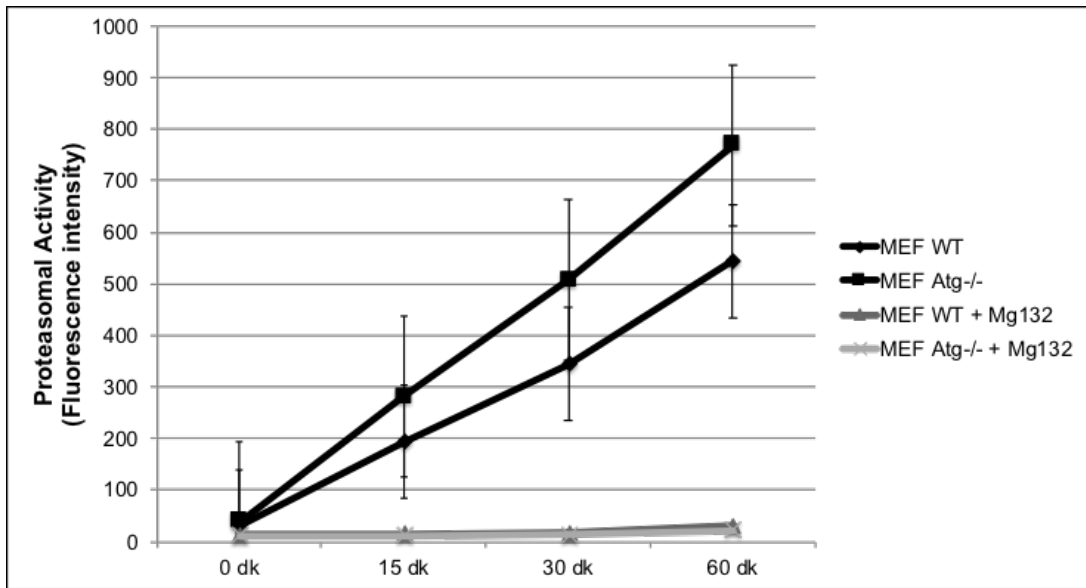


Figure 3.1.5 2: Proteasomal activity measurement results of WT and ATG5 KO MEF cells. WT and ATG5 KO MEF cells. Seeded in 6 well plates and following treatment with DMSO and MG132 (20 μ M), proteasome activities were measured according to protocol described in method chapter (N=4 experiments, not significant).

Next, the effect of ATG5 deficiency in cellular ATP level was measured in WT and ATG5 knockout MEF cells under control and oligomycin treated conditions. As shown in Figure 3.1.5 3, ATG5 knockout resulted in significant decrease in ATP production as a hint for mitochondrial defect.

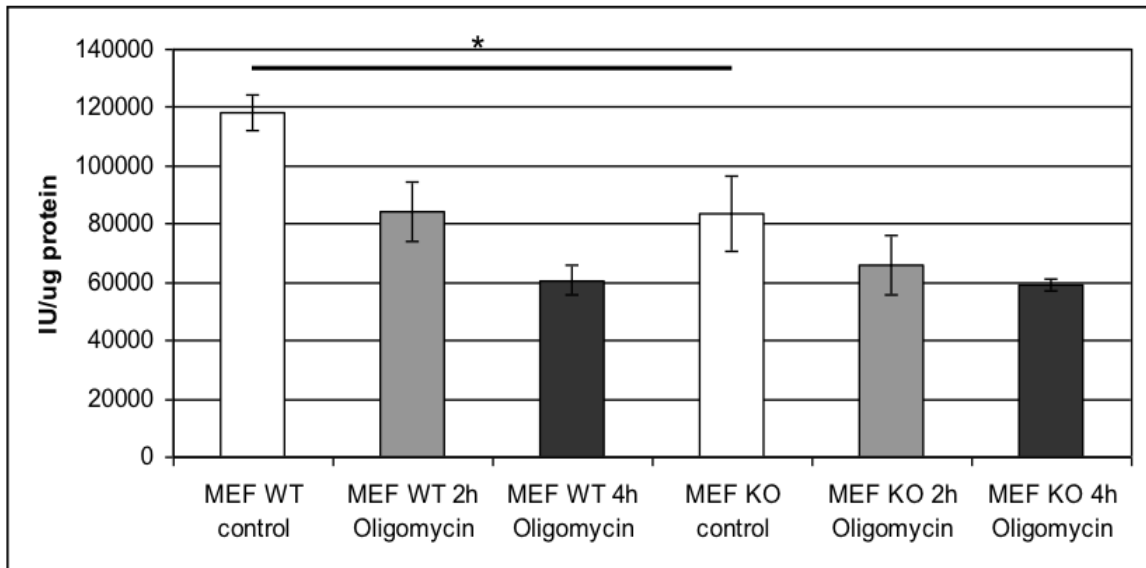


Figure 3.1.5 3: ATP assay results of WT and ATG5 KO MEF cells in response to Oligomycin treatment. WT and ATG5 KO MEF cells were seeded in 6 well plates. Following DMSO and Oligomycin treatment, cellular ATP level was determined (Oligomycin 5 ug/ml, N=3 independent experiments, * $p \leq 0.05$).

Then the effect of knockdown PSMA7 on autophagy was investigated. SiRNA-mediated knockdown of PSMA7 resulted in enhanced LC3-II shift therefore enhanced autophagic activity (Figure 3.1.5 4). Additionally, the effect of PSMA7 deficiency was analysed in terms LC3 puncta formation and validated the activatory effect of knock down PSMA7 on autophagy (Figure 3.1.5 5).

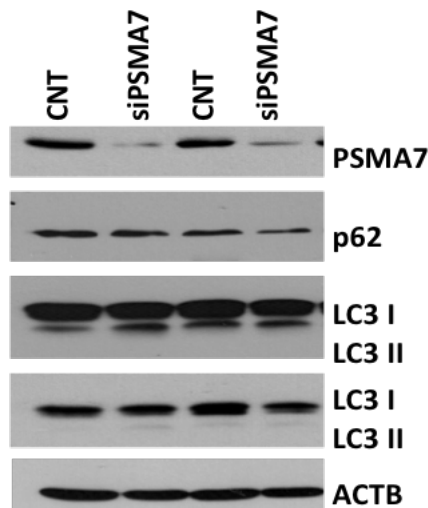


Figure 3.1.5 4: The siRNA-mediated knockdown effect of PSMA7 enhanced autophagic activity in HEK/293T cells. HEK/293T cells following PSMA7 specific siRNA transfection, grown for further 48 h. Cell lysates were separated through 15% SDS-PAGE. PSMA7, p62, LC3 and β -ACTIN antibodies were used for immunoblotting.

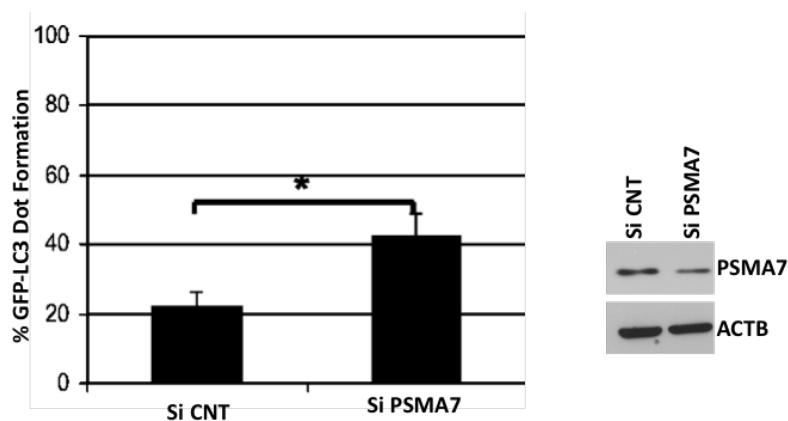


Figure 3.1.5 5: The results of PSMA7 knockdown on LC3 dot formation analyses in HEK/293T cells. HEK/293T cells were cultured on coverslides and co-transfected with pEGFP-LC3 and either non-targeting or PSMA7-targeting siRNA oligos for 48 h. The knockdown efficiency was checked by western blotting (right panel) by using PSMA7 and ACTIN antibodies. *ACTB*, β -ACTIN was used as loading control. For GFP-LC3 dot formation, cells were fixed with 4% PFA and analyzed under fluorescent microscope (left panel, mean \pm S.D. n=5 independent experiments).

Following observations of the global effects of each protein on the protein degradation mechanisms, we further analyzed the effect of the proteins on a target selective autophagy, mitophagy in HEK/293T and HELA cells. To start with, functional tests of PSMA7 was performed at several different stages of mitophagy process as listed in Figure 3.1.5 6.

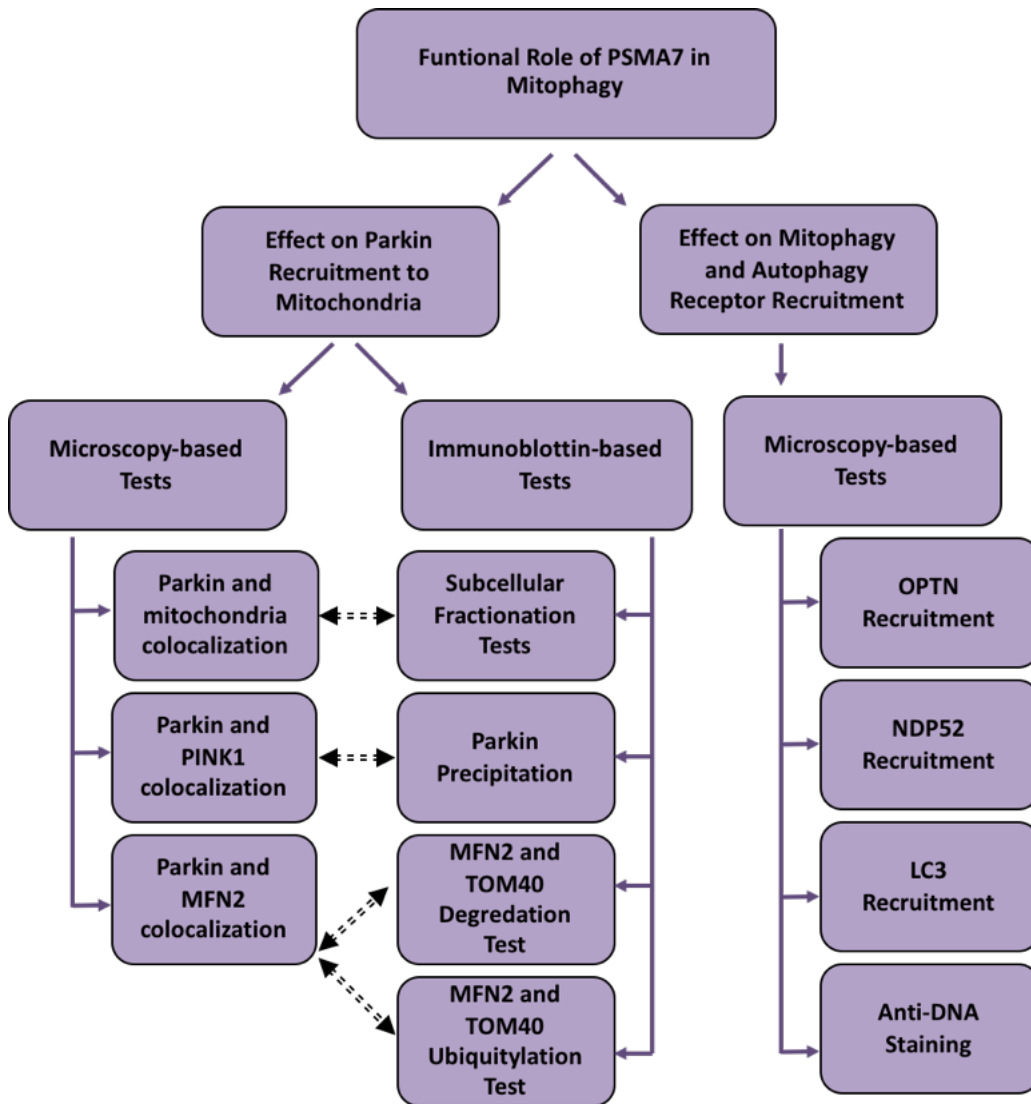


Figure 3.1.5 6: The effect of knockdown PSMA7 analyzed on mitophagy in terms of several different aspects.

To do that initially, the effect of knockdown PSMA7 on CCCP-mediated Parkin recruitment was analyzed by colocalization tests in HEK/293T (Figure 3.1.5 7) and HELA cells (Figure 3.1.5 8). In both of the cell lines, siRNA-mediated knock down of PSMA7 resulted in decrease in CCCP-induced Parkin translocation from cytoplasm to mitochondria.

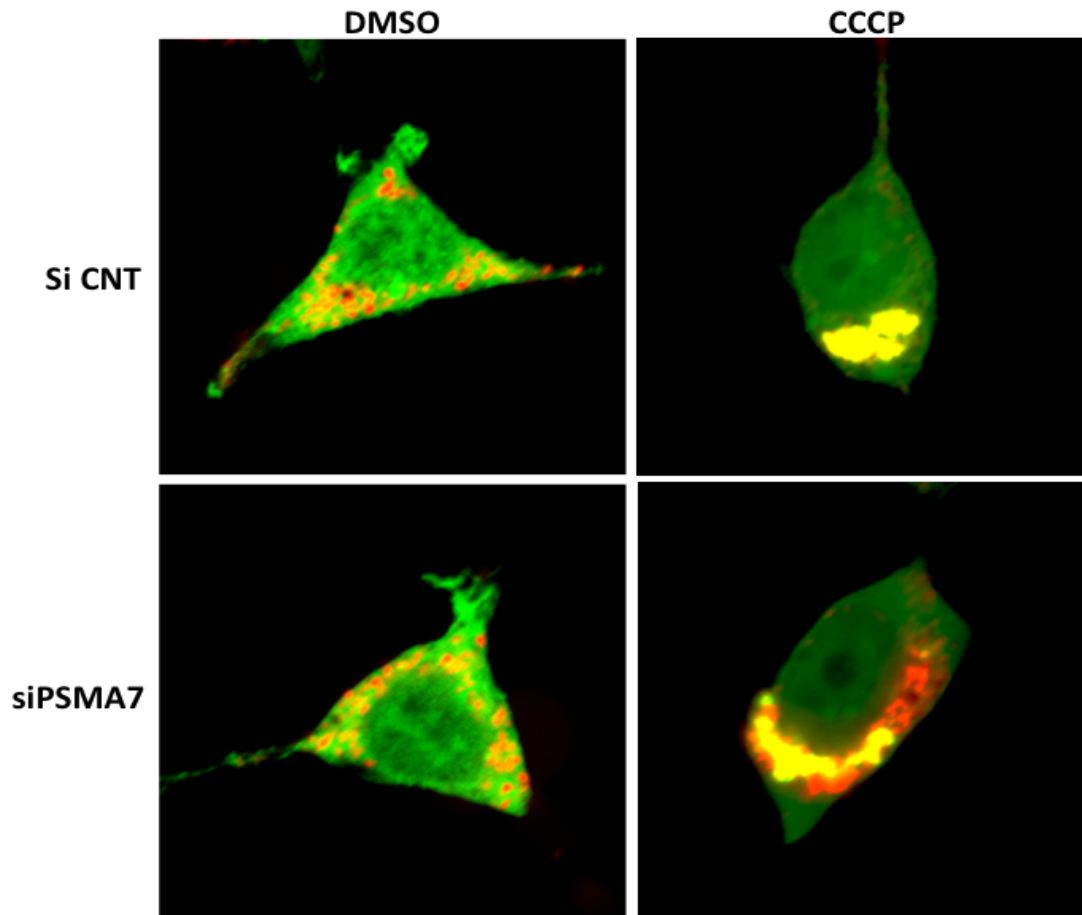


Figure 3.1.5 7: The effect of knock down PSMA7 on Parkin translocation onto mitochondria in HEK/293T cells. HEK/293T cells were grown on coverslides and co-transfected with YFP-tagged Parkin (Green) and mito-dsRed (Red) constructs together with either PSMA7-targeting siRNA or non-targeting siRNAs for 48 h. Following CCCP treatment for 12 h with a concentration of 10 μ M, colocalization tests were performed under confocal microscope. N=3 independent experiments performed.

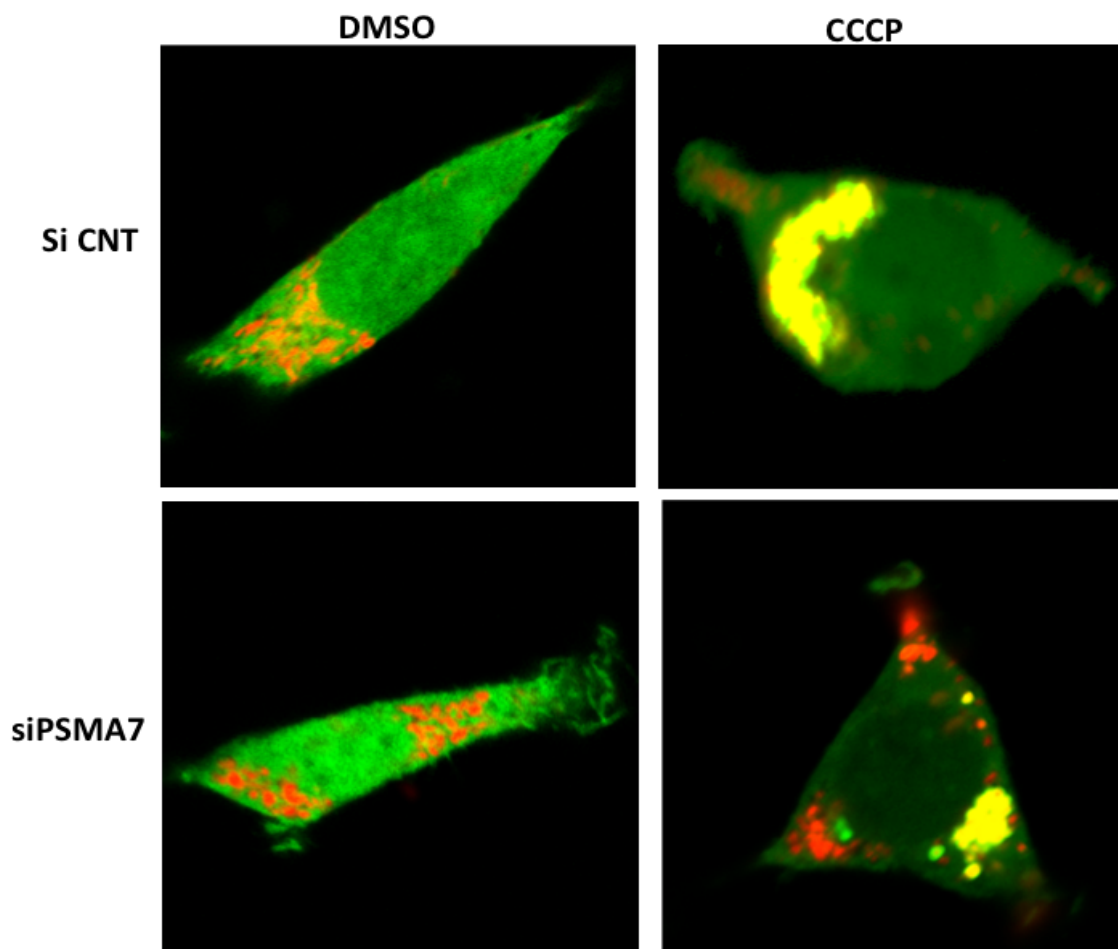


Figure 3.1.5 8: The effect of knock down PSMA7 on Parkin translocation onto mitochondria in HELA cells. HELA cells were grown on coverslides and co-transfected with YFP-tagged Parkin (Green) and mito-dsRed (Red) constructs together with either PSMA7-targeting siRNA or non-targeting siRNAs for 48 h. Following CCCP treatment for 12 h with a concentration of 10 μ M, colocalization tests were performed under confocal microscope. N=3 independent experiments performed.

Parkin translocation from cytoplasm to mitochondria was also analyzed by subcellular fractionation experiments in addition to colocalization tests. The decrease in PSMA7 protein level, correlated with the decrease in CCCP-stimulated Parkin recruitment (Figure 3.1.5 9).

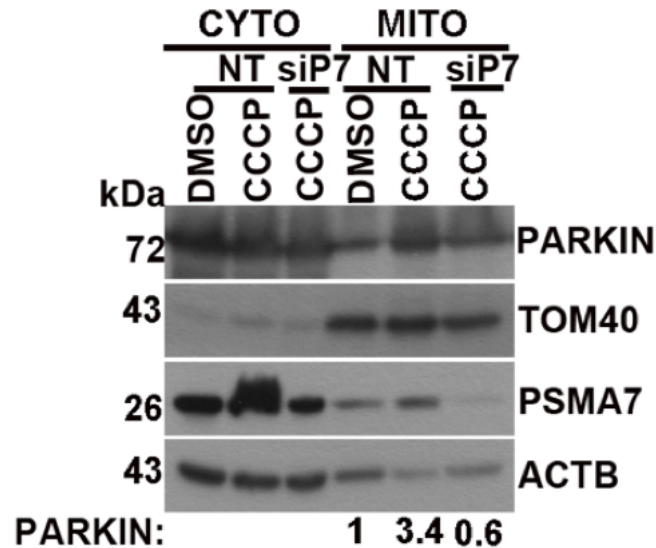


Figure 3.1.5 9: Western blotting results of subcellular fractionation tests for the analysis of PSMA7 deficiency on Parkin recruitment in HEK/293T cells. HEK/293T cells were co-transfected with YFP-tagged Parkin construct and either with PSMA7-targeting siRNA or non-targeting siRNA for 48 h. Following DMSO or CCCP treatment for 12 h with a concentration of 10 μ M, through series of differential centrifugation, cells were separated into cytoplasmic and mitochondrial fractions. Cytoplasmic and mitochondrial proteins then further separated through 12% SDS-PAGE. Parkin, TOM40, PSMA7 and β -Actin were used for immunoblotting. TOM40 and β -Actin were used to check the quality and the purity of subcellular fractionation step.

Next, the effect of PSMA7 on the CCCP-induced PINK1-Parkin interaction was evaluated in HEK/293T and HELA cells by performing colocalization (Figure 3.1.5 10) and immunoprecipitation tests (Figure 3.1.5 11). When HELA cells treated with CCCP, Parkin and PINK1 proteins showed increased interaction. However, PSMA7 knock down resulted in decrease in CCCP-induced interaction between Parkin and PINK1 proteins (Figure 3.1.5 10). Similar results were obtained in immunoprecipitation tests (Figure 3.1.5 11).

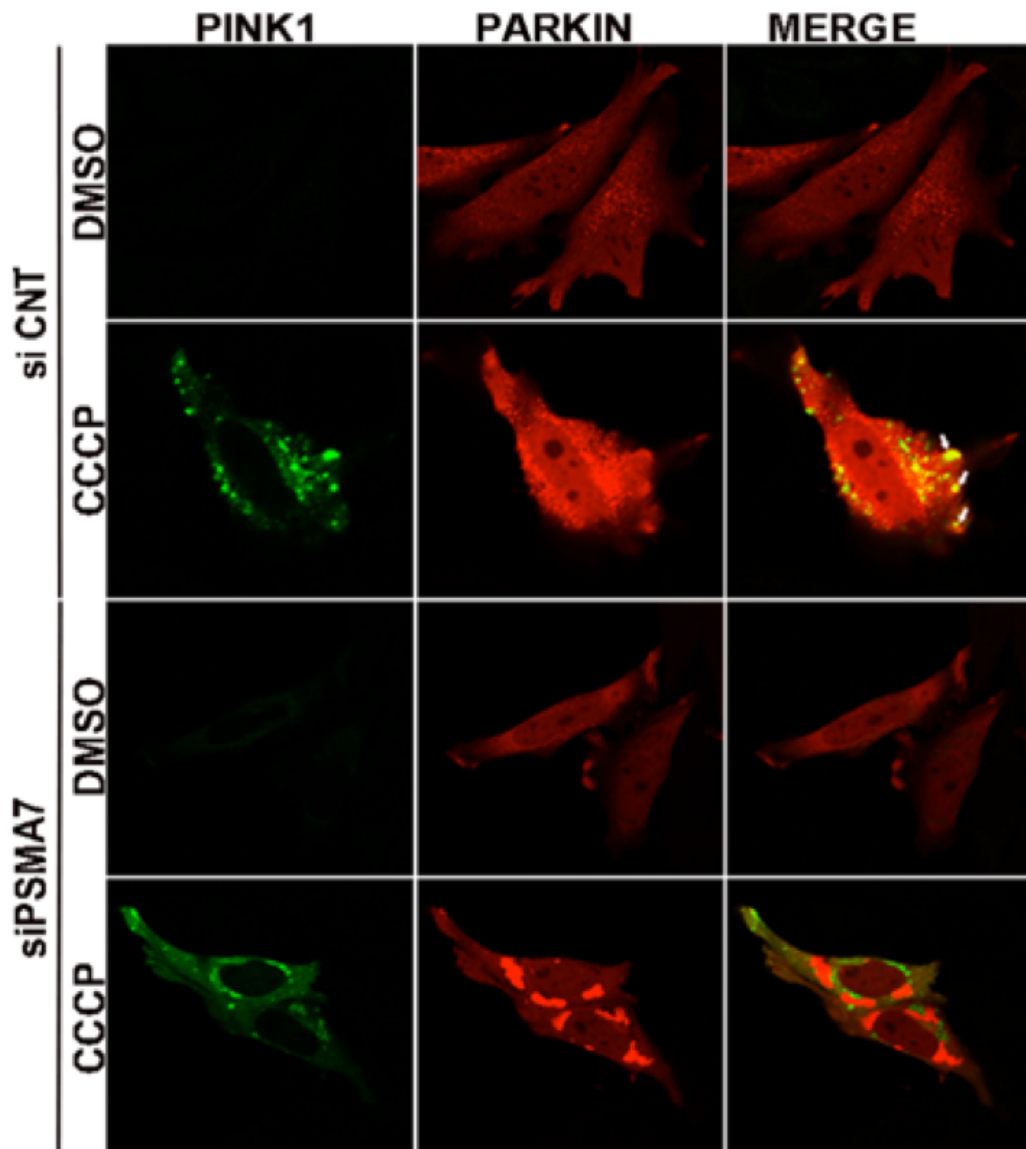


Figure 3.1.5 10: Colocalization analyses showing the role of PSMA7 on PINK1 and Parkin interaction in HELA cells. HELA cells were grown on cover slides and co-transfected with C-terminal GFP-tagged PINK1 (Green), pmCherry-tagged Parkin (Red) and together with siRNA CNT (non-targeting) or PSMA7-targeting siRNA for 48 h. Following treatment with DMSO and CCCP, colocalization of the proteins were analyzed under confocal microscope. *Merge*, the overlay of Green and Red signals. Representative data of n=3 independent experiments.

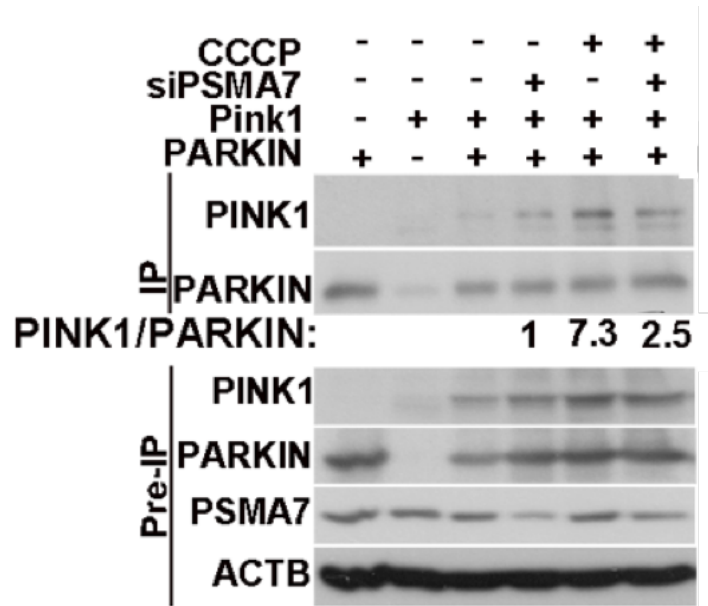


Figure 3.1.5 11: Myc-tagged immunoprecipitation results for analyzing the effect of PSMA7 on PINK1 and Parkin interaction in HEK/293T cells. HEK/293T cells were co-transfected with C-GFP-tagged PINK1 and Myc-tagged Parkin together with either PSMA7-targeting siRNA or non-targeting siRNA for 48 h. After DMSO or CCCP treatment (10 μ M, 12 h), cell lysates were incubated with myc-beads for overnight at 4°C. Co-precipitated proteins were analyzed by SDS-PAGE followed by immunoblotting. PINK1, Parkin and PSMA7 antibodies were used. *Pre-IP*, lysate controls; *IP*, immunoprecipitation and *ACTB*, β -Actin.

Due to the regulatory role of PSMA7 on Parkin translocation, we next checked the effect of PSMA7 on the interaction between Parkin and its degradation targets as well as the degradation level of the Parkin targets such as MFN2 in HEK/293T and HELA cells (Figure 3.1.5 12 and Figure 3.1.5 14).

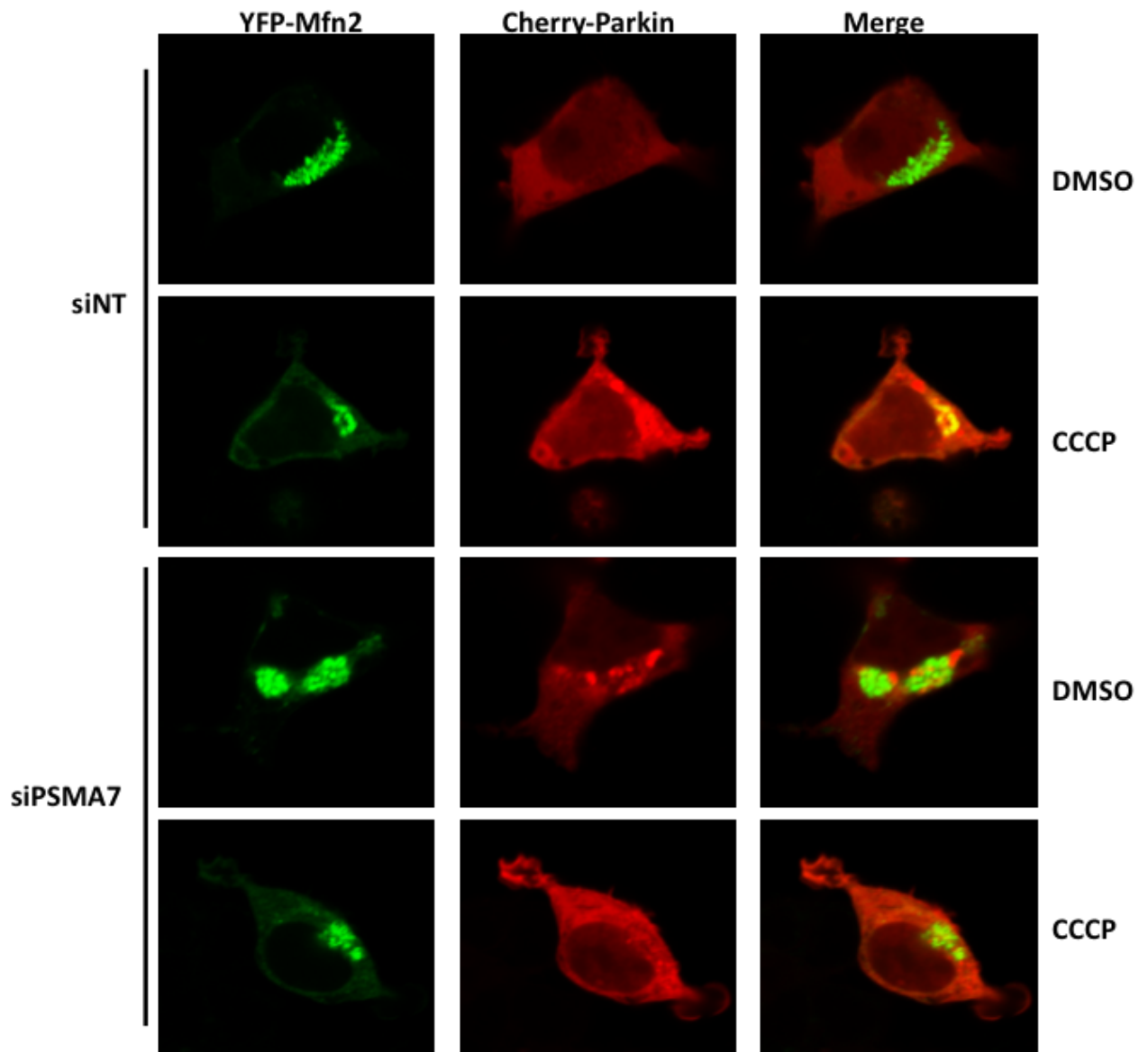


Figure 3.1.5 12: Colocalization test to check the effect of knock down PSMA7 on MFN2 and Parkin interaction in HEK/293T cells. HEK/293T cells were cultured on cover slips and co-transfected with YFP-tagged MFN2 (Green) and pmCherry-tagged Parkin (Red) together with either PSMA7-targeting or non-targeting siRNAs. *Merge*, overlay of the red and green signals. N=3 independent experiments performed.

In order to understand that, first colocalization tests were performed and knock down PSMA7 significantly restored CCCP-induced MFN2 and Parkin colocalization in HEK/293T (Figure 3.1.5 12-13) and HELA cells (Figure 3.1.5 14-15).

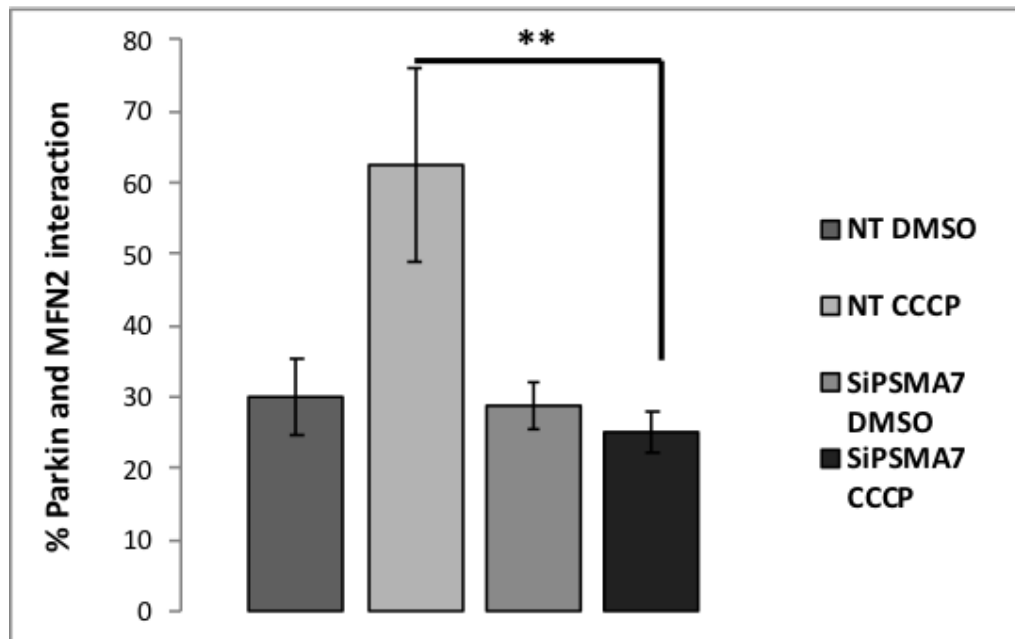


Figure 3.1.5 13: The quantification graphic of Parkin and MFN2 colocalization in HEK/293T cells. At least 50 cells per condition per experiment quantified, mean \pm S.D. n=3 independent experiments, p value: 0,009848.

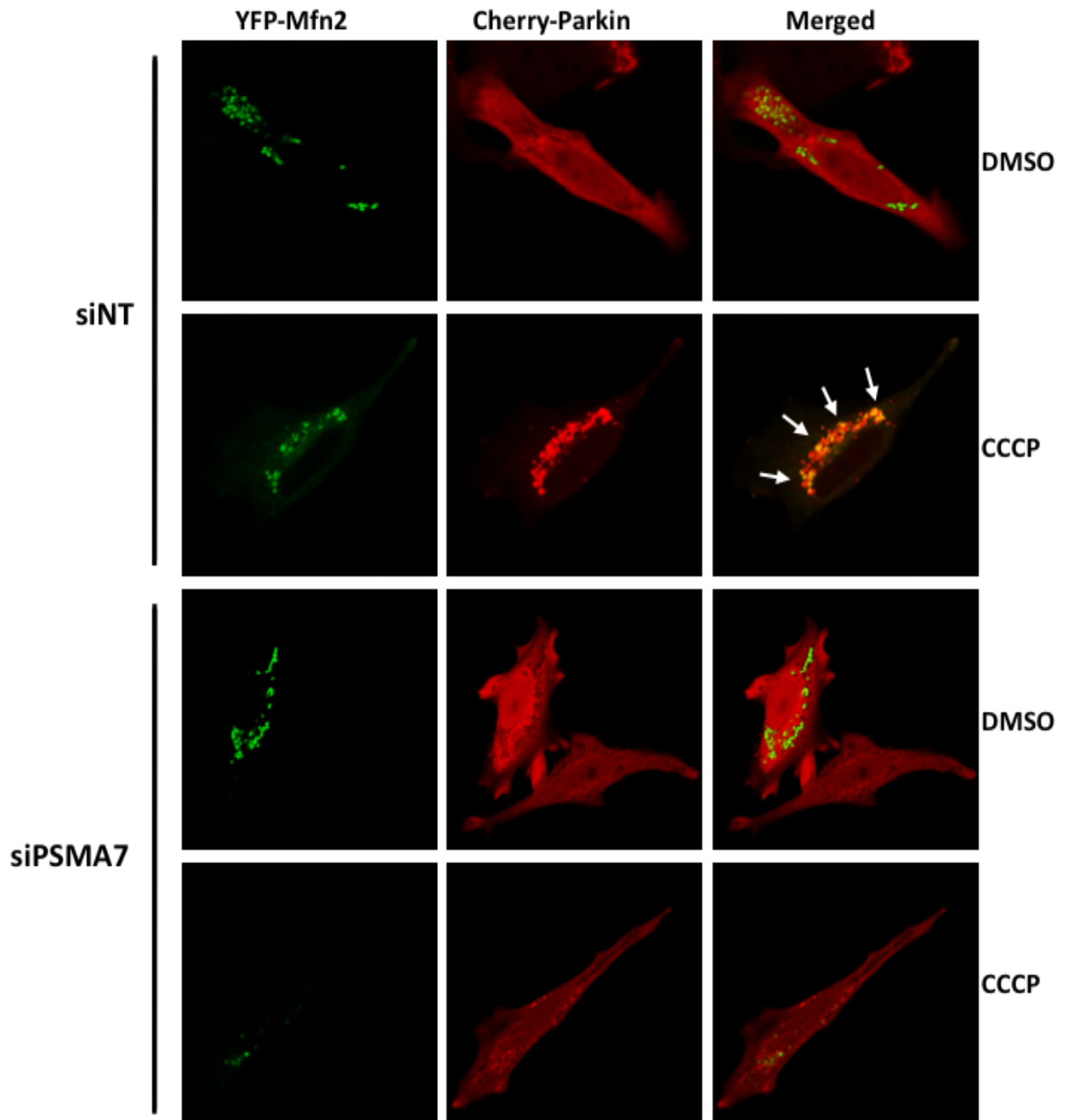


Figure 3.1.5 14: Colocalization test to check the effect of knock down PSMA7 on MFN2 and Parkin interaction in HELA cells. HELA cells were cultured on cover slips and co-transfected with YFP-tagged MFN2 (Green) and pmCherry-tagged Parkin (Red) together with either PSMA7-targeting or non-targeting siRNAs. *Merge*, overlay of the red and green signals. N=3 independent experiments performed.

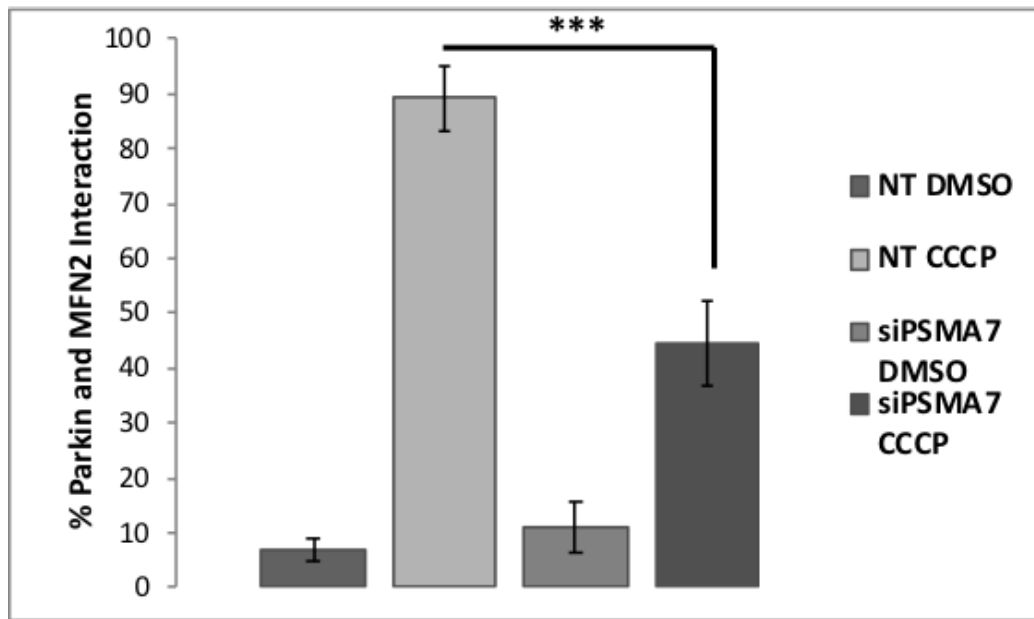


Figure 3.1.5 15: The quantification graphic of Parkin and MFN2 colocalization in HELA cells. At least 50 cells per condition per experiment quantified, mean \pm S.D. n=3 independent experiments, p value: 0,0002.

Then, the effect of PSMA7 on the degradation of outer mitochondrial membrane proteins, MFN2 (Figure 3.1.5 16) and TOM40 (Figure 3.1.5 17) were checked by western blotting experiments. Correlating the colocalization results of Parkin and MFN2 proteins, knock down PSMA7 significantly blocked CCCP-induced MFN2 and TOM40 degradation.

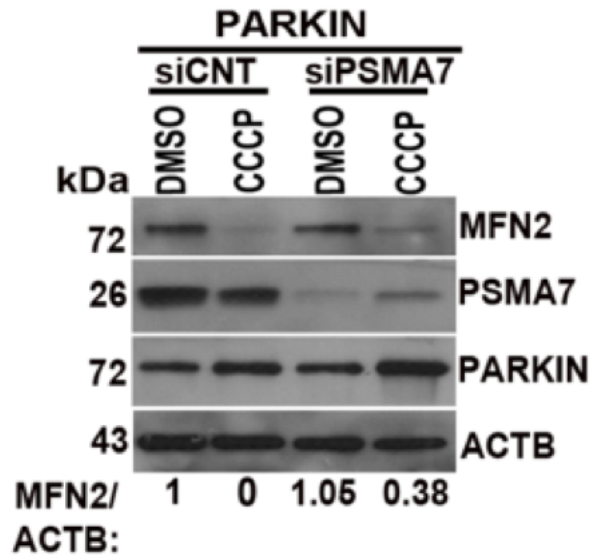


Figure 3.1.5 16: Effect of knockdown PSMA7 on MFN2 degradation in HEK/293T cells. HEK/293T cells were transfected with YFP-tagged Parkin and together with either PSMA7-targeting siRNA or non-targeting siRNA for 48 h. Following DMSO or CCCP treatment, protein lysates were isolated and separated through 12% SDS-PAGE. MFN2, PSMA7 and Parkin antibodies were used for immunoblotting. ACTB, β -Actin used for loading control. Image J software was used for band intensity measurement (N=3 independent experiments were performed).

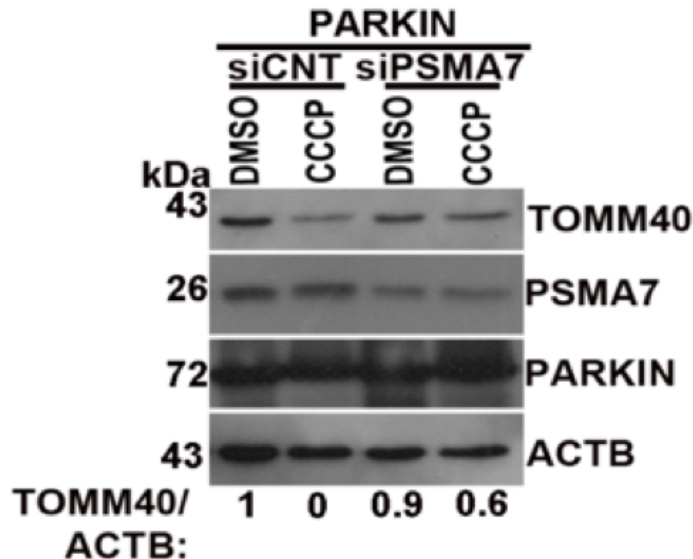


Figure 3.1.5 17: Effect of knock down PSMA7 on TOM40 degradation in HEK/293T cells. HEK/293T cells were transfected with YFP-tagged Parkin and together with either PSMA7-targeting siRNA or non-targeting siRNA for 48 h. Following DMSO or CCCP treatment, protein lysates were isolated and separated through 12% SDS-PAGE. TOM40,

PSMA7 and Parkin antibodies were used for immunoblotting. ACTB, β -Actin used for loading control. Image J software was used for band intensity measurement (N=3 independent experiments were performed).

Since Parkin is an E3-ligase and it has been linked to mitophagy through its ubiquitylation capacity of outer mitochondrial membrane proteins. Therefore, we next checked ubiquitylation levels of the mitochondrial proteins by performing ubiquitin immunoprecipitation experiments in HEK/293T cells (Figure 3.1.4 18). PSMA7 knock down decreased degradation of OMM proteins such as TOM40 and VDAC1 in line with the previous data, but interestingly, CCCP treatment could still increased the ubiquitylation levels of these protein suggesting that other E3 ligases could also contribute to PINK/Parkin-dependent mitophagy.

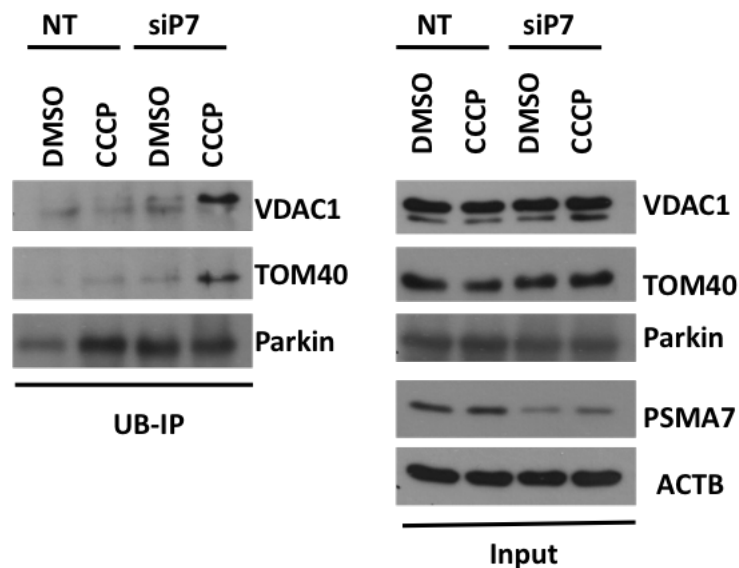


Figure 3.1.4 18: The effect of PSMA7 on ubiquitylation levels OMM proteins of HEK/293T cells. HEK/293T cells were transfected with YFP-tagged Parkin and together with either PSMA7-targeting siRNA or non-targeting siRNA for 48 h. Following DMSO or CCCP treatment, protein lysates were isolated and incubated with ubiquitin antibody coupled protein A agarose beads overnight. Eluted proteins were separated through 12% SDS-PAGE. VDAC1, TOM40, PSMA7 and Parkin antibodies were used for immunoblotting. ACTB, β -Actin used for loading control. *Input*, lysate controls; *UB-IP*,

ubiquitin immunoprecipitation. Image J software was used for band intensity measurement (N=2 independent experiments were performed).

So far cumulative data shows that, PSMA7 has critical role in recruitment of Parkin protein to mitochondria through interfering its interaction with PINK1. Not only the recruitment, but also CCCP-induced Parkin mediated ubiquitylation of OMM proteins and therefore their degradation was shown to strongly correlated with PSMA7 protein. But strikingly, knockdown PSMA7 did not change CCCP-stimulated ubiquitylation pattern of OMM proteins suggesting the involvement of other cytoplasmic or mitochondrial E3 ligases in this process.

Next, we analyzed the effect of PSMA7 on the recruitment of selective mitophagy adaptor proteins such as OPTN and NDP52 in HELA cells by confocal microscopy (Figure 3.1.5 19- Figure 3.1.5 21). According to Figure 3.1.5 19 and its quantification shown in Figure 3.1.5 20, CCCP-induced mitochondria associated GFP-OPTN dots significantly decreased when PSMA7 was knocked down. In addition to OPTN, NDP52 as another mitophagy receptor recruitment was also blocked upon PSMA7 knock down (Figure 3.1.5 21).

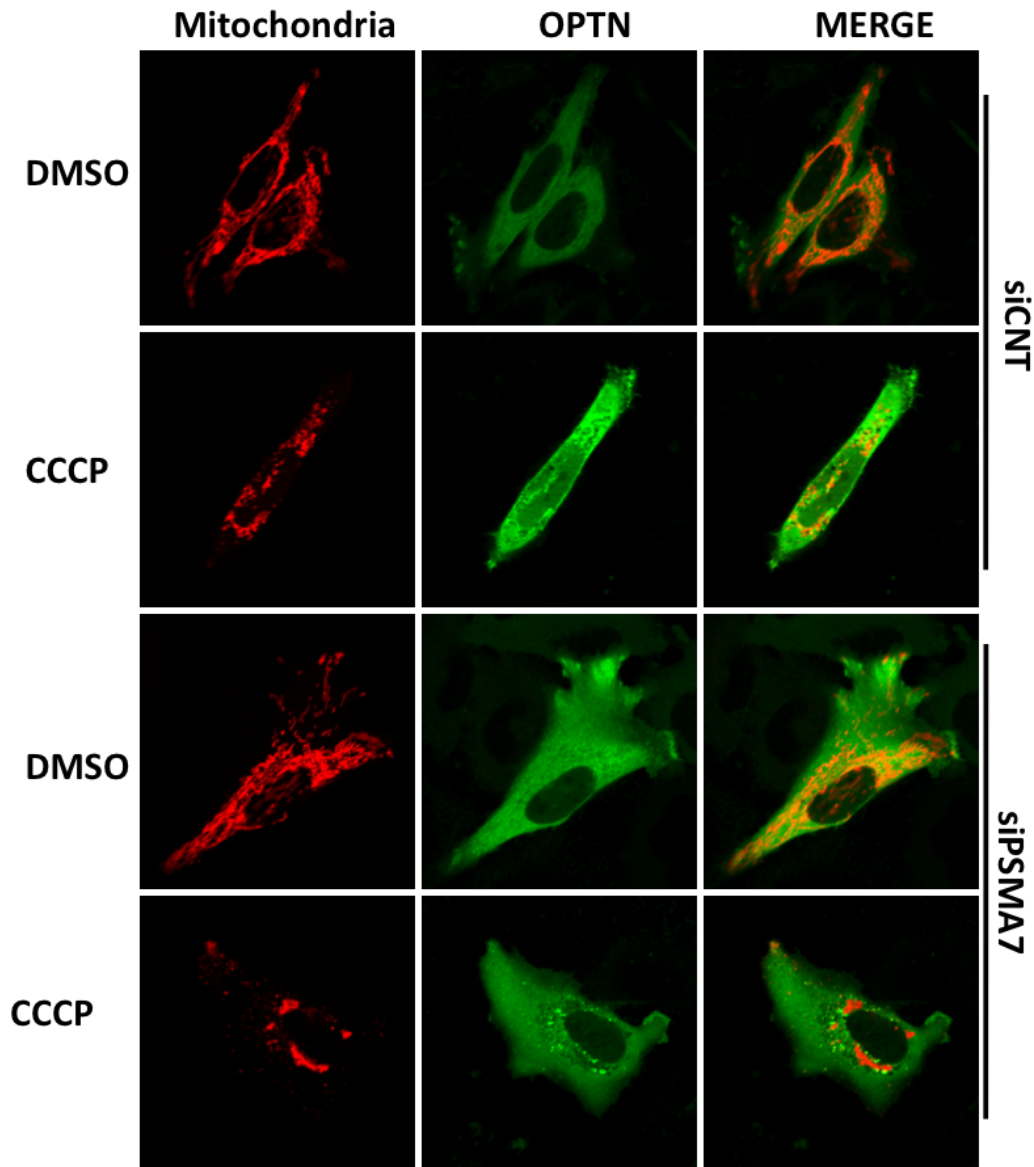


Figure 3.1.5 19: The effect of knock down PSMA7 on mitochondria associated GFP-OPTN dot formation in HELA cells. HELA cells co-transfected with EGFP-tagged OPTN (Green), mito-dsRed (Red) and together with either PSMA7-targeting or non-targeting siRNA for 48 h. Following treatment with DMSO or CCCP (10 μ M, 12 h), cells were fixed with 4% PFA and dot formation was analyzed under confocal microscope. *Merge*, overlay of green and red signals (Representative data of N=3 independent experiments).

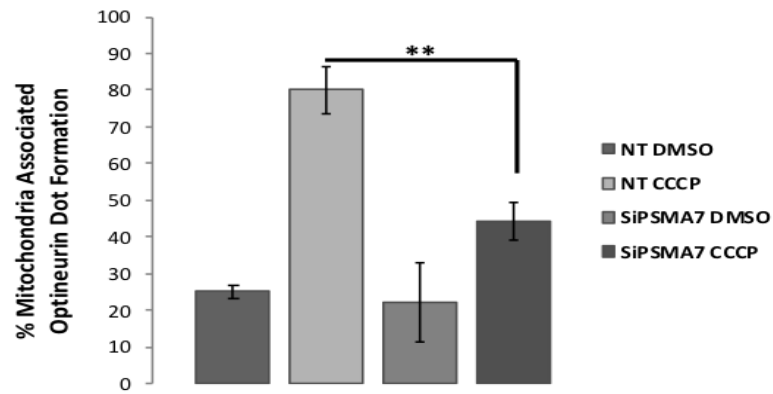


Figure 3.1.5 20: The quantification of mitochondria associated GFP-OPTN dot formation in HELA cells. At least 50 cells per condition per experiment quantified, mean \pm S.D. n=3 independent experiments, p value: 0,001825.

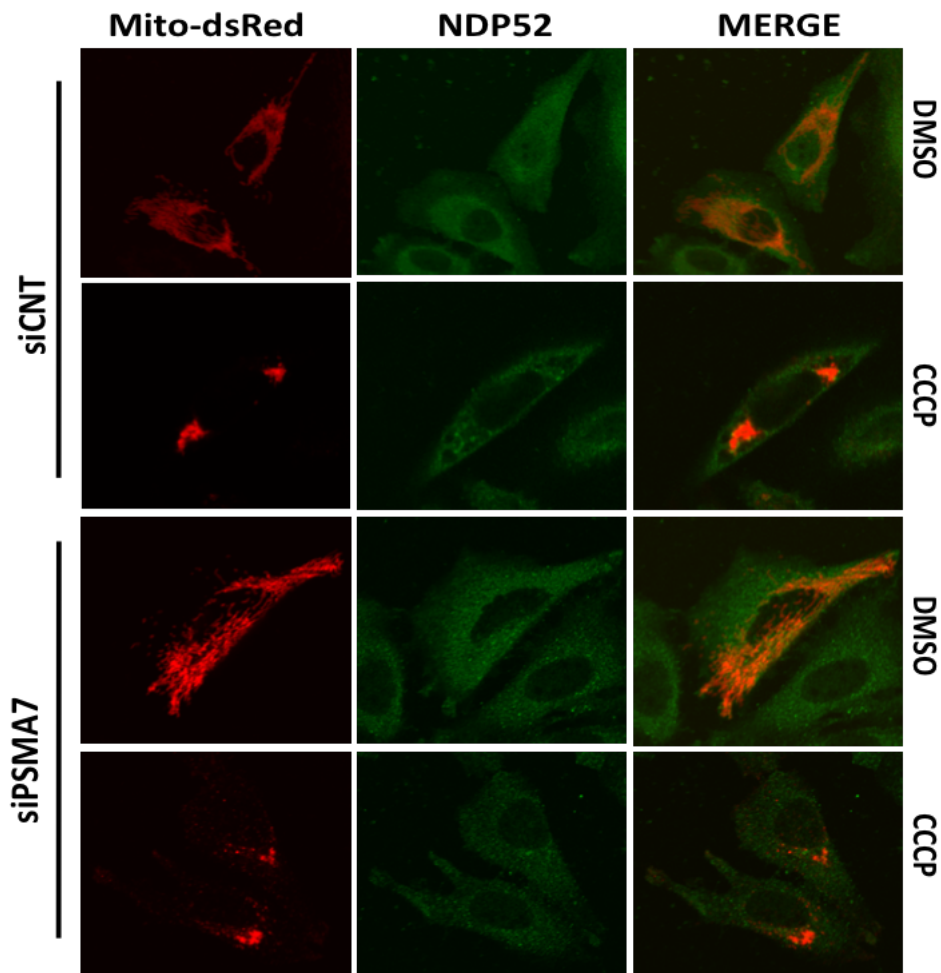


Figure 3.1.4 21: The effect of knockdown PSMA7 on mitochondria associated NDP52 dot formation in HELA cells. HELA cells co-transfected with mito-dsRed (Red) and together with either PSMA7-targeting or non-targeting siRNA for 48 h. Following treatment with DMSO or CCCP (10 μ M, 12 h), cells were fixed with 4% PFA. Fixed samples were permeabilized and then sequentially incubated with NDP52 primary

antibody and Alexa Fluor 488 rabbit secondary antibody and then analyzed under confocal microscope. *Merge*, overlay of green and red signals (Representative data of N=3 independent experiments)

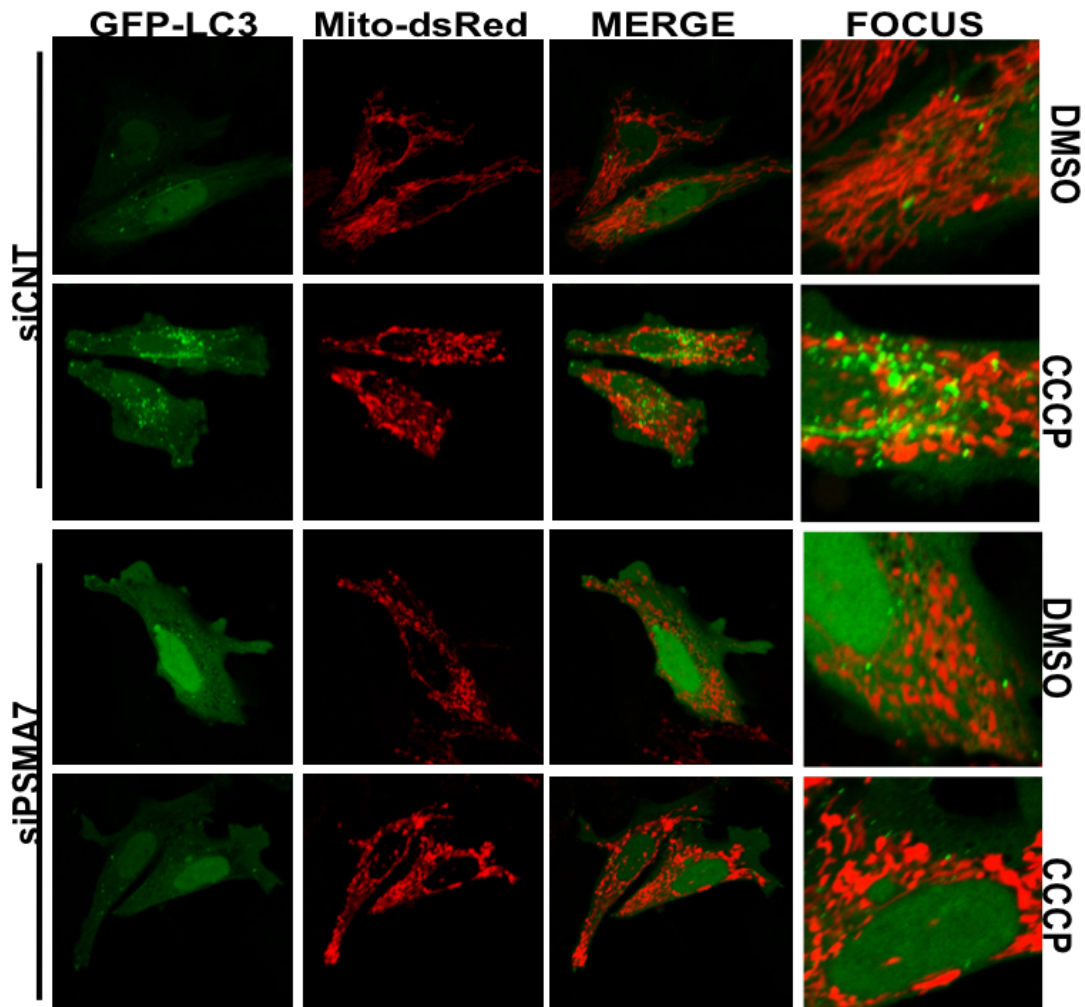


Figure 3.1.5 22: The effect of siRNA-mediated knock down of PSMA7 on mitochondria associated GFP-LC3 dot formation. HELA cells co-transfected with pEGFP-tagged LC3 (Green), mito-dsRed (Red) and together with either PSMA7-targeting or non-targeting siRNA for 48 h. Following treatment with DMSO or CCCP (10 μ M, 12 h), cells were fixed with 4% PFA and mitochondria associated dot formation was analyzed under confocal microscope. *Merge*, overlay of green and red signals (Representative data of N=4 independent experiments).

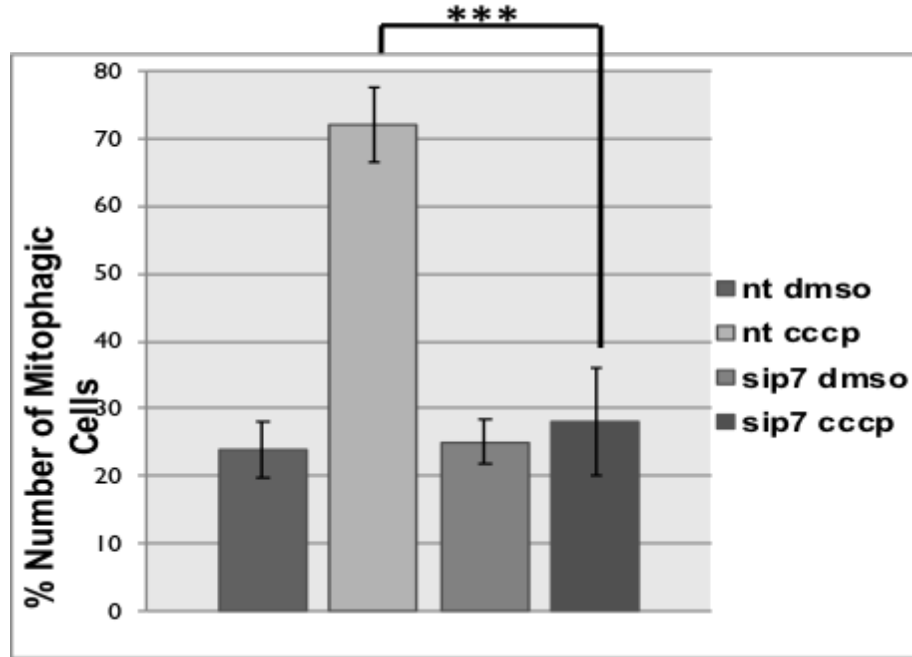


Figure 3.1.5 23: The quantification of mitochondria associated GFP-LC3 dot formation in HELA cells. At least 50 cells per condition per experiment quantified, mean \pm S.D. n=3 independent experiments, p value: 0,000196.

Afterwards, as an mitophagy test rather than previous mitochondrial protein degradation, GFP-LC3 dots that were localizing on mitochondria were analyzed with confocal microscope and quantified in HELA (Figure 3.1.5 22 and 3.1.4 23) and HEK/293T cells (Figure 3.1.5 24 and 3.1.5 25). Accordingly, it was observed that knock down PSMA7 significantly blocked cellular mitophagy levels by interfering the LC3 dot and mitochondria association in HELA and HEK/293T cells.

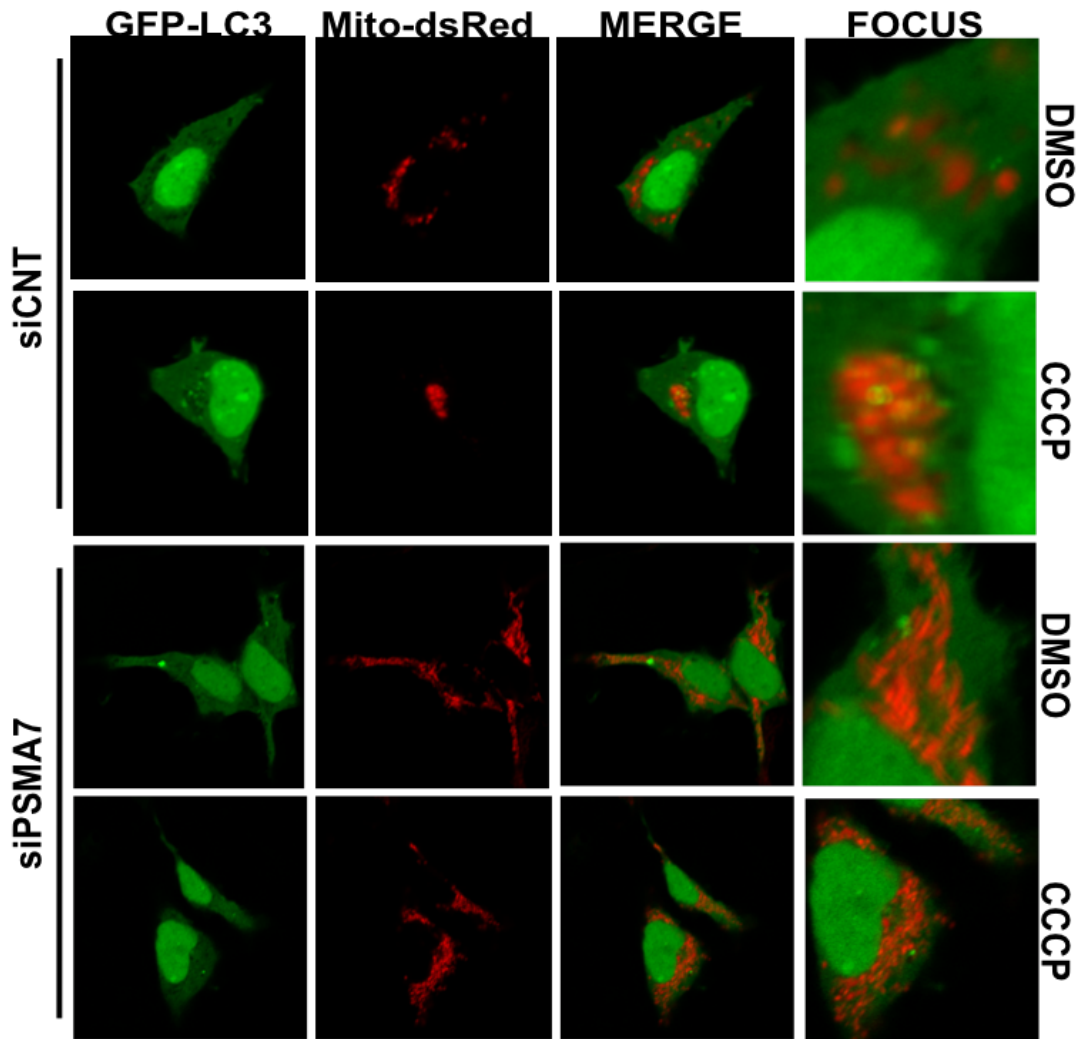


Figure 3.1.5 24: The effect of knock down PSMA7 on mitochondria associated GFP-LC3 dot formation in HEK/293T cells. HEK/293T cells co-transfected with pEGFP-tagged LC3 (Green), mito-dsRed (Red) and together with either PSMA7-targeting or non-targeting siRNA for 48 h. Following treatment with DMSO or CCCP (10 μ M, 12 h), cells were fixed with 4% PFA and mitochondria associated dot formation was analyzed under confocal microscope. *Merge*, overlay of green and red signals (Representative data of N=4 independent experiments).

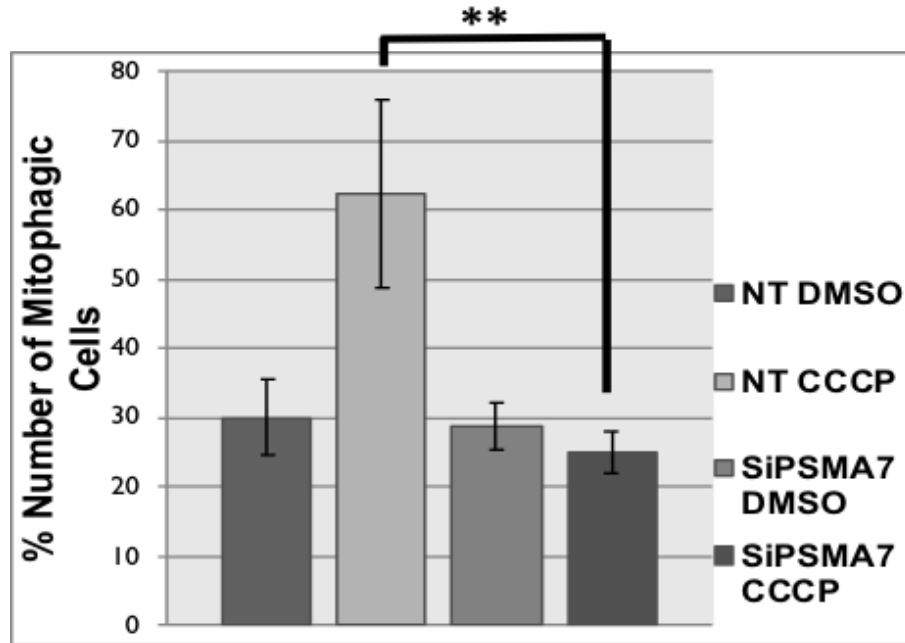


Figure 3.1.5 25: The quantification of GFP-LC3 dot associated mitochondria of HEK/293T cells at least 50 cells per condition per experiment quantified, mean \pm S.D. n=4 independent experiments, p value: 0,009848.

Next, the effect of PSMA7 on mitophagy was checked by the means of staining cellular DNA and subtracting nuclear DNA from that total DNA content, alterations in mitochondrial DNA was evaluated under confocal microscopy (Figure 3.1.5 26) and quantified (Figure 3.1.5 27).

Based on the data shown in Figure 3.1.5 26 and Figure 3.1.5 27, knockdown PSMA7 significantly blocked CCCP mediated mitochondrial clearance in other words PSMA7 was introduced as novel regulator of mitochondrial DNA and mitophagy.

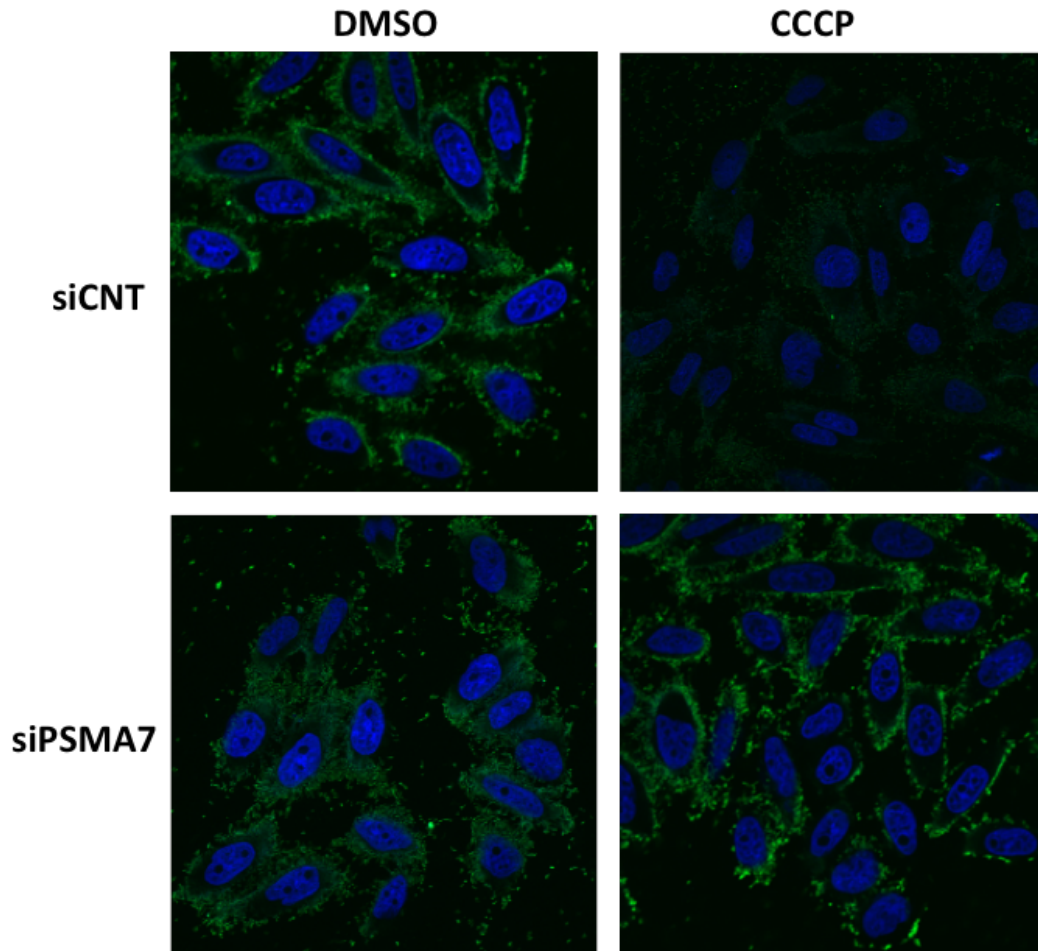


Figure 3.1.5 26: Anti-DNA staining results of HELA cells to analyze mitochondrial DNA in HELA cells. HELA cells were co-transfected with MYC-tagged Parkin and PSMA7-targeting or non-targeting siRNAs. Following treatment with DMSO or CCCP (10 μ M, 12 h), cells were fixed with 4% PFA and permeabilized with BSA and saponin solution. Then permeabilized cells were incubated with Anti-DNA primary antibody and Alexa Fluor-488 (Green) secondary antibody. After washes, stained with DAPI (Blue) for differentiation of nuclear DNA. Slides were analyzed by confocal microscopy (Representative data of n=3 independent experiments).

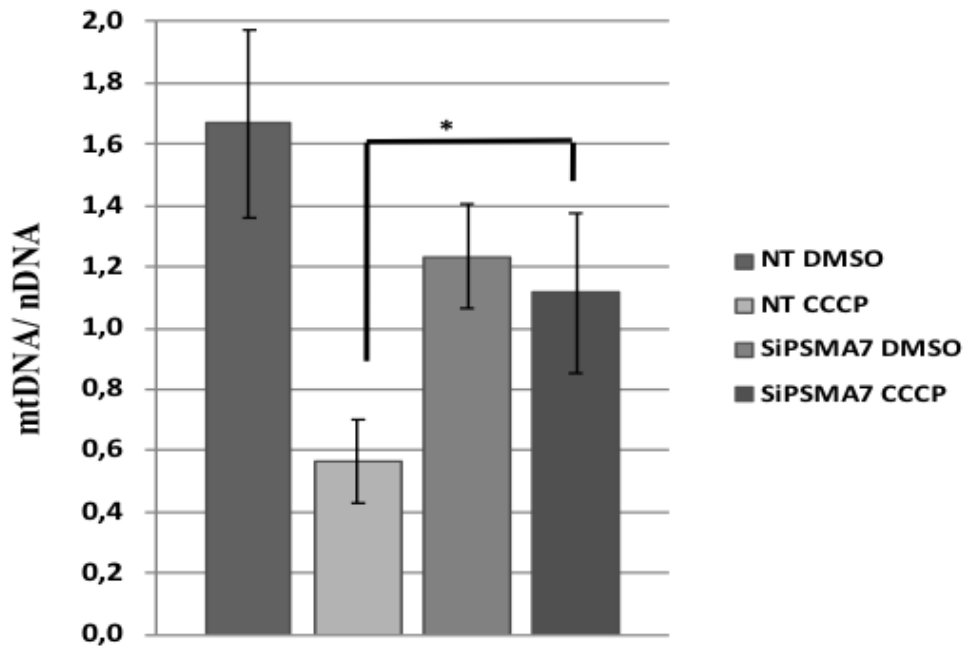


Figure 3.1.5 27: The quantification of mitochondrial DNA amount of HELA cells at least 100 cells were considered per condition in experiment, mean \pm S.D. of n=3 independent experiments, p value \leq 0.05.

Furthermore, the dependence on proteasomal activity of ATG5 onto the mitochondria was tested by using chemical proteasome inhibitor rather than genetic manipulation.

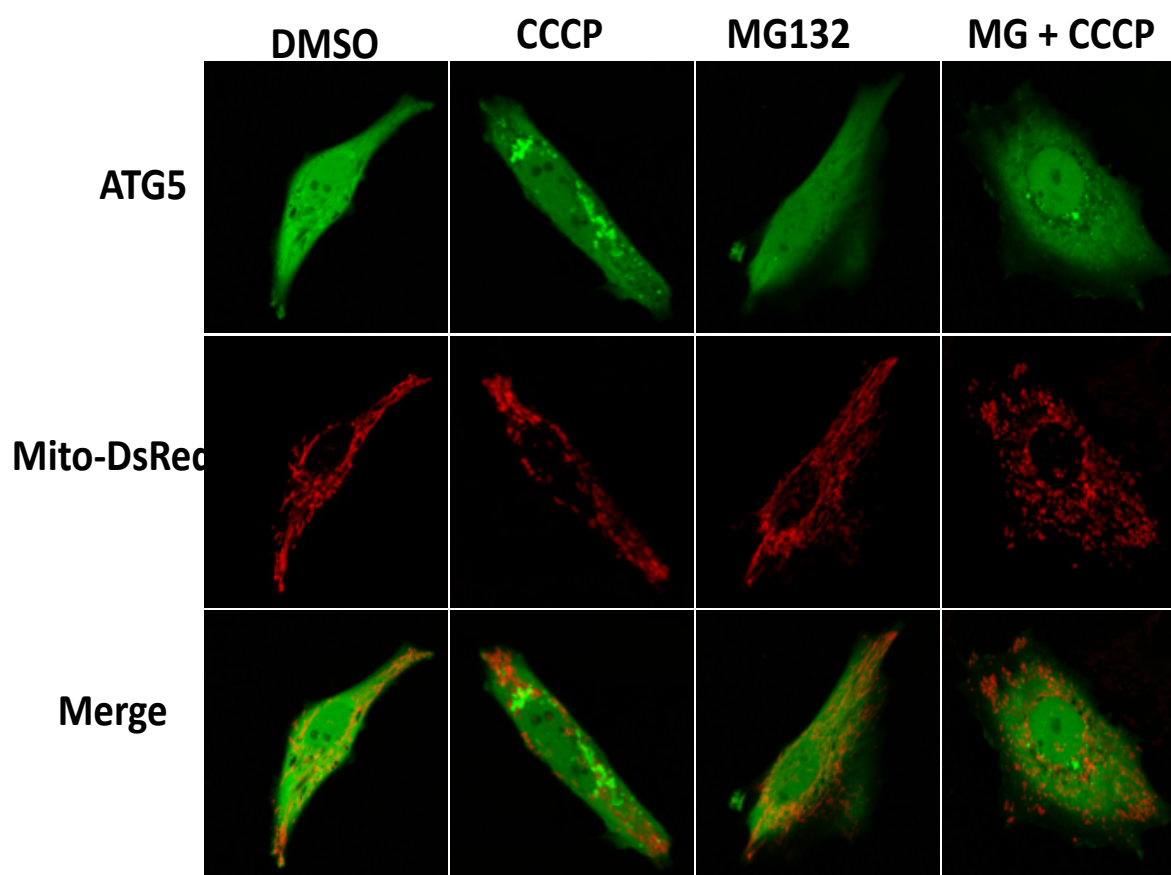


Figure 3.1.5 28: The effect of proteasomal activity on ATG5 recruitment onto mitochondria in Parkin stable HeLa cells. HeLa cells were co-transfected with mito-dsRed (Red) and GFP-tagged ATG5 (Green) constructs for 48 h. Following treatment with DMSO or CCCP (20 μ M), MG132 (30 μ M) and MG132 combination with CCCP, cells were fixed with 4% PFA and analyzed under confocal microscope. *Merge*, overlay of green and red signals (n=3 independent experiments performed).

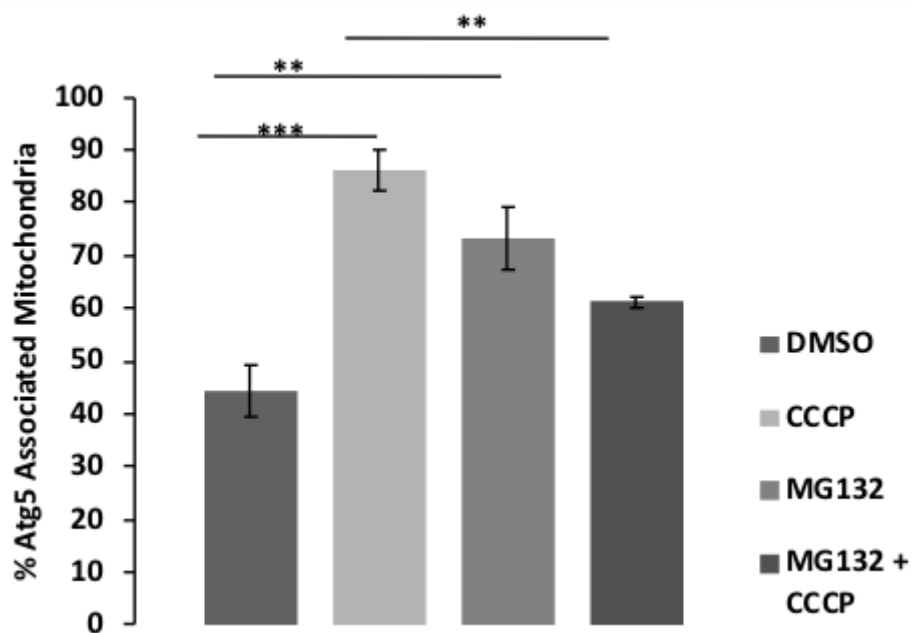


Figure 3.1.5 29: Quantification of mitochondria associated ATG5 in HeLa cells at least 30 cells were considered per condition in an experiment, mean \pm S.D. of n=3 independent experiments, p value \leq 0.05)

According to colocalization tests (Figure 3.1.5 28) and its quantification (Figure 3.1.5 29), it's observed that upon proteasome inhibition compare to DMSO condition ATG5 accumulated onto the mitochondria however when combined with CCCP, CCCP-mediated recruitment of ATG5 was decreased.

All these data obtained from this study showed that PSMA7 by forming complexes with ATG5 and Parkin, regulates Parkin translocation from cytoplasm to mitochondria therefore determines the mitochondrial amount and mitophagy level in cells.

In the similar context, we also analyzed the role of ATG5 in several stages of mitophagy as listed in Figure 3.1.5 30.

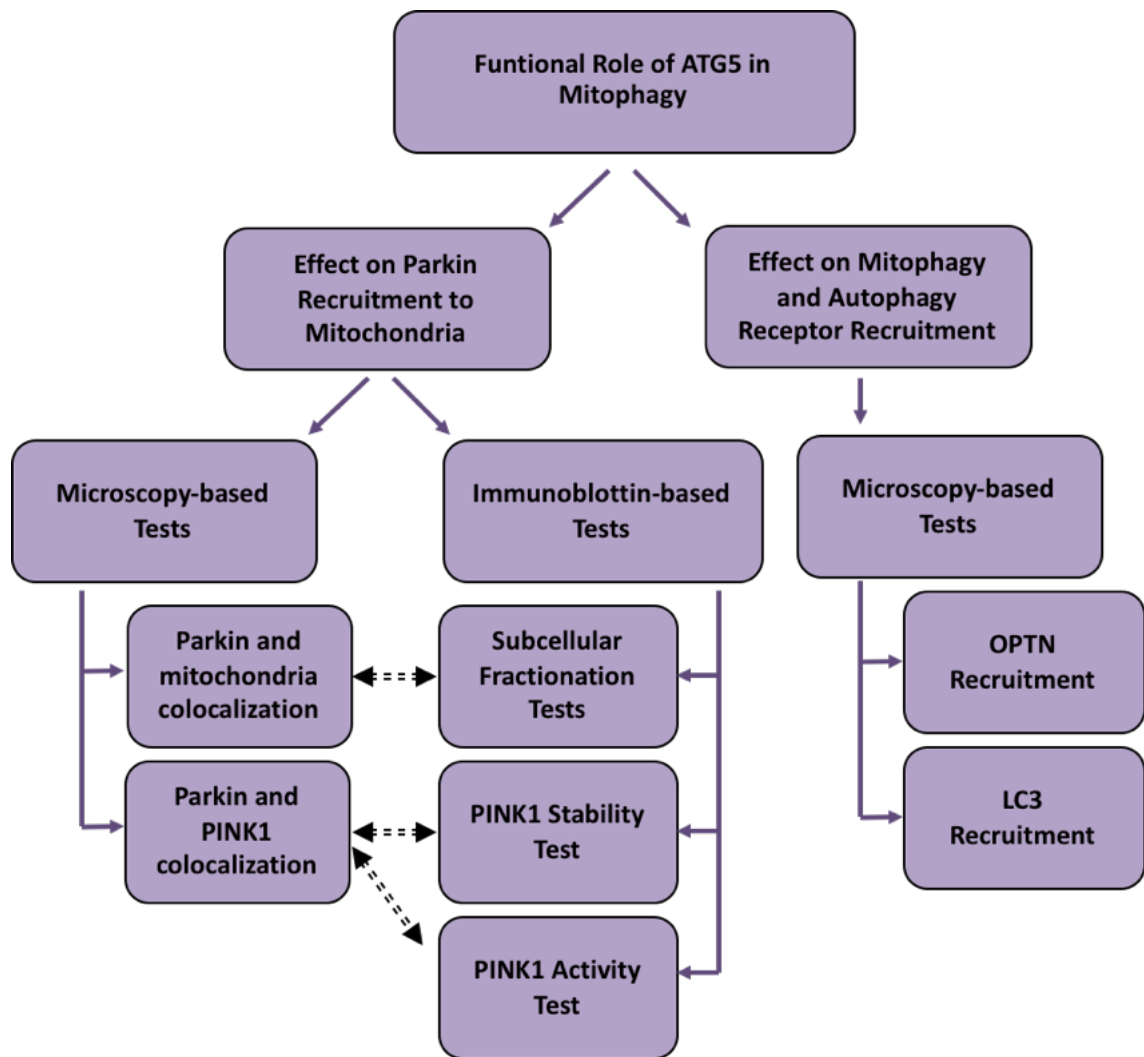


Figure 3.1.5 30: The effect of ATG5 deficiency on mitophagy was investigated in different stages of mitophagy.

First, at a wider perspective knock down effect of ATG5 on mitophagy was checked with colocalization tests by confocal microscopy in HEK/293T (Figure 3.1.5 31) and HELA (Figure 3.1.5 32) cells. In both of the cell lines, ATG5 knock down resulted in decrease in LC3 dot association with mitochondria therefore inhibiting mitochondrial clearance.

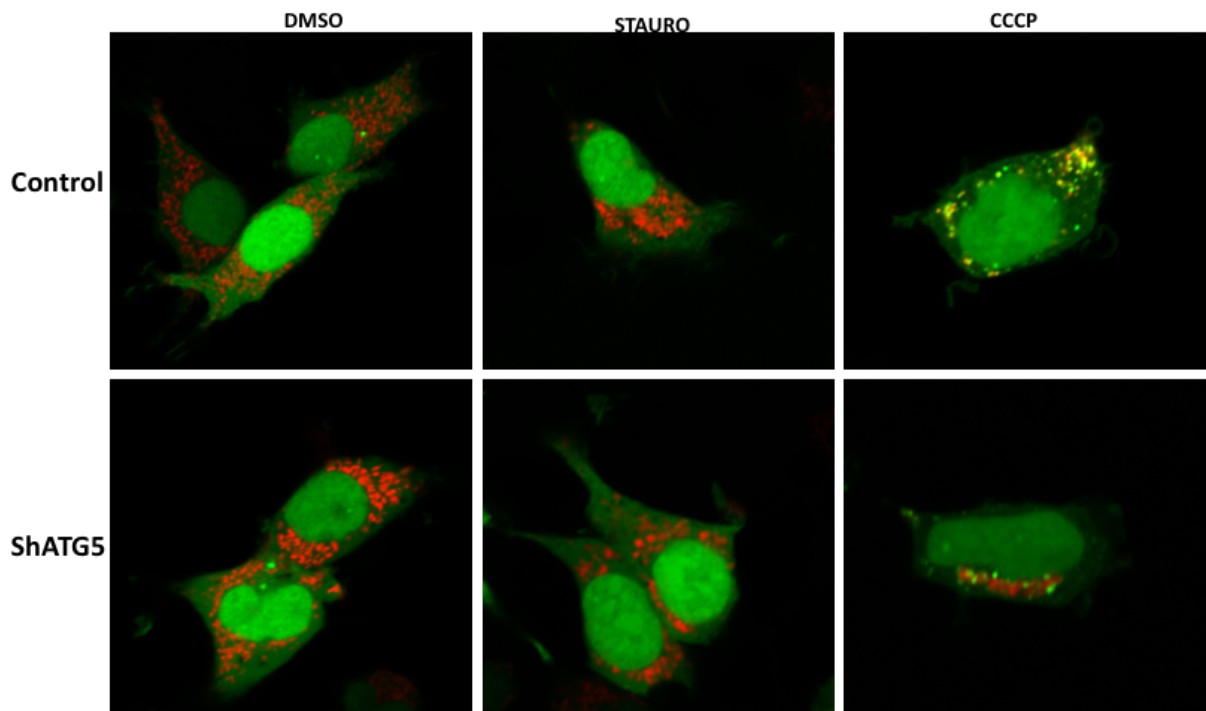


Figure 3.1.5 31: The effect of ShRNA-mediated knockdown of ATG5 on mitophagy in HEK/293T cells was analyzed under confocal microscope. HEK/293T cells co-transfected with pEGFP-LC3 (Green), mito-dsRed (Red) and together with pCDNA3.1 as control or shRNA ATG5 for 72 h. Following treatment with DMSO, Staurosporine and CCCP, cells were fixed and analyzed under confocal microscope (Representative data of n=3 independent experiments, images belong to the merge pictures of each condition).

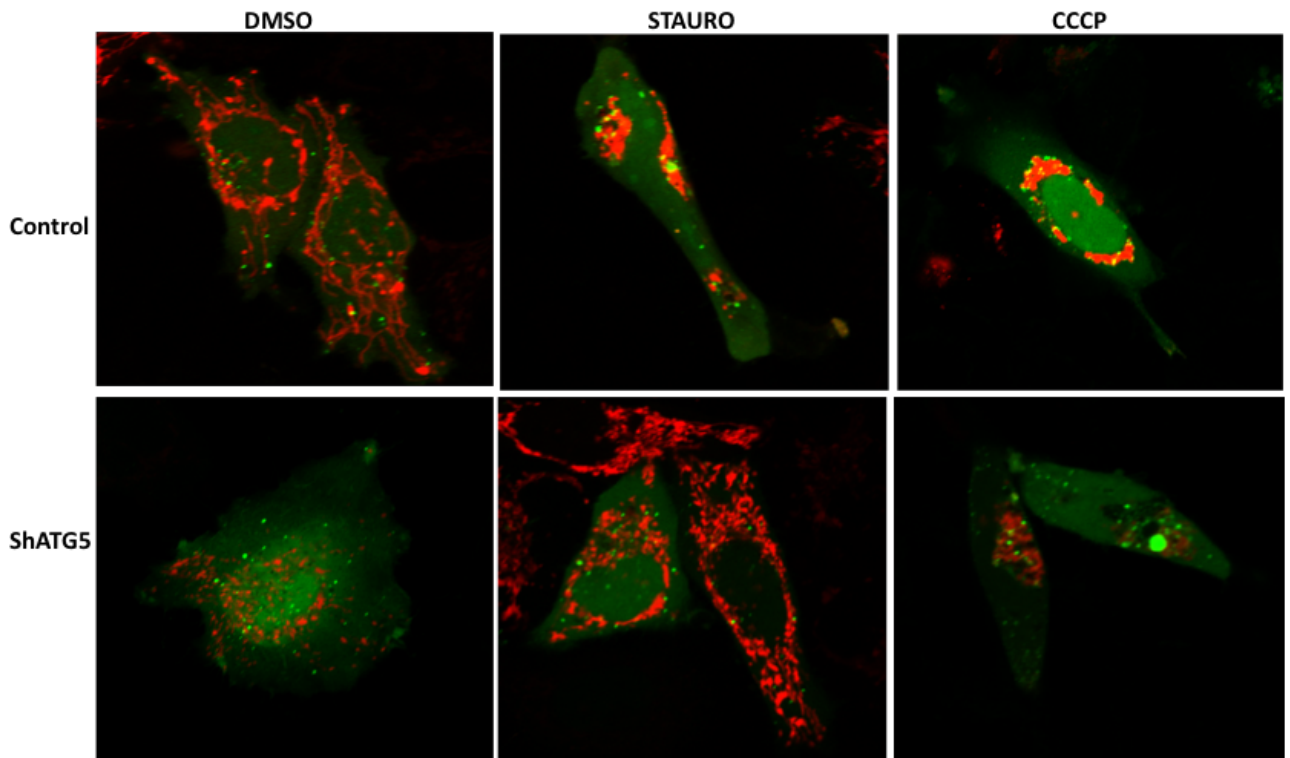


Figure 3.1.5 32: The effect of ShRNA-mediated knockdown of ATG5 on mitophagy in HELA cells was analyzed under confocal microscope. HELA cells co-transfected with pEGFP-LC3 (Green), mito-dsRed (Red) and together with pCDNA3.1 as control or shRNA ATG5 for 72 h. Following treatment with DMSO, Staurosporine and CCCP, cells were fixed and analyzed under confocal microscope (Representative data of n=3 independent experiments, images belong to the merge pictures of each condition).

Next, the effect of ATG5 on mitochondrial optineurin dot formation was analyzed in HELA cells (Figure 3.1.5 33 and Figure 3.1.5 34). Considering the data shown below, deficiency in ATG5 attenuated significantly CCCP-stimulated OPTN puncta formation which were localized on mitochondria in HELA cells.

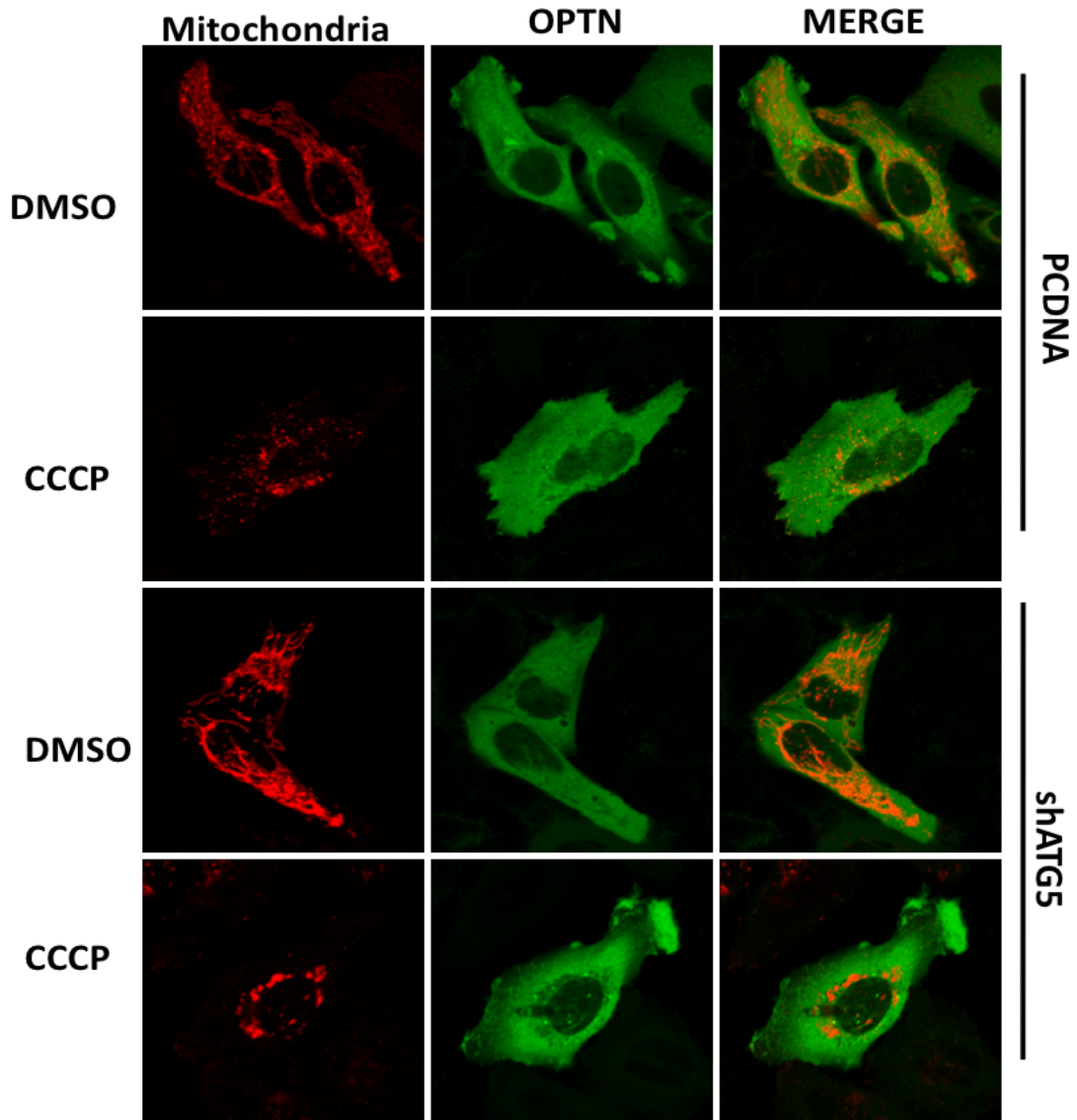


Figure 3.1.5 33: The effect of shRNA mediated knock down of ATG5 on mitochondria associated GFP-OPTN dot formation in HELA cells. HELA cells co-transfected with EGFP-tagged OPTN (Green), mito-dsRed (Red) and together with either pCDNA3.1 or shRNA ATG5 for 72 h. Following treatment with DMSO or CCCP (10 μ M, 12 h), cells were fixed with 4% PFA and dot formation was analyzed under confocal microscope. *Merge*, overlay of green and red signals (Representative data of N=3 independent experiments).

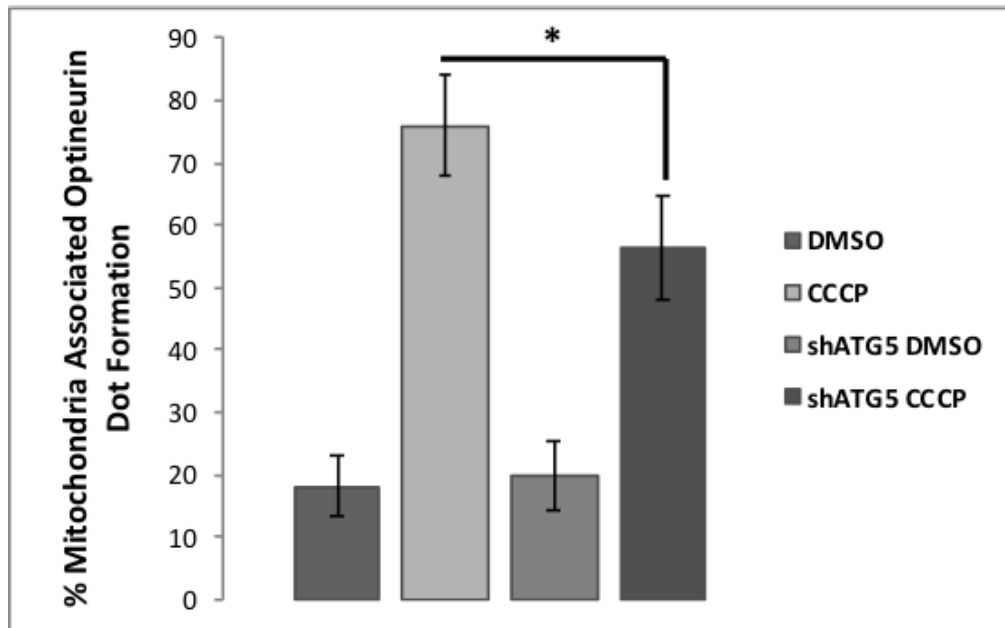


Figure 3.1.5 34: The quantification of mitochondria associated GFP-OPTN dot formation in HELA cells at least 50 cells per condition per experiment quantified, mean \pm S.D. n= 3 independent experiments, P value: 0,044831.

So far, knock down of ATG5 has been shown to have an inhibitory effect on mitophagy through altering OPTN recruitment to mitochondria.

Furthermore, the role of ATG5 on Parkin recruitment was evaluated by colocalization tests and its quantification in HELA cells (Figure 3.1.5 35 and Figure 3.1.5 36). In accordance with data exhibited below, shRNA-mediated ATG5 knockdown had an enhancing effect for recruiting mitochondria.

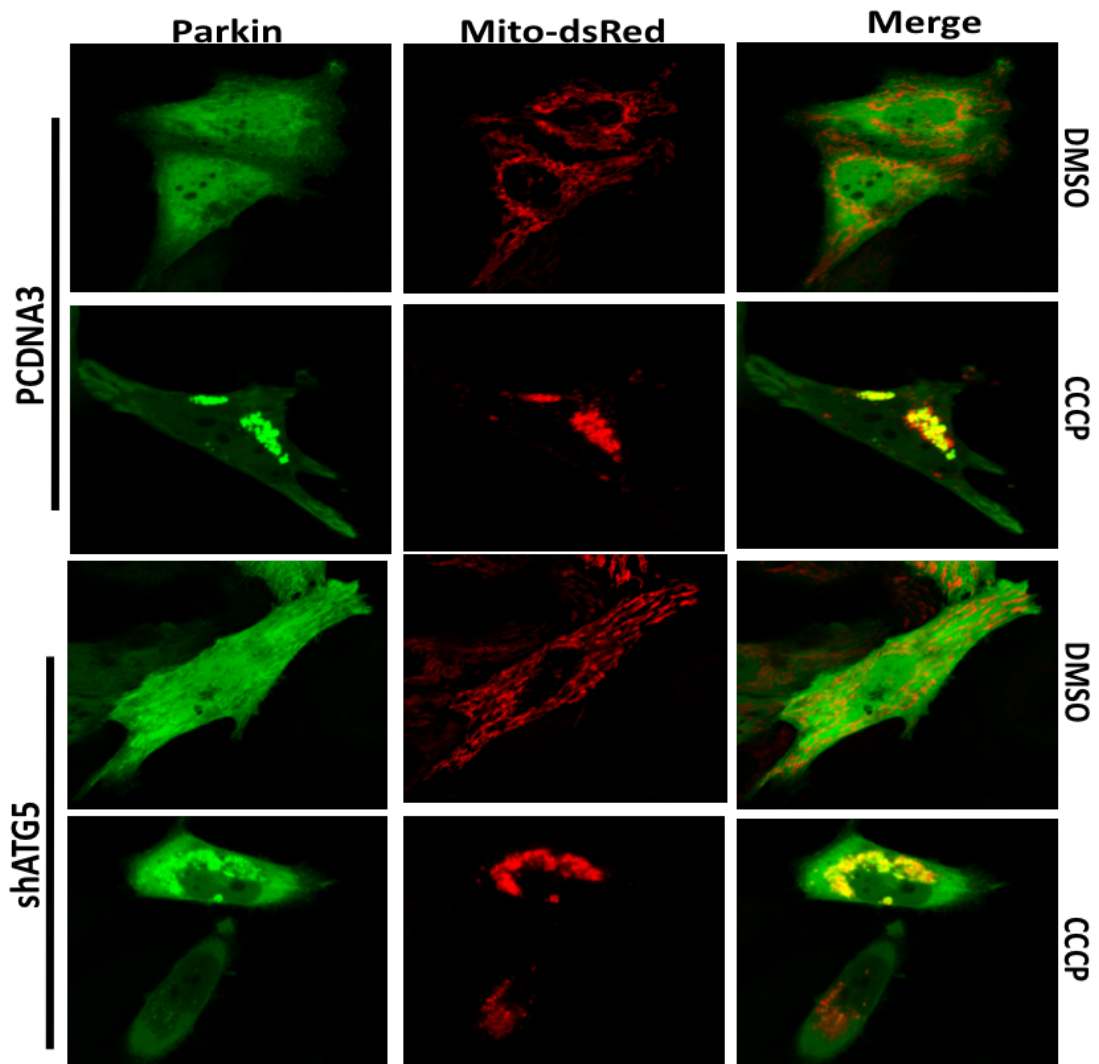


Figure 3.1.5 35: The effect of knock down ATG5 on Parkin recruitment to mitochondria in HELA cells. HELA cells were co-transfected with YFP-tagged Parkin (Green) and mito-dsRed (Red) constructs together with pCDNA3.1 as control or shRNA ATG5 for 72 h. After DMSO or CCCP treatment (10 μ M, for 12 h), cells were fixed with 4% PFA and analyzed under confocal microscope. *Merge*, overlay of green and red signals (Representative data of N=3 independent experiments).

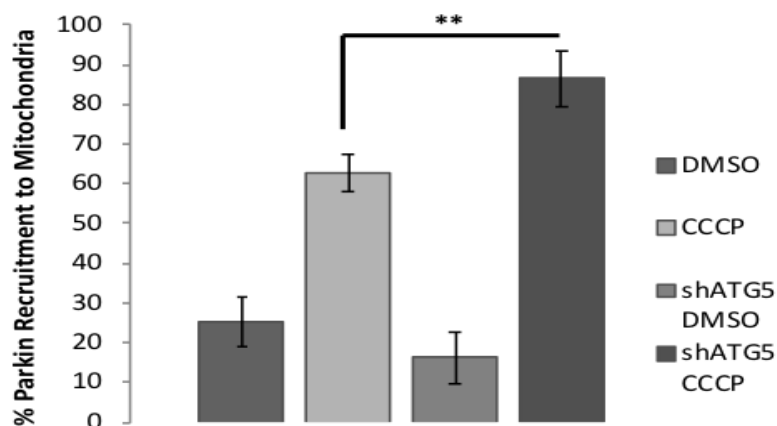


Figure 3.1.5 36: The quantification of Parkin translocation onto mitochondria of HELA cells at least 30 cells were considered per condition in experiments, mean \pm S.D. of n=3 independent experiments, p value \leq 0.05.

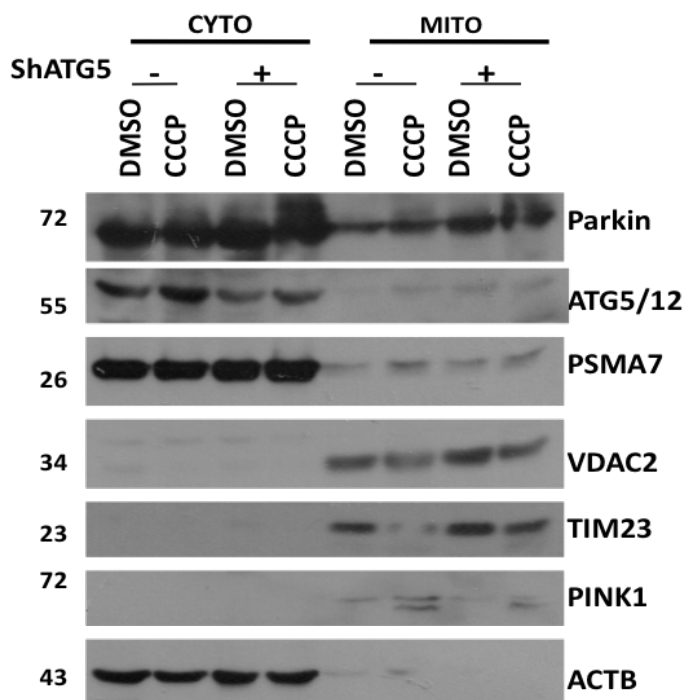


Figure 3.1.5 37: Subcellular fractionations tests of HEK/293T cells. HEK/293T cells co-transfected with YFP-tagged Parkin construct together with pCDNA3.1 as control or shRNA ATG5 for 72 h. After DMSO or CCCP treatment (10 μ M, for 12 h), cells were harvested and pellets were subjected to series of differential centrifugation steps for the isolation of mitochondrial and cytoplasmic fractions. For immunoblots, Parkin, ATG5, PSMA7, VDAC1, TIM23, PINK1 antibodies were used. *ACTB*, β -Actin was used for the purification control of the isolation.

To further validate the results of colocalization tests, by performing subcellular fractionation experiments in HEK/293T cells. As shown in Figure 3.1.5 37, knock down ATG5 resulted in accumulation of Parkin on mitochondria, not only CCCP conditions but also under steady state levels. However, blocked mitophagy in terms of decreasing the CCCP-mediated degradation capacity on OMM and IMM proteins.

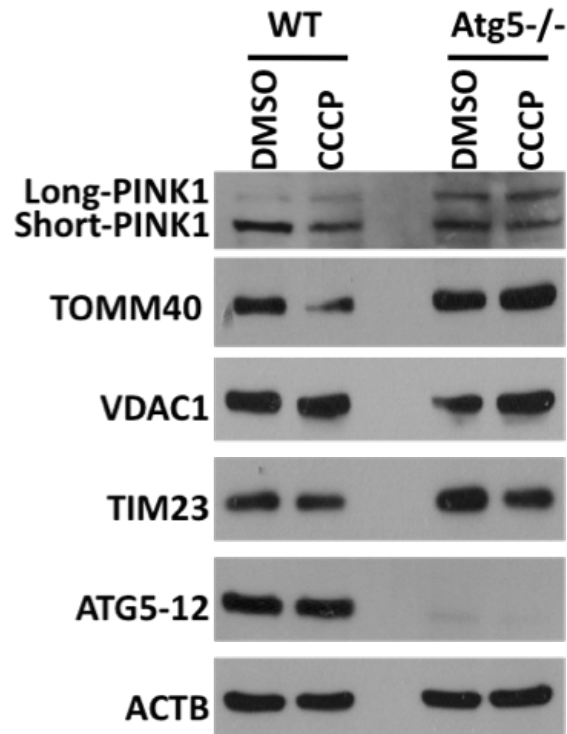


Figure 3.1.5 38: The effect of ATG5 deficiency in MEF cells. WT and ATG5 $-/-$ MEF cells were seeded in 6-well plates with a density of 250.000 cells per well. Following DMSO or CCCP treatment (10 μ M, for 12 h), cells were harvested and proteins were extracted. Denaturated protein samples were separated through 12% SDS-PAGE. For immunoblots, PINK1, TOM40, VDAC1, TIM23 and ATG5 antibodies were used. *ACTB*, β -Actin was used for loading control. *WT*, wild type and *ATG5-/-*, ATG5 Knockout cells. N=3 independent experiments performed.

Additionally, the global effect of ATG5 deficiency was checked in wild type and ATG5 knockout MEF cells (Figure 3.1.5 38). According to immunoblotting results, it is observed that CCCP-mediated degradation of mitochondrial proteins, including TOM40 and TIM23 blocked in ATG5^{-/-} MEF cells. But more interestingly, PINK1 protein become stabilized in response to ATG5 deficiency in its long, unprocessed form suggesting that ATG5 has more complex regulation in mitophagy not only recruiting autophagic membranes but also regulating PINK1 function.

In order to validate the data obtained from MEF cells, ATG5 knockout HeLa cells were generated by using Crispr/Cas9 strategy. Polyclones were tested according to their ATG5 levels and followed by monoclonal selection in puromycine containing selective medium. Two different monoclones were determined according to their ATG5-12 levels and their basal autophagy levels for further use in the experiments (Figure 3.1.5 39).

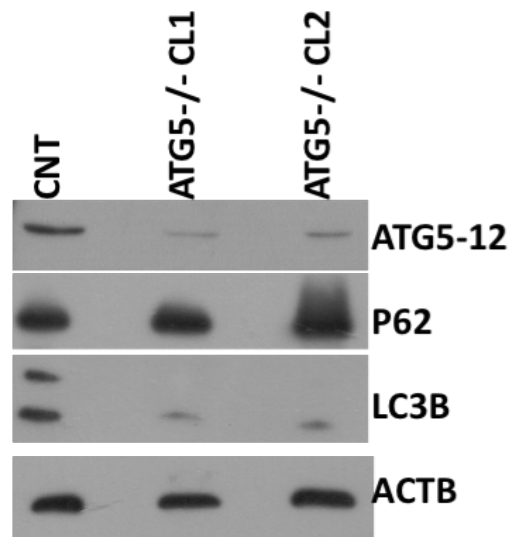


Figure 3.1.5 39: Confirmation of ATG5^{-/-} HeLa clones. Selected HELA clones were harvested and protein lysates were prepared using RIPA buffer. Denaturated samples were separated through 15% SDS-PAGE. For immunoblots, ATG5, P62 and LC3 antibodies were used. *ACTB*, β -Actin was used for loading control.

With selected monoclonals, the effect of ATG5 on mitochondrial protein in HeLa cells were tested (Figure 3.1.5 40). According to data shown in Figure 3.1.5 40, CCCP-mediated degradation of mitochondrial proteins were reduced with ATG5 knockout in line with the MEF cell results.

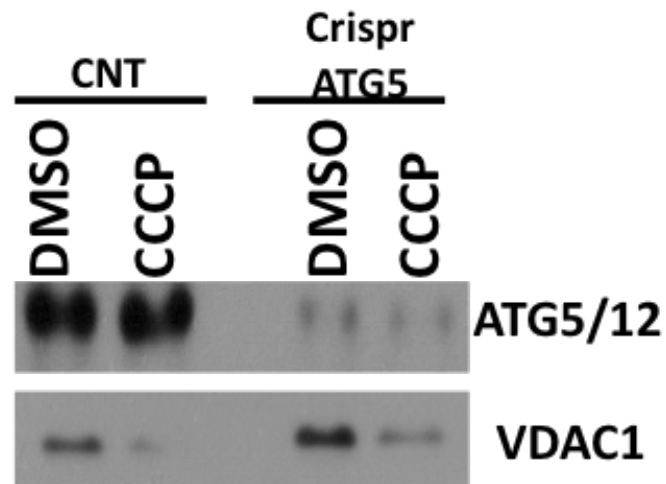


Figure 3.1.5 40: The effect of ATG5 mitochondrial protein levels was analysed in CNT and ATG5^{-/-} HeLa cells. HELA cells were seeded in 6-well plates with a cell density of 250.000 cells per well. Following DMSO or CCCP treatment (10 μ M, for 12 h), cells were harvested and proteins were extracted. Denaturated protein samples were separated through 12% SDS-PAGE. For immunoblots, ATG5 and VDAC1 antibodies were used.

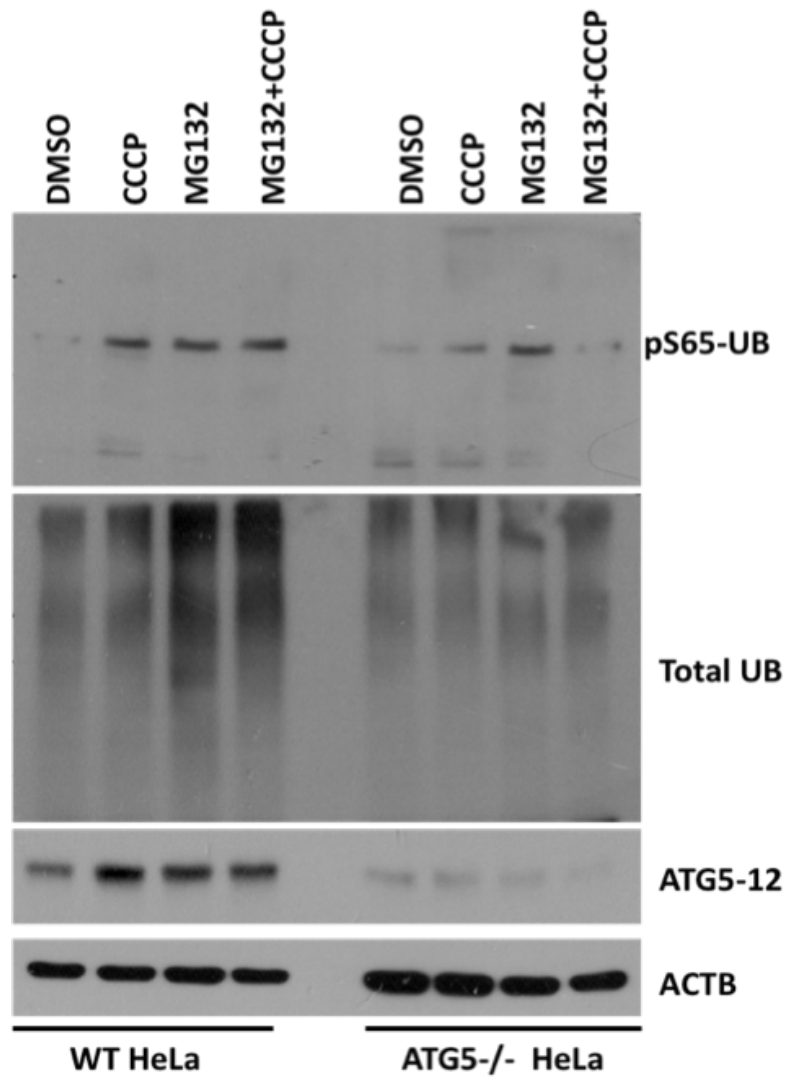


Figure 3.1.5 41: The effect of ATG5 on ubiquitin phosphorylation as a readout of PINK1 activity. HELA cells were seeded in 6-well plates with a cell density of 250.000 cells per well. Cells were treated with DMSO, CCCP treatment (20 μ M), MG132 (30 μ M) and MG132 combined with CCCP. Then cells were harvested and phospho-proteins were extracted. Denaturated protein samples were separated through 12% SDS-PAGE. For immunoblots, ATG5, UB, pSER65-UB and β -Actin antibodies were used. *ACTB*, β -Actin was used for loading control (Representative data of n=2 independent experiments).

Based on the stability effect of ATG5 on PINK1, the data led us to analyze the effect of ATG5 on PINK1 kinase activity. To do that, one of the phosphorylation targets of PINK1, Ser65 phosphorylation of ubiquitin levels were analyzed in WT and ATG5^{-/-} HeLa cells (Figure 3.1.5 41). According to Figure 3.1.5 41, in WT cells, CCCP induced ubiquitin phosphorylation and MG132 mediated proteasome inhibition had no effect on phosphorylation status of ubiquitin. In ATG5^{-/-} cells, CCCP induced ubiquitin phosphorylation but not as much as in the case of WT cells suggesting that ATG5 has regulatory role in kinase activity of PINK1.

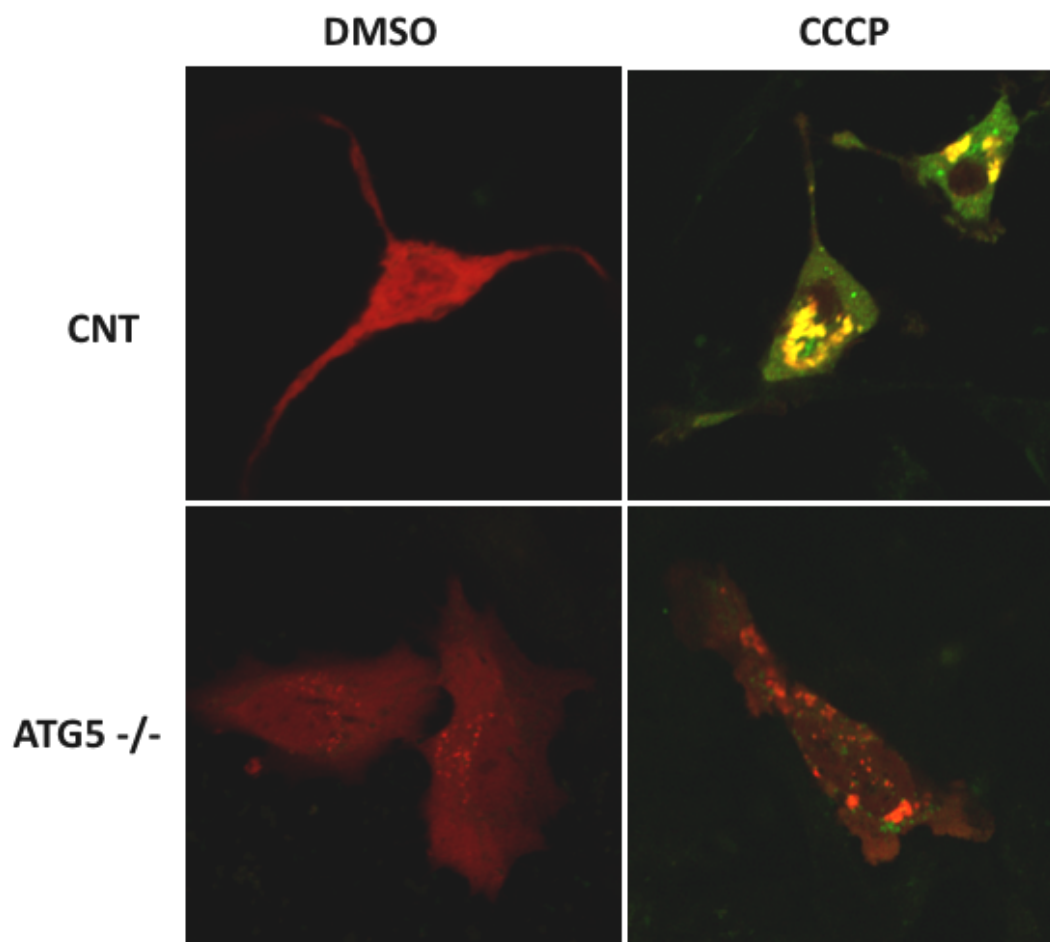


Figure 3.1.5 42: The effect of ATG5 deficiency in PINK1- Parkin interaction in HeLa cells. WT and ATG5^{-/-} HELA cells were cultured on cover slides in 12-well plates at a cell density of 25.000 cells per well. Cells were co-transfected with GFP-tagged PINK1 (Green) and pmCherry-tagged Parkin (Red) constructs for 48 h. After DMSO or CCCP treatment (10 μ M, for 12 h), cells were fixed with 4% PFA and analyzed under confocal

microscope. *Merge*, overlay of green and red signals (Representative data of N=3 independent experiments).

Observed functional and stability regulation of PINK1 by ATG5 protein were further analyzed in terms the PINK1-Parkin interaction by colocalization test respesented in Figure 3.1.5 42. According to microscopy tests, CCCP treatment enhanced PINK1 and Parkin colocalization whereas PINK1 and Parkin remained in different regions as accumulation around perinuclear area in ATG5^{-/-} cells.

So far, all these data suggest that ATG5 and PSMA7 has differential role in the regulation of mitochondrial homeostasis.

3.1.6 The Effect of Other Proteasomal Subunits on Mitophagy

One of the catalytic β subunit, PSMB5 was found in enriched protein-protein complex with ATG5 protein under CCCP treatment condition when compared with DMSO treated control condition in mass spectrometry analyses (Figure 3.1.6 1).

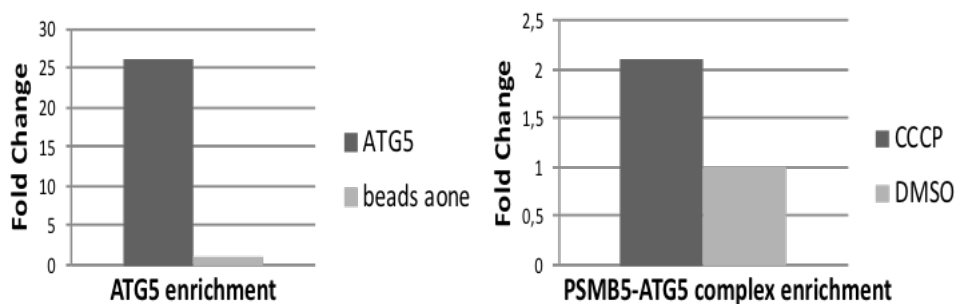


Figure 3.1.6 1: SILAC-based LC-MS/MS analysis. The fold change graphs were compared with beads alone (left); enrichment of PSMB5-ATG5 complex under CCCP condition were compared with DMSO control condition (right) (n=1).

Due to the presence of PSMA7 in cells is both proteasomal and non-proteasomal, the subcellular localization of PSMB5 was analyzed in order to understand the observed effect of PSMA7 is associated with proteasome or not. To investigate the subcellular localization of PSMB5, DMSO and CCCP treated HEK/293T cells were exposed subcellular fractionation tests and their cytoplasm and mitochondria are separated. According to Figure 3.1.6 2, PSMA7 and PSMB5 were predominantly found in cytoplasm and their amount stable upon treatment in cytoplasm. However, in the case of mitochondria, under basal condition there is small amount of PSMA7 and PSMB5 on mitochondria. The presence of PSMA7-PSMB5 complex suggesting the proteasomal abundance onto mitochondria significantly stimulated when cells treated with CCCP. This increase is correlated with enhanced translocation of Parkin onto mitochondria and decreased mitochondrial inner membrane protein, TIM23.

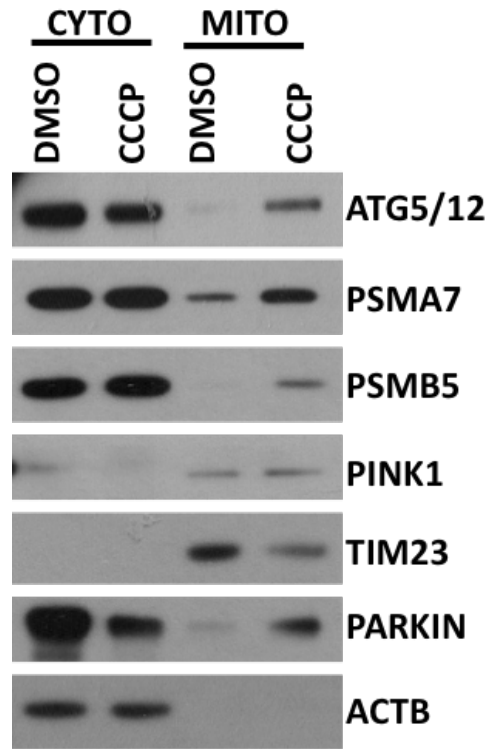


Figure 3.1.6 2: CCCP induces other proteasomal subunits to mitochondria. HEK/293T cells were subjected to 48 h of YFP-Parkin transfection and last 12 h treated with 10 μ M CCCP or DMSO as control. Subcellular fractionation analyses performed. Following fractionation, cytoplasmic and mitochondrial lysates were separated through 12% SDS-PAGE (representative data of n=3 independent experiments). For immunoblotting, ATG5, PSMA7, PSMB5, PARKIN, PINK1 and TIM23 were utilized. *ACTB*, β -Actin was used for purification control of the isolation.

Based on these data, the effect of other proteasomal subunits in fact PSMB5 was investigated on mitophagy process as listed layers in Figure 3.1.6 3.

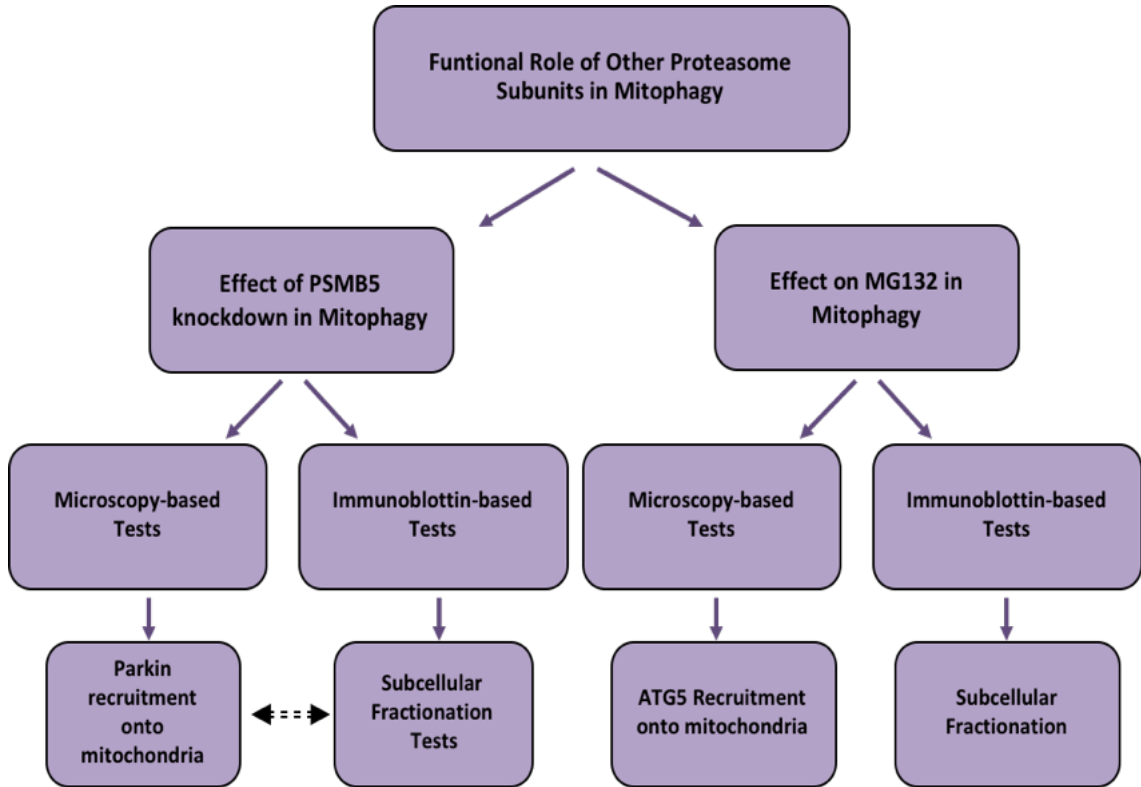


Figure 3.1.6. 3: The effect of other proteasomal subunits and overall proteasome activity on mitophagy in terms of recruitment of regulators investigated.

First, the effect of PSMB5 on Parkin recruitment by confocal microscopy is checked. As shown in Figure 3.1.6. 4, CCCP-induced parkin recruitment onto mitochondria was significantly altered when cellular PSMB5 level is limiting.

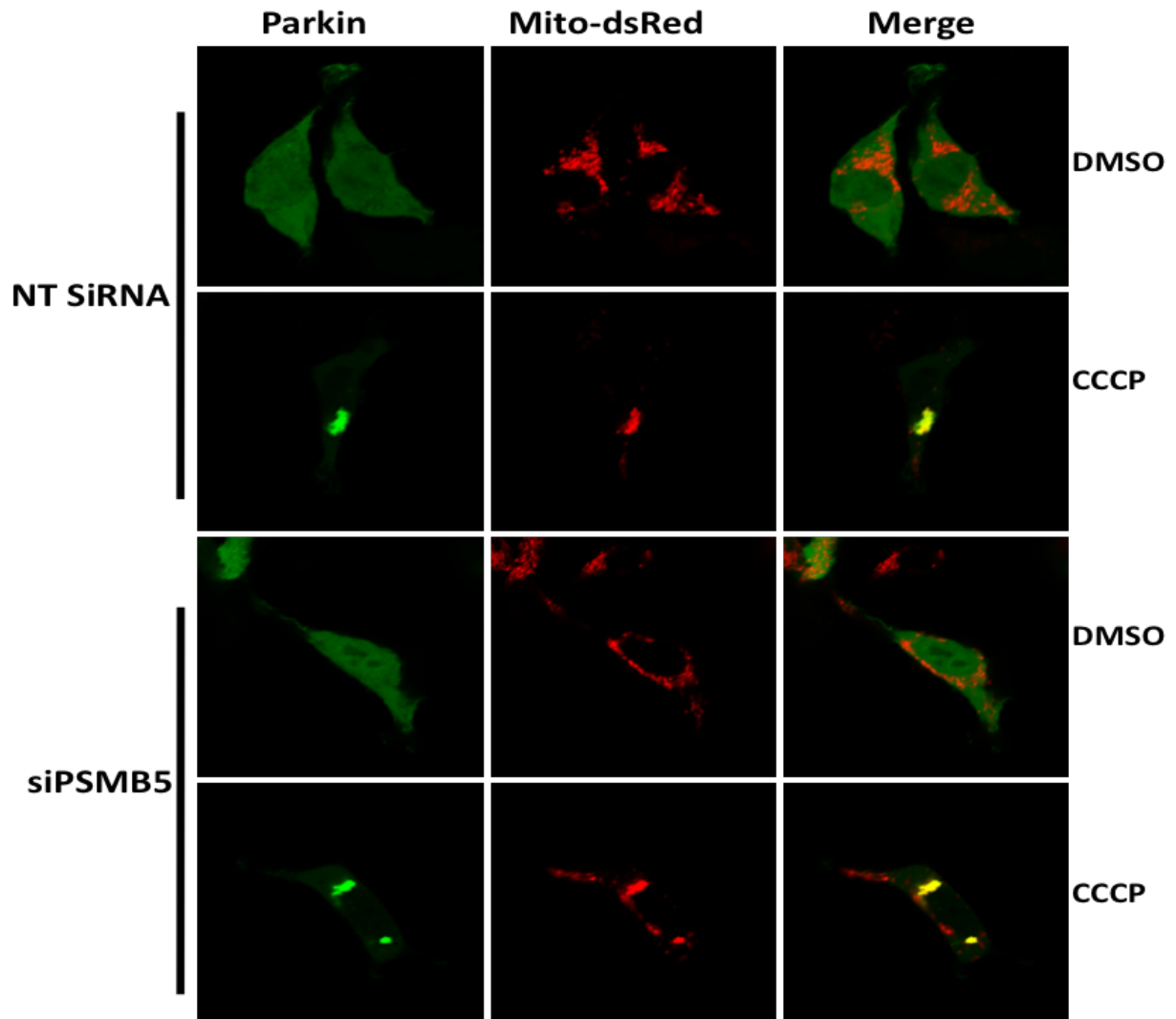


Figure 3.1.6. 4: The effect of siRNA-mediated knockdown of PSMB5 on Parkin recruitment to mitochondria. HEK/293T cells were co-transfected with YFP-tagged Parkin (Green) and mito-dsRed (Red) constructs together with PSMB5-targeting siRNA or non-targeting siRNA for 48 h. After DMSO or CCCP treatment (10 μ M, for 12 h), cells were fixed with 4% PFA and analyzed under confocal microscope. *Merge*, overlay of green and red signals (Representative data of N=3 independent experiments).

Next, the effect of knockdown PSMB5 on Parkin recruitment was analyzed by subcellular fractionation experiments. According to immunoblotting results represented in Figure 3.1.6 5, CCCP-induced Parkin recruitment onto mitochondria abolished when PSMB5 is knocked down using specific siRNAs.

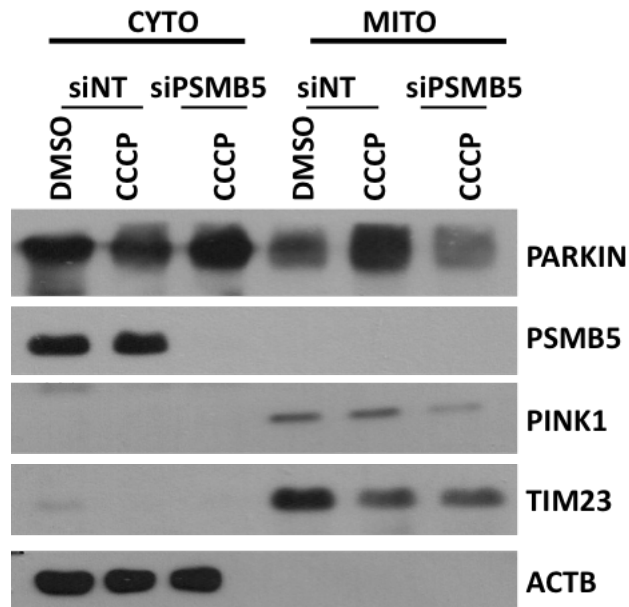


Figure 3.1.6 5: SiRNA mediated knockdown of PSMB5 resulted in decrease in CCCP-induced Parkin translocation onto mitochondria. HEK/293T cells were grown in 15 cm² plates with a cell density of 4x10⁶ cells per plate. For each condition 6 plates of cells seeded. Cells were co-transfected with YFP-tagged Parkin constructs together with PSMB5-targeting siRNA or non-targeting siRNA for 48 h. After DMSO or CCCP treatment (10 μM, for 12 h), cells were harvested and subcellular fractionation protocol was followed. Mitochondrial and cytoplasmic fractions were further separated through 12% SDS-PAGE. For immunoblotting, Parkin, TIM23, PSMB5, PINK1 and ACTIN antibodies were used. Representative data of n=3 independent experiments. β-Actin was used for purification control of the isolation.

These observations obtained from independent experimental set ups suggest that not only PSMA7 but also PSMB5 and therefore whole proteasome itself has crucial role in CCCP-induced cellular repositioning of E3 ligase, Parkin.

Next, we checked whether proteasome itself or proteasomal activity was also required for Parkin and autophagy protein, ATG5 recruitment or not. In order to figure it out, chemical proteasome inhibitor MG132 was utilized and by performing subcellular fractionation the recruitment of proteins onto mitochondria analyzed in both transiently Parkin overexpressed (Figure 3.1.6 6) and stable Parkin expressing (Figure 3.1.6 7) HEK/293T cells.

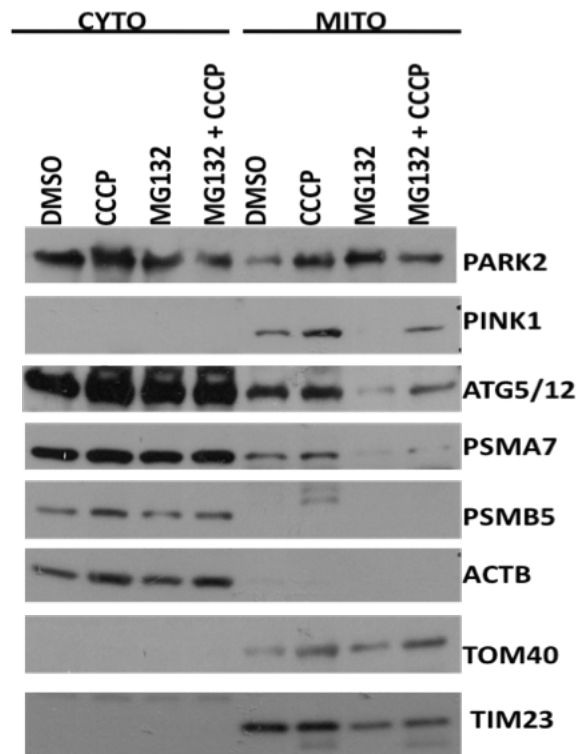


Figure 3.1.6 6: The effect of Proteasome inhibition on protein recruitment onto mitochondria in HEK/293T cells. HEK/293T cells were grown in 15 cm² plates with a cell density of 4x10⁶ cells per plate. For each condition 6 plates of cells seeded. Cells were co-transfected with YFP-tagged Parkin constructs for 48 h. Following treatments with DMSO, CCCP (20 μM), MG132 (30 μM) and MG132 combined with CCCP, cells were harvested and subcellular fractionation performed. After denaturation, mtochondrial and cytoplasmic proteins separated through 12% SDS-PAGE. Immunoblots were incubated with TIM23, TOM40, PSMA7, PSMB5, ATG5, PINK1 nad Parkin antibodies. ACTB, β-Actin was used for purification control of the isolation. *CYTO*, cytoplasm and *MITO*, mitochondria (representative data of n=4 independent experiments).

According to data shown in Figure 3.1.6 6 and Figure 3.1.6 7, CCCP-induced mitochondrial recruitment of ATG5 and Parkin required functional proteasomes in cells.

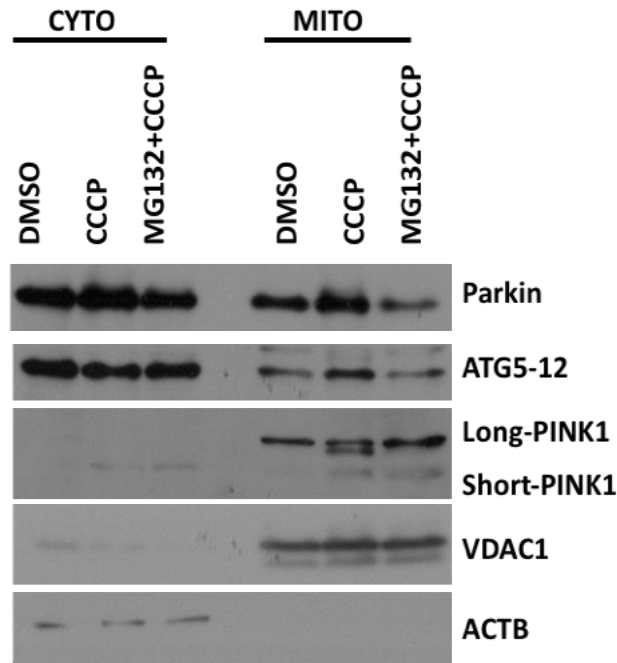


Figure 3.1.6 7: The effect of Proteasome inhibition on protein recruitment onto mitochondria in Parkin stable HEK/293T cells. Parkin stable HEK/293T cells were grown in 15 cm² plates with a cell density of 4x10⁶ cells per plate. For each condition 6 plates of cells seeded. Cells were co-transfected with YFP-tagged Parkin constructs for 48 h. Following treatments with DMSO, CCCP (20 μM), MG132 (30 μM) and MG132 combined with CCCP, cells were harvested and subcellular fractionation performed. After denaturation, mtochondrial and cytoplasmic proteins separated through 12% SDS-PAGE. Immunoblots were incubated with TIM23, TOM40, PSMA7, PSMB5, ATG5, PINK1 nad Parkin antibodies. ACTB, β-Actin was used for purification control of the isolation. *CYTO*, cytoplasm and *MITO*, mitochondria (Representative data of n=3 independent experiments).

Untill so far, observations showed that CCCP treatment resulted in increased positioning of ATG5, Parkin, PSMA7 and PSMB5 onto mitochondria and Parkin recruitment and ATG5 recruitment were tightly regulated by the cellular proteasome abundance and proteasomal activity. Additionally, cellular PSMA7 and ATG5 levels differentially regulates Parkin recruitment to mitochondria in response to CCCP-mediated mitochondrial dysfunction.

3.1.7 Target Prediction on Mitochondria for ATG5 Localization

After validation of the ATG5 occurrence, next, we checked the potential mitochondrial proteins for CCCP-induced mitochondrial positioning of ATG5 protein. To start with, SILAC-based ATG5 interactome results were critically analyzed in terms of the enhanced complex formation upon mitochondrial stress, CCCP.

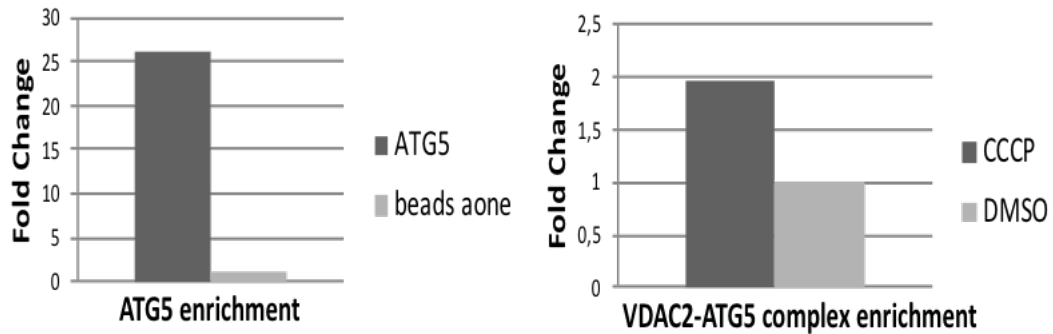


Figure 3.1.7 1: SILAC-based LC-MS/MS analysis. The fold change graphs were compared with beads alone (left); enrichment of VDAC2-ATG5 complex under CCCP conditions were compared with DMSO control condition (right) (n=1).

Among the long list, it is observed that mitochondrial voltage channel VDAC2 increased the complex formation with ATG5 protein upon CCCP treatment (Figure 3.1.7 1). CCCP-induced ATG5 and VDAC2 interaction was investigated by using protein-protein interaction techniques, including immunoprecipitation (Figure 3.1.7 2) and colocalization tests in HEK/293T and HeLa cells (Figure 3.1.7 3 and Figure 3.1.7 4).

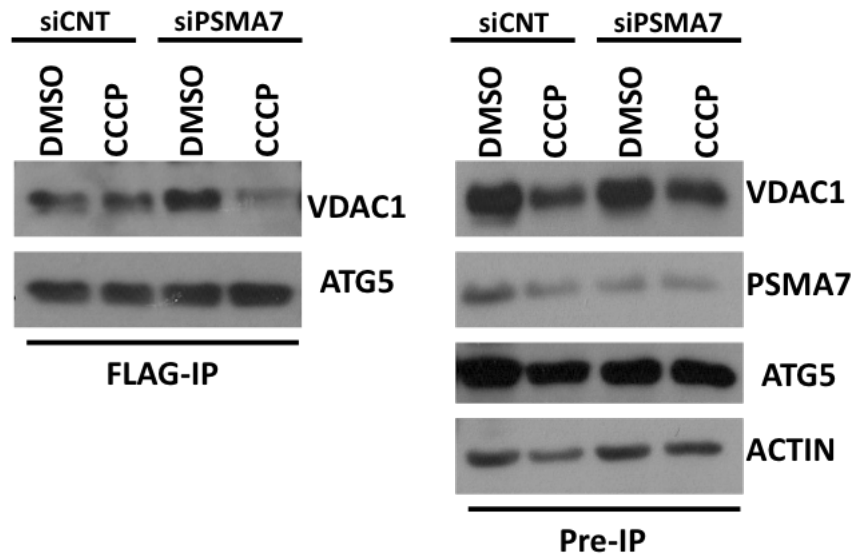


Figure 3.1.7 2: ATG5 immunoprecipitation experiments to test VDAC2 binding in HEK/293T cells. HEK/293T cells were grown in 10 cm² plates for overnight prior to desired transfection. Cells were transfected with YFP-tagged Parkin and Flag-tagged ATG5 construct together with and without PSMA7-targeting siRNA for 48 h. Following treatments with DMSO or CCCP (10 μM, 12 h), cells were harvested and proteins were isolated. Cell lysates were incubated with Flag-beads overnight at 4°C. Immunoprecipitants were extracted with 3X loading dye by boiling for 10 minutes, at 95°C. Samples were separated through 12% SDS-PAGE. For immunoblots, ATG5, VDAC1 and PSMA7 antibodies were used. *ACTIN*, β-Actin was used for loading control. *FLAG-IP*, Flag immunoprecipitation and *Pre-IP*, protein lysate control (n=3 independent experiment performed in HEK/293T cells).

ATG5 immunoprecipitation experiments and colocalization tests revealed that VDAC1 is one of the mitochondria residing proteins potentially targets ATG5 to mitochondria through physical interaction. CCCP increased ATG5 and VDAC1 interaction. In line with the previous data, siRNA-mediated knockdown of PSMA7 decreased CCCP-induced ATG5-VDAC1 interaction (Figure 3.1.7 2, Figure 3.1.7 3 and Figure 3.1.7 4).

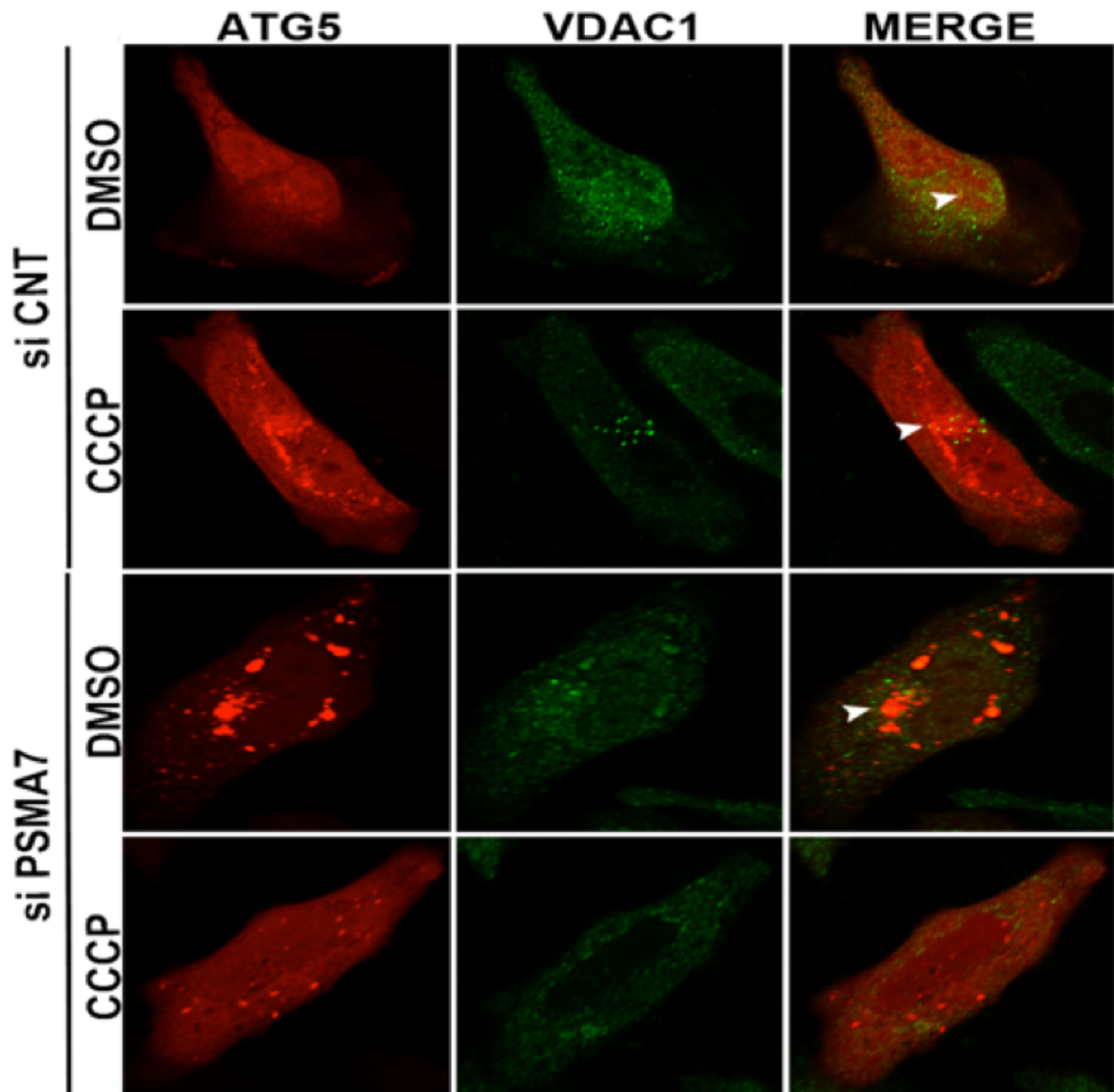


Figure 3.1.7 3: Colocalization tests of endogenous ATG5 and VDAC1 by immunostaining of HEK/293T cells. HEK/293T cells were grown on poly-L-Lysine coated cover slides in 12-well plates. Cells were transfected with MYC-tagged Pakin and together with or without PSMA7-targeting siRNA for 48 h. Following 12 h of DMSO or CCCP treatment, cells were fixed with 4% PFA and permeabilized with Saponin/BSA solution. Following primary and secondary antibody incubations, cells were analyzed under confocal microscope.

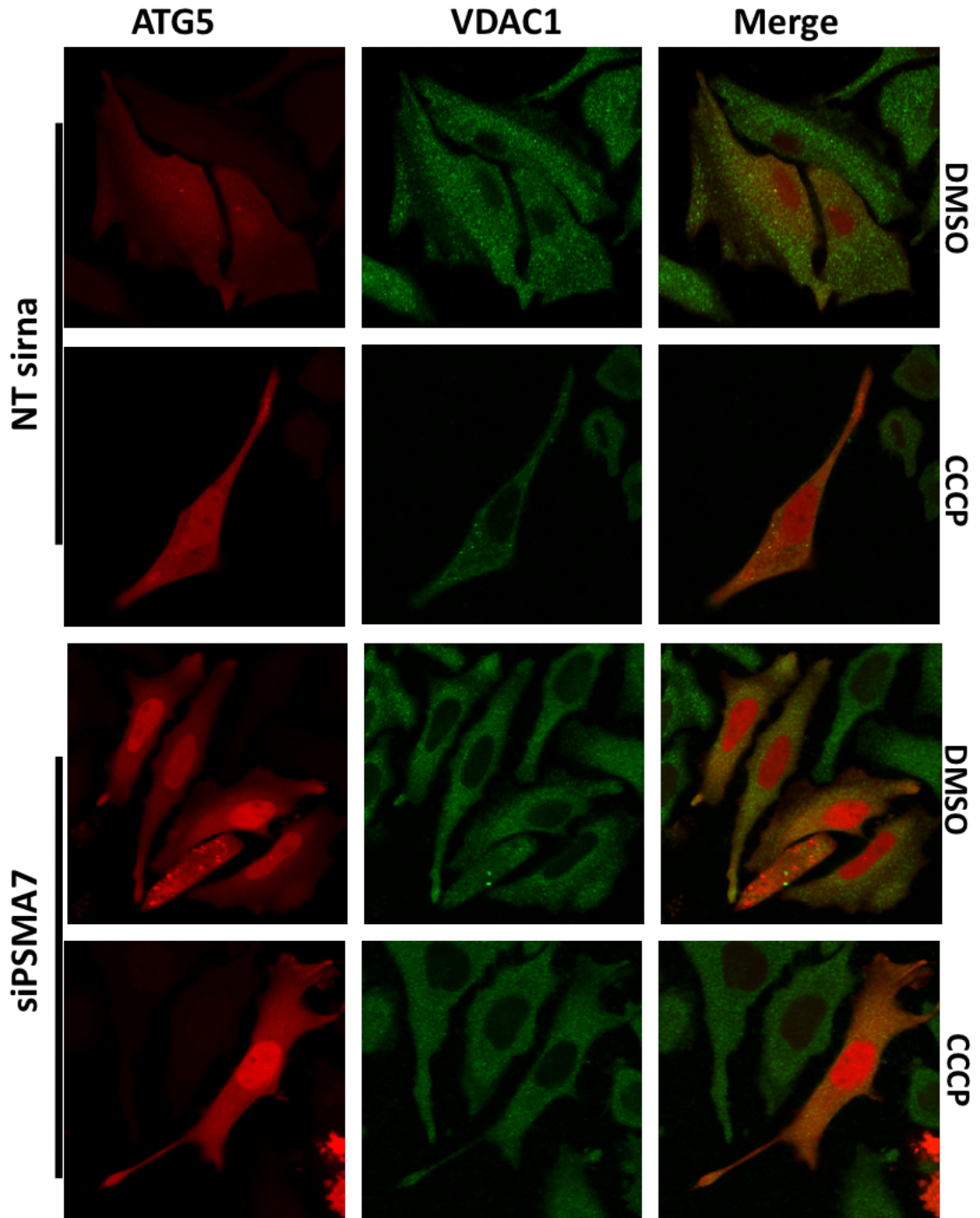


Figure 3.1.7 4: Colocalization tests of endogenous ATG5 and VDAC1 by immunostaining of HeLa cells. HELA cells were grown on poly-L-Lysine coated cover slides in 12-well plates. Cells were transfected with MYC-tagged Pakin and together with or without PSMA7-targeting siRNA for 48 h. Following 12 h of DMSO or CCCP treatment, cells were fixed with 4% PFA and permeabilized with Saponin/BSA solution. Following primary and secondary antibody incubations, cells were analyzed under confocal microscope.

Next, mitochondrial ATG5 and VDAC1 interaction was tested endogenously in stable Parkin expressing HEK/293T (Figure 3.1.7 5) and HeLa cells (Figure 3.1.7 6) by immunoprecipitating VDAC1 protein from isolated mitochondrial extracts. According to data shown below in Figure 3.1.7 5 and 3.1.7 6, VDAC1 and ATG5 interaction further verified under both basal and CCCP-induced conditions as well as in both cell lines.

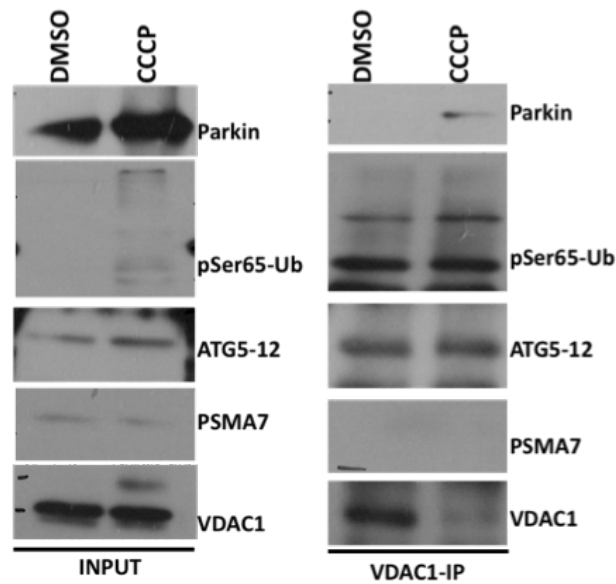


Figure 3.1.7 5: Mitochondrial VDAC1-ATG5 interaction tests in Parkin stable HEK/293T cells. Stable HEK/293T cells were seeden in 15 cm² plates with a cell density of 4x10⁶ cells. For each condition, 6 plates of cells used. Following subcellular fractionation, mitochondrial proteins were incubated with VDAC1 antibody coupled agarose beads overnight at 4°C. Precipitated proteins were eluted in loading dye. Denaturated samples were separated through 12% SDS-PAGE. For immunoblots, Parkin, pSer65-Ub, ATG5, PSMA7 and VDAC1 antibodies were used. *Input*, lysate control and *VDAC1-IP*, VDAC immunoprecipitation.

Obtained results suggest that VDAC1 protein could be one of the landing zone for ATG5 protein locating on mitochondria and PSMA7 has crucial role in directing ATG5 and Parkin proteins to mitochondria.

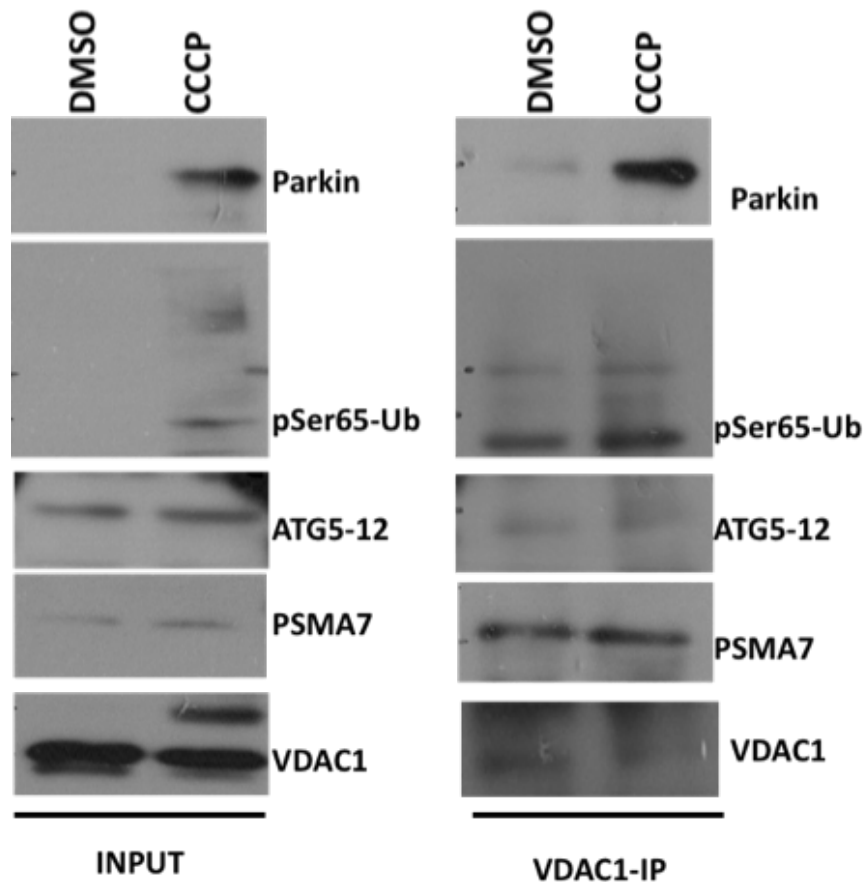


Figure 3.1.7 6: VDAC1-ATG5 interaction test on mitochondria in Parkin stable HeLa cells. Stable HELA cells were seeded in 15 cm² plates with a cell density of 4x10⁶ cells. For each condition, 6 plates of cells used. Following subcellular fractionation, mitochondrial proteins were incubated with VDAC1 antibody coupled agarose beads overnight at 4°C. Precipitated proteins were eluted in loading dye. Denaturated samples were separated through 12% SDS-PAGE. For immunoblots, Parkin, pSer65-Ub, ATG5, PSMA7 and VDAC1 antibodies were used. *Input*, lysate control and *VDAC1-IP*, VDAC immunoprecipitation.

Based on curiosity, other mitochondrial outer membrane proteins, including TOM40 (Figure 3.1.7 7 and Figure 3.1.7 8) and MFN2 (Figure 3.1.7 9 and Figure 3.1.7 10) were also tested for their potential interaction target residing on mitochondria for ATG5 to govern mitophagy in both Parkin expressing HEK/293T and Hela cells.

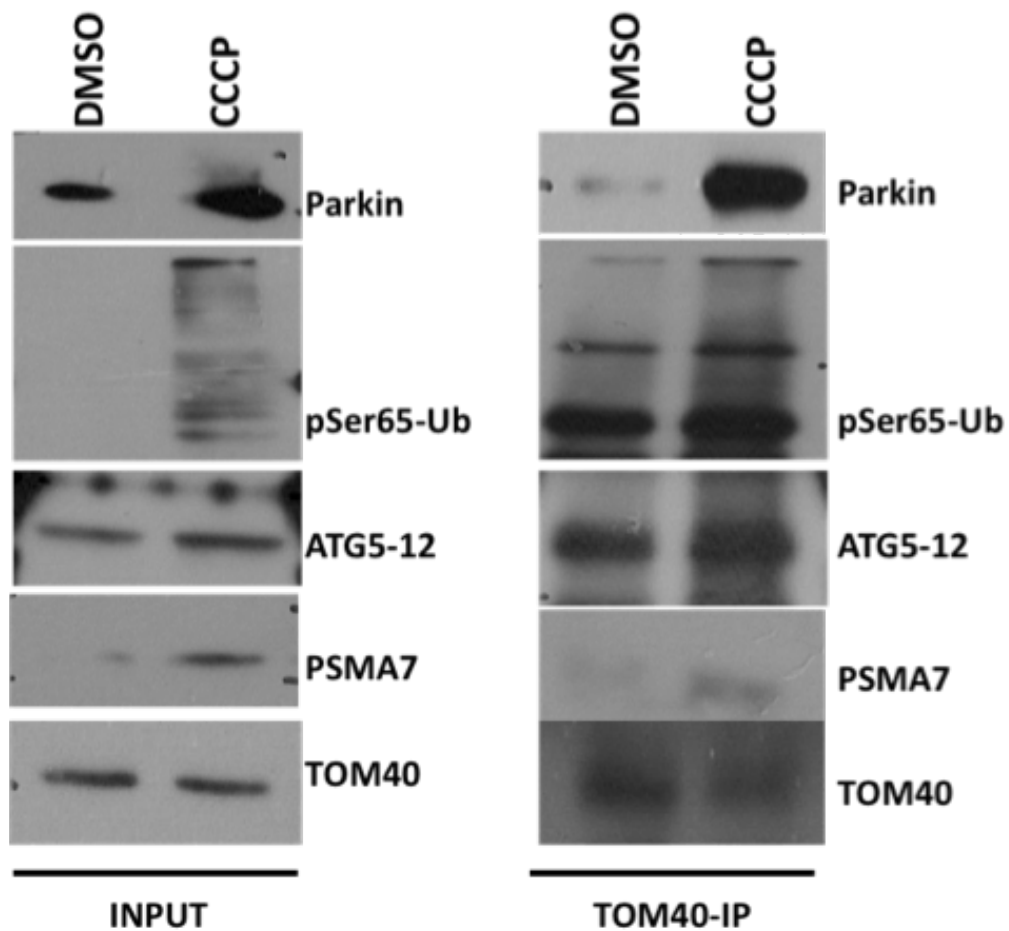


Figure 3.1.7 7: TOM40-ATG5 interaction test on mitochondria in Parkin stable HEK/293T cells. Stable HEK/293T cells were seeded in 15 cm² plates with a cell density of 4x10⁶ cells. For each condition, 6 plates of cells used. Following subcellular fractionation, mitochondrial proteins were incubated with TOM40 antibody coupled agarose beads overnight at 4°C. Precipitated proteins were eluted in loading dye. Denaturated samples were separated through 12% SDS-PAGE. For immunoblots, Parkin, pSer65-Ub, ATG5, PSMA7 and TOM40 antibodies were used. *Input*, lysate control and *TOM40-IP*, TOM40 immunoprecipitation.

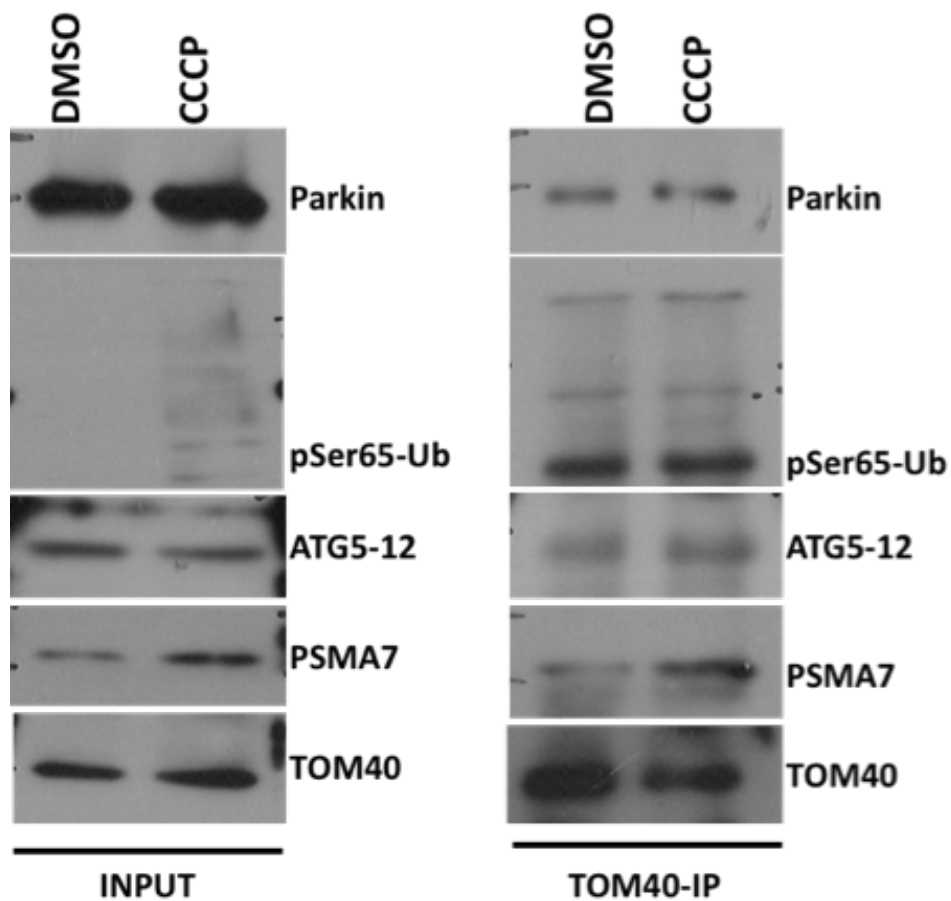


Figure 3.1.7 8: TOM40-ATG5 interaction test on mitochondria in Parkin stable HeLa cells. Stable HELA cells were seeded in 15 cm² plates with a cell density of 4x10⁶ cells. For each condition, 6 plates of cells used. Following subcellular fractionation, mitochondrial proteins were incubated with TOM40 antibody coupled agarose beads overnight at 4°C. Precipitated proteins were eluted in loading dye. Denaturated samples were separated through 12% SDS-PAGE. For immunoblots, Parkin, pSer65-Ub, ATG5, PSMA7 and TOM40 antibodies were used. *Input*, lysate control and *TOM40-IP*, TOM40 immunoprecipitation.

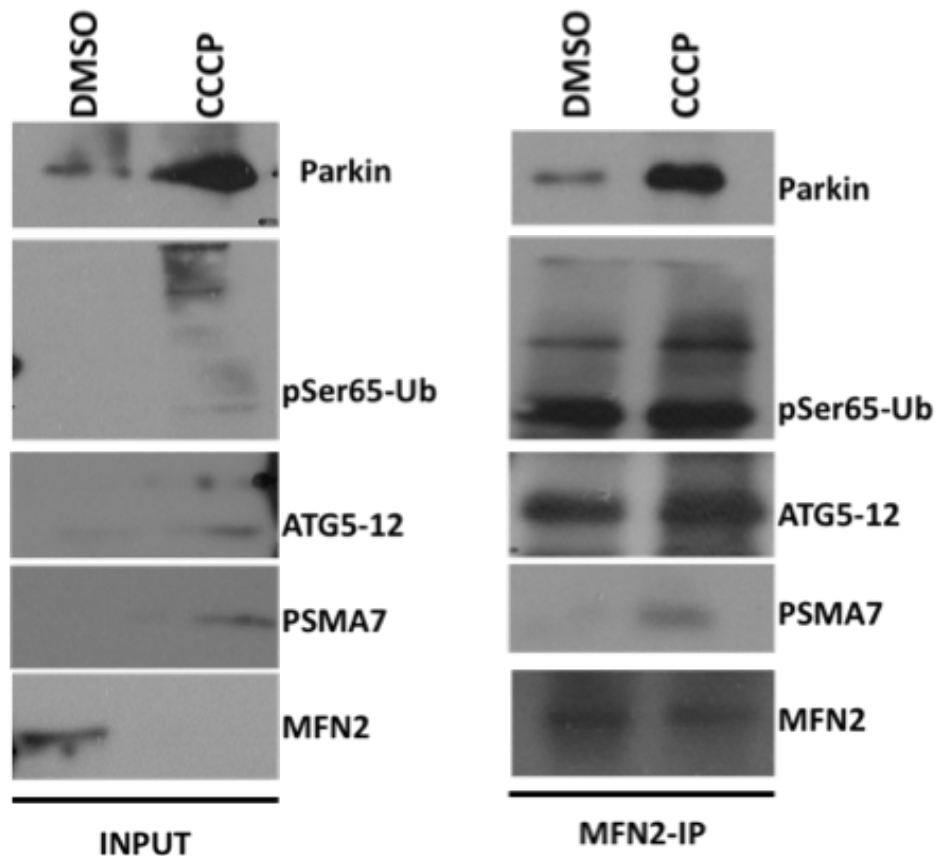


Figure 3.1.7 9: MFN2-ATG5 interaction test on mitochondria in Parkin stable HEK/293T cells. Stable HEK/293T cells were seeded in 15 cm² plates with a cell density of 4x10⁶ cells. For each condition, 6 plates of cells used. Following subcellular fractionation, mitochondrial proteins were incubated with MFN2 antibody coupled agarose beads overnight at 4°C. Precipitated proteins were eluted in loading dye. Denaturated samples were separated through 12% SDS-PAGE. For immunoblots, Parkin, pSer65-Ub, ATG5, PSMA7 and MFN2 antibodies were used. *Input*, lysate control and *MFN2-IP*, MFN2 immunoprecipitation.

Even though their protein levels decreased with CCCP, both TOM40 and MFN2 proteins showed increased binding with ATG5 protein suggesting that not only through VDAC1 protein but also via other tested mitochondrial proteins mitochondria were eliminated.

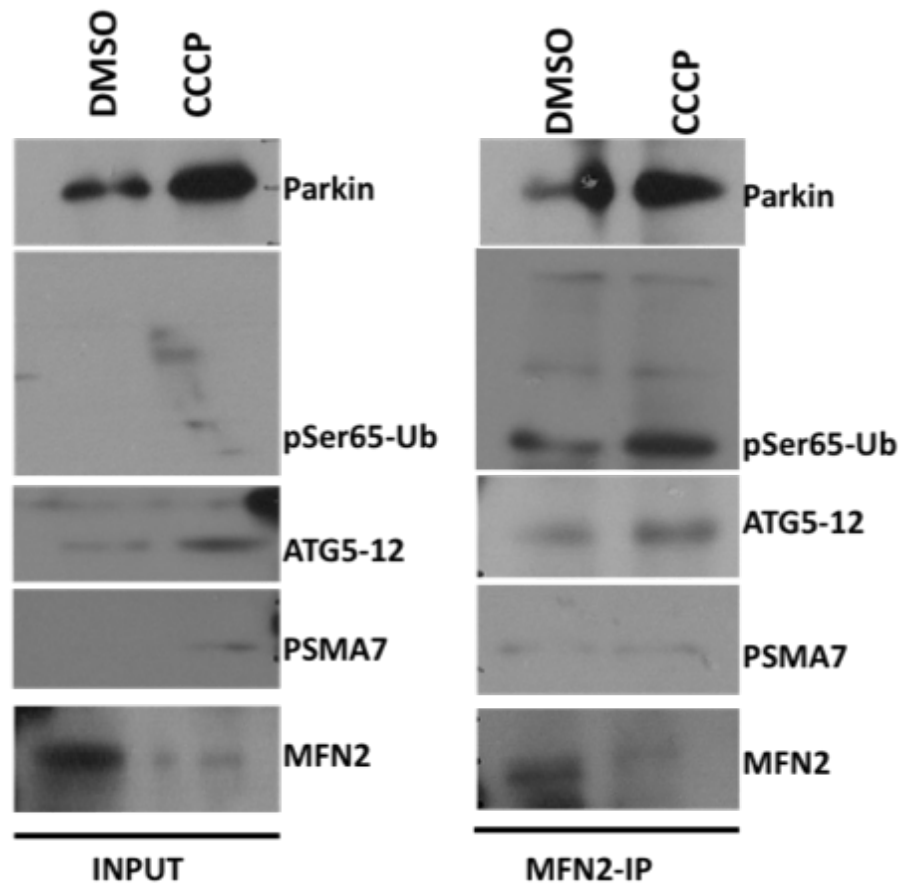


Figure 3.1.7 10: MFN2-ATG5 interaction test on mitochondria in Parkin stable HeLa cells. Stable HELA cells were seeden in 15 cm² plates with a cell density of 4x10⁶ cells. For each condition, 6 plates of cells used. Following subcellular fractionation, mitochondrial proteins were incubated with MFN2 antibody coupled agarose beads overnight at 4°C. Precipitated proteins were eluted in loading dye. Denaturated samples were separated through 12% SDS-PAGE. For immunoblots, Parkin, pSer65-Ub, ATG5, PSMA7 and MFN2 antibodies were used. *Input*, lysate control and *MFN2-IP*, MFN2 immunoprecipitation.

In this section, all the given data suggested that ATG5 could have various outer mitochondrial membrane targets, including VDAC1, TOM40 and MFN2. These observations showed that mitophagy is not a process starting from at a certain point and remove whole organelle. Conversely, it could start from several locations on mitochondria to eliminate dysfunctional mitochondria for the safe of the cell as soon as possible.

3.2 IDENTIFICATION OF OTHER PROTEASOMAL COMPONENTS AS DIRECT INTERACTORS OF ATG5

3.2.1 SILAC-Based Screening

SILAC-based ATG5 interactome analyses revealed that there are various CCP-induced interaction partners that are associated with the UPS system, including the E1 enzyme UBA1 and the E2 enzyme UBE2L3 (Figure 3.2.1 1).

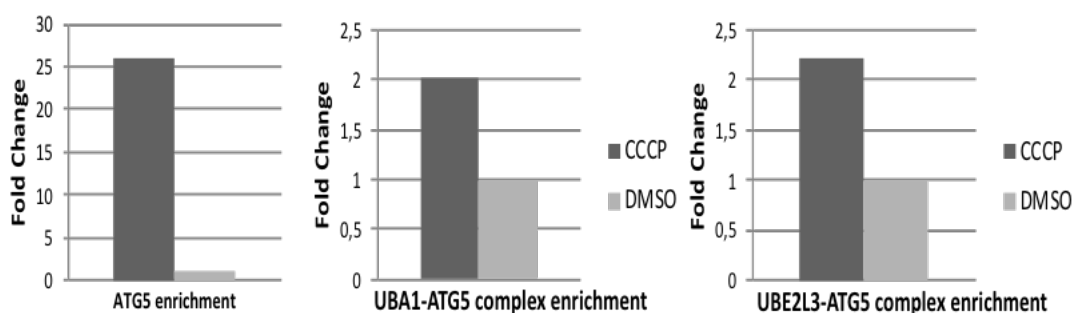


Figure 3.2.1 1: SILAC-based LC-MS/MS analysis. The fold change graphs were compared with beads alone (left); enrichment of UBA1-ATG5 complex under CCCP conditions (middle) and UBE2L3-ATG5 complex under CCCP (right) were compared with DMSO control condition (n=1).

This data suggests potential and more complex cellular roles of ATG5 which could be associated with stress stimuli and its autophagic as well as non-autophagic functions. Additionally, according to the list given below in Table 3.2.1 1, in different stress conditions, there are several other UPS related components such as E3 ligases in ATG5 interactome which will be tested as a follow-up study of this thesis.

3.2.2 Validation of SILAC-based ATG5 Interaction Partners

Proteomic analyses then confirmed by using co-immunoprecipitation tests HEK/293T cells. According to immunoblots represented in Figure 3.2.2 1, CCCP treatment significantly increased ATG5 binding with both the UPS-associated components, UBA1 and UBE2L3. Interestingly, the presence of an E3 ligase Parkin did not enhanced the interaction yet, had no effect on UBA1 binding and inhibitory effect on UBE2L3 binding.

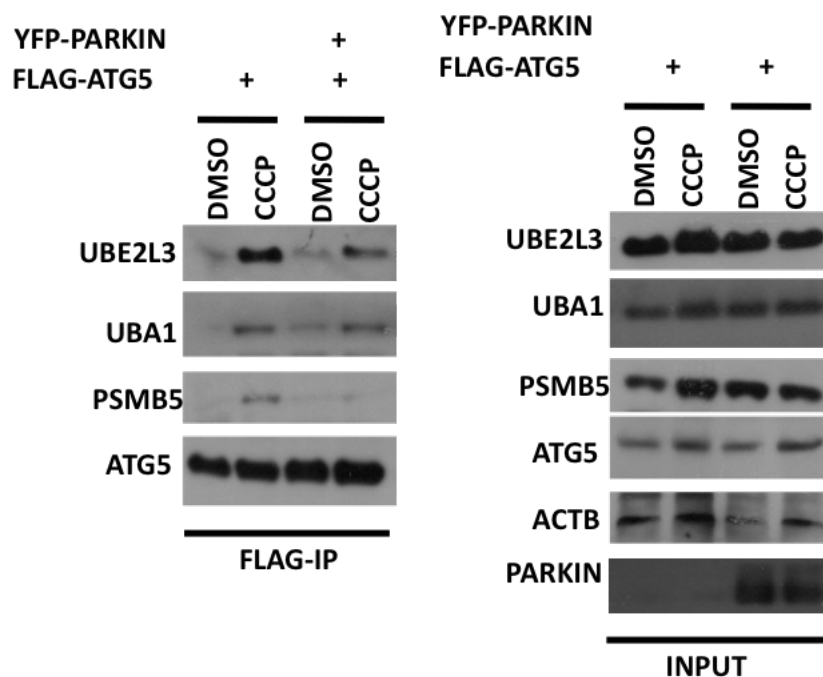


Figure 3.2.2 1: Co-immunoprecipitation test for the validation of proteomic data in HEK/293T cells. HEK/293T cells were splitted into 10 cm² plates with a 1.5x10⁶ cell density. Cells were transfected with Flag-tagged ATG5 construct alone or together with YFP-tagged Parkin for 48 h. Following 12 h of DMSO od CCCP treatment (10 μM), cells were harvested and proteins were extracted. Cell lysates were incubated with Flag-beads overnight, at 4°C. Immunoprecipitated proteins were eluted by boiling for 10 minutes at 954°C in loading dye. Denaturated samples were separated through 12% SDS-PAGE.

Blots were incubated with UBA1, UBE2L3, PSMB5, Parkin and ATG5 antibodies. *ACTB*, β -Actin was used as loading control. *Input*, cell lysate control and *Flag-IP*, Flag Immunoprecipitation.

Next, cellular localization of UBA1 and UBE2L3 enzymes were determined by performing cytoplasmic and mitochondrial isolation. Due to the involvement of the both enzymes in the fast reactions of ubiquitylation, to increase the efficiency of detection for cellular dynamics, chemical-crosslinking was performed prior to subcellular isolation.

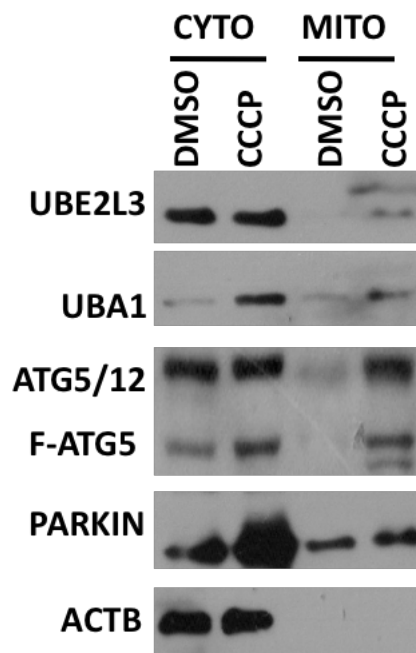


Figure 3.2.2 2: Subcellular localization of UBA1 and UBE2L3 enzymes in HEK/293T cells. HEK/293T cells were seeded into 15 cm² plates with a cell density of 4x10⁶ cells per plate. Cells were transfected with Flag-tagged ATG5 and YFP-tagged Parkin constructs for 48 h. Following 12 h of DMSO or CCCP (10 μ M), cells were harvested and by using glutaraldehyde protein-protein interactions were fixed prior to subcellular isolation (For more detail, please see the method section). Through differential centrifugation steps, cytoplasm and mitochondria out of the cell pellets were separated. Denaturated protein sanples from cytoplasmic and mitochondrial parts, run through 12% SDS-PAGE. For immunoblotting, UBA1, UBE2L3, PARKIN and ATG5 antibodies were used. *ACTB*, β -Actin was used as loading control. *CYTO*, cytoplasm and *MITO*, mitochondria (n=4 independent experiment performed).

According to immunoblots represented in Figure 3.2.2 2, in cells UBA1 and UBE2L3 had differential distribution pattern. In cytoplasm, DMSO or CCCP treatment had no effect on UBE2L3 level, whereas cytoplasmic UBA1 level significantly enhanced in response to CCCP. However, for both UBA1 and UBE2L3 proteins, CCCP enhanced their presence on mitochondria together with ATG5 and PARKIN.

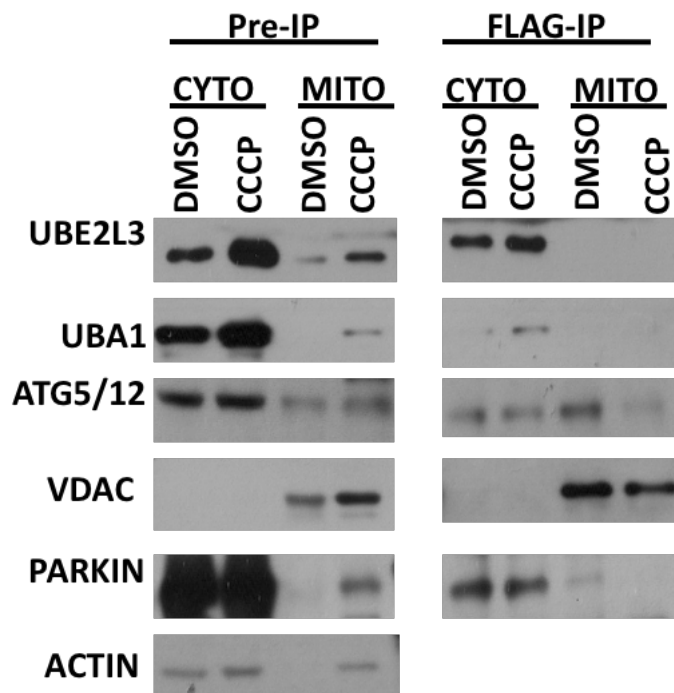


Figure 3.2.2 3: Determination of the cellular ATG5-UBA1 and ATG5-UBE2L3 interaction by subcellular fractionation followed by immunoprecipitation tests in HEK/293T cells. HEK/293T cells were seeded into 15 cm² plates with a cell density of 4x10⁶ cells per plate. Cells were transfected with Flag-tagged ATG5 and YFP-tagged Parkin constructs for 48 h. Following 12 h of DMSO or CCCP (10 μM), cells were harvested and by using glutaraldehyde protein-protein interactions were fixed prior to subcellular isolation (For more detail, please see the method section). Through differential centrifugation steps, cytoplasm and mitochondria out of the cell pellets were separated. Protein lysates were incubated with Flag-beads overnight at 4°C. Co-precipitated proteins were eluted in loading dye by boiling for 10 minutes at 95°C.

Denaturated protein sanples from cytoplasmic and mitochondrial parts, run through 12% SDS-PAGE. For immunoblotting, UBA1, UBE2L3, PARKIN and ATG5 antibodies were used. *ACTB*, β -Actin was used as loading control. *CYTO*, cytoplasm; *MITO*, mitochondria; *Pre-IP*, lysate controls and *Flag-IP*, Flag immunoprecipitation (n=2 independent experiment performed).

Subsequently, we wanted to check the localization of ATG5 and ubiquitylation-related enzymes in cells. To do that, mitochondrial and cytoplasmic ATG5 proteins precipitated and co-precipitating proteins were analyzed by immublotting with specific antibodies. As represented in Figure 3.2.2 3 that ATG5 binding to both proteins, UBA1 and UBE2L2 occurred in cytoplasm.

There are other various ubiquitin-proteasome system components that have been identified by SILAC-based proteomic screenings in response to CCCP condition (Table 3.2.2 1) as well as other autophagy-inducing conditions, including starvation and Torin1 (Table 3.2.2 2).

Table 3.2.2 1: CCCP induced UPS-associated ATG5 Interactome List of HEK/293T

Gene	Protein Name
PSMA7	Proteasome subunit alpha type-7
USP10	Ubiquitin carboxyl-terminal hydrolase 10
UBA1	Ubiquitin-like modifier-activating enzyme 1
UBE2L3	Ubiquitin-conjugating enzyme E2 L3

Table 3.2.2 2: CCCP induced UPS-associated PSMA7 Interactome List of HEK/293T

Gene Name	Protein Name
CAPRIN1	Caprin-1
PSMG4	Proteasome assembly chaperone 4
SCYL2	SCY1-like protein 2
PSMB5	Proteasome subunit beta type-5
PSME4	Proteasome activator complex subunit 4
PSMG1	Proteasome assembly chaperone 1
PSME3	Proteasome activator complex subunit 3
KCTD2	BTB/POZ domain-containing protein KCTD2
KCTD17	BTB/POZ domain-containing protein KCTD17
PSMG3	Proteasome assembly chaperone 3
KCTD5	BTB/POZ domain-containing protein KCTD5
STUB1	E3 ubiquitin-protein ligase CHIP
ANKFY1	Rabankyrin-5
SUPT16H	FACT complex subunit SPT16

Additionally, mitochondrial and cytoplasmic SILAC-based ATG5 interactome analyses were also enlighten the possibility as well as the complexity of other direct interactions between The UPS and autophagy system based on the subcellular location of the components (Table 3.2.2 4 and Table 3.2.2 5).

Table 3.2.2 3: UPS-associated ATG5 Interactome Combined List with Differential Autophagy Inducing Conditions (CCCp, STV or Torin1) in HEK/293T cells

Gene Name	Protein Name
UBA1	Ubiquitin-like modifier-activating enzyme 1
UBE2N / UBE2NL	Ubiquitin-conjugating enzyme E2 N
UBR5	E3 ubiquitin-protein ligase UBR5
UFD1L	Ubiquitin fusion degradation protein 1 homolog
USP9X	Probable ubiquitin carboxyl-terminal hydrolase FAF-X
ATXN10	Ataxin-10
SUMO2	Small ubiquitin-related modifier 2
TRIM21	E3 ubiquitin-protein ligase TRIM21
USP10	Ubiquitin carboxyl-terminal hydrolase 10
USP14	Ubiquitin carboxyl-terminal hydrolase 14
ATXN2	Ataxin-2
KCTD2	BTB/POZ domain-containing protein KCTD2
KCTD5	BTB/POZ domain-containing protein KCTD5
NDFIP1	NEDD4 family-interacting protein 1
PARK2	E3 ubiquitin-protein ligase parkin
RBBP6	E3 ubiquitin-protein ligase RBBP6
TRIM21	E3 ubiquitin-protein ligase TRIM21
UBR4	E3 ubiquitin-protein ligase UBR4

Table 3.2.2 4: CCCP induced UPS-associated Cytoplasmic ATG5 Interactome List of HEK/293T cells

Gene Name	Protein Name
PSMA7	Proteasome subunit alpha type-7
Park2	Parkin
RBBP6	E3 ubiquitin-protein ligase RBBP6
KCTD2	BTB/POZ domain-containing protein KCTD2
ATXN2	Ataxin 2
MIB1	E3 ubiquitin-protein ligase MIB1
DCAF13	DDB1- and CUL4-associated factor 13
KCTD5	BTB/POZ domain-containing protein KCTD5
UBR4	E3 ubiquitin-protein ligase UBR4
PSMD4	26S proteasome non-ATPase regulatory subunit 4
PSMD2	26S proteasome non-ATPase regulatory subunit 2
PSMD1	26S proteasome non-ATPase regulatory subunit 1
PSMC5	26S protease regulatory subunit 8

Table 3.2.2 5: CCCP induced UPS-associated Mitochondrial ATG5 Interactome List of HEK/293T cells

Gene Name	Protein Name
Park2	Parkin E3 ligase
PSMC2	26S protease regulatory subunit 7
KCTD5	BTB/POZ domain-containing protein KCTD5
KCTD2	BTB/POZ domain-containing protein KCTD2
NDFIP1	NEDD4 family-interacting protein 1

Untill so far, it was confirmed that the UPS components E1 enzyme UBA1 and E2 enzyme UBE2L3 localized mostly in cytoplasm and upon CCCP treatment they translocated onto mitochondria together with ATG5 and Parkin proteins. CCCP treatment also enhanced ATG5 binding to UBA1 and UBE2L3 proteins, yet mostly detected in cytoplasm and proposed model for UBA1 and UBE2L3 in CCCP-induced cellular homeostasis represented in Figure 3.2.2 4. Yet, there are many other differentially regulated proteasomal system components that found as ATG5 and PSMA7 interacting hits and some common partners also exist. Confirmation technics for at least some interesting candidates or all are required.

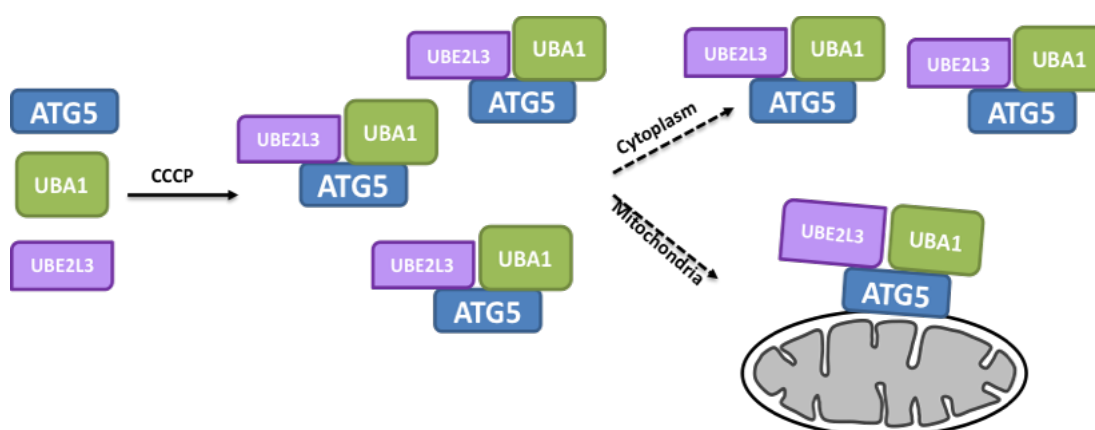


Figure 3.2.2 4: Proposed model for CCCP-induced UBA1 and UBE2L3 regulation in cells.

3.3 MITOCHONDRIAL MOTILITY CONTROL THROUGH ATG5 INTERACTORS

Mitochondria are highly dynamic organelles and their movement is critical for the energy supply to the cells. The mitochondria motility is maintained so far through microtubules, dyneins and basically cytoskeleton. Upon mitochondrial stress like CCCP, mitochondrial morphology is highly affected, and this alteration would change the cellular movement of the mitochondria.

3.3.1 The Role of PSMA7 on Mitochondrial Motility

In order to test the mitochondrial movement, following DMSO and CCCP HeLa cells were analyzed under confocal microscopy. As seen in Figure 3.3.1 1, CCCP abolished mitochondria and fibrillar actin connections and deregulated mitochondrial motility.

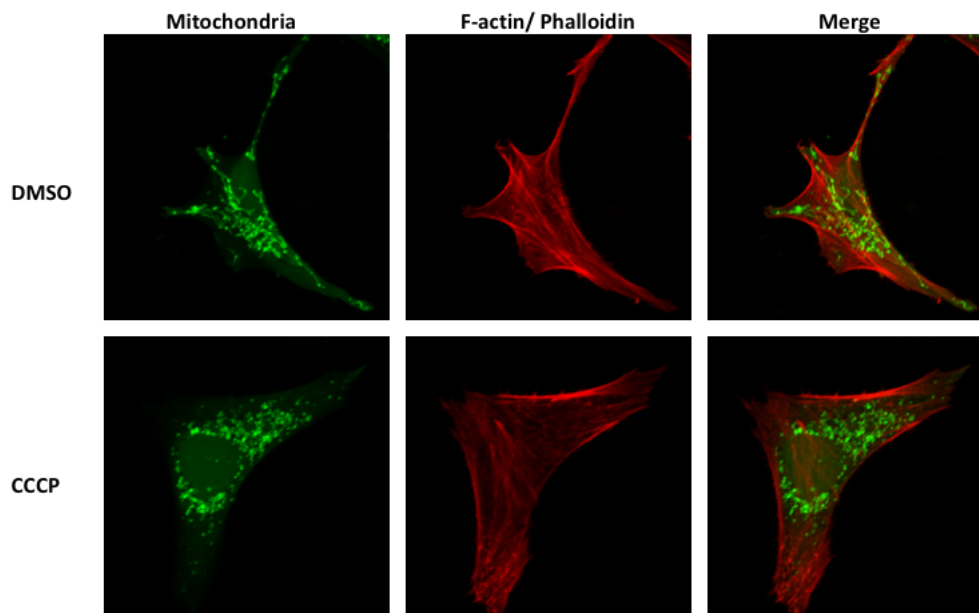


Figure 3.3.1 1: The effect of CCCP on mitochondrial motility analyzed in HeLa cells.

HeLa cells were grown on cover slips in 12-well plates and transfected with pmTurquoise-mito construct. Following 12 h treatment of DMSO as control or CCCP (10 μ M), cells were fixed with 4 % PFA and stained with phalloidin. After staining, cells were analyzed under confocal microscope.

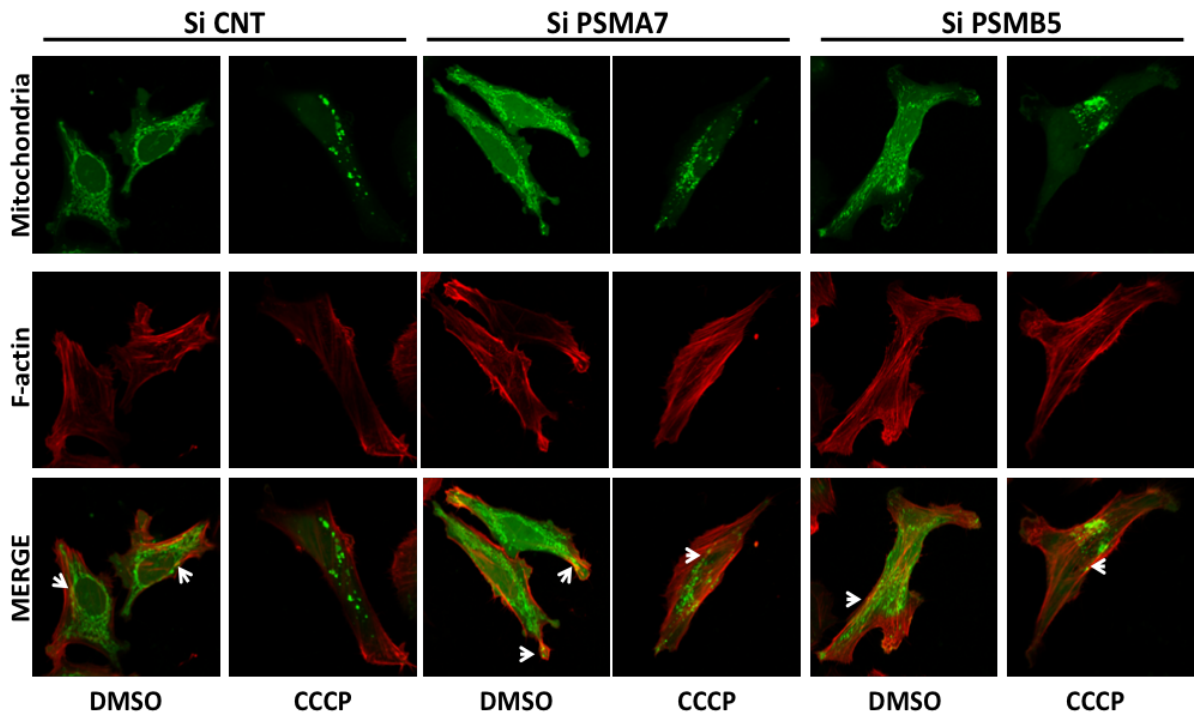


Figure 3.3.1 2: The effect of siRNA-mediated knockdown of PSMA7 and PSMB5 on mitochondrial motility analyzed in HeLa cells. HeLa cells grown on cover slips in 12-well plates and transfected with pmTurquoise-mito construct together with PSMA7-targeting or PSMB5-targeting or non-targeting siRNAs for 48 h. Following treatment of DMSO as control or CCCP, cells were fixed with PFA and stained with phalloidin. After staining, cells were analyzed under confocal microscope (n=3 independent experiment performed).

Next, the effect of ATG5 interactors, including PSMA7 and PSMB5 on mitochondrial motility was checked in HeLa cells (Figure 3.3.1 2). According to confocal microscopy results, CCCP-mediated loss of contact with fibrillar actin was

restored in both PSMA7 and PSMB5 knockdown conditions. These observations suggested that proteasome is a key regulator of both mitochondrial removal and motility.

siRNA-mediated knockdown effect of PSMA7 on mitochondria and cytoskeleton connection was further analyzed through microtubule association by tubulin staining in HeLa cells. According to given below in Figure 3.3.1 3, mitochondria and microtubule connection was decreased even lost upon CCCP treatment. However, deficiency in PSMA7 had no significant effect on CCCP-derived loss of mitochondria and microtubule connection.

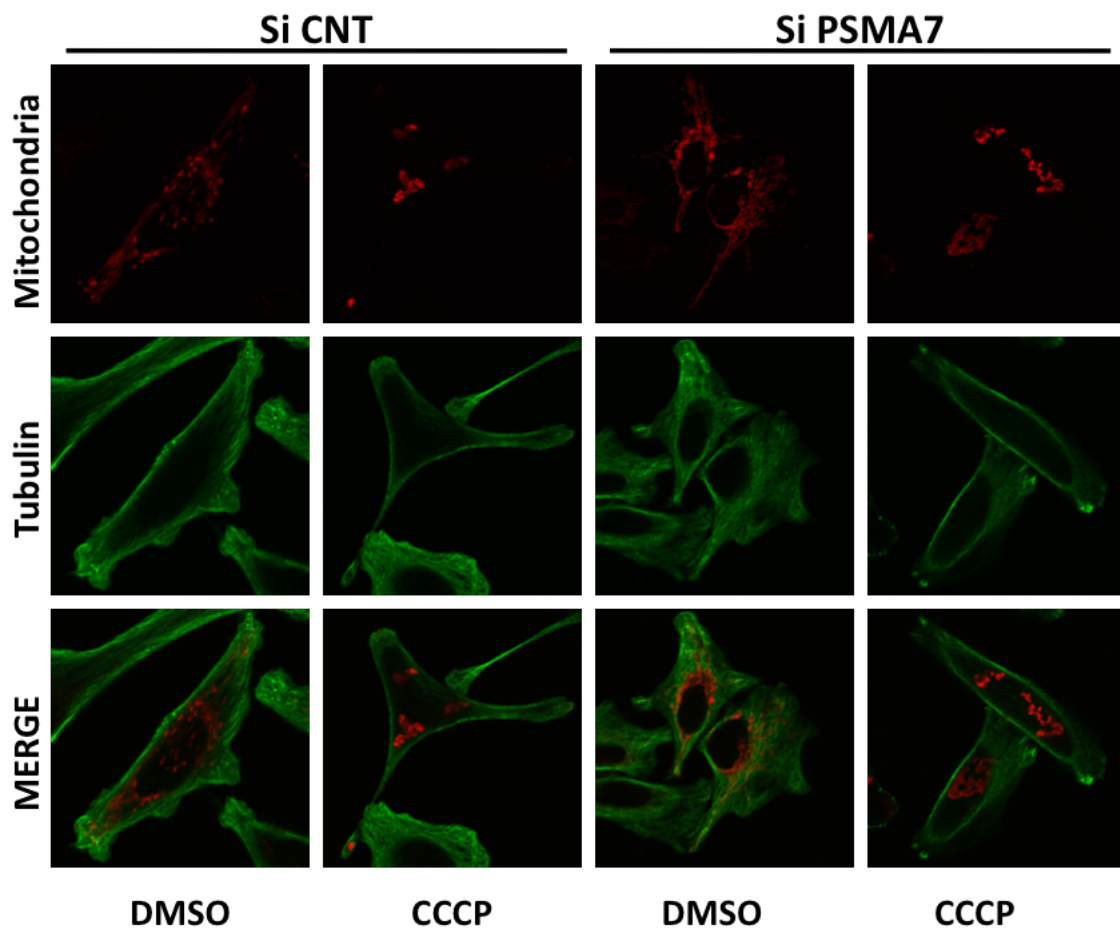


Figure 3.3.1 3: The effect of siRNA-mediated knockdown of PSMA7 on mitochondrial motility analyzed in HeLa cells. HeLa cells grown on cover slips in 12-well plates and transfected with pmTurquoise-mito construct together with PSMA7-targeting or PSMB5-targeting or non-targeting siRNAs for 48 h. Following treatment of DMSO as control or CCCP, cells were fixed with PFA and incubated with Tubulin primary and Alexa-Flour 488-mouse secondary antibodies. Then cells were analyzed under confocal microscope (N=3 independent experiment performed).

So far, these data indicate that CCCP treatment significantly inhibited tubulin polymerization, reduced the association of mitochondria and microtubules (MT) and microfibriles (MF). Knockdown PSMA7 and PSMB5 could successfully restore the loss of MF-mitochondria connection but not MT-mitochondria connection.

3.3.2 The Effect of DIAPH1 on Mitochondrial Motility and Mitophagy

CCCP-stimulated ATG5 interactome analysis revealed that one of the best hits of the interaction partners is DIAPH1 protein (shown in the Table 3.3.2 1). DIAPH1 protein is a diaphanous-related formin family member protein and is a Rho effector proteins regulating cell movement and migration by organizing polymerization of microtubules and microfilaments (Watanabe et al., 1997).

Table 3.3.2 1: List of Top 4 Significant Hits from SILAC-based ATG5 Interactome Screen in HEK/293T cells.

		CCCP	DMSO	
Ratio M/L IP	Ratio H/L IP	Ratio M/L IP significant t	Ratio H/L IP significant t	Gene names
5,03	5,07	+	+	ATG12
4,68	4,77	+	+	ATG5
3,56	3,66	+	+	ATG16L1
1,99	-0,58	+		DIAPH1

Additionally, it has been shown that ACTH signaling through increasing cellular cAMP level and PKA potentiated phosphorylation and activation of RhoA regulated

organelle positioning in cells. Phosphorylated RhoA interacted with DIAPH1 and the formation of this complex, resulted in the microtubule-dependent movement in a close proximity of ER (represented in Figure 3.3.2 1, (Li and Sewer, 2010)).

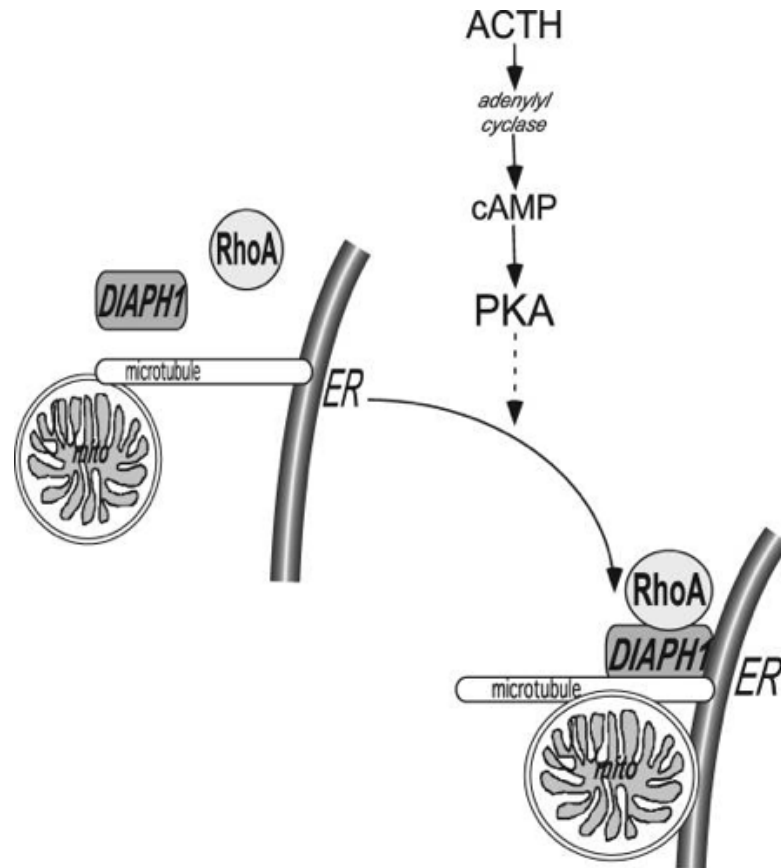


Figure 3.3.2 1: DIAPH1 regulated mitochondrial repositioning in cells.(Retrieved from (Li and Sewer, 2010)).

First of all, proteomic data was verified by using classical protein-protein interaction test, co-immunoprecipitation. By precipitating overexpressed ATG5, co-precipitated DIAPH1 protein was analyzed. According to immunoblots represented in Figure 3.3.2 2, under basal condition DIAPH1 and ATG5 barely interacted. Yet, CCCP significantly enhanced their binding, in line with the proteomic data.

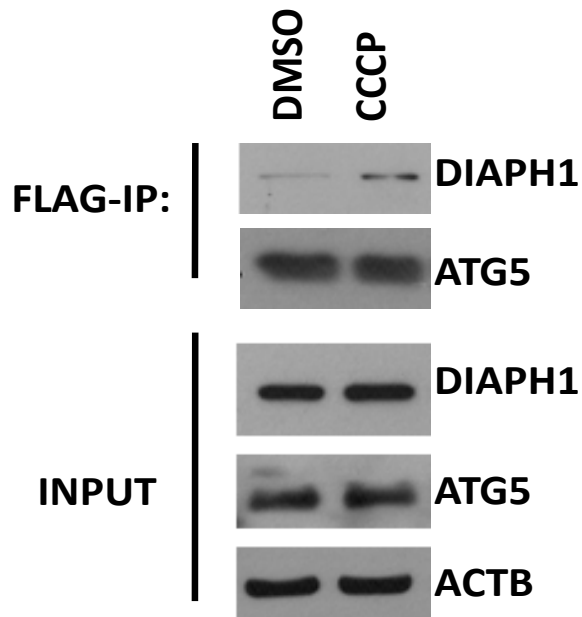


Figure 3.3.2 2: Confirmation of ATG5 and DIAPH1 interaction by immunoprecipitation tests in HEK/293T cells. HEK/293T cells were seeded in 10 cm² plates with a cell density of 1.5x10⁶. 16 h post seeding, cells were transfected with Flag-tagged ATG5 construct for 48 h. Cells were treated with DMSO or CCCP for 12 h. After treatment, cells were harvested and proteins were isolated. Cell lysates were further incubated with Flag-beads overnight at 4°C. Precipitated proteins were eluted in sample buffer by boiling for 10 minutes at 95°C. Denaturated samples were separated through 12% SDS gel. For immunoblots, ATG5 and DIAPH1 antibodies were used. *ACTB*, β -Actin was used as loading control. *Pre-IP*, lysate controls and *Flag-IP*, Flag immunoprecipitation (n=3 independent experiments performed).

Next, endogenous ATG5 binding to DIAPH1 protein was tested in HEK/293T (Figure 3.3.2 3) and HeLa (Figure 3.3.2 4) cells. Endogenous ATG5 protein could also successfully precipitated DIAPH1 protein, when cells exposed to mitochondrial stress conditions, including CCCP and Staurosporine in both cell lines.

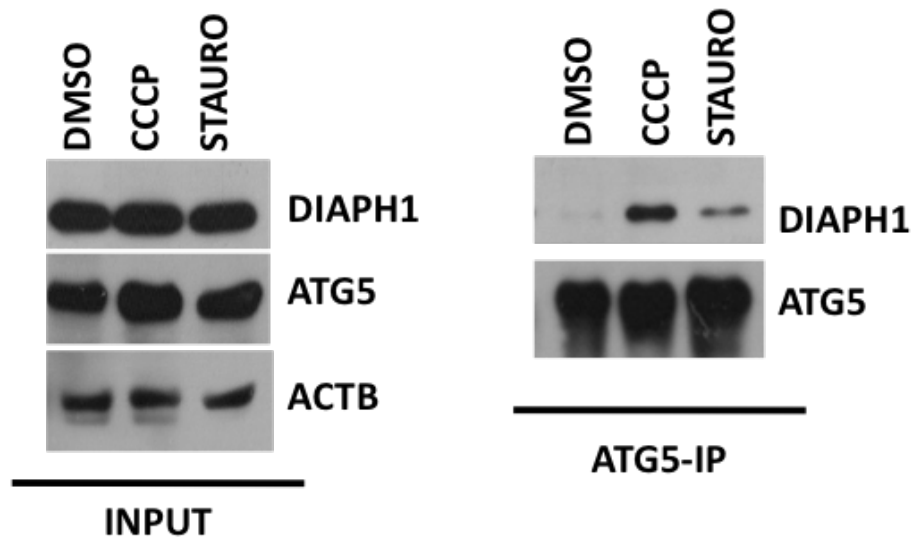


Figure 3.3.2 3: Endogenous ATG5 binding test for DIAPH1 protein in HEK/293T cells. HEK/293T cells were seeded into 15 cm² plates with a cell density of 4x10⁶ cells for 72 h. Cells were treated with DMSO, CCCP or Staurosporine for 12 h. Then cells were harvested and lysates were incubated with ATG5 coupled beads for overnight at 4°C. Precipitated proteins were eluted in sample buffer by boiling for 10 minutes at 95°C. Denaturated samples were separated through 12% SDS gel. For immunoblots, ATG5 and DIAPH1 antibodies were used. *ACTB*, β -Actin was used as loading control. *Pre-IP*, lysate controls and *Flag-IP*, Flag immunoprecipitation (n=3 independent experiments performed).

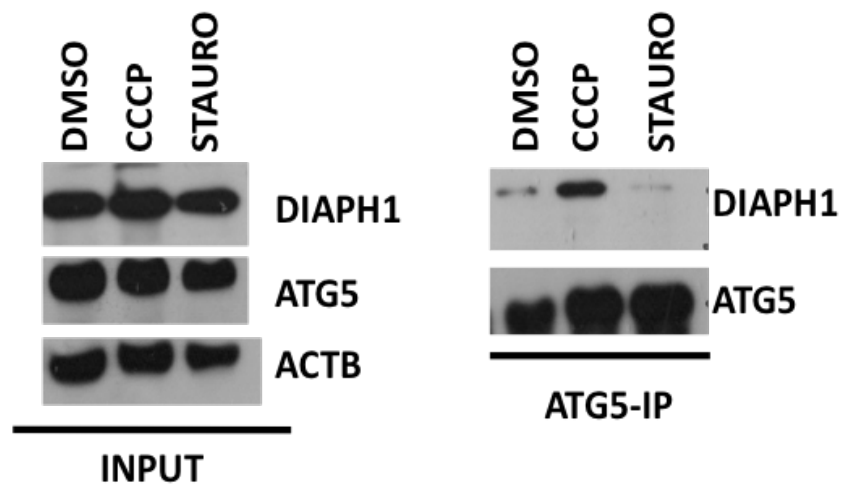


Figure 3.3.2 4: Endogenous ATG5 binding test for DIAPH1 protein in HeLa cells. HELA cells were seeded into 15 cm² plates with a cell density of 4x10⁶ cells for 72 h.

Cells were treated with DMSO, CCCP or Staurosporine for 12 h. Then cells were harvested and lysates were incubated with ATG5 coupled beads for overnight at 4°C. Precipitated proteins were eluted in sample buffer by boiling for 10 minutes at 95°C. Denaturated samples were separated through 12% SDS gel. For immunoblots, ATG5 and DIAPH1 antibodies were used. *ACTB*, β -Actin was used as loading control. *Pre-IP*, lysate controls and *Flag-IP*, Flag immunoprecipitation (n=3 independent experiments performed).

Next, the subcellular localization of DIAPH1 was investigated by performing subcellular fractionation (Figure 3.3.2 5) due to the hint of its role in mitochondrial repositioning and mitochondrial stress-stimulated interaction with ATG5. According to data shown in Figure 3.3.2 5, in basal and CCCP-stimulated conditions, DIAPH1 was found predominantly in cytoplasm. Under basal situation, there was almost no detectable DIAPH1 and ATG5 on mitochondria and with CCCP-treatment the presence of both DIAPH1 and ATG5 proteins increased onto the mitochondria suggesting its functionality at organeller base.

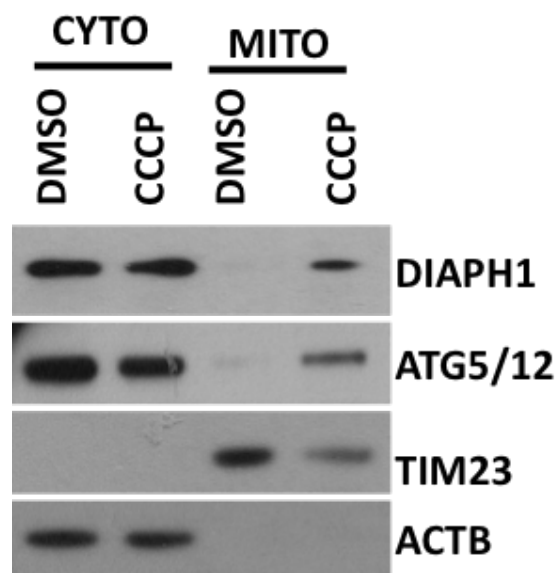


Figure 3.3.2 5: DIAPH1 was found on mitochondria upon CCCP treatment in HEK/293T cells. HEK/293T cells were seeded into 15 cm² plates with a cell density of 4x10⁶ cells

for 72 h. Cells were treated with DMSO or CCCP for 12 h. Then cells were harvested and subcellular fractionation performed. Protein lysates were further separated through 12% SDS gel. For immunoblots, ATG5, TIM23, ACTIN and DIAPH1 antibodies were used. *ACTB*, β -Actin was used as purification control of the isolation. *Pre-IP*, lysate controls and *Flag-IP*, Flag immunoprecipitation (n=3 independent experiments performed).

Next, the functional role of DIAPH1 on mitochondrial elimination was checked by siRNA-mediated knockdown experiments in HEK/293T (Figure 3.3.2 6) and HeLa cells (Figure 3.3.2 7). CCCP-stimulated mitochondrial protein degradation was enhanced upon cellular DIAPH1 level was limiting in both HEK/293T and HeLa cells. These findings suggest that DIAPH1 has critical role in restricting cellular mitochondrial loss by autophagic degradation.

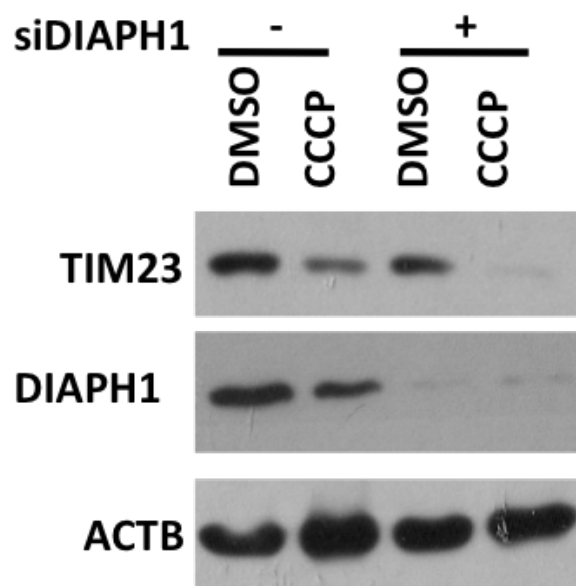


Figure 3.3.2 6: The effect of knockdown DIAPH1 on mitophagy in HEK/293T cells. HEK/293T cells were seeded in 6-well plates with a cell density of 300.000 cells/well. Cells were transfected with DIAPH1-targeting siRNA or non-targeting siRNA for 48 h. Following DMSO or CCCP treatment, cells were harvested and proteins were extracted. Protein lysates were further separated through 12% SDS gel. For immunoblots, TIM23, DIAPH1 and ACTIN antibodies were used. *ACTB*, β -Actin was used as loading control.

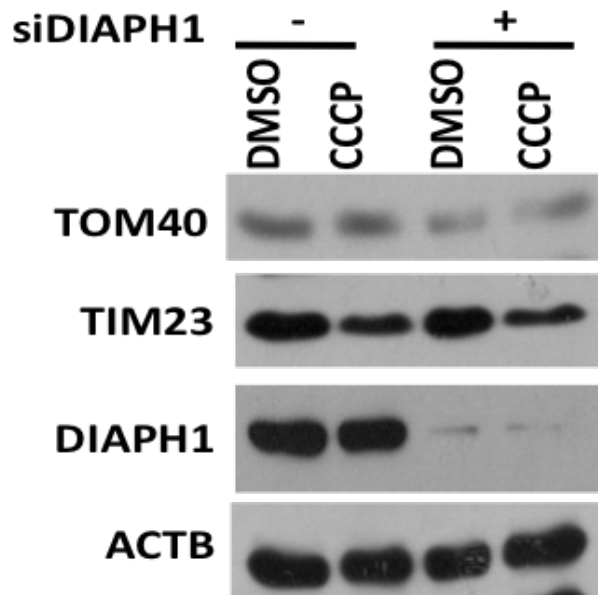


Figure 3.3.2 7: The effect of knockdown DIAPH1 on mitophagy in HeLa cells. HELA cells were seeded in 6-well plates with a cell density of 300.000 cells/well. Cells were transfected with DIAPH1-targeting siRNA or non-targeting siRNA for 48 h. Following DMSO or CCCP treatment, cells were harvested and proteins were extracted. Protein lysates were further separated through 12% SDS gel. For immunoblots, TIM23, DIAPH1 and ACTIN antibodies were used. *ACTB*, β -Actin was used as loading control.

Next, we tested the functional role of DIAPH1 protein in mitochondria and microtubule association, microtubule formation and therefore potentially motility in HeLa cells (Figure 3.3.2 8). According to confocal microscopy analyses, tubulin polymerization and its connection with mitochondria decreased with CCCP. These decrease further stimulated when DIAPH1 is knocked down.

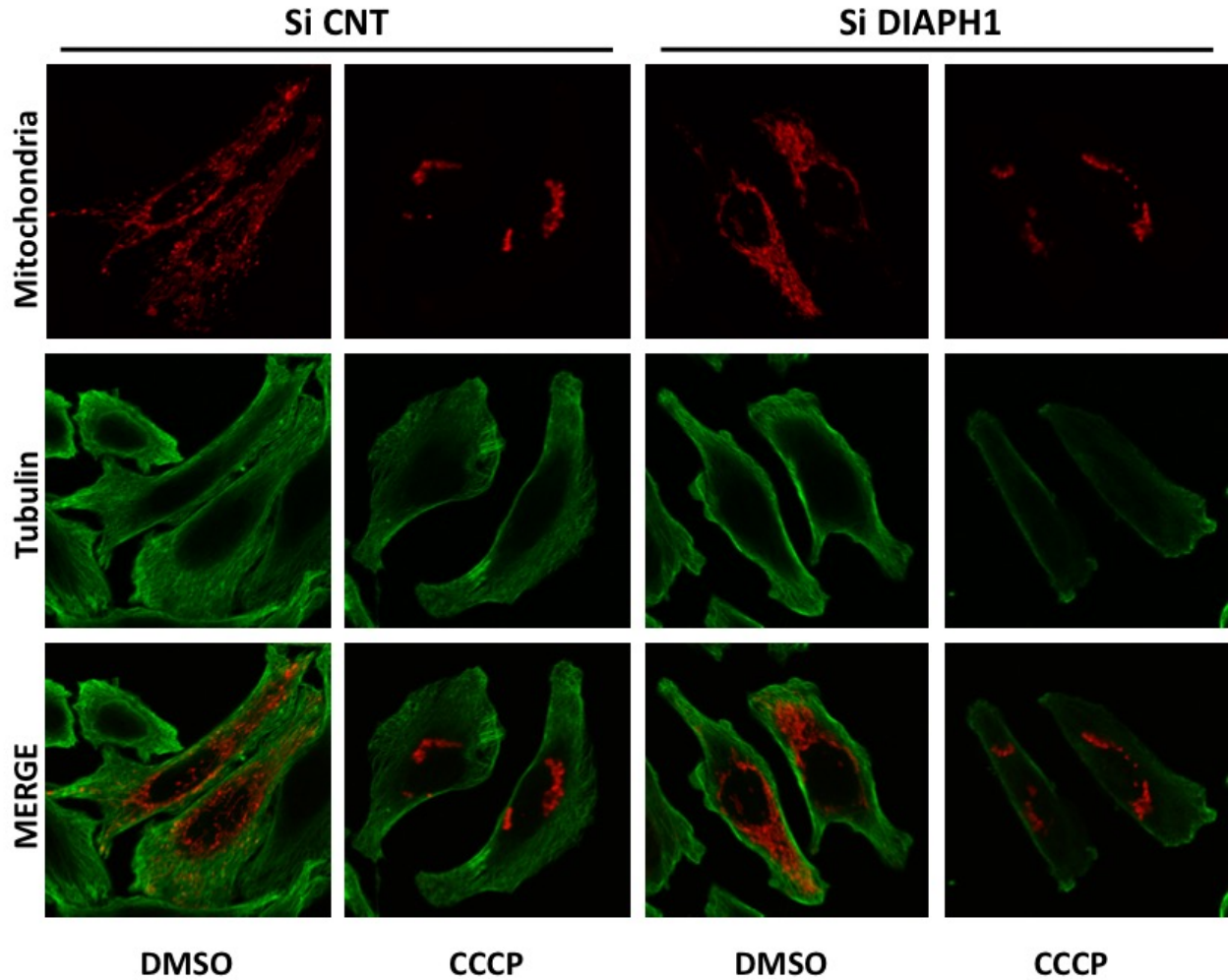


Figure 3.3.2 8: The effect of knockdown DIAPH1 on Mitochondria and Cytoskeleton Connection in HeLa cells. HeLa cells were seeded on cover slips and transfected with mito-dsRed (Red) construct together with or without DIAPH1-targeting siRNA. Following DMSO or CCCP treatment, cells were fixed with 4% PFA. Then, cells were permeabilized with BSA/Saponin solution. Permeabilized samples were incubated with Tubulin primary antibody and Alexa-Fluor 488 anti-Mouse secondary antibody. Cells were analyzed under confocal microscope.

Along with this thesis, due to the confirmed interaction with ATG5 and PSMA7, we checked the effect of PSMA7 on ATG5 binding to DIAPH1 in order to get the idea of its binding site on ATG5. To do that, cells expressing PSMA7 at a normal level and deficit in PSMA7 used for further ATG5 immunoprecipitation tests HEK/293T. According to

immunoblots shown in Figure 3.3.2 9, siRNA-mediated knockdown of PSMA7 has no significant effect on ATG5 and DIAPH1 binding suggesting that PSMA7 and DIAPH1 did not compete for ATG5 binding.

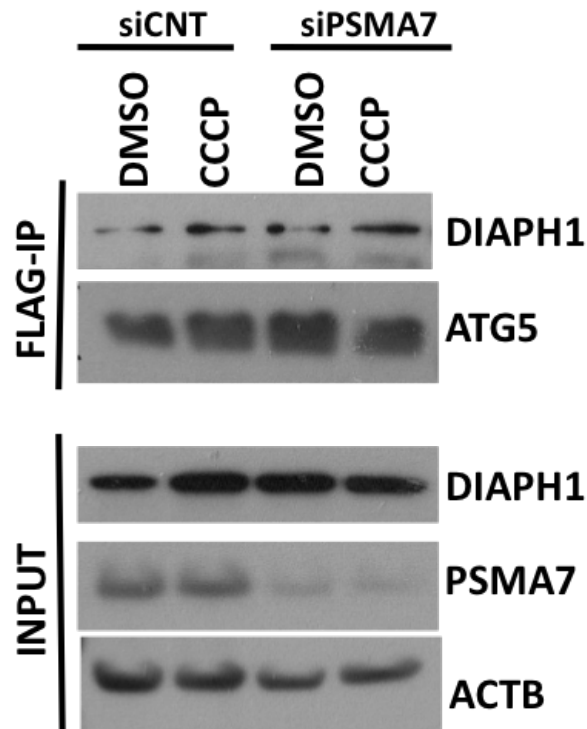


Figure 3.3.2 9: Immunoprecipitation experiments to check the effect of PSMA7 on ATG5 and DIAPH1 interaction performed in HEK/293T cells. HEK/293T cells were seeded in 10 cm² plates with a cell density of 1.5-2x10⁶ cells. Cells were transfected with Flag-tagged ATG5 together with and without PSMA7-targeting siRNA for 48 h. Following 12 h of DMSO or CCCP treatment, cell lysates were incubated with Flag-beads overnight. Precipitated proteins were eluted by boiling for 10 minutes at 95°C. Denaturated samples were separated through 12% SDS-PAGE. For immunoblots, DIAPH1, PSMA7 and ATG5 antibodies were used. *ACTB*, β-Actin was used as loading control. *Input*, cell lysate control and *Flag-IP*, Flag Immunoprecipitation (Representative data of n=4 experiments).

Due to their CCCP-mediated enhanced interaction with ATG5 as well as their increased localization onto mitochondria, next, we tested whether PSMA7 and DIAPH1 were interacting or not. According to immunoprecipitation experiment results shown in

Figure 3.3.2 10, endogenous PSMA7 found in a complex formation with DIAPH1 and this complex abundance increased with CCCP and Staurosporine.

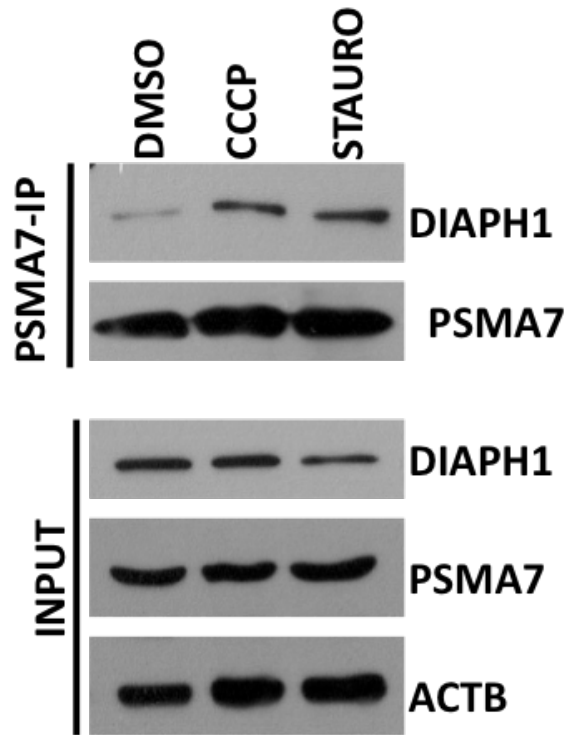


Figure 3.3.2 10: Immunoprecipitation experiments to test endogenous PSMA7 and DIAPH1 binding in HEK/293T cells. HEK/293T cells were seeded in 15 cm² plates with a cell density of 4x10⁶ cells. Following 12 h of DMSO, Staurosporine or CCCP treatment, cell lysates were incubated with PSMA7 antibody coupled-beads overnight. Precipitated proteins were eluted by boiling for 10 minutes at 95°C. Denaturated samples were separated through 12% SDS-PAGE. For immunoblots, DIAPH1, PSMA7 and ATG5 antibodies were used. *ACTB*, β -Actin was used as loading control. *Input*, cell lysate control and *PSMA7-IP*, PSMA7 Immunoprecipitation (Representative data of n=3 experiments).

All these data indicated that, PSMA7 and ATG5 bind the same interaction partner, DIAPH1 in order to regulate mitochondrial motility. DIAPH1 binding for both ATG5 and PSMA7 was upregulated with CCCP treatment. Knockdown DIAPH1 resulted in enhanced mitophagy and knockdown PSMA7 enhanced DIAPH1 and ATG5 binding.

Additionally, knockdown of proteasomal subunits restored CCCP-mediated loss of cytoskeleton and mitochondria connection whereas knockdown DIAPH1 worsened the loss of contact.

Proposed model for PSMA7 and DIAPH1 regulation of mitochondrial motility was represented in Figure 3.3.2 11.

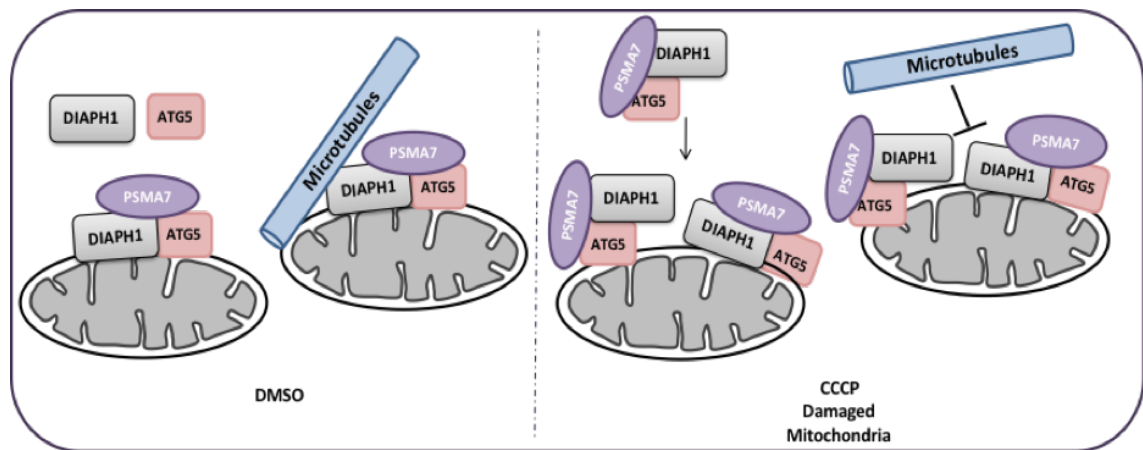


Figure 3.3.2 11: Mitochondrial motility control by PSMA7 and DIAPH1.

4. DISCUSSION

Autophagy and the ubiquitin proteasome systems are major degradation systems in mammalian cells that allow recycling of cellular contents ranging from soluble proteins to intracellular organelles. Although their mode of action and their requirements for substrate recognition are different, there are several overlaps and interconnections between the UPS and autophagy pathways.

Ubiquitin is a common signal for both the UPS and autophagy. It was proposed that, ubiquitin chain type could determine the pathway of choice for protein degradation. K48-linked ubiquitylation was proposed to be a signal for the UPS, whereas K63 linked ubiquitylation directed proteins for autophagosomal degradation (Herhaus and Dikic, 2015). Yet, a number of independent studies provided evidence that both ubiquitylation types could lead to autophagic degradation of substrates (Wandel et al., 2017). Moreover, recent studies underline the importance of ubiquitin phosphorylation as an event increasing the affinity of autophagy receptors to the targets of selective autophagy (Kane et al., 2014; Koyano et al., 2014). Additionally, non-ubiquitin modifications (e.g., acetylation, sumoylation, neddylation etc.) were shown to affect protein degradation as well (Hwang and Lee, 2017). Therefore, a barcode of ubiquitin and other modifications seem to prime proteins for one or the other degradation pathway and determine their fate. As another level of regulation, deconjugating enzymes such as DUBs may counteract or redirect proteins for different degradation systems.

In this thesis, rather than previously mentioned indirect regulations, the first direct links between the ubiquitin-proteasome system and autophagy was introduced and its cellular function deeply analyzed which was mainly through ATG5 and PSMA7 and PSMB5. The interactions of PSMA7 and PSMB5 with ATG5 were confirmed by various protein-protein interaction techniques, including co-immunoprecipitation, colocalization tests, endogenous immunoprecipitation and gel filtration tests. By structural modelling,

several critical residues at C-terminal part of the PSMA7 suggested as critical points for interaction and these data was verified by immunoprecipitating truncated fragments of PSMA7 that are generated by PCR-based cloning.

The interaction between ATG5 and PSMA7 was observed in both cytoplasm and on mitochondria, yet investigated more on mitochondria due to their CCCP and staurosporine-mediated increased dynamic complex formation on mitochondria. Increased mitochondrial localization of this complex was verified by using subcellular fractionation and colocalization tests. In fact, proteasomes are themselves selective target for autophagic degradation (Marshall et al., 2015). To figure out the observed interaction was due to the proteasomal degradation of not, the expression pattern of proteasomal subunits such as PSMA7 and PSMB5 were analyzed in response to various autophagy activators, proteasomal inhibitors and as well as mitochondrial stress inducers and no significant degradation of PSMA7 was observed in listed conditions. Therefore PSMA7 is not a degradation target of autophagy in our case and could have regulatory role in mitochondrial dynamic such as mitophagy. In line with this hypothesis, the functional role of the interaction was analyzed.

Based on gel filtration experiment results, in cytoplasm ATG5, PSMA7, PINK1 and Parkin were found as big complex. Yet, there are observed two big complexes on mitochondria containing differential amount of ATG5 and PSMA7 proteins. In one complex, there are ATG5, PINK1 and Parkin, in the other PSMA7, PSMB5, Parkin and decreasing fractions of ATG5 adding complexity to the regulation of mitochondrial dynamics. When the potential candidates of outer mitochondrial membrane proteins, it was observed that VDAC1, MFN2 and TOM40 were all interacted with ATG5.

In functional studies, it was observed that PSMA7 knockdown resulted decrease in Parkin translocation to mitochondria through its deregulated interaction with PINK1 and its ubiquitylation targets. Additionally, deficiency in PSMA7, restored CCCP-induced mitochondrial elimination, mitophagy. Interestingly, other proteasomal subunit, PSMB5 knockdown as well as chemical inhibition of proteasome gave similar results suggesting that proteasomal abundance and proteasomal activity regulates repositioning of Parkin, ATG5 and subsequently mitophagy.

Furthermore, from the ATG5 perspective, the deficiency in ATG5 resulted in downregulated mitophagy and enhanced Parkin translocation onto mitochondria in line with the accumulation of dysfunctional mitochondria recruited more Parkin could not become eliminated. Another striking observation was increased cellular stability of PINK1 which normally has short half life and only stabilized in response to mitochondrial stress. When ATG5 regulation on PINK1 protein was investigated, it was seen that not only the stability but also the PINK1 kinase activity was affected with cellular ATG5 abundance. In ATG5^{-/-} HeLa cells, CCCP induced PINK1-mediated ubiquitin phosphorylation was blocked. In fact, these differential regulation of ATG5 and PSMA7 were not surprising due to our two different complex formation onto mitochondria.

According to data obtained in this phd study, there have been identified various protein complexes containing ATG5, PSMA7 (proteasomal form; so the proteasome due to the involvement of the PSMB5) and Parkin onto the mitochondria and the formation of these complexes. Identified protein complexes on mitochondria depicted in Figure 4. 1. As shown in the Figure 4. 1, complex I is composed of PINK1, Parkin, VDAC1, ATG5, UBA1 and UBE2L3. In complex II, involved proteins are found as TOM40, ATG5, PSMA7, Parkin, UBA1 and UBE2L3. In the third one, MFN2, ATG5, PSMA7, Parkin, UBA1 and UBE2L3 were described as complex components. Because the ubiquitin conjugation reaction is a rapid system, the involvement of the E1 enzyme UBA1 and the E2 enzyme UBE2L3 in the complexes through ATG5 binding is not stable on mitochondria. These interactions were also dynamic and eventhough their localization on mitochondria were also enhanced with CCCP the predominant interaction between these enzymes and ATG5 in cytoplasm.

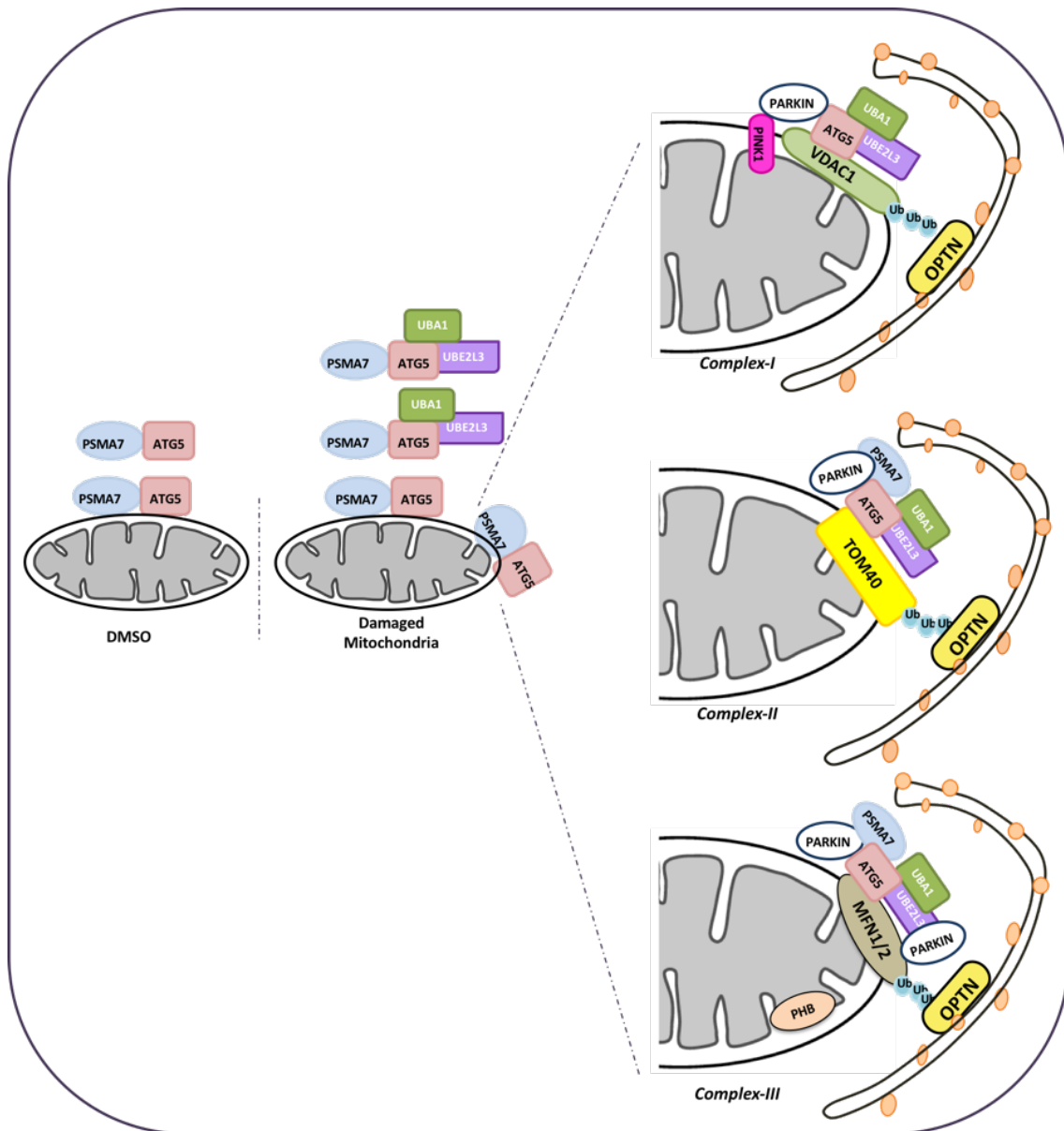


Figure 4. 1: Proposed interaction model for CCCP-induced protein complex formation onto mitochondria.

The proposed model for mitophagy regulation by ATG5-PSMA7 or in another word, by ATG5-proteasome complex was resresented in Figure 4.2 and Figure 4. 3.

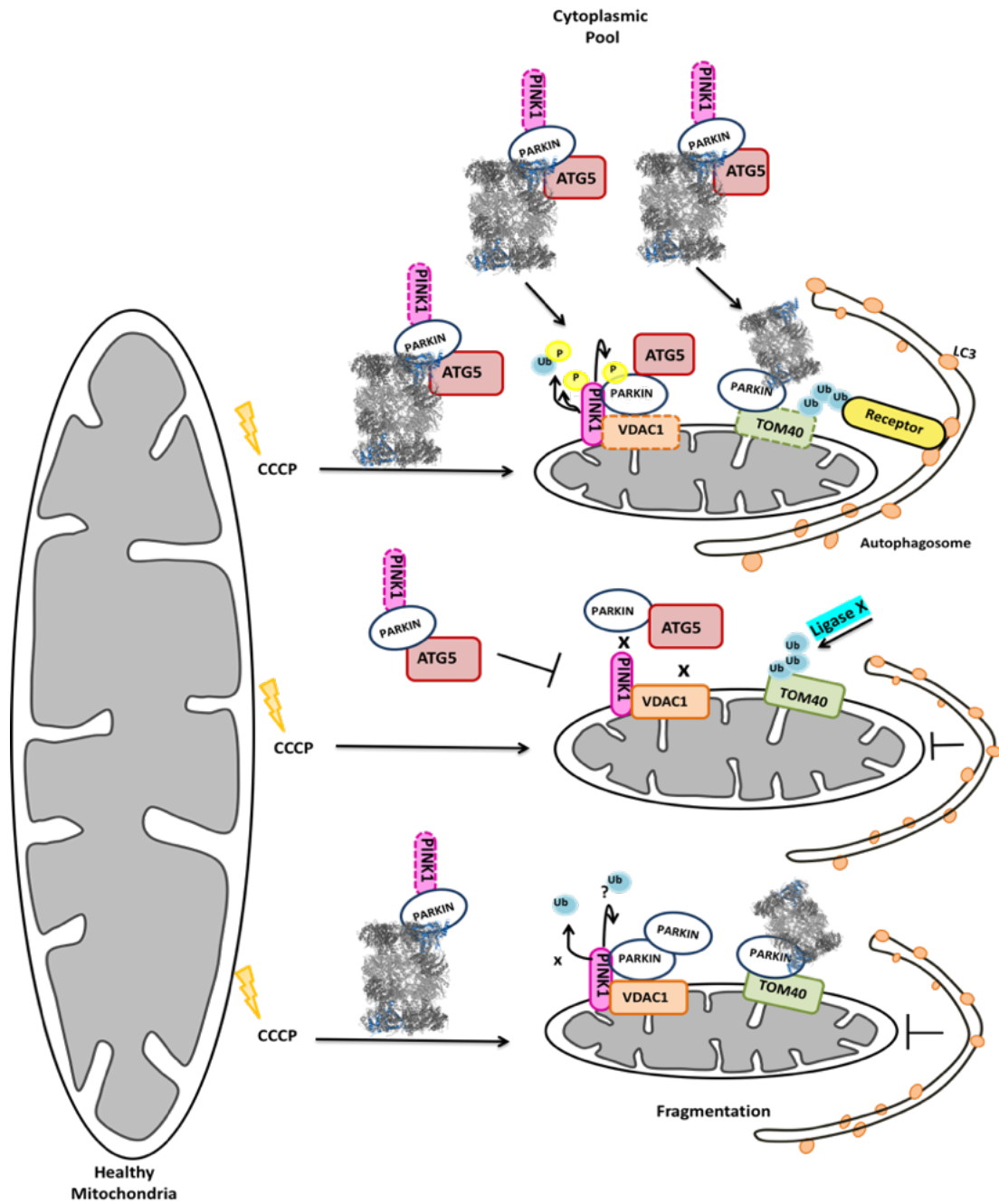


Figure 4.2: Detailed model-1 for proposed hypothesis in the regulation of mitophagy.

According to proposed models in Figure 4. 2, under steady-state conditions, proteasome, ATG5, PINK1 and Parkin are found as complex in cytoplasm. CCCP enhances their recruitment onto mitochondria. On the organelle, components of the complex disassociates to form 3 different complexes which involve different outer

mitochondrial membrane proteins to regulate from several points as fast reaction of proper mitophagy. These complexes also contain PSMA7 and PINK1 proteins differentially. Knockdown of PSMA7 and PSMB5 as well as chemical proteasome inhibition, decreased Parkin and ATG5 recruitment onto mitochondria by interfering with PINK1-Parkin interaction and blocked mitophagy receptor recruitment and LC3 associated autophagosomal membrane engulfment. Differentially, deficiency in ATG5 increased PINK1 stability and Parkin recruitment onto mitochondria. However interferes with mitophagy blockage through deregulating PINK1 kinase activity and recruitment of mitophagy receptors and autophagic machinery.

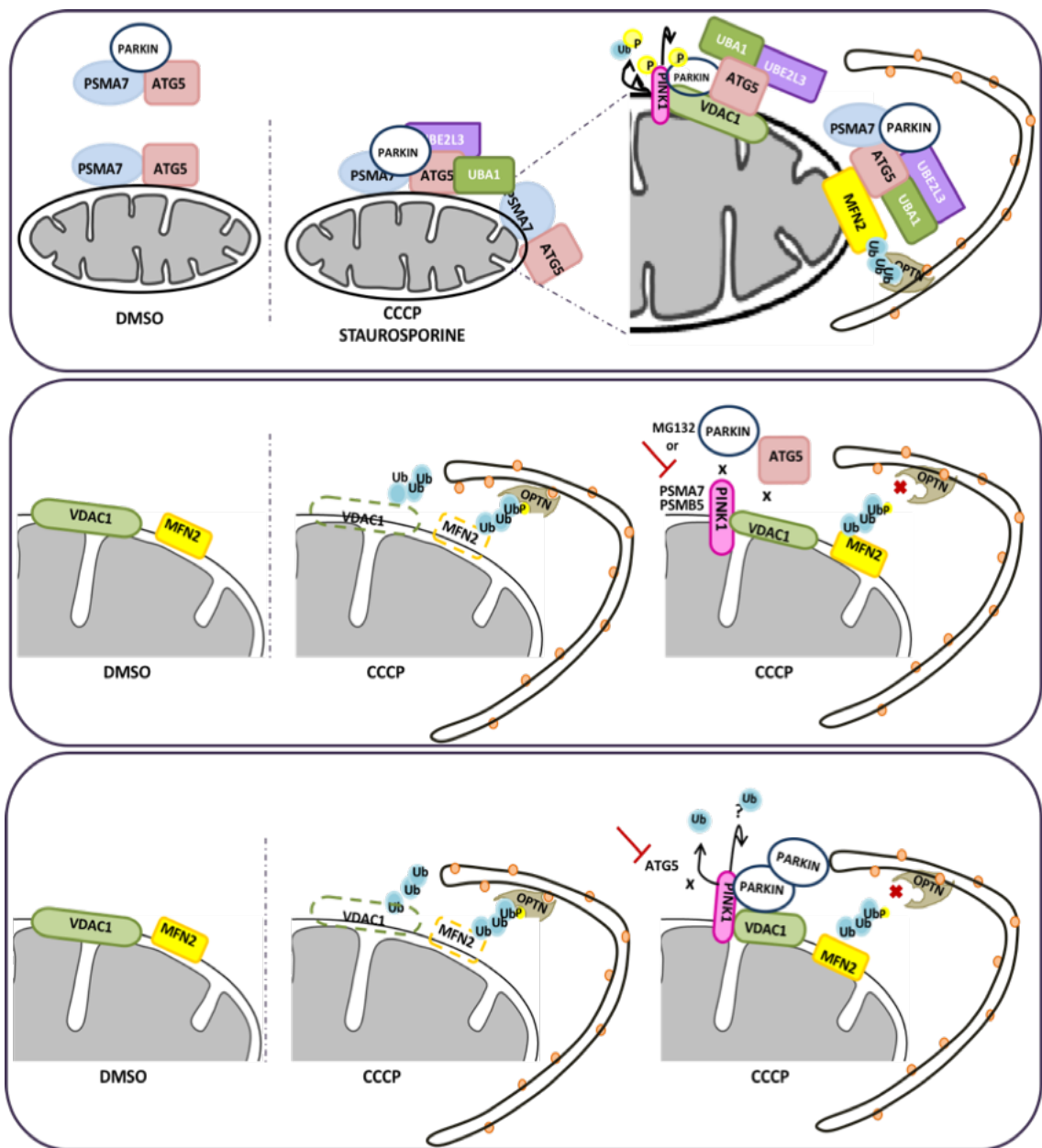


Figure 4.3: Detailed model-2 for proposed hypothesis in the regulation of mitophagy.

Similarly in proposed model-2 represented in Figure 4. 3, ATG5, PSMA7 and Parkin were found together in cytoplasm. With CCCP-mediated mitochondrial depolarization, ATG5, Parkin and PSMA7 are recruited onto mitochondria in order to form 3 different complexes during mitochondrial removal. ATG5 also interacts with E1 and E2 enzymes on CCCP-exposed mitochondria that are possibly involved in the ubiquitylation reactions of outer mitochondrial membrane proteins. When PSMA7 knocked down, the recruitment of ATG5 and Parkin proteins onto mitochondria decreased. Parkin and PINK1 protein interaction blocked. And furthermore, mitophagy receptor, OPTN and general autophagy receptor LC3 recruitment onto mitochondria reduced, degradation of outer mitochondrial membrane proteins and mitophagy is blocked. However, the ubiquitylation of the outer mitochondrial membrane proteins are not effected suggesting the involvement of other E3 ligases in the process to compensate reduced recruitment of Parkin to damaged mitochondria. On the other hand, when ATG5 is deficient, Parkin protein recruitment onto mitochondria is upregulated. Both short and long forms of PINK1 stability is enhanced, yet kinase function decreased. Mitophagy and autophagy receptor recruitment and subsequently mitophagy is blocked.

Based on the data and representations in the Figure 4.2 and 4. 3, ATG5 forms a bridge between mitochondrial outer membrane proteins and conjugating system providing prominent environment for the ubiquitylation of the mitochondrial proteins. PSMA7 has a dual function: first, playing a critical role for shuttling E3 ligase Parkin protein and through ATG5 binding autophagy machinery and second, involved in the degradation process of ubiquitylated outer mitochondrial membrane proteins. All these data suggest that first, there are many identified direct links between the UPS and autophagy system could include the same key regulators due to their differential subcellular localizations. Even on the same compartment of the cell, one regulator could have differential roles depending on its binding partners.

Mitochondrial movement based on cellular need, is critical to reveal potential regulators of this process. SILAC-based proteomic analyses suggested DIAPH1 as a potential ATG5 interacting protein. This data was verified by using immunoprecipitation tests and enhanced with CCCP, decreased with staurosporine. Interestingly, PSMA7 and ATG5 bound the same protein, DIAPH1 in order to regulate mitochondrial motility. Knockdown of DIAPH1 resulted in enhanced mitophagy and knockdown of PSMA7

enhanced DIAPH1 and ATG5 binding. Additionally, knockdown of proteasomal subunits restored CCCP-mediated loss of cytoskeleton and mitochondria connection whereas knockdown DIAPH1 worsened the loss of contact. Eventhough there are missing questions such as these regulations are linked to autophagic role of ATG5 or not, but still is a novel regulation of ATG5 on mitochondria movement as well as the role of proteasome in the same context.

Considering the importance of protein catabolism for cellular and organismal homeostasis and health, a better understanding of individual systems as well as the direct links between systems will be most rewarding from both a basic science perspective and with regards to clinical management of diseases involving protein quality control problems.

5. CONCLUSION AND FUTURE ASPECTS

In this thesis, PSMA7 was introduced as novel ATG5 interacting protein and a key mitophagy regulator. Possible regulatory mechanisms from ATG5 and PSMA7 corner in mitophagy coordination were suggested. ATG5 and other UPS-related components UBA1 and UBE2L3 interactions were identified which has potentially cytoplasmic regulation rather than mitochondria. ATG5 and DIAPH1 interaction was identified showing the role of ATG5 in mitochondrial motility in cells. Furthermore, other ATG5 and PSMA7 interaction partners were also identified by using SILAC-based proteomic analyses.

We believe that, obtained data from this doctoral work will first show that ubiquitin-proteasome system and autophagy system are regulating cellular homeostasis directly together. Second, these findings will improve our understanding of how complex regulations are exist in a cell and due to dynamic nature of the cell we are able to see as far as the cell allow us. Yet, there are still remaining questions in the picture. For example, first, eventhough we identified that C-terminal part of the PSMA7 is critical for ATG5 binding the key residue is unknown. We have shortened the possibbility into 4 potential aminoacids and further mutagenesis studies need to be performed. Second, in order to prove the direct interaction, *in vitro* binding tests for ATG5-PSMA7, ATG5-UBA1 and ATG5-UBE2L3 will be performed. Third, several key experiments will be repeated by using different agents including, Antimycin A, Oligomycin and Ivermectin in stably Parkin expressing cells. Forth, other phosphorylation target of PINK1 protein will be tested as another proof of ATG5-regulated PINK1 kinase activity. Fifth, thanks to our new collaborations with hospitals, skin biopsy material from Parkinson's Disease bearing patients will be obtained and primary cells will be isolated. Following their trans-differentiation into dopaminergic neurons, our key findings will be tested in these induced dopaminergic neurons.

The mitochondrial motility part will be analyzed by live cell microscopy with additional controls of chemical polymerization inhibitors. The role of ATG5 on mitochondria movement will be tested in WT and ATG5^{-/-} HeLa and MEF cells maybe combined with PSMA7 overexpression due to the competition between DIAPH1 and PSMA7 for ATG5 binding.

6. REFERENCES

- Abdelmohsen, K., Srikantan, S., Yang, X., Lal, A., Kim, H. H., Kuwano, Y., et al. (2009). Ubiquitin-mediated proteolysis of HuR by heat shock. *EMBO J.* doi:10.1038/emboj.2009.67.
- Aerbajinai, W., Giattina, M., Lee, Y. T., Raffeld, M., and Miller, J. L. (2003). The proapoptotic factor Nix is coexpressed with Bcl-xL during terminal erythroid differentiation. *Blood* 102, 712–717. doi:10.1182/blood-2002-11-3324.
- Altieri, D. C. (2010). Survivin and IAP proteins in cell-death mechanisms. *Biochem. J.* doi:10.1042/BJ20100814.
- Ambivero, C. T., Cilenti, L., Main, S., and Zervos, A. S. (2014). Mulan E3 ubiquitin ligase interacts with multiple E2 conjugating enzymes and participates in mitophagy by recruiting GABARAP. *Cell. Signal.* 26, 2921–2929. doi:10.1016/j.cellsig.2014.09.004.
- An, H., and Harper, J. W. (2018). Systematic analysis of ribophagy in human cells reveals bystander flux during selective autophagy. *Nat. Cell Biol.* 20, 135–143. doi:10.1038/s41556-017-0007-x.
- Antonioli, M., Albiero, F., Nazio, F., Vescovo, T., Perdomo, A. B., Corazzari, M., et al. (2014a). AMBRA1 interplay with cullin E3 Ubiquitin ligases regulates autophagy dynamics. *Dev. Cell* 31, 734–746. doi:10.1016/j.devcel.2014.11.013.
- Antonioli, M., Ciccocanti, F., Dengjel, J., and Fimia, G. M. (2017). “Methods to Study the BECN1 Interactome in the Course of Autophagic Responses,” in *Methods in Enzymology* doi:10.1016/bs.mie.2016.09.069.
- Antonioli, M., Di Rienzo, M., Piacentini, M., Fimia, G. M., Albiero, F., Nazio, F., et al. (2014b). AMBRA1 interplay with cullin E3 Ubiquitin ligases regulates autophagy dynamics. *Dev. Cell* 31, 734–746. doi:10.1016/j.devcel.2014.11.013.
- Apcher, G.-S., Maitland, J., Dawson, S., Sheppard, P., and Mayer, R. J. (2004). The alpha4 and alpha7 subunits and assembly of the 20S proteasome. *FEBS Lett.* doi:10.1016/j.febslet.2004.05.067.

- Apcher, G. S., Heink, S., Zantopf, D., Kloetzel, P. M., Schmid, H. P., Mayer, R. J., et al. (2003). Human immunodeficiency virus-1 Tat protein interacts with distinct proteasomal alpha and beta subunits. *FEBS Lett.* doi:S0014579303010251 [pii] ET - 2003/10/11.
- Arora, V., Cheung, H. H., Plenchette, S., Micali, O. C., Liston, P., and Korneluk, R. G. (2007). Degradation of survivin by the X-linked Inhibitor of Apoptosis (XIAP)-XAF1 complex. *J. Biol. Chem.* 282, 26202–26209. doi:10.1074/jbc.M700776200.
- Banning, A., Deubel, S., Kluth, D., Zhou, Z., and Brigelius-Flohe, R. (2005a). The GI-GPx Gene Is a Target for Nrf2. *Mol. Cell. Biol.* 25, 4914–4923. doi:10.1128/MCB.25.12.4914-4923.2005.
- Banning, A., Deubel, S., Kluth, D., Zhou, Z., and Brigelius-Flohe, R. (2005b). The GI-GPx Gene Is a Target for Nrf2. *Mol. Cell. Biol.* 25, 4914–4923. doi:10.1128/MCB.25.12.4914-4923.2005.
- Bansal, M., Moharir, S. C., Sailasree, S. P., Sirohi, K., Sudhakar, C., Sarathi, D. P., et al. (2018). Optineurin promotes autophagosome formation by recruiting the autophagy-related Atg12-5-16L1 complex to phagophores containing the Wipi2 protein. *J. Biol. Chem.* doi:10.1074/jbc.M117.801944.
- Behrends, C., and Harper, J. W. (2011). Constructing and decoding unconventional ubiquitin chains. *Nat. Struct. Mol. Biol.* 18, 520–528. doi:10.1038/nsmb.2066.
- Behrends, C., Sowa, M. E., Gygi, S. P., and Harper, J. W. (2010). Network organization of the human autophagy system. *Nature.* doi:10.1038/nature09204.
- Bellot, G., Garcia-Medina, R., Gounon, P., Chiche, J., Roux, D., Pouyssegur, J., et al. (2009). Hypoxia-Induced Autophagy Is Mediated through Hypoxia-Inducible Factor Induction of BNIP3 and BNIP3L via Their BH3 Domains. *Mol. Cell. Biol.* 29, 2570–2581. doi:10.1128/MCB.00166-09.
- Benanti, J. A. (2012). Coordination of cell growth and division by the ubiquitin-proteasome system. *Semin. Cell Dev. Biol.* 23, 492–498. doi:10.1016/j.semcdb.2012.04.005.
- Bennett, E. J., Rush, J., Gygi, S. P., and Harper, J. W. (2010). Dynamics of cullin-RING ubiquitin ligase network revealed by systematic quantitative proteomics. *Cell.* doi:10.1016/j.cell.2010.11.017.
- Bhat, K. P., Yan, S., Wang, C.-E., Li, S., and Li, X.-J. (2014). Differential ubiquitination and degradation of huntingtin fragments modulated by ubiquitin-protein ligase E3A. *Proc. Natl. Acad. Sci.* 111, 5706–5711.

doi:10.1073/pnas.1402215111.

- Bingol, B., Tea, J. S., Phu, L., Reichelt, M., Bakalarski, C. E., Song, Q., et al. (2014). The mitochondrial deubiquitinase USP30 opposes parkin-mediated mitophagy. *Nature* 510, 370–375. doi:10.1038/nature13418.
- Birgisdottir, Á. B., Lamark, T., Johansen, T., Alemu, E. A., Lamark, T., Torgersen, K. M., et al. (2013). The LIR motif - crucial for selective autophagy. *J. Cell Sci.* 126, 3237–47. doi:10.1242/jcs.126128.
- Blomen, V. A., Májek, P., Jae, L. T., Bigenzahn, J. W., Nieuwenhuis, J., Staring, J., et al. (2015). Gene essentiality and synthetic lethality in haploid human cells. *Science* (80-.). doi:10.1126/science.aac7557.
- Bloom, J., Peschiaroli, A., DeMartino, G., and Pagano, M. (2006). Modification of Cull1 regulates its association with proteasomal subunits. *Cell Div.* doi:10.1186/1747-1028-1-5.
- Bodemann, B. O., Orvedahl, A., Cheng, T., Ram, R. R., Ou, Y. H., Formstecher, E., et al. (2011). RalB and the exocyst mediate the cellular starvation response by direct activation of autophagosome assembly. *Cell.* doi:10.1016/j.cell.2010.12.018.
- Bogunovic, D., Byun, M., Durfee, L. A., Abhyankar, A., Sanal, O., Mansouri, D., et al. (2012). Mycobacterial disease and impaired IFN- γ immunity in humans with inherited ISG15 deficiency. *Science* (80-.). 337, 1684–1688. doi:10.1126/science.1224026.
- Boldt, K., Van Reeuwijk, J., Lu, Q., Koutroumpas, K., Nguyen, T. M. T., Texier, Y., et al. (2016). An organelle-specific protein landscape identifies novel diseases and molecular mechanisms. *Nat. Commun.* doi:10.1038/ncomms11491.
- Bousquet-Dubouch, M.-P., Baudalet, E., Guérin, F., Matondo, M., Uttenweiler-Joseph, S., Burlet-Schiltz, O., et al. (2009). Affinity Purification Strategy to Capture Human Endogenous Proteasome Complexes Diversity and to Identify Proteasome-interacting Proteins. *Mol. Cell. Proteomics.* doi:10.1074/mcp.M800193-MCP200.
- Bowman, C. J., Ayer, D. E., and Dynlacht, B. D. (2014). Foxk proteins repress the initiation of starvation-induced atrophy and autophagy programs. *Nat. Cell Biol.* 16, 1202–1214. doi:10.1038/ncb3062.
- Braschi, E., Zunino, R., and McBride, H. M. (2009). MAPL is a new mitochondrial SUMO E3 ligase that regulates mitochondrial fission. *EMBO Rep.* 10, 748–754. doi:10.1038/embor.2009.86.
- Buchan, J. R., Kolaitis, R. M., Taylor, J. P., and Parker, R. (2013). XEukaryotic stress

- granules are cleared by autophagy and Cdc48/VCP function. *Cell* 153, 1461–1474. doi:10.1016/j.cell.2013.05.037.
- Budanov, A. V, and Karin, M. (2009). The p53-regulated Sestrin gene products inhibit mTOR signaling. *October* 134, 451–460. doi:10.1016/j.cell.2008.06.028.
- Byron, A., Humphries, J. D., Craig, S. E., Knight, D., and Humphries, M. J. (2012). Proteomic analysis of $\alpha 4\beta 1$ integrin adhesion complexes reveals α -subunit-dependent protein recruitment. *Proteomics*. doi:10.1002/pmic.201100487.
- Carvalho, A. F., Pinto, M. P., Grou, C. P., Alencastre, I. S., Fransen, M., Sá-Miranda, C., et al. (2007). Ubiquitination of mammalian Pex5p, the peroxisomal import receptor. *J. Biol. Chem.* 282, 31267–31272. doi:10.1074/jbc.M706325200.
- Cassavaugh, J. M., Hale, S. A., Wellman, T. L., Howe, A. K., Wong, C., and Lounsbury, K. M. (2011). Negative regulation of HIF-1 α by an FBW7-mediated degradation pathway during hypoxia. *J. Cell. Biochem.* doi:10.1002/jcb.23321.
- Chen, C., Pore, N., Behrooz, A., Ismail-Beigi, F., and Maity, A. (2001). Regulation of glut1 mRNA by hypoxia-inducible factor-1: Interaction between H-ras and hypoxia. *J. Biol. Chem.* doi:10.1074/jbc.M010144200.
- Chen, D., Fan, W., Lu, Y., Ding, X., Chen, S., and Zhong, Q. (2012). A Mammalian Autophagosome Maturation Mechanism Mediated by TECPR1 and the Atg12-Atg5 Conjugate. *Mol. Cell.* doi:10.1016/j.molcel.2011.12.036.
- Chen, M., Chen, Z., Wang, Y., Tan, Z., Zhu, C., Li, Y., et al. (2016). Mitophagy receptor FUNDC1 regulates mitochondrial dynamics and mitophagy. *Autophagy* 12, 689–702. doi:10.1080/15548627.2016.1151580.
- Chen, Y., and Klionsky, D. J. (2011). The regulation of autophagy - unanswered questions. *J. Cell Sci.* 124, 161–170. doi:10.1242/jcs.064576.
- Chen, Y., Yang, L.-N., Cheng, L., Tu, S., Guo, S.-J., Le, H.-Y., et al. (2013). Bcl2-associated Athanogene 3 Interactome Analysis Reveals a New Role in Modulating Proteasome Activity. *Mol. Cell. Proteomics*. doi:10.1074/mcp.M112.025882.
- Chen, Z.-H., Cao, J.-F., Zhou, J.-S., Liu, H., Che, L.-Q., Mizumura, K., et al. (2014). Interaction of caveolin-1 with ATG12-ATG5 system suppresses autophagy in lung epithelial cells. *AJP Lung Cell. Mol. Physiol.* doi:10.1152/ajplung.00268.2013.
- Chen, Z., Liu, L., Cheng, Q., Li, Y., Wu, H., Zhang, W., et al. (2017). Mitochondrial E3 ligase MARCH5 regulates FUNDC1 to fine-tune hypoxic mitophagy. *EMBO Rep.* 18, 495–509. doi:10.15252/embr.201643309.
- Cho, S., Choi, Y. J., Kim, J. M., Jeong, S. T., Kim, J. H., Kim, S. H., et al. (2001).

- Binding and regulation of HIF-1 α by a subunit of the proteasome complex, PSMA7. *FEBS Lett.* doi:10.1016/S0014-5793(01)02499-1.
- Christianson, J. C., Olzmann, J. A., Shaler, T. A., Sowa, M. E., Bennett, E. J., Richter, C. M., et al. (2012). Defining human ERAD networks through an integrative mapping strategy. *Nat. Cell Biol.* doi:10.1038/ncb2383.
- Cianfanelli, V., De Zio, D., Di Bartolomeo, S., Nazio, F., Strappazzon, F., and Cecconi, F. (2015). Ambra1 at a glance. *J. Cell Sci.* 128, 2003–2008. doi:10.1242/jcs.168153.
- Ciani, B., Layfield, R., Cavey, J. R., Sheppard, P. W., and Searle, M. S. (2003). Structure of the ubiquitin-associated domain of p62 (SQSTM1) and implications for mutations that cause Paget's disease of bone. *J. Biol. Chem.* 278, 37409–37412. doi:10.1074/jbc.M307416200.
- Ciechanover, A. (2012). Intracellular protein degradation: From a vague idea through the lysosome and the ubiquitin-proteasome system and onto human diseases and drug targeting. *ASH Educ. B.* 2006. doi:10.1182/asheducation-2006.1.1.
- Clague, M. J., Heride, C., and Urbé, S. (2015). The demographics of the ubiquitin system. *Trends Cell Biol.* 25, 417–426. doi:10.1016/j.tcb.2015.03.002.
- Clausen, T. H., Lamark, T., Isakson, P., Finley, K., Larsen, K. B., Brech, A., et al. (2010). p62/SQSTM1 and ALFY interact to facilitate the formation of p62 bodies/ALIS and their degradation by autophagy. *Autophagy* 6, 330–344. doi:10.4161/auto.6.3.11226.
- Claverol, S., Burlet-Schiltz, O., Girbal-Neuhauser, E., Gairin, J. E., and Monsarrat, B. (2002). Mapping and Structural Dissection of Human 20 S Proteasome Using Proteomic Approaches. *Mol. Cell. Proteomics.* doi:10.1074/mcp.M200030-MCP200.
- Codogno, P., and Meijer, A. J. (2006). Atg5: More than an autophagy factor. *Nat. Cell Biol.* doi:10.1038/ncb1006-1045.
- Cohen-kaplan, V., Livneh, I., Avni, N., Fabre, B., Ziv, T., and Tae, Y. (2016). autophagy of the mammalian 26S proteasome. doi:10.1073/pnas.1615455113.
- Collins, C. A., De Mazière, A., Van Dijk, S., Carlsson, F., Klumperman, J., and Brown, E. J. (2009). Atg5-independent sequestration of ubiquitinated mycobacteria. *PLoS Pathog.* 5. doi:10.1371/journal.ppat.1000430.
- Collins, G. A., and Goldberg, A. L. (2017). The Logic of the 26S Proteasome. *Cell* 169, 792–806. doi:10.1016/j.cell.2017.04.023.

- Copetti, T., Bertoli, C., Dalla, E., Demarchi, F., and Schneider, C. (2009). p65/RelA Modulates BECN1 Transcription and Autophagy. *Mol. Cell. Biol.* 29, 2594–2608. doi:10.1128/MCB.01396-08.
- Cornelissen, T., Haddad, D., Wauters, F., Van Humbeeck, C., Mandemakers, W., Koentjoro, B., et al. (2014). The deubiquitinase USP15 antagonizes Parkin-mediated mitochondrial ubiquitination and mitophagy. *Hum. Mol. Genet.* 23, 5227–5242. doi:10.1093/hmg/ddu244.
- Crighton, D., Wilkinson, S., O’Prey, J., Syed, N., Smith, P., Harrison, P. R., et al. (2006). DRAM, a p53-Induced Modulator of Autophagy, Is Critical for Apoptosis. *Cell.* doi:10.1016/j.cell.2006.05.034.
- Cuervo, A. M., Palmer, A., Rivett, A. J., and Knecht, E. (1995). Degradation of Proteasomes by Lysosomes in Rat Liver. *Eur. J. Biochem.* 227, 792–800. doi:10.1111/j.1432-1033.1995.0792p.x.
- Dan, H. C., and Baldwin, A. S. (2008). Differential Involvement of I B Kinases and in Cytokine- and Insulin-Induced Mammalian Target of Rapamycin Activation Determined by Akt. *J. Immunol.* 180, 7582–7589. doi:10.4049/jimmunol.180.11.7582.
- Deas, E., Plun-Favreau, H., Gandhi, S., Desmond, H., Kjaer, S., Loh, S. H. Y., et al. (2011). PINK1 cleavage at position A103 by the mitochondrial protease PARL. *Hum. Mol. Genet.* 20, 867–879. doi:10.1093/hmg/ddq526.
- Delgado, M. E., Dyck, L., Laussmann, M. A., and Rehm, M. (2014). Modulation of apoptosis sensitivity through the interplay with autophagic and proteasomal degradation pathways. *Cell Death Dis.* 5, e1011-8. doi:10.1038/cddis.2013.520.
- Demishtein, A., Fraiberg, M., Berko, D., Tirosh, B., Elazar, Z., and Navon, A. (2017). SQSTM1 / p62-mediated autophagy compensates for loss of proteasome polyubiquitin recruiting capacity. 8627. doi:10.1080/15548627.2017.1356549.
- Dengjel, J., Akimov, V., Olsen, J. V, Bunkenborg, J., Mann, M., Blagoev, B., et al. (2007). Quantitative proteomic assessment of very early cellular signaling events. *Nat. Biotechnol.* doi:10.1038/nbt1301.
- Dengjel, J., Høyer-Hansen, M., Nielsen, M. O., Eisenberg, T., Harder, L. M., Schandorff, S., et al. (2012). Identification of Autophagosome-associated Proteins and Regulators by Quantitative Proteomic Analysis and Genetic Screens. *Mol. Cell. Proteomics.* doi:10.1074/mcp.M111.014035.
- Deosaran, E., Larsen, K. B., Hua, R., Sargent, G., Wang, Y., Kim, S., et al. (2013).

- NBR1 acts as an autophagy receptor for peroxisomes. *J. Cell Sci.* 126, 939–952. doi:10.1242/jcs.114819.
- Deribe, Y. L., Wild, P., Chandrashaker, A., Curak, J., Schmidt, M. H. H., Kalaidzidis, Y., et al. (2009). Regulation of epidermal growth factor receptor trafficking by lysine deacetylase hdac6. *Sci. Signal.* doi:10.1126/scisignal.2000576.
- Dikic, I. (2017). Proteasomal and Autophagic Degradation Systems. *Annu. Rev. Biochem.* 86, 193–224. doi:10.1146/annurev-biochem-061516-044908.
- Dikic, I., and Bremm, A. (2014). DUBs counteract parkin for efficient mitophagy. *EMBO J.* 33, 2442–3. doi:10.15252/embj.201490101.
- Ding, W.-X., Ni, H.-M., Li, M., Liao, Y., Chen, X., Stolz, D. B., et al. (2010). Nix is critical to two distinct phases of mitophagy: reactive oxygen species (ROS)-mediated autophagy induction and Parkin-ubiquitin-p62-mediated mitochondria priming. *J. Biol. Chem.* doi:10.1074/jbc.M110.119537.
- Djavaheri-Mergny, M., Amelotti, M., Mathieu, J., Besançon, F., Bauvy, C., Souquère, S., et al. (2006). NF- κ B activation represses tumor necrosis factor- α -induced autophagy. *J. Biol. Chem.* 281, 30373–30382. doi:10.1074/jbc.M602097200.
- Dong, J., Chen, W., Welford, A., and Wandinger-Ness, A. (2004). The proteasome α -subunit XAPC7 interacts specifically with Rab7 and late endosomes. *J. Biol. Chem.* doi:10.1074/jbc.M401022200.
- Dooley, H. C., Razi, M., Polson, H. E. J., Girardin, S. E., Wilson, M. I., and Tooze, S. A. (2014). WIPI2 Links LC3 Conjugation with PI3P, Autophagosome Formation, and Pathogen Clearance by Recruiting Atg12-5-16L1. *Mol. Cell.* doi:10.1016/j.molcel.2014.05.021.
- Drissi, R., Dubois, M.-L., Douziech, M., and Boisvert, F.-M. (2015). Quantitative Proteomics Reveals Dynamic Interactions of the Minichromosome Maintenance Complex (MCM) in the Cellular Response to Etoposide Induced DNA Damage. *Mol. Cell. Proteomics.* doi:10.1074/mcp.M115.048991.
- Du, H., Kim, S., Hur, Y.-S., Lee, M.-S., Lee, S.-H., and Cheon, C.-I. (2015). A cytosolic thioredoxin acts as a molecular chaperone for peroxisome matrix proteins as well as antioxidant in peroxisome. *Mol. Cells.* doi:10.14348/molcells.2015.2277.
- Durcan, T. M., and Fon, E. A. (2015). USP8 and PARK2/parkin-mediated mitophagy. *Autophagy* 11, 428–429. doi:10.1080/15548627.2015.1009794.
- Durcan, T. M., Tang, M. Y., Perusse, J. R., Dashti, E. A., Aguilera, M. A., McLelland,

- G.-L., et al. (2014). USP8 regulates mitophagy by removing K6-linked ubiquitin conjugates from parkin. *EMBO J.* 33, 2473–2491. doi:10.15252/embj.201489729.
- Dzierzak, E., and Philipsen, S. (2013). Erythropoiesis : Development and Differentiation. 1–16.
- Egan, D. F., Shackelford, D. B., Mihaylova, M. M., Gelino, S., Kohnz, R. A., Mair, W., et al. (2011). Phosphorylation of ULK1 (hATG1) by AMP-activated protein kinase connects energy sensing to mitophagy. *Science (80-)*. 331, 456–461. doi:10.1126/science.1196371.
- Elliott, P. R., Leske, D., Hrdinka, M., Bagola, K., Fiil, B. K., McLaughlin, S. H., et al. (2016). SPATA2 Links CYLD to LUBAC, Activates CYLD, and Controls LUBAC Signaling. *Mol. Cell*. doi:10.1016/j.molcel.2016.08.001.
- Emdal, K. B., Pedersen, A. K., Bekker-Jensen, D. B., Tsafou, K. P., Horn, H., Lindner, S., et al. (2015). Temporal proteomics of NGF-TrkA signaling identifies an inhibitory role for the E3 ligase Cbl-b in neuroblastoma cell differentiation. *Sci. Signal*. doi:10.1126/scisignal.2005769.
- Erbil, S., Oral, O., Mitou, G., Kig, C., Durmaz-Timucin, E., Guven-Maiorov, E., et al. (2016). RACK1 is an interaction partner of ATG5 and a novel regulator of autophagy. *J. Biol. Chem*. doi:10.1074/jbc.M115.708081.
- Ertych, N., Stolz, A., Valerius, O., Braus, G. H., and Bastians, H. (2016). *CHK2 – BRCA1* tumor-suppressor axis restrains oncogenic Aurora-A kinase to ensure proper mitotic microtubule assembly. *Proc. Natl. Acad. Sci*. doi:10.1073/pnas.1525129113.
- Esteban-Martínez, L., Sierra-Filardi, E., McGreal, R. S., Salazar-Roa, M., Mariño, G., Seco, E., et al. (2017). Programmed mitophagy is essential for the glycolytic switch during cell differentiation. *EMBO J.* 36, 1688–1706. doi:10.15252/embj.201695916.
- Ewing, R. M., Chu, P., Elisma, F., Li, H., Taylor, P., Climie, S., et al. (2007). Large-scale mapping of human protein-protein interactions by mass spectrometry. *Mol. Syst. Biol*. doi:10.1038/msb4100134.
- Fan, T., Huang, Z., Wang, W., Zhang, B., Xu, Y., Mao, Z., et al. (2018). Proteasome inhibition promotes autophagy and protects from endoplasmic reticulum stress in rat alveolar macrophages exposed to hypoxia-reoxygenation injury. 1–11. doi:10.1002/jcp.26516.
- Farny, N. G., Kedersha, N. L., and Silver, P. A. (2009). Metazoan stress granule

- assembly is mediated by P-eIF2a-dependent and -independent mechanisms. 1814–1821. doi:10.1261/rna.1684009.initiation.
- Feng, Y., Longo, D. L., and Ferris, D. K. (2001). Polo-like kinase interacts with proteasomes and regulates their activity. *Cell Growth Differ.*
- Feng, Z., Hu, W., De Stanchina, E., Teresky, A. K., Jin, S., Lowe, S., et al. (2007). The regulation of AMPK β 1, TSC2, and PTEN expression by p53: Stress, cell and tissue specificity, and the role of these gene products in modulating the IGF-1-AKT-mTOR pathways. *Cancer Res.* 67, 3043–3053. doi:10.1158/0008-5472.CAN-06-4149.
- Filimonenko, M., Isakson, P., Finley, K. D., Anderson, M., Jeong, H., Melia, T. J., et al. (2010). The Selective Macroautophagic Degradation of Aggregated Proteins Requires the PI3P-Binding Protein Alfy. *Mol. Cell* 38, 265–279. doi:10.1016/j.molcel.2010.04.007.
- Finley, D. (2009). Recognition and Processing of Ubiquitin-Protein Conjugates by the Proteasome. *Annu. Rev. Biochem.* doi:10.1146/annurev.biochem.78.081507.101607.
- Fiskin, E., Bionda, T., Dikic, I., and Behrends, C. (2016). Global Analysis of Host and Bacterial Ubiquitinome in Response to Salmonella Typhimurium Infection. *Mol. Cell* 62, 967–981. doi:10.1016/j.molcel.2016.04.015.
- Flugel, D., Gorlach, a, and Kietzmann, T. (2012a). GSK-3beta regulates cell growth, migration, and angiogenesis via Fbw7 and USP28-dependent degradation of HIF-1alpha. *Blood* 119, 1292–1301. doi:10.1182/blood-2011-08-375014 [pii]r10.1182/blood-2011-08-375014.
- Flugel, D., Gorlach, a, and Kietzmann, T. (2012b). GSK-3beta regulates cell growth, migration, and angiogenesis via Fbw7 and USP28-dependent degradation of HIF-1alpha. *Blood* 119, 1292–1301. doi:10.1182/blood-2011-08-375014 [pii]r10.1182/blood-2011-08-375014.
- Foster, M. W., Thompson, J. W., Forrester, M. T., Sha, Y., McMahon, T. J., Bowles, D. E., et al. (2013). Proteomic analysis of the NOS2 interactome in human airway epithelial cells. *Nitric Oxide.* doi:10.1016/j.niox.2013.02.079.
- Fracchiolla, D., Sawa-Makarska, J., Zens, B., de Ruiter, A., Zaffagnini, G., Brezovich, A., et al. (2016). Mechanism of cargo-directed Atg8 conjugation during selective autophagy. *Elife.* doi:10.7554/eLife.18544.
- Franco, L. H., Nair, V. R., Scharn, C. R., Xavier, R. J., Torrealba, J. R., Shiloh, M. U.,

- et al. (2017). The Ubiquitin Ligase Smurf1 Functions in Selective Autophagy of Mycobacterium tuberculosis and Anti-tuberculous Host Defense. *Cell Host Microbe*. doi:10.1016/j.chom.2016.11.002.
- Fricke, B., Heink, S., Steffen, J., Kloetzel, P. M., and Krüger, E. (2007). The proteasome maturation protein POMP facilitates major steps of 20S proteasome formation at the endoplasmic reticulum. *EMBO Rep*. doi:10.1038/sj.embor.7401091.
- Froment, C., Uttenweiler-Joseph, S., Bousquet-Dubouch, M. P., Matondo, M., Borges, J. P., Esmenjaud, C., et al. (2005). A quantitative proteomic approach using two-dimensional gel electrophoresis and isotope-coded affinity tag labeling for studying human 20S proteasome heterogeneity. in *Proteomics* doi:10.1002/pmic.200401281.
- Fu, M., St-Pierre, P., Shankar, J., Wang, P. T. C., Joshi, B., and Nabi, I. R. (2013). Regulation of mitophagy by the Gp78 E3 ubiquitin ligase. *Mol. Biol. Cell* 24, 1153–1162. doi:10.1091/mbc.E12-08-0607.
- Fu, W., Ma, Q., Chen, L., Li, P., Zhang, M., Ramamoorthy, S., et al. (2009). MDM2 acts downstream of p53 as an E3 ligase to promote FOXO ubiquitination and degradation. *J. Biol. Chem.* 284, 13987–14000. doi:10.1074/jbc.M901758200.
- Fuertes, G., Villarroya, A., and Knecht, E. (2003). Role of proteasomes in the degradation of short-lived proteins in human fibroblasts under various growth conditions. *Int. J. Biochem. Cell Biol.* 35, 651–664. doi:10.1016/S1357-2725(02)00382-5.
- Fujii, K., Kitabatake, M., Sakata, T., and Ohno, M. (2012). 40S subunit dissociation and proteasome-dependent RNA degradation in nonfunctional 25S rRNA decay. *EMBO J.* 31, 2579–2589. doi:10.1038/emboj.2012.85.
- Fujita, N., Morita, E., Itoh, T., Tanaka, A., Nakaoka, M., Osada, Y., et al. (2013). Recruitment of the autophagic machinery to endosomes during infection is mediated by ubiquitin. *J. Cell Biol.* 203, 115–128. doi:10.1083/jcb.201304188.
- Funderburk, S. F., Wang, Q. J., and Yue, Z. (2010). The Beclin 1-VPS34 complex - at the crossroads of autophagy and beyond. *Trends Cell Biol.* doi:10.1016/j.tcb.2010.03.002.
- Gamerding, M., Kaya, A. M., Wolfrum, U., Clement, A. M., and Behl, C. (2011). BAG3 mediates chaperone-based aggresome-targeting and selective autophagy of misfolded proteins. *EMBO Rep.* 12, 149–156. doi:10.1038/embor.2010.203.

- Gammoh, N., Florey, O., Overholtzer, M., and Jiang, X. (2013). Interaction between FIP200 and ATG16L1 distinguishes ULK1 complex-dependent and-independent autophagy. *Nat. Struct. Mol. Biol.* doi:10.1038/nsmb.2475.
- Gao, F., Chen, D., Si, J., Hu, Q., Qin, Z., Fang, M., et al. (2015). The mitochondrial protein BNIP3L is the substrate of PARK2 and mediates mitophagy in PINK1/PARK2 pathway. *Hum. Mol. Genet.* 24, 2528–2538. doi:10.1093/hmg/ddv017.
- Gao, Y., Lecker, S., Post, M. J., Hietaranta, A. J., Li, J., Volk, R., et al. (2000). Inhibition of ubiquitin-proteasome pathway-mediated I kappa B alpha degradation by a naturally occurring antibacterial peptide. *J. Clin. Invest.* doi:10.1172/JCI9826.
- Gao, Z., Gammoh, N., Wong, P. M., Erdjument-Bromage, H., Tempst, P., and Jiang, X. (2010). Processing of autophagic protein LC3 by the 20S proteasome. *Autophagy.* doi:10.4161/auto.6.1.10928.
- Garrett, H., Thompson, R., Harris, J. W., and Brody, J. P. (2004). Post-translationally modified S12, absent in transformed breast epithelial cells, is not associated with the 26S proteasome and is induced by proteasome inhibitor. *Int. J. Cancer.* doi:10.1002/ijc.20261.
- Ge, P., Zhang, J., Wang, X., Meng, F., Li, W., Luan, Y., et al. (2009). Inhibition of autophagy induced by proteasome inhibition increases cell death in human SHG-44 glioma cells. 1046–1052. doi:10.1038/aps.2009.71.
- Geisler, S., Holmström, K. M., Skujat, D., Fiesel, F. C., Rothfuss, O. C., Kahle, P. J., et al. (2010). PINK1/Parkin-mediated mitophagy is dependent on VDAC1 and p62/SQSTM1. *Nat. Cell Biol.* 12, 119–131. doi:10.1038/ncb2012.
- Giannone, R. J., McDonald, H. W., Hurst, G. B., Shen, R. F., Wang, Y., and Liu, Y. (2010). The protein network surrounding the human telomere repeat binding factors TRF1, TRF2, and POT1. *PLoS One.* doi:10.1371/journal.pone.0012407.
- Glotzer, M., Murray, A. W., and Kirschner, M. W. (1991). Cyclin is degraded by the ubiquitin pathway. *Nature* 349, 132–138. doi:10.1038/349132a0.
- Goodall, M. L., Fitzwalter, B. E., Zahedi, S., Wu, M., Rodriguez, D., Mulcahy-Levy, J. M., et al. (2016). The Autophagy Machinery Controls Cell Death Switching between Apoptosis and Necroptosis. *Dev. Cell.* doi:10.1016/j.devcel.2016.04.018.
- Griffin, T. A., Nandi, D., Cruz, M., Fehling, H. J., Kaer, L. V, Monaco, J. J., et al. (1998). Immunoproteasome assembly: cooperative incorporation of interferon gamma (IFN-gamma)-inducible subunits. *J. Exp. Med.* 187, 97–104.

doi:10.1084/jem.187.1.97.

- Groll, M., and Huber, R. (2003). Substrate access and processing by the 20S proteasome core particle. *Int. J. Biochem. Cell Biol.* 35, 606–616. doi:10.1016/S1357-2725(02)00390-4.
- Groll, M., and Huber, R. (2004). Inhibitors of the eukaryotic 20S proteasome core particle: A structural approach. *Biochim. Biophys. Acta - Mol. Cell Res.* 1695, 33–44. doi:10.1016/j.bbamcr.2004.09.025.
- Grou, C. P., Pinto, M. P., Mendes, A. V., Domingues, P., and Azevedo, J. E. (2015). The de novo synthesis of ubiquitin: Identification of deubiquitinases acting on ubiquitin precursors. *Sci. Rep.* 5, 1–16. doi:10.1038/srep12836.
- Gutierrez, M. G., Master, S. S., Singh, S. B., Taylor, G. A., Colombo, M. I., and Deretic, V. (2004). Autophagy is a defense mechanism inhibiting BCG and Mycobacterium tuberculosis survival in infected macrophages. *Cell* 119, 753–766. doi:10.1016/j.cell.2004.11.038.
- Hamazaki, J., Sasaki, K., Kawahara, H., Hisanaga, S. -i., Tanaka, K., and Murata, S. (2007). Rpn10-Mediated Degradation of Ubiquitinated Proteins Is Essential for Mouse Development. *Mol. Cell. Biol.* doi:10.1128/MCB.00509-07.
- Hanada, T., Noda, N. N., Satomi, Y., Ichimura, Y., Fujioka, Y., Takao, T., et al. (2007). The Atg12-Atg5 conjugate has a novel E3-like activity for protein lipidation in autophagy. *J. Biol. Chem.* 282, 37298–37302. doi:10.1074/jbc.C700195200.
- Hara, K., Yonezawa, K., Weng, Q. P., Kozlowski, M. T., Belham, C., and Avruch, J. (1998). Amino acid sufficiency and mTOR regulate p70 S6 kinase and eIF-4E BP1 through a common effector mechanism. *J. Biol. Chem.* doi:10.1074/jbc.273.23.14484.
- Hara, T., Nakamura, K., Matsui, M., Yamamoto, A., Nakahara, Y., Suzuki-Migishima, R., et al. (2006). Suppression of basal autophagy in neural cells causes neurodegenerative disease in mice. *Nature* 441, 885–889. doi:10.1038/nature04724.
- Hasson, S. A., Kane, L. A., Yamano, K., Huang, C. H., Sliter, D. A., Buehler, E., et al. (2013). High-content genome-wide RNAi screens identify regulators of parkin upstream of mitophagy. *Nature* 504, 291–295. doi:10.1038/nature12748.
- Havugimana, P. C., Hart, G. T., Nepusz, T., Yang, H., Turinsky, A. L., Li, Z., et al. (2012). A census of human soluble protein complexes. *Cell.* doi:10.1016/j.cell.2012.08.011.

- He, M., Zhou, Z., Shah, A. A., Zou, H., Tao, J., Chen, Q., et al. (2016). The emerging role of deubiquitinating enzymes in genomic integrity, diseases, and therapeutics. *Cell Biosci.* 6, 1–15. doi:10.1186/s13578-016-0127-1.
- Heath, R. J., Goel, G., Baxt, L. A., Rush, J. S., Mohanan, V., Paulus, G. L. C., et al. (2016). RNF166 Determines Recruitment of Adaptor Proteins during Antibacterial Autophagy. *Cell Rep.* doi:10.1016/j.celrep.2016.11.005.
- Hein, M. Y., Hubner, N. C., Poser, I., Cox, J., Nagaraj, N., Toyoda, Y., et al. (2015). A Human Interactome in Three Quantitative Dimensions Organized by Stoichiometries and Abundances. *Cell.* doi:10.1016/j.cell.2015.09.053.
- Heinemeyer, W., Ramos, P. C., and Dohmen, R. J. (2004). Ubiquitin-proteasome system. *Cell. Mol. Life Sci.* doi:10.1007/s00018-004-4130-z.
- Hendriks, I. A., D'Souza, R. C. J., Yang, B., Verlaan-De Vries, M., Mann, M., and Vertegaal, A. C. O. (2014). Uncovering global SUMOylation signaling networks in a site-specific manner. *Nat. Struct. Mol. Biol.* 21, 927–936. doi:10.1038/nsmb.2890.
- Hendriks, I. A., and Vertegaal, A. C. O. (2016). A comprehensive compilation of SUMO proteomics. *Nat. Rev. Mol. Cell Biol.* 17, 581–595. doi:10.1038/nrm.2016.81.
- Heo, J. M., Ordureau, A., Paulo, J. A., Rinehart, J., and Harper, J. W. (2015). The PINK1-PARKIN Mitochondrial Ubiquitylation Pathway Drives a Program of OPTN/NDP52 Recruitment and TBK1 Activation to Promote Mitophagy. *Mol. Cell* 60, 7–20. doi:10.1016/j.molcel.2015.08.016.
- Herhaus, L., and Dikic, I. (2015). Expanding the ubiquitin code through post-translational modification. *EMBO Rep.* 16, 1071–1083. doi:10.15252/embr.201540891.
- Hershko, A. (1983). Ubiquitin: Roles in protein modification and breakdown. *Cell.* doi:10.1016/0092-8674(83)90131-9.
- Hershko, A. (2005). The ubiquitin system for protein degradation and some of its roles in the control of the cell-division cycle (Nobel Lecture). *Angew. Chemie - Int. Ed.* doi:10.1002/anie.200501724.
- Hershko, A., and Ciechanover, A. (1998). The ubiquitin system. *Annu. Rev. Biochem.* doi:10.1146/annurev.biochem.67.1.425.
- Higgins, R., Gendron, J. M., Rising, L., Mak, R., Webb, K., Kaiser, S. E., et al. (2015). The Unfolded Protein Response Triggers Site-Specific Regulatory Ubiquitylation

- of 40S Ribosomal Proteins. *Mol. Cell* 59, 35–49.
doi:10.1016/j.molcel.2015.04.026.
- Hirano, Y., Hayashi, H., Iemura, S. ichiro, Hendil, K. B., Niwa, S. ichiro, Kishimoto, T., et al. (2006). Cooperation of Multiple Chaperones Required for the Assembly of Mammalian 20S Proteasomes. *Mol. Cell*. doi:10.1016/j.molcel.2006.11.015.
- Hochstrasser, M. (2009). Origin and function of ubiquitin-like proteins. *Nature* 458, 422–429. doi:10.1038/nature07958.
- Honda, S., Arakawa, S., Nishida, Y., Yamaguchi, H., Ishii, E., and Shimizu, S. (2014). Ulk1-mediated Atg5-independent macroautophagy mediates elimination of mitochondria from embryonic reticulocytes. *Nat. Commun.* 5, 1–13.
doi:10.1038/ncomms5004.
- Honsho, M., Yamashita, S. ichi, and Fujiki, Y. (2016). Peroxisome homeostasis: Mechanisms of division and selective degradation of peroxisomes in mammals. *Biochim. Biophys. Acta - Mol. Cell Res.* 1863, 984–991.
doi:10.1016/j.bbamcr.2015.09.032.
- Huang, H., Regan, K. M., Wang, F., Wang, D., Smith, D. I., van Deursen, J. M. A., et al. (2005). Skp2 inhibits FOXO1 in tumor suppression through ubiquitin-mediated degradation. *Proc. Natl. Acad. Sci.* 102, 1649–1654.
doi:10.1073/pnas.0406789102.
- Huang, H., and Tindall, D. J. (2011). Regulation of FOXO protein stability via ubiquitination and proteasome degradation. *Biochim. Biophys. Acta - Mol. Cell Res.* doi:10.1016/j.bbamcr.2011.01.007.
- Huang, L., Kinnucan, E., Wang, G., Beaudenon, S., Howley, P. M., Huibregtse, J. M., et al. (1999). Structure of an E6AP-UbcH7 complex: Insights into ubiquitination by the E2-E3 enzyme cascade. *Science (80-.)*. doi:10.1126/science.286.5443.1321.
- Huett, A., Heath, R. J., Begun, J., Sassi, S. O., Baxt, L. A., Vyas, J. M., et al. (2012). The LRR and RING domain protein LRSAM1 is an E3 ligase crucial for ubiquitin-dependent autophagy of intracellular salmonella typhimurium. *Cell Host Microbe* 12, 778–790. doi:10.1016/j.chom.2012.10.019.
- Humphries, J. D., Byron, A., Bass, M. D., Craig, S. E., Pinney, J. W., Knight, D., et al. (2009). Proteomic analysis of integrin-associated complexes identifies RCC2 as a dual regulator of Rac1 and Arf6. *Sci. Signal.* doi:10.1126/scisignal.2000396.
- Huttlin, E. L., Bruckner, R. J., Paulo, J. A., Cannon, J. R., Ting, L., Baltier, K., et al. (2017). Architecture of the human interactome defines protein communities and

- disease networks. *Nature*. doi:10.1038/nature22366.
- Huttlin, E. L., Ting, L., Bruckner, R. J., Gebreab, F., Gygi, M. P., Szpyt, J., et al. (2015). The BioPlex Network: A Systematic Exploration of the Human Interactome. *Cell*. doi:10.1016/j.cell.2015.06.043.
- Hwang, S. P., and Lee, D. H. (2017). Autophagy mediates SUMO-induced degradation of a polyglutamine protein ataxin-3. *Animal Cells Syst. (Seoul)*. 21, 169–176. doi:10.1080/19768354.2017.1330765.
- Ichimura, Y., Kumanomidou, T., Sou, Y. S., Mizushima, T., Ezaki, J., Ueno, T., et al. (2008). Structural basis for sorting mechanism of p62 in selective autophagy. *J. Biol. Chem.* 283, 22847–22857. doi:10.1074/jbc.M802182200.
- Iioka, H., Iemura, S. I., Natsume, T., and Kinoshita, N. (2007). Wnt signalling regulates paxillin ubiquitination essential for mesodermal cell motility. *Nat. Cell Biol.* doi:10.1038/ncb1607.
- Ikeda, K., Nakano, R., Uraoka, M., Nakagawa, Y., Koide, M., Katsume, A., et al. (2009a). Identification of ARIA regulating endothelial apoptosis and angiogenesis by modulating proteasomal degradation of cIAP-1 and cIAP-2. *Proc. Natl. Acad. Sci.* doi:10.1073/pnas.0806780106.
- Ikeda, Y., DeMartino, G. N., Brown, M. S., Lee, J. N., Goldstein, J. L., and Ye, J. (2009b). Regulated endoplasmic reticulum-associated degradation of a polytopic protein: p97 recruits proteasomes to Insig-1 before extraction from membranes. *J. Biol. Chem.* doi:10.1074/jbc.M109.044875.
- Ishii, K., Noda, M., Yagi, H., and Thammaphorn, R. (2015). Disassembly of the self-assembled, double-ring structure of proteasome $\alpha 7$ homo-tetradecamer by $\alpha 6$. *Nat. Publ. Gr.* doi:10.1038/srep18167.
- Ishimura, R., Tanaka, K., and Komatsu, M. (2014). Dissection of the role of p62/Sqstm1 in activation of Nrf2 during xenophagy. *FEBS Lett.* 588, 822–828. doi:10.1016/j.febslet.2014.01.045.
- Ito, C., Saito, Y., Nozawa, T., Fujii, S., Sawa, T., Inoue, H., et al. (2013). Endogenous nitrated nucleotide is a key mediator of autophagy and innate defense against bacteria. *Mol. Cell* 52, 794–804. doi:10.1016/j.molcel.2013.10.024.
- Itoh, T., Fujita, N., Kanno, E., Yamamoto, A., Yoshimori, T., and Fukuda, M. (2008). Golgi-resident small GTPase Rab33B interacts with Atg16L and modulates autophagosome formation. *Mol. Biol. Cell*. doi:10.1091/mbc.E07-12-1231.
- Iwata, A., Riley, B. E., Johnston, J. A., and Kopito, R. R. (2005). HDAC6 and

- microtubules are required for autophagic degradation of aggregated Huntingtin. *J. Biol. Chem.* 280, 40282–40292. doi:10.1074/jbc.M508786200.
- Jaakkola, P., Jaakkola, P., Mole, D. R., Tian, Y., Kriegsheim, A. Von, Hebestreit, H. F., et al. (2014). Targeting of HIF- α to the von Hippel – Lindau Ubiquitylation Complex by O₂-Regulated Prolyl Hydroxylation. 468. doi:10.1126/science.1059796.
- Jager, S. (2004). Role for Rab7 in maturation of late autophagic vacuoles. *J. Cell Sci.* 117, 4837–4848. doi:10.1242/jcs.01370.
- Jain, A., Lamark, T., Sjøttem, E., Larsen, K. B., Awuh, J. A., Øvervatn, A., et al. (2010). p62/SQSTM1 is a target gene for transcription factor NRF2 and creates a positive feedback loop by inducing antioxidant response element-driven gene transcription. *J. Biol. Chem.* 285, 22576–22591. doi:10.1074/jbc.M110.118976.
- Jana, N. R., Dikshit, P., Goswami, A., Kotliarova, S., Murata, S., Tanaka, K., et al. (2005). Co-chaperone CHIP associates with expanded polyglutamine protein and promotes their degradation by proteasomes. *J. Biol. Chem.* 280, 11635–11640. doi:10.1074/jbc.M412042200.
- Jayarapu, K., and Griffin, T. A. (2004). Protein-protein interactions among human 20S proteasome subunits and proteasomelin. *Biochem. Biophys. Res. Commun.* doi:10.1016/j.bbrc.2003.12.119.
- Jayarapu, K., and Griffin, T. A. (2007). Differential intra-proteasome interactions involving standard and immunosubunits. *Biochem. Biophys. Res. Commun.* doi:10.1016/j.bbrc.2007.05.011.
- Jia, Y., Song, T., Wei, C., Ni, C., Zheng, Z., Xu, Q., et al. (2009). Negative Regulation of MAVS-Mediated Innate Immune Response by PSMA7. *J. Immunol.* doi:10.4049/jimmunol.0901646.
- Jiang, L., Hara-kuge, S., Yamashita, S., and Fujiki, Y. (2015a). Peroxin Pex14p is the key component for coordinated autophagic degradation of mammalian peroxisomes by direct binding to LC3-II. 36–49. doi:10.1111/gtc.12198.
- Jiang, S., Park, D. W., Gao, Y., Ravi, S., Darley-Usmar, V., Abraham, E., et al. (2015b). Participation of proteasome-ubiquitin protein degradation in autophagy and the activation of AMP-activated protein kinase. *Cell. Signal.* doi:10.1016/j.cellsig.2015.02.024.
- Jin, S. M., Lazarou, M., Wang, C., Kane, L. A., Narendra, D. P., and Youle, R. J. (2010). Mitochondrial membrane potential regulates PINK1 import and proteolytic

- destabilization by PARL. *J. Cell Biol.* 191, 933–942. doi:10.1083/jcb.201008084.
- Jin, S., Tian, S., Chen, Y., Zhang, C., Xie, W., Xia, X., et al. (2016). USP19 modulates autophagy and antiviral immune responses by deubiquitinating Beclin-1. *EMBO J.* 35, 866–880. doi:10.15252/emboj.201593596.
- Johnston, J. A., Ward, C. L., and Kopito, R. R. (2012). A Cellular Response to Misfolded Proteins Aggregates : *Cell* 143, 1883–1898. doi:10.1083/jcb.143.7.1883.
- Ju, J. S., Miller, S. E., Hanson, P. I., and Weihl, C. C. (2008). Impaired protein aggregate handling and clearance underlie the pathogenesis of p97/VCP-associated disease. *J. Biol. Chem.* 283, 30289–30299. doi:10.1074/jbc.M805517200.
- Juenemann, K., Schipper-Krom, S., Wiemhoefer, A., Kloss, A., Sanz, A. S., and Reits, E. A. J. (2013). Expanded polyglutamine-containing N-terminal huntingtin fragments are entirely degraded by mammalian proteasomes. *J. Biol. Chem.* 288, 27068–27084. doi:10.1074/jbc.M113.486076.
- Kabeya, Y. (2004). LC3, GABARAP and GATE16 localize to autophagosomal membrane depending on form-II formation. *J. Cell Sci.* 117, 2805–2812. doi:10.1242/jcs.01131.
- Kane, L. A., Lazarou, M., Fogel, A. I., Li, Y., Yamano, K., Sarraf, S. A., et al. (2014). PINK1 phosphorylates ubiquitin to activate parkin E3 ubiquitin ligase activity. *J. Cell Biol.* 205, 143–153. doi:10.1083/jcb.201402104.
- Kang, Y.-A., Sanalkumar, R., O’Geen, H., Linnemann, A. K., Chang, C.-J., Bouhassira, E. E., et al. (2012). Autophagy Driven by a Master Regulator of Hematopoiesis. *Mol. Cell Biol.* 32, 226–239. doi:10.1128/MCB.06166-11.
- Kato, S., Ding, J., Pisch, E., Jhala, U. S., and Du, K. (2008). COP1 functions as a FoxO1 ubiquitin E3 ligase to regulate FoxO1-mediated gene expression. *J. Biol. Chem.* 283, 35464–35473. doi:10.1074/jbc.M801011200.
- Kaushik, S., and Cuervo, A. M. (2018). The coming of age of chaperone-mediated autophagy. *Nat. Rev. Mol. Cell Biol.* 2018. doi:10.1038/s41580-018-0001-6.
- Kawaguchi, Y., Kovacs, J. J., McLaurin, A., Vance, J. M., Ito, A., and Yao, T. P. (2003). The deacetylase HDAC6 regulates aggresome formation and cell viability in response to misfolded protein stress. *Cell* 115, 727–738. doi:10.1016/S0092-8674(03)00939-5.
- Kazlauskaitė, A., Kondapalli, C., Gourlay, R., Campbell, D. G., Ritorto, M. S., Hofmann, K., et al. (2014). Parkin is activated by PINK1-dependent

- phosphorylation of ubiquitin at Ser⁶⁵. *Biochem. J.* 460, 127–141.
doi:10.1042/BJ20140334.
- Kedersha, N., Cho, M. R., Li, W., Yacono, P. W., Chen, S., Gilks, N., et al. (2000). Dynamic shuttling of TIA-1 accompanies the recruitment of mRNA to mammalian stress granules. *J. Cell Biol.* 151, 1257–1268. doi:10.1083/jcb.151.6.1257.
- Kedersha, N., Panas, M. D., Achorn, C. A., Lyons, S., Tisdale, S., Hickman, T., et al. (2016). G3BP-Caprin1-USP10 complexes mediate stress granule condensation and associate with 40S subunits. *J. Cell Biol.* 212, 845–860.
doi:10.1083/jcb.201508028.
- Kedersha, N., Stoecklin, G., Ayodele, M., Yacono, P., Lykke-Andersen, J., Fitzler, M. J., et al. (2005). Stress granules and processing bodies are dynamically linked sites of mRNP remodeling. *J. Cell Biol.* doi:10.1083/jcb.200502088.
- Kenzelmann Broz, D., Mello, S. S., Biegging, K. T., Jiang, D., Dusek, R. L., Brady, C. A., et al. (2013). Global genomic profiling reveals an extensive p53-regulated autophagy program contributing to key p53 responses. *Genes Dev.*
doi:10.1101/gad.212282.112.
- Kırlı, K., Karaca, S., Dehne, H. J., Samwer, M., Pan, K. T., Lenz, C., et al. (2015). A deep proteomics perspective on CRM1-mediated nuclear export and nucleocytoplasmic partitioning. *Elife*. doi:10.7554/eLife.11466.
- Kim, J. H., Hong, S. B., Lee, J. K., Han, S., Roh, K. H., Lee, K. E., et al. (2015). Insights into autophagosome maturation revealed by the structures of ATG5 with its interacting partners. *Autophagy*. doi:10.4161/15548627.2014.984276.
- Kim, J. W., Tchernyshyov, I., Semenza, G. L., and Dang, C. V. (2006). HIF-1-mediated expression of pyruvate dehydrogenase kinase: A metabolic switch required for cellular adaptation to hypoxia. *Cell Metab.* doi:10.1016/j.cmet.2006.02.002.
- Kim, P. K., Hailey, D. W., Mullen, R. T., and Lippincott-Schwartz, J. (2008). Ubiquitin signals autophagic degradation of cytosolic proteins and peroxisomes. *Proc. Natl. Acad. Sci.* 105, 20567–20574. doi:10.1073/pnas.0810611105.
- Kirisako, T., Ichimura, Y., Okada, H., Kabeya, Y., Mizushima, N., Yoshimori, T., et al. (2000). The reversible modification regulates the membrane-binding state of Apg8/Aut7 essential for autophagy and the cytoplasm to vacuole targeting pathway. *J. Cell Biol.* 151, 263–275. doi:10.1083/jcb.151.2.263.
- Kirkegaard, K., Taylor, M. P., and Jackson, W. T. (2004). Cellular autophagy: Surrender, avoidance and subversion by microorganisms. *Nat. Rev. Microbiol.*

doi:10.1038/nrmicro865.

- Kirkin, V., McEwan, D. G., Novak, I., and Dikic, I. (2009). A Role for Ubiquitin in Selective Autophagy. *Mol. Cell* 34, 259–269. doi:10.1016/j.molcel.2009.04.026.
- Klionsky, D. J. (2007). Autophagy: From phenomenology to molecular understanding in less than a decade. *Nat. Rev. Mol. Cell Biol.* doi:10.1038/nrm2245.
- Kobayashi, A., Kang, M., Okawa, H., Zenke, Y., Chiba, T., Igarashi, K., et al. (2004). Oxidative Stress Sensor Keap1 Functions as an Adaptor for Cul3-Based E3 Ligase To Regulate Proteasomal Degradation of Nrf2 Oxidative Stress Sensor Keap1 Functions as an Adaptor for Cul3-Based E3 Ligase To Regulate Proteasomal Degradation of Nrf2. *Mol. Cell. Biol.* 24, 7130–7139. doi:10.1128/MCB.24.16.7130.
- Kobayashi, E. H., Suzuki, T., Funayama, R., Nagashima, T., Hayashi, M., Sekine, H., et al. (2016). Nrf2 suppresses macrophage inflammatory response by blocking proinflammatory cytokine transcription. *Nat. Commun.* 7, 1–14. doi:10.1038/ncomms11624.
- Koch, H. B., Zhang, R., Verdoodt, B., Bailey, A., Zhang, C. D., Yates, J. R., et al. (2007). Large-scale identification of c-MYC-associated proteins using a combined TAP/MudPIT approach. *Cell Cycle*. doi:10.4161/cc.6.2.3742.
- Koh, M. Y., Darnay, B. G., and Powis, G. (2008). Hypoxia-Associated Factor, a Novel E3-Ubiquitin Ligase, Binds and Ubiquitinates Hypoxia-Inducible Factor 1 , Leading to Its Oxygen-Independent Degradation. *Mol. Cell. Biol.* doi:10.1128/MCB.00773-08.
- Komander, D., Clague, M. J., and Urbé, S. (2009). Breaking the chains: Structure and function of the deubiquitinases. *Nat. Rev. Mol. Cell Biol.* 10, 550–563. doi:10.1038/nrm2731.
- Komatsu, M., Kurokawa, H., Waguri, S., Taguchi, K., Kobayashi, A., Ichimura, Y., et al. (2010). The selective autophagy substrate p62 activates the stress responsive transcription factor Nrf2 through inactivation of Keap1. *Nat. Cell Biol.* doi:10.1038/ncb2021.
- Komatsu, M., Waguri, S., Chiba, T., Murata, S., Iwata, J. I., Tanida, I., et al. (2006). Loss of autophagy in the central nervous system causes neurodegeneration in mice. *Nature*. doi:10.1038/nature04723.
- Komatsu, M., Waguri, S., Koike, M., Sou, Y. shin, Ueno, T., Hara, T., et al. (2007). Homeostatic Levels of p62 Control Cytoplasmic Inclusion Body Formation in

- Autophagy-Deficient Mice. *Cell* 131, 1149–1163. doi:10.1016/j.cell.2007.10.035.
- Komatsu, M., Waguri, S., Ueno, T., Iwata, J., Murata, S., Tanida, I., et al. (2005). Impairment of starvation-induced and constitutive autophagy in Atg7-deficient mice. *J. Cell Biol.* doi:10.1083/jcb.200412022.
- Kondapalli, C., Kazlauskaite, A., Zhang, N., Woodroof, H. I., Campbell, D. G., Gourlay, R., et al. (2012). PINK1 is activated by mitochondrial membrane potential depolarization and stimulates Parkin E3 ligase activity by phosphorylating Serine 65. *Open Biol.* 2, 120080–120080. doi:10.1098/rsob.120080.
- Kopito, R. R. (2000). Aggresomes, inclusion bodies and protein aggregation. *Trends Cell Biol.* 10, 524–530. doi:10.1016/S0962-8924(00)01852-3.
- Korac, J., Schaeffer, V., Kovacevic, I., Clement, A. M., Jungblut, B., Behl, C., et al. (2013). Ubiquitin-independent function of optineurin in autophagic clearance of protein aggregates. *J. Cell Sci.* 126, 580–592. doi:10.1242/jcs.114926.
- Korolchuk, V. I., Mansilla, A., Menzies, F. M., and Rubinsztein, D. C. (2009a). Autophagy Inhibition Compromises Degradation of Ubiquitin-Proteasome Pathway Substrates. *Mol. Cell* 33, 517–527. doi:10.1016/j.molcel.2009.01.021.
- Korolchuk, V. I., Mansilla, A., Menzies, F. M., and Rubinsztein, D. C. (2009b). Autophagy Inhibition Compromises Degradation of Ubiquitin-Proteasome Pathway Substrates. *Mol. Cell* 33, 517–527. doi:10.1016/j.molcel.2009.01.021.
- Korolchuk, V. I., Menzies, F. M., and Rubinsztein, D. C. (2009c). A novel link between autophagy and the ubiquitin-proteasome system. *Autophagy*. doi:10.4161/auto.8840.
- Korolchuk, V. I., Menzies, F. M., and Rubinsztein, D. C. (2010). Mechanisms of cross-talk between the ubiquitin-proteasome and autophagy-lysosome systems. *FEBS Lett.* 584, 1393–1398. doi:10.1016/j.febslet.2009.12.047.
- Koyano, F., Okatsu, K., Kosako, H., Tamura, Y., Go, E., Kimura, M., et al. (2014). Ubiquitin is phosphorylated by PINK1 to activate parkin. *Nature* 510, 162–166. doi:10.1038/nature13392.
- Kraft, C., Deplazes, A., Sohrmann, M., and Peter, M. (2008). Mature ribosomes are selectively degraded upon starvation by an autophagy pathway requiring the Ubp3p/Bre5p ubiquitin protease. *Nat. Cell Biol.* 10, 602–610. doi:10.1038/ncb1723.
- Kraft, C., and Peter, M. (2008). Is the Rsp5 ubiquitin ligase involved in the regulation of

- ribophagy? *Autophagy* 4, 838–840. doi:10.4161/auto.6603.
- Kravtsova-ivantsiv, Y., Ciechanover, A., Kravtsova-ivantsiv, Y., and Ciechanover, A. (2015). The ubiquitin-proteasome system and activation of NF- κ B : involvement of the ubiquitin ligase KPC1 in p105 processing and tumor suppression The ubiquitin-proteasome system and activation of NF- κ B : involvement of the ubiquitin ligase KPC1 in p105 proc. 3556. doi:10.1080/23723556.2015.1054552.
- Kristensen, A. R., Gsponer, J., and Foster, L. J. (2012). A high-throughput approach for measuring temporal changes in the interactome. *Nat. Methods*. doi:10.1038/nmeth.2131.
- Kroemer, G., Mariño, G., and Levine, B. (2010). Autophagy and the Integrated Stress Response. *Mol. Cell* 40, 280–293. doi:10.1016/j.molcel.2010.09.023.
- Kuchay, S., Duan, S., Schenkein, E., Peschiaroli, A., Saraf, A., Florens, L., et al. (2013). FBXL2- and PTPL1-mediated degradation of p110-free p85 β regulatory subunit controls the PI(3)K signalling cascade. *Nat. Cell Biol.* doi:10.1038/ncb2731.
- Kulikov, R., Letienne, J., Kaur, M., Grossman, S. R., Arts, J., and Blattner, C. (2010). Mdm2 facilitates the association of p53 with the proteasome. *Proc. Natl. Acad. Sci.* doi:10.1073/pnas.0911716107.
- Kundu, M., Lindsten, T., Yang, C. Y., Wu, J., Zhao, F., Zhang, J., et al. (2008). Ulk1 plays a critical role in the autophagic clearance of mitochondria and ribosomes during reticulocyte maturation. *Blood* 112, 1493–1502. doi:10.1182/blood-2008-02-137398.
- Kwon, Y. T., and Ciechanover, A. (2017). The Ubiquitin Code in the Ubiquitin-Proteasome System and Autophagy. *Trends Biochem. Sci.* 42, 873–886. doi:10.1016/j.tibs.2017.09.002.
- Kyrychenko, V. O., Nagibin, V. S., Tumanovska, L. V., Pashevin, D. O., Gurianova, V. L., Moibenko, A. A., et al. (2013). Knockdown of PSMB7 induces autophagy in cardiomyocyte cultures: Possible role in endoplasmic reticulum stress. *Pathobiology* 81, 8–14. doi:10.1159/000350704.
- Lamark, T., and Johansen, T. (2012). Aggrephagy: Selective disposal of protein aggregates by macroautophagy. *Int. J. Cell Biol.* 2012. doi:10.1155/2012/736905.
- Lamb, C. A., Yoshimori, T., and Tooze, S. A. (2013). The autophagosome: Origins unknown, biogenesis complex. *Nat. Rev. Mol. Cell Biol.* 14, 759–774. doi:10.1038/nrm3696.
- Lander, G. C., Estrin, E., Matyskiela, M. E., Bashore, C., Nogales, E., and Martin, A.

- (2012). Complete subunit architecture of the proteasome regulatory particle. *Nature* 482, 186–191. doi:10.1038/nature10774.
- Law, K. B., Bronte-tinkew, D., Pietro, E. Di, Snowden, A., Jones, O., Moser, A., et al. (2017). The peroxisomal AAA ATPase complex prevents pexophagy and development of peroxisome biogenesis disorders. *Autophagy* 13, 868–884. doi:10.1080/15548627.2017.1291470.
- Lazarou, M., Jin, S. M., Kane, L. A., and Youle, R. J. (2012). Role of PINK1 Binding to the TOM Complex and Alternate Intracellular Membranes in Recruitment and Activation of the E3 Ligase Parkin. *Dev. Cell* 22, 320–333. doi:10.1016/j.devcel.2011.12.014.
- Lazarou, M., Sliter, D. A., Kane, L. A., Sarraf, S. A., Wang, C., Burman, J. L., et al. (2015). The ubiquitin kinase PINK1 recruits autophagy receptors to induce mitophagy. *Nature* 524, 309–314. doi:10.1038/nature14893.
- Lee, D. F., Kuo, H. P., Chen, C. Te, Hsu, J. M., Chou, C. K., Wei, Y., et al. (2007). IKK β Suppression of TSC1 Links Inflammation and Tumor Angiogenesis via the mTOR Pathway. *Cell* 130, 440–455. doi:10.1016/j.cell.2007.05.058.
- Lee, I. H., Cao, L., Mostoslavsky, R., Lombard, D. B., Liu, J., Bruns, N. E., et al. (2008). A role for the NAD-dependent deacetylase Sirt1 in the regulation of autophagy. *Proc. Natl. Acad. Sci.* doi:10.1073/pnas.0712145105.
- Lee, J. H., Elly, C., Park, Y., Lee, J. H., Elly, C., Park, Y., et al. (2015). Inducible Factor-1 a to Maintain Regulatory T Cell Stability and Suppressive Capacity Article E3 Ubiquitin Ligase VHL Regulates Hypoxia-Inducible Factor-1 a to Maintain Regulatory T Cell Stability and Suppressive Capacity. *Immunity* 42, 1062–1074. doi:10.1016/j.immuni.2015.05.016.
- Lee, J. J., Sanchez-Martinez, A., Zarate, A. M., Benincá, C., Mayor, U., Clague, M. J., et al. (2018). Basal mitophagy is widespread in *Drosophila* but minimally affected by loss of Pink1 or parkin. *J. Cell Biol.*, jcb.201801044. doi:10.1083/jcb.201801044.
- Lee, J. Y., Koga, H., Kawaguchi, Y., Tang, W., Wong, E., Gao, Y. S., et al. (2010). HDAC6 controls autophagosome maturation essential for ubiquitin-selective quality-control autophagy. *EMBO J.* 29, 969–980. doi:10.1038/emboj.2009.405.
- Lee, M. J., Lee, B.-H., Hanna, J., King, R. W., and Finley, D. (2011). Trimming of Ubiquitin Chains by Proteasome-associated Deubiquitinating Enzymes. *Mol. Cell. Proteomics* 10, R110.003871. doi:10.1074/mcp.R110.003871.

- Lee, M. Y., Sumpter, R., Zou, Z., Sirasanagandla, S., Wei, Y., Mishra, P., et al. (2017). Peroxisomal protein PEX13 functions in selective autophagy. *EMBO Rep.* doi:10.15252/embr.201642443.
- Lemasters, J. J. (2005). John j. lemasters. 8, 3–5.
- Li, D., Dong, Q., Tao, Q., Gu, J., Cui, Y., Jiang, X., et al. (2015). c-Abl regulates proteasome abundance by controlling the ubiquitin-proteasomal degradation of PSMA7 subunit. *Cell Rep.* doi:10.1016/j.celrep.2014.12.044.
- Li, D., and Sewer, M. B. (2010). RhoA and DIAPH1 mediate adrenocorticotropin-stimulated cortisol biosynthesis by regulating mitochondrial trafficking. *Endocrinology.* doi:10.1210/en.2010-0044.
- Li, N., Zhang, Z., Zhang, W., and Wei, Q. (2011). Calcineurin B subunit interacts with proteasome subunit alpha type 7 and represses hypoxia-inducible factor-1 α activity via the proteasome pathway. *Biochem. Biophys. Res. Commun.* doi:10.1016/j.bbrc.2011.01.055.
- Li, Q., Chen, P., Zeng, Z., Liang, F., Song, Y., Xiong, F., et al. (2016). Yeast two-hybrid screening identified WDR77 as a novel interacting partner of TSC22D2. *Tumor Biol.* doi:10.1007/s13277-016-5113-z.
- Li, S., Wandel, M. P., Li, F., Liu, Z., He, C., Wu, J., et al. (2013). Sterical hindrance promotes selectivity of the autophagy cargo receptor NDP52 for the danger receptor galectin-8 in antibacterial autophagy. *Sci. Signal.* 6, 1–7. doi:10.1126/scisignal.2003730.
- Li, W. W., Li, J., and Bao, J. K. (2012). Microautophagy: Lesser-known self-eating. *Cell. Mol. Life Sci.* 69, 1125–1136. doi:10.1007/s00018-011-0865-5.
- Li, Z., Na, X., Wang, D., Schoen, S. R., Messing, E. M., and Wu, G. (2002a). Ubiquitination of a novel deubiquitinating enzyme requires direct binding to von Hippel-Lindau tumor suppressor protein. *J. Biol. Chem.* 277, 4656–4662. doi:10.1074/jbc.M108269200.
- Li, Z., Wang, D., Na, X., Schoen, S. R., Messing, E. M., and Wu, G. (2002b). Identification of a deubiquitinating enzyme subfamily as substrates of the von Hippel-Lindau tumor suppressor. *Biochem. Biophys. Res. Commun.* doi:10.1016/S0006-291X(02)00534-X.
- Liggett, A., Crawford, L. J., Walker, B., Morris, T. C. M., and Irvine, A. E. (2010). Methods for measuring proteasome activity: Current limitations and future developments. *Leuk. Res.* doi:10.1016/j.leukres.2010.07.003.

- Lim, P. J., Danner, R., Liang, J., Doong, H., Harman, C., Srinivasan, D., et al. (2009). Ubiquilin and p97/VCP bind erasin, forming a complex involved in ERAD. *J. Cell Biol.* 187, 201–217. doi:10.1083/jcb.200903024.
- Lin, Q., Dai, Q., Meng, H., Sun, A., Wei, J., Peng, K., et al. (2017). The HECT E3 ubiquitin ligase NEDD4 interacts with and ubiquitylates SQSTM1 for inclusion body autophagy. doi:10.1242/jcs.207068.
- Ling, J., Kang, Y., Zhao, R., Xia, Q., Lee, D. F., Chang, Z., et al. (2012). Kras G12D-Induced IKK2/ β /NF- κ B Activation by IL-1 α and p62 Feedforward Loops Is Required for Development of Pancreatic Ductal Adenocarcinoma. *Cancer Cell* 21, 105–120. doi:10.1016/j.ccr.2011.12.006.
- Liu, J., Xia, H., Kim, M., Xu, L., Li, Y., Zhang, L., et al. (2011). Beclin1 controls the levels of p53 by regulating the deubiquitination activity of USP10 and USP13. *Cell* 147, 223–234. doi:10.1016/j.cell.2011.08.037.
- Liu, X., Huang, W., Li, C., Li, P., Yuan, J., Li, X., et al. (2006). Interaction between c-Abl and Arg Tyrosine Kinases and Proteasome Subunit PSMA7 Regulates Proteasome Degradation. *Mol. Cell.* doi:10.1016/j.molcel.2006.04.007.
- Liu, Z., Chen, P., Gao, H., Gu, Y., Yang, J., Peng, H., et al. (2014). Ubiquitylation of Autophagy Receptor Optineurin by HACE1 Activates Selective Autophagy for Tumor Suppression. *Cancer Cell* 26, 106–120. doi:10.1016/j.ccr.2014.05.015.
- Lobato-Márquez, D., and Mostowy, S. (2017). *Salmonella* ubiquitination: ARIH1 enters the fray. *EMBO Rep.* 18, 1476–1477. doi:10.15252/embr.201744672.
- Long, J., Gallagher, T. R. A., Cavey, J. R., Sheppard, P. W., Ralston, S. H., Layfield, R., et al. (2008). Ubiquitin recognition by the ubiquitin-associated domain of p62 involves a novel conformational switch. *J. Biol. Chem.* 283, 5427–5440. doi:10.1074/jbc.M704973200.
- Lu, K., Psakhye, I., and Jentsch, S. (2014). Autophagic clearance of PolyQ proteins mediated by ubiquitin-Atg8 adaptors of the conserved CUET protein family. *Cell* 158, 549–563. doi:10.1016/j.cell.2014.05.048.
- Lu, L., Hu, S., Wei, R., Qiu, X., Lu, K., Fu, Y., et al. (2013). The HECT type ubiquitin ligase NEDL2 is degraded by anaphase-promoting complex/cyclosome (APC/C)-Cdh1, and its tight regulation maintains the metaphase to anaphase transition. *J. Biol. Chem.* doi:10.1074/jbc.M113.472076.
- Mammucari, C., Milan, G., Romanello, V., Masiero, E., Rudolf, R., Del Piccolo, P., et al. (2007). FoxO3 Controls Autophagy in Skeletal Muscle In Vivo. *Cell Metab.* 6,

- 458–471. doi:10.1016/j.cmet.2007.11.001.
- Manzanillo, P. S., Ayres, J. S., Watson, R. O., Collins, A. C., Souza, G., Rae, C. S., et al. (2013). The ubiquitin ligase parkin mediates resistance to intracellular pathogens. *Nature* 501, 512–516. doi:10.1038/nature12566.
- Mao, J., Xia, Q., Liu, C., Ying, Z., Wang, H., and Wang, G. (2017). A critical role of Hrd1 in the regulation of optineurin degradation and aggresome formation. *Hum. Mol. Genet.* 26, 1877–1889. doi:10.1093/hmg/ddx096.
- Marshall, R. S., Li, F., Gemperline, D. C., Book, A. J., and Vierstra, R. D. (2015). Autophagic Degradation of the 26S Proteasome Is Mediated by the Dual ATG8/Ubiquitin Receptor RPN10 in Arabidopsis. *Mol. Cell* 58, 1053–1066. doi:10.1016/j.molcel.2015.04.023.
- Matsumoto, M., Hatakeyama, S., Oyamada, K., Oda, Y., Nishimura, T., and Nakayama, K. I. (2005). Large-scale analysis of the human ubiquitin-related proteome. *Proteomics*. doi:10.1002/pmic.200401280.
- Matsushita, M., Suzuki, N. N., Obara, K., Fujioka, Y., Ohsumi, Y., and Inagaki, F. (2007). Structure of Atg5-Atg16, a complex essential for autophagy. *J. Biol. Chem.* doi:10.1074/jbc.M609876200.
- Matthias, P., Yoshida, M., and Khochbin, S. (2008). HDAC6 a new cellular stress surveillance factor. *Cell Cycle* 7, 7–10. doi:10.4161/cc.7.1.5186.
- Mauthe, M., Jacob, A., Freiburger, S., Hentschel, K., Stierhof, Y. D., Codogno, P., et al. (2011). Resveratrol-mediated autophagy requires WIPI-1-regulated LC3 lipidation in the absence of induced phagophore formation. *Autophagy* 7, 1448–1461. doi:10.4161/auto.7.12.17802.
- Mazroui, R., Di Marco, S., Kaufman, R. J., and Gallouzi, I.-E. (2007). Inhibition of the Ubiquitin-Proteasome System Induces Stress Granule Formation. *Mol. Biol. Cell.* doi:10.1091/mbc.E06.
- Mehrpour, M., Esclatine, A., Beau, I., and Codogno, P. (2010). Overview of macroautophagy regulation in mammalian cells. *Cell Res.* 20, 748–762. doi:10.1038/cr.2010.82.
- Meier, F., Abeywardana, T., Dhall, A., Marotta, N. P., Varkey, J., Langen, R., et al. (2012). Semisynthetic, site-specific ubiquitin modification of α -synuclein reveals differential effects on aggregation. *J. Am. Chem. Soc.* 134, 5468–5471. doi:10.1021/ja300094r.
- Menzies, F. M., Garcia-Arencibia, M., Imarisio, S., O’Sullivan, N. C., Ricketts, T.,

- Kent, B. A., et al. (2015). Calpain inhibition mediates autophagy-dependent protection against polyglutamine toxicity. *Cell Death Differ.* 22, 433–444. doi:10.1038/cdd.2014.151.
- Mishra, A., Godavarthi, S. K., Maheshwari, M., Goswami, A., and Jana, N. R. (2009). The ubiquitin ligase E6-AP is induced and recruited to aggresomes in response to proteasome inhibition and may be involved in the ubiquitination of Hsp70-bound misfolded proteins. *J. Biol. Chem.* 284, 10537–10545. doi:10.1074/jbc.M806804200.
- Mizushima, N. (2018). A brief history of autophagy from cell biology to physiology and disease. *Nat. Cell Biol.* doi:10.1038/s41556-018-0092-5.
- Morimoto, D., Walinda, E., Fukada, H., Sou, Y. S., Kageyama, S., Hoshino, M., et al. (2015). The unexpected role of polyubiquitin chains in the formation of fibrillar aggregates. *Nat. Commun.* 6, 1–10. doi:10.1038/ncomms7116.
- Moscat, J., and Diaz-Meco, M. T. (2009). p62 at the Crossroads of Autophagy, Apoptosis, and Cancer. *Cell* 137, 1001–1004. doi:10.1016/j.cell.2009.05.023.
- Nakagawa, T., Shirane, M., Lemura, S. I., Natsume, T., and Nakayama, K. I. (2007). Anchoring of the 26S proteasome to the organellar membrane by FKBP38. *Genes to Cells.* doi:10.1111/j.1365-2443.2007.01086.x.
- Nakamura, N., Kimura, Y., Tokuda, M., Honda, S., and Hirose, S. (2006). MARCH-V is a novel mitofusin 2- and Drp1-binding protein able to change mitochondrial morphology. *EMBO Rep.* 7, 1019–1022. doi:10.1038/sj.embor.7400790.
- Nakashima, H., Nguyen, T., Goins, W. F., and Chiocca, E. A. (2015). Interferon-stimulated gene 15 (ISG15) and ISG15-linked proteins can associate with members of the selective autophagic process, histone deacetylase 6 (HDAC6) and SQSTM1/p62. *J. Biol. Chem.* 290, 1485–1495. doi:10.1074/jbc.M114.593871.
- Nakatogawa, H., Ichimura, Y., and Ohsumi, Y. (2007). Atg8, a Ubiquitin-like Protein Required for Autophagosome Formation, Mediates Membrane Tethering and Hemifusion. *Cell* 130, 165–178. doi:10.1016/j.cell.2007.05.021.
- Nakayama, K., Frew, I. J., Hagensen, M., Skals, M., Habelhah, H., Bhoumik, A., et al. (2004). Siah2 regulates stability of prolyl-hydroxylases, controls HIF1 α abundance, and modulates physiological responses to hypoxia. *Cell* 117, 941–952. doi:10.1016/j.cell.2004.06.001.
- Nandi, D., Woodward, E., Ginsburg, D. B., and Monaco, J. J. (1997). Intermediates in the formation of mouse 20S proteasomes: Implications for the assembly of

- precursor β subunits. *EMBO J.* doi:10.1093/emboj/16.17.5363.
- Narendra, D. P., Kane, L. A., Hauser, D. N., Fearnley, I. M., and Youle, R. J. (2010). p62/SQSTM1 is required for Parkin-induced mitochondrial clustering but not mitophagy; VDAC1 is dispensable for both. *Autophagy* 6, 1090–1106. doi:10.4161/auto.6.8.13426.
- Narendra, D., Tanaka, A., Suen, D. F., and Youle, R. J. (2008). Parkin is recruited selectively to impaired mitochondria and promotes their autophagy. *J. Cell Biol.* 183, 795–803. doi:10.1083/jcb.200809125.
- Nazio, F., Strappazon, F., Antonioli, M., Bielli, P., Cianfanelli, V., Bordi, M., et al. (2013). mTOR inhibits autophagy by controlling ULK1 ubiquitylation, self-association and function through AMBRA1 and TRAF6. *Nat. Cell Biol.* 15, 406–416. doi:10.1038/ncb2708.
- Nezis, I. P., Simonsen, A., Sagona, A. P., Finley, K., Gaumer, S., Contamine, D., et al. (2008). Ref(2)P, the *Drosophila melanogaster* homologue of mammalian p62, is required for the formation of protein aggregates in adult brain. *J. Cell Biol.* 180, 1065–1071. doi:10.1083/jcb.200711108.
- Nie, J., Xie, P., Liu, L., Xing, G., Chang, Z., Yin, Y., et al. (2010). Smad ubiquitylation regulatory factor 1/2 (Smurf1/2) promotes p53 degradation by stabilizing the E3 ligase MDM2. *J. Biol. Chem.* 285, 22818–22830. doi:10.1074/jbc.M110.126920.
- Noad, J., Von Der Malsburg, A., Pathe, C., Michel, M. A., Komander, D., and Randow, F. (2017). LUBAC-synthesized linear ubiquitin chains restrict cytosol-invading bacteria by activating autophagy and NF- κ B. *Nat. Microbiol.* doi:10.1038/nmicrobiol.2017.63.
- Norman, J. A., and Shiekhhattar, R. (2006). Analysis of Nedd8-associated polypeptides: A model for deciphering the pathway for ubiquitin-like modifications. *Biochemistry.* doi:10.1021/bi052435a.
- Novak, I., Kirkin, V., McEwan, D. G., Zhang, J., Wild, P., Rozenknop, A., et al. (2010). Nix is a selective autophagy receptor for mitochondrial clearance. *EMBO Rep.* 11, 45–51. doi:10.1038/embor.2009.256.
- Ogawa, M., Yoshimori, T., Suzuki, T., Sagara, H., Mizushima, N., and Sasakawa, C. (2005). Escape of intracellular *Shigella* from autophagy. *Science (80-)*. 307, 727–731. doi:10.1126/science.1106036.
- Ohh, M., Park, C. W., Ivan, M., Hoffman, M. A., Kim, T., Huang, L. E., et al. (2000). Ubiquitination of hypoxia-inducible factor requires direct binding to the β -domain

- of the von Hippel – Lindau protein. *2*, 423–427.
- Ohsumi, Y., and Mizushima, N. (2004). Two ubiquitin-like conjugation systems essential for autophagy. *Semin. Cell Dev. Biol.* doi:10.1016/j.semcdb.2003.12.004.
- Okamoto, K., Kondo-Okamoto, N., and Ohsumi, Y. (2009). Mitochondria-Anchored Receptor Atg32 Mediates Degradation of Mitochondria via Selective Autophagy. *Dev. Cell* 17, 87–97. doi:10.1016/j.devcel.2009.06.013.
- Okatsu, K., Saisho, K., Shimanuki, M., Nakada, K., Shitara, H., Sou, Y. S., et al. (2010). P62/SQSTM1 cooperates with Parkin for perinuclear clustering of depolarized mitochondria. *Genes to Cells* 15, 887–900. doi:10.1111/j.1365-2443.2010.01426.x.
- Okerlund, N. D., Schneider, K., Leal-Ortiz, S., Montenegro-Venegas, C., Kim, S. A., Garner, L. C., et al. (2018). Erratum: Bassoon Controls Presynaptic Autophagy through Atg5 (*Neuron* (2017) 93(4) (897–913.e7)(S0896627317300508)(10.1016/j.neuron.2017.01.026)). *Neuron*. doi:10.1016/j.neuron.2018.01.010.
- Okumoto, K., Misono, S., Miyata, N., Matsumoto, Y., Mukai, S., and Fujiki, Y. (2011). Cysteine ubiquitination of PTS1 receptor Pex5p regulates Pex5p recycling. *Traffic* 12, 1067–1083. doi:10.1111/j.1600-0854.2011.01217.x.
- Oláh, J., Vincze, O., Virók, D., Simon, D., Bozsó, Z., Tokési, N., et al. (2011). Interactions of pathological hallmark proteins: Tubulin polymerization promoting protein/p25, β -amyloid, and α -synuclein. *J. Biol. Chem.* doi:10.1074/jbc.M111.243907.
- Olzmann, J. A., Li, A., Chudaev, M. V., Chen, J., Perez, F. A., Palmiter, R. D., et al. (2007). Parkin-mediated K63-linked polyubiquitination targets misfolded DJ-1 to aggresomes via binding to HDAC6. *J. Cell Biol.* 178, 1025–1038. doi:10.1083/jcb.200611128.
- Orian, A., Gonen, H., Bercovich, B., Fajerman, I., Eytan, E., Israe, A., et al. (2000). SCF b -TrCP ubiquitin ligase-mediated processing of NF- k B p105 requires phosphorylation of its C-terminus by I k B kinase. 19.
- Ossareh-Nazari, B., Bonizec, M., Cohen, M., Dokudovskaya, S., Delalande, F., Schaeffer, C., et al. (2010). Cdc48 and Ufd3, new partners of the ubiquitin protease Ubp3, are required for ribophagy. *EMBO Rep.* 11, 548–554. doi:10.1038/embor.2010.74.
- Ossareh-Nazari, B., Niño, C. A., Bengtson, M. H., Lee, J. W., Joazeiro, C. A. P., and

- Dargemont, C. (2014). Ubiquitylation by the Ltn1 E3 ligase protects 60S ribosomes from starvation-induced selective autophagy. *J. Cell Biol.* 204, 909–917. doi:10.1083/jcb.201308139.
- Otomo, C., Metlagel, Z., Takaesu, G., and Otomo, T. (2013). Structure of the human ATG12~ATG5 conjugate required for LC3 lipidation in autophagy. *Nat. Struct. Mol. Biol.* doi:10.1038/nsmb.2431.
- Palikaras, K., Lionaki, E., and Tavernarakis, N. (2015). Coordination of mitophagy and mitochondrial biogenesis during ageing in *C. elegans*. *Nature* 521, 525–528. doi:10.1038/nature14300.
- Pan, J. A., Sun, Y., Jiang, Y. P., Bott, A. J., Jaber, N., Dou, Z., et al. (2016). TRIM21 Ubiquitylates SQSTM1/p62 and Suppresses Protein Sequestration to Regulate Redox Homeostasis. *Mol. Cell* 61, 720–733. doi:10.1016/j.molcel.2016.02.007.
- Pankiv, S., Clausen, T. H., Lamark, T., Brech, A., Bruun, J. A., Outzen, H., et al. (2007). p62/SQSTM1 binds directly to Atg8/LC3 to facilitate degradation of ubiquitinated protein aggregates by autophagy*[S]. *J. Biol. Chem.* 282, 24131–24145. doi:10.1074/jbc.M702824200.
- Paul, S., Kashyap, A. K., Jia, W., He, Y. W., and Schaefer, B. C. (2012). Selective Autophagy of the Adaptor Protein Bcl10 Modulates T Cell Receptor Activation of NF-κB. *Immunity*. doi:10.1016/j.immuni.2012.04.008.
- Peth, A., Besche, H. C., and Goldberg, A. L. (2009). Ubiquitinated Proteins Activate the Proteasome by Binding to Usp14/Ubp6, which Causes 20S Gate Opening. *Mol. Cell* 36, 794–804. doi:10.1016/j.molcel.2009.11.015.
- Petroski, M. D., and Deshaies, R. J. (2005). Function and regulation of cullin-RING ubiquitin ligases. *Nat. Rev. Mol. Cell Biol.* 6, 9–20. doi:10.1038/nrm1547.
- Pichler, A., Fatouros, C., Lee, H., and Eisenhardt, N. (2017). SUMO conjugation - A mechanistic view. *Biomol. Concepts* 8, 13–36. doi:10.1515/bmc-2016-0030.
- Pickart, C. M., and Eddins, M. J. (2004). Ubiquitin: Structures, functions, mechanisms. *Biochim. Biophys. Acta - Mol. Cell Res.* 1695, 55–72. doi:10.1016/j.bbamcr.2004.09.019.
- Pinto-Fernandez, A., and Kessler, B. M. (2016). DUBbing cancer: Deubiquitylating enzymes involved in epigenetics, DNA damage and the cell cycle as therapeutic targets. *Front. Genet.* 7, 1–13. doi:10.3389/fgene.2016.00133.
- Platta, H. W., Abrahamsen, H., Thoresen, S. B., and Stenmark, H. (2012). Nedd4-dependent lysine-11-linked polyubiquitination of the tumour suppressor Beclin 1.

- Biochem. J.* 441, 399–406. doi:10.1042/BJ20111424.
- Platta, H. W., El Magraoui, F., Baumer, B. E., Schlee, D., Girzalsky, W., and Erdmann, R. (2009). Pex2 and Pex12 Function as Protein-Ubiquitin Ligases in Peroxisomal Protein Import. *Mol. Cell. Biol.* 29, 5505–5516. doi:10.1128/MCB.00388-09.
- Protter, D. S. W., and Parker, R. (2016). Principles and Properties of Stress Granules. *Trends Cell Biol.* 26, 668–679. doi:10.1016/j.tcb.2016.05.004.
- Pyo, J. O., Jang, M. H., Kwon, Y. K., Lee, H. J., Jun, J. Il, Woo, H. N., et al. (2005). Essential roles of Atg5 and FADD in autophagic cell death: Dissection of autophagic cell death into vacuole formation and cell death. *J. Biol. Chem.* doi:10.1074/jbc.M413934200.
- Qing, G., Yan, P., Qu, Z., Liu, H., and Xiao, G. (2007). Hsp90 regulates processing of NF- κ B2 p100 involving protection of NF- κ B-inducing kinase (NIK) from autophagy-mediated degradation. *Cell Res.* 17, 520–530. doi:10.1038/cr.2007.47.
- Qiu, Y., Hofmann, K., Coats, J. E., Schulman, B. A., and Kaiser, S. E. (2013). Binding to E1 and E3 is mutually exclusive for the human autophagy E2 Atg3. *Protein Sci.* doi:10.1002/pro.2381.
- Randow, F., and Youle, R. J. (2014). Self and nonself: How autophagy targets mitochondria and bacteria. *Cell Host Microbe* 15, 403–411. doi:10.1016/j.chom.2014.03.012.
- Ravikumar, B., Moreau, K., Jahreiss, L., Puri, C., and Rubinsztein, D. C. (2010). Plasma membrane contributes to the formation of pre-autophagosomal structures. *Nat. Cell Biol.* doi:10.1038/ncb2078.
- Reichard, J. F., Motz, G. T., and Puga, A. (2007). Heme oxygenase-1 induction by NRF2 requires inactivation of the transcriptional repressor BACH1. *Nucleic Acids Res.* 35, 7074–7086. doi:10.1093/nar/gkm638.
- Reineke, L. C., and Lloyd, R. E. (2013). Diversion of stress granules and P-bodies during viral infection. *Virology.* doi:10.1016/j.virol.2012.11.017.
- Renna, M., Jimenez-Sanchez, M., Sarkar, S., and Rubinsztein, D. C. (2010). Chemical inducers of autophagy that enhance the clearance of mutant proteins in neurodegenerative diseases. *J. Biol. Chem.* 285, 11061–11067. doi:10.1074/jbc.R109.072181.
- Richter, B., Sliter, D. A., Herhaus, L., Stolz, A., Wang, C., Beli, P., et al. (2016). Phosphorylation of OPTN by TBK1 enhances its binding to Ub chains and promotes selective autophagy of damaged mitochondria. *Proc. Natl. Acad. Sci.*

- 113, 4039–4044. doi:10.1073/pnas.1523926113.
- Riley, B. E., Kaiser, S. E., Shaler, T. A., Ng, A. C. Y., Hara, T., Hipp, M. S., et al. (2010). Ubiquitin accumulation in autophagy-deficient mice is dependent on the Nrf2-mediated stress response pathway: A potential role for protein aggregation in autophagic substrate selection. *J. Cell Biol.* 191, 537–552. doi:10.1083/jcb.201005012.
- Rogov, V., Dötsch, V., Johansen, T., and Kirkin, V. (2014). Interactions between Autophagy Receptors and Ubiquitin-like Proteins Form the Molecular Basis for Selective Autophagy. *Mol. Cell* 53, 167–178. doi:10.1016/j.molcel.2013.12.014.
- Rolland, T., Taşan, M., Charloteaux, B., Pevzner, S. J., Zhong, Q., Sahni, N., et al. (2014). A proteome-scale map of the human interactome network. *Cell.* doi:10.1016/j.cell.2014.10.050.
- Sakowski, E. T., Koster, S., Portal Celhay, C., Park, H. S., Shrestha, E., Hetzenecker, S. E., et al. (2015). Ubiquilin 1 Promotes IFN- γ -Induced Xenophagy of *Mycobacterium tuberculosis*. *PLoS Pathog.* 11, 1–18. doi:10.1371/journal.ppat.1005076.
- Sanchez, A. M. J., Csibi, A., Raibon, A., Cornille, K., Gay, S., Bernardi, H., et al. (2012). AMPK promotes skeletal muscle autophagy through activation of forkhead FoxO3a and interaction with Ulk1. *J. Cell. Biochem.* 113, 695–710. doi:10.1002/jcb.23399.
- Sandoval, H., Thiagarajan, P., Dasgupta, S. K., Schumacher, A., Prchal, J. T., Chen, M., et al. (2008). Essential role for Nix in autophagic maturation of erythroid cells. *Nature* 454, 232–235. doi:10.1038/nature07006.
- Sang, L., Miller, J. J., Corbit, K. C., Giles, R. H., Brauer, M. J., Otto, E. A., et al. (2011). Mapping the NPHP-JBTS-MKS protein network reveals ciliopathy disease genes and pathways. *Cell.* doi:10.1016/j.cell.2011.04.019.
- Sargent, G., Zutphen, T. Van, Shatseva, T., Zhang, L., Giovanni, V. Di, Bandsma, R., et al. (2016). PEX2 is the E3 ubiquitin ligase required for pexophagy during starvation. 214. doi:10.1083/jcb.201511034.
- Sarraf, S. A., Raman, M., Guarani-Pereira, V., Sowa, M. E., Huttlin, E. L., Gygi, S. P., et al. (2013). Landscape of the PARKIN-dependent ubiquitylome in response to mitochondrial depolarization. *Nature* 496, 372–376. doi:10.1038/nature12043.
- Sasaki, M., Sukegawa, J., Miyosawa, K., Yanagisawa, T., Ohkubo, S., and Nakahata, N. (2007). Low expression of cell-surface thromboxane A2 receptor beta-isoform

- through the negative regulation of its membrane traffic by proteasomes.
Prostaglandins Other Lipid Mediat. doi:10.1016/j.prostaglandins.2006.12.001.
- Scanlon, T. C., Gottlieb, B., Durcan, T. M., Fon, E. A., Beitel, L. K., and Trifiro, M. A. (2009). Isolation of human proteasomes and putative proteasome-interacting proteins using a novel affinity chromatography method. *Exp. Cell Res.* doi:10.1016/j.yexcr.2008.10.027.
- Schell-Steven, A., Stein, K., Amoros, M., Landgraf, C., Volkmer-Engert, R., Rottensteiner, H., et al. (2005). Identification of a novel, intraperoxisomal pex14-binding site in pex13: association of pex13 with the docking complex is essential for peroxisomal matrix protein import. *Mol. Cell. Biol.* doi:10.1128/MCB.25.8.3007-3018.2005.
- Schrader, J., Henneberg, F., Mata, R. A., Tittmann, K., Schneider, T. R., Stark, H., et al. (2016). The inhibition mechanism of human 20S proteasomes enables next-generation inhibitor design. *Science (80-.)*. doi:10.1126/science.aaf8993.
- Schwartz, A. L., and Ciechanover, A. (2009). Targeting Proteins for Destruction by the Ubiquitin System: Implications for Human Pathobiology. *Annu. Rev. Pharmacol. Toxicol.* doi:10.1146/annurev.pharmtox.051208.165340.
- Schweers, R. L., Zhang, J., Randall, M. S., Loyd, M. R., Li, W., Dorsey, F. C., et al. (2007). NIX is required for programmed mitochondrial clearance during reticulocyte maturation. *Proc. Natl. Acad. Sci. U. S. A.* 104, 19500–5. doi:10.1073/pnas.0708818104.
- Sdek, P., Ying, H., Chang, D. L. F., Qiu, W., Zheng, H., Touitou, R., et al. (2005). MDM2 promotes proteasome-dependent ubiquitin-independent degradation of retinoblastoma protein. *Mol. Cell.* doi:10.1016/j.molcel.2005.10.017.
- Seguin, S. J., Morelli, F. F., Vinet, J., Amore, D., De Biasi, S., Poletti, A., et al. (2014). Inhibition of autophagy, lysosome and VCP function impairs stress granule assembly. *Cell Death Differ.* 21, 1838–1851. doi:10.1038/cdd.2014.103.
- Selimovic, D., Porzig, B. B. O. W., El-Khattouti, A., Badura, H. E., Ahmad, M., Ghanjati, F., et al. (2013). Bortezomib/proteasome inhibitor triggers both apoptosis and autophagy-dependent pathways in melanoma cells. *Cell. Signal.* 25, 308–318. doi:10.1016/j.cellsig.2012.10.004.
- Sengupta, S., Peterson, T. R., and Sabatini, D. M. (2010). Regulation of the mTOR Complex 1 Pathway by Nutrients, Growth Factors, and Stress. *Mol. Cell* 40, 310–322. doi:10.1016/j.molcel.2010.09.026.

- Sha, Z., Schnell, H. M., Ruoff, K., and Goldberg, A. (2018). Rapid induction of p62 and GABARAPL1 upon proteasome inhibition promotes survival before autophagy activation. *J. Cell Biol.* doi:10.1083/jcb.201708168.
- Shaid, S., Brandts, C. H., Serve, H., and Dikic, I. (2013). Ubiquitination and selective autophagy. *Cell Death Differ.* 20, 21–30. doi:10.1038/cdd.2012.72.
- Shen, H., Korutla, L., Champtiaux, N., Toda, S., LaLumiere, R., Vallone, J., et al. (2007). NAC1 Regulates the Recruitment of the Proteasome Complex into Dendritic Spines. *J. Neurosci.* doi:10.1523/JNEUROSCI.1571-07.2007.
- Shi, C. S., and Kehrl, J. H. (2010). TRAF6 and A20 regulate lysine 63-linked ubiquitination of Beclin-1 to control TLR4-induced Autophagy. *Sci. Signal.* 3, 1–10. doi:10.1126/scisignal.2000751.
- Shiba-Fukushima, K., Arano, T., Matsumoto, G., Inoshita, T., Yoshida, S., Ishihama, Y., et al. (2014). Phosphorylation of Mitochondrial Polyubiquitin by PINK1 Promotes Parkin Mitochondrial Tethering. *PLoS Genet.* 10. doi:10.1371/journal.pgen.1004861.
- Shiba-Fukushima, K., Imai, Y., Yoshida, S., Ishihama, Y., Kanao, T., Sato, S., et al. (2012). PINK1-mediated phosphorylation of the Parkin ubiquitin-like domain primes mitochondrial translocation of Parkin and regulates mitophagy. *Sci. Rep.* 2, 1–8. doi:10.1038/srep01002.
- Shloush, J., Vlassov, J. E., Engson, I., Duan, S., Saridakis, V., Dhe-paganon, S., et al. (2011). Structural and functional comparison of the RING domains of two p53 E3 ligases, Mdm2 and Pirh2. *J. Biol. Chem.* 286, 4796–4808. doi:10.1074/jbc.M110.157669.
- Shpilka, T., Weidberg, H., Pietrokovski, S., and Elazar, Z. (2011). Atg8: An autophagy-related ubiquitin-like protein family. *Genome Biol.* 12. doi:10.1186/gb-2011-12-7-226.
- Smith, D. M., Chang, S. C., Park, S., Finley, D., Cheng, Y., and Goldberg, A. L. (2007). Docking of the Proteasomal ATPases' Carboxyl Termini in the 20S Proteasome's α Ring Opens the Gate for Substrate Entry. *Mol. Cell* 27, 731–744. doi:10.1016/j.molcel.2007.06.033.
- Sowter, H. M., Ratcliffe, P. J., Watson, P., Greenberg, A. H., and Harris, A. L. (2001). HIF-1-dependent regulation of hypoxic induction of the cell death factors BNIP3 and NIX in human tumors. *Cancer Res.* 61, 6669–6673. doi:10.1158/0008-5472.can-04-4130.

- Spinnenhirn, V., Farhan, H., Basler, M., Aichem, A., Canaan, A., and Groettrup, M. (2014). The ubiquitin-like modifier FAT10 decorates autophagy-targeted Salmonella and contributes to Salmonella resistance in mice. *J. Cell Sci.* 127, 4883–4893. doi:10.1242/jcs.152371.
- Sriramachandran, A. M., and Dohmen, R. J. (2014). SUMO-targeted ubiquitin ligases. *Biochim. Biophys. Acta - Mol. Cell Res.* 1843, 75–85. doi:10.1016/j.bbamcr.2013.08.022.
- Stitt, T. N., Drujan, D., Clarke, B. A., Panaro, F., Timofeyeva, Y., Kline, W. O., et al. (2004). The IGF-1/PI3K/Akt pathway prevents expression of muscle atrophy-induced ubiquitin ligases by inhibiting FOXO transcription factors. *Mol. Cell* 14, 395–403. doi:10.1016/S1097-2765(04)00211-4.
- Stolz, A., Ernst, A., and Dikic, I. (2014). Cargo recognition and trafficking in selective autophagy. *Nat. Cell Biol.* 16, 495–501. doi:10.1038/ncb2979.
- Strappazon, F., and Cecconi, F. (2015). AMBRA1-induced mitophagy: A new mechanism to cope with cancer? *Mol. Cell. Oncol.* 2, e975647. doi:10.4161/23723556.2014.975647.
- Strappazon, F., Nazio, F., Corrado, M., Cianfanelli, V., Romagnoli, A., Fimia, G. M., et al. (2015). AMBRA1 is able to induce mitophagy via LC3 binding, regardless of PARKIN and p62/SQSTM1. *Cell Death Differ.* 22, 419–432. doi:10.1038/cdd.2014.139.
- Sun, A., Li, C., Chen, R., Huang, Y., Chen, Q., Cui, X., et al. (2016). GSK-3 β controls autophagy by modulating LKB1-AMPK pathway in prostate cancer cells. *Prostate.* doi:10.1002/pros.23106.
- Sun, A., Wei, J., Childress, C., Shaw, J. H., Peng, K., Shao, G., et al. (2017). The E3 ubiquitin ligase NEDD4 is an LC3-interactive protein and regulates autophagy. *Autophagy* 13, 522–537. doi:10.1080/15548627.2016.1268301.
- Suraweera, A., Münch, C., Hanssum, A., and Bertolotti, A. (2012). Failure of amino acid homeostasis causes cell death following proteasome inhibition. *Mol. Cell* 48, 242–253. doi:10.1016/j.molcel.2012.08.003.
- Susmita Kaushik and Ana Maria Cuervo (2013). NIH Public Access. 22, 407–417. doi:10.1016/j.tcb.2012.05.006.Chaperone-mediated.
- Suvorova, E. S., Lucas, O., Weisend, C. M., Rollins, M. C. F., Merrill, G. F., Capecchi, M. R., et al. (2009). Cytoprotective Nrf2 pathway is induced in chronically Txnrd 1-deficient hepatocytes. *PLoS One* 4. doi:10.1371/journal.pone.0006158.

- Svendsen, J. M., Smogorzewska, A., Sowa, M. E., O'Connell, B. C., Gygi, S. P., Elledge, S. J., et al. (2009). Mammalian BTBD12/SLX4 Assembles A Holliday Junction Resolvase and Is Required for DNA Repair. *Cell* 138, 63–77. doi:10.1016/j.cell.2009.06.030.
- Szargel, R., Shani, V., Elghani, F. A., Mekies, L. N., Liani, E., Rott, R., et al. (2015). The PINK1, synphilin-1 and SIAH-1 complex constitutes a novel mitophagy pathway. *Hum. Mol. Genet.* 25, 3476–3490. doi:10.1093/hmg/ddw189.
- Takaesu, G., Kobayashi, T., and Yoshimura, A. (2012). TGF β -activated kinase 1 (TAK1)-binding proteins (TAB) 2 and 3 negatively regulate autophagy. *J. Biochem.* doi:10.1093/jb/mvr123.
- Tan, J. M. M., Wong, E. S. P., Dawson, V. L., Dawson, T. M., and Lim, K. L. (2008). Lysine 63-linked polyubiquitin potentially partners with p62 to promote the clearance of protein inclusions by autophagy. *Autophagy* 4, 251–253. doi:10.4161/auto.5444.
- Tanaka, Y., Guhde, G., Suter, A., Eskelinen, E. L., Hartmann, D., Lüllmann-Rauch, R., et al. (2000). Accumulation of autophagic vacuoles and cardiomyopathy LAMP-2-deficient mice. *Nature* 406, 902–906. doi:10.1038/35022595.
- Tandle, A. T., Calvani, M., Uranchimeg, B., Zahavi, D., Melillo, G., and Libutti, S. K. (2009). Endothelial monocyte activating polypeptide-II modulates endothelial cell responses by degrading hypoxia-inducible factor-1 α through interaction with PSMA7, a component of the proteasome. *Exp. Cell Res.* doi:10.1016/j.yexcr.2009.03.021.
- Tang, B., Cai, J., Sun, L., Li, Y., Qu, J., Snider, B. J., et al. (2014). Proteasome inhibitors activate autophagy involving inhibition of PI3K-Akt-mTOR pathway as an anti-oxidation defense in human RPE cells. *PLoS One* 9, 3–10. doi:10.1371/journal.pone.0103364.
- Tanida, I., Ueno, T., and Kominami, E. (2004). Human light chain 3/MAP1LC3B Is cleaved at its carboxyl-terminal Met 121 to expose Gly120 for lipidation and targeting to autophagosomal membranes. *J. Biol. Chem.* 279, 47704–47710. doi:10.1074/jbc.M407016200.
- Tannous, P., Zhu, H., Nemchenko, A., Berry, J. M., Johnstone, J. L., Shelton, J. M., et al. (2008). Intracellular protein aggregation is a proximal trigger of cardiomyocyte autophagy. *Circulation* 117, 3070–3078. doi:10.1161/CIRCULATIONAHA.107.763870.

- Tasdemir, E., Maiuri, M. C., Galluzzi, L., Vitale, I., Djavaheri-Mergny, M., D'Amelio, M., et al. (2008a). Regulation of autophagy by cytoplasmic p53. *Nat. Cell Biol.* 10, 676–687. doi:10.1038/ncb1730.
- Tasdemir, E., Maiuri, M. C., Morselli, E., Criollo, A., D'Amelio, M., Djavaheri-Mergny, M., et al. (2008b). A dual role of p53 in the control of autophagy. *Autophagy*. doi:10.4161/auto.6486.
- Tattoli, I., Sorbara, M. T., Vuckovic, D., Ling, A., Soares, F., Carneiro, L. A. M., et al. (2012). Amino acid starvation induced by invasive bacterial pathogens triggers an innate host defense program. *Cell Host Microbe* 11, 563–575. doi:10.1016/j.chom.2012.04.012.
- Tattoli, I., Sorbara, M. T., Yang, C., Tooze, S. A., Philpott, D. J., and Girardin, S. E. (2013). Listeria phospholipases subvert host autophagic defenses by stalling pre-autophagosomal structures. *EMBO J.* 32, 3066–3078. doi:10.1038/emboj.2013.234.
- Thompson, J. W., Nagel, J., Hoving, S., Gerrits, B., Bauer, A., Thomas, J. R., et al. (2014). Quantitative Lys- ϵ -Gly-Gly (diGly) proteomics coupled with inducible RNAi reveals ubiquitin-mediated proteolysis of DNA damage-inducible transcript 4 (DDIT4) by the E3 Ligase HUWE1. *J. Biol. Chem.* doi:10.1074/jbc.M114.573352.
- Thurston, T. L. M. (2009). The tbk1 adaptor and autophagy receptor ndp52 restricts the proliferation of ubiquitin-coated bacteria. *Nat. Immunol.* 10, 1215–1222. doi:10.1038/ni.1800.
- Till, A., Lakhani, R., Burnett, S. F., and Subramani, S. (2012). Pexophagy: The selective degradation of peroxisomes. *Int. J. Cell Biol.* 2012. doi:10.1155/2012/512721.
- Tipler, C. P., Hutchon, S. P., Hendil, K., Tanaka, K., Fishel, S., and Mayer, R. J. (1997). Purification and characterization of 26S proteasomes from human and mouse spermatozoa. *Mol. Hum. Reprod.* doi:10.1093/molehr/3.12.1053.
- Tomkinson, B., and Lindås, A. C. (2005). Tripeptidyl-peptidase II: A multi-purpose peptidase. *Int. J. Biochem. Cell Biol.* 37, 1933–1937. doi:10.1016/j.biocel.2005.02.009.
- Tourrière, H., Chebli, K., Zekri, L., Courselaud, B., Blanchard, J. M., Bertrand, E., et al. (2003). The RasGAP-associated endoribonuclease G3BP assembles stress granules. *J. Cell Biol.* doi:10.1083/jcb.200212128.

- Tracy, K., Dibling, B. C., Spike, B. T., Knabb, J. R., Schumacker, P., and Macleod, K. F. (2007). BNIP3 Is an RB/E2F Target Gene Required for Hypoxia-Induced Autophagy. *Mol. Cell. Biol.* 27, 6229–6242. doi:10.1128/MCB.02246-06.
- Trempe, J. F., Sauvé, V., Grenier, K., Seirafi, M., Tang, M. Y., Meñade, M., et al. (2013). Structure of parkin reveals mechanisms for ubiquitin ligase activation. *Science (80-.)*. 340, 1451–1455. doi:10.1126/science.1237908.
- Tripathi, D. N., Zhang, J., Jing, J., Dere, R., and Lyn, C. (2016). A new role for ATM in selective autophagy of peroxisomes (pexophagy). *Autophagy* 12, 711–712. doi:10.1080/15548627.2015.1123375.
- Turcu Francisca E. Reyes, Ventii Karen H., W. K. D. (2010). NIH Public Access. *Annu Rev Biochem*, 363–397. doi:10.1146/annurev.biochem.78.082307.091526.Regulation.
- Van Humbeeck, C., Cornelissen, T., Hofkens, H., Mandemakers, W., Gevaert, K., De Strooper, B., et al. (2011). Parkin Interacts with Ambra1 to Induce Mitophagy. *J. Neurosci.* 31, 10249–10261. doi:10.1523/JNEUROSCI.1917-11.2011.
- Varjosalo, M., Keskitalo, S., VanDrogen, A., Nurkkala, H., Vichalkovski, A., Aebersold, R., et al. (2013). The Protein Interaction Landscape of the Human CMGC Kinase Group. *Cell Rep.* doi:10.1016/j.celrep.2013.03.027.
- Verma, R., Oania, R. S., Kolawa, N. J., and Deshaies, R. J. (2013). Cdc48/p97 promotes degradation of aberrant nascent polypeptides bound to the ribosome. *Elife* 2013, 1–17. doi:10.7554/eLife.00308.
- Vijay-Kumar, S., Bugg, C. E., Wilkinson, K. D., Vierstra, R. D., Hatfield, P. M., and Cook, W. J. (1987). Comparison of the three-dimensional structures of human, yeast, and oat ubiquitin. *J. Biol. Chem.*
- Vinayagam, A., Stelzl, U., Foulle, R., Plassmann, S., Zenkner, M., Timm, J., et al. (2011). A directed protein interaction network for investigating intracellular signal transduction. *Sci. Signal.* doi:10.1126/scisignal.2001699.
- Walter, K. M., Schönenberger, M. J., Trötz Müller, M., Horn, M., Elsässer, H. P., Moser, A. B., et al. (2014). Hif-2 α Promotes degradation of mammalian peroxisomes by selective autophagy. *Cell Metab.* 20, 882–897. doi:10.1016/j.cmet.2014.09.017.
- Wan, C., Borgeson, B., Phanse, S., Tu, F., Drew, K., Clark, G., et al. (2015). Panorama of ancient metazoan macromolecular complexes. *Nature*. doi:10.1038/nature14877.
- Wandel, M. P., Pathe, C., Werner, E. I., Ellison, C. J., Boyle, K. B., von der Malsburg,

- A., et al. (2017). GBPs Inhibit Motility of *Shigella flexneri* but Are Targeted for Degradation by the Bacterial Ubiquitin Ligase IpaH9.8. *Cell Host Microbe* 22, 507–518.e5. doi:10.1016/j.chom.2017.09.007.
- Wanders, R. J. A., Waterham, H. R., and Ferdinandusse, S. (2016). Metabolic Interplay between Peroxisomes and Other Subcellular Organelles Including Mitochondria and the Endoplasmic Reticulum. *Front. Cell Dev. Biol.* 3, 1–15. doi:10.3389/fcell.2015.00083.
- Wang, J., Huo, K., Ma, L., Tang, L., Li, D., Huang, X., et al. (2011). Toward an understanding of the protein interaction network of the human liver. *Mol. Syst. Biol.* doi:10.1038/msb.2011.67.
- Wang, W., and Subramani, S. (2017). Role of PEX5 ubiquitination in maintaining peroxisome dynamics and homeostasis. 4101. doi:10.1080/15384101.2017.1376149.
- Wang, X., Chen, C. F., Baker, P. R., Chen, P. L., Kaiser, P., and Huang, L. (2007). Mass spectrometric characterization of the affinity-purified human 26S proteasome complex. *Biochemistry*. doi:10.1021/bi061994u.
- Wang, X. J., Yu, J., Wong, S. H., Cheng, A. S., Chan, F. K., Ng, S. S., et al. (2013). A novel crosstalk between two major protein degradation systems. *Autophagy* 9, 1500–1508. doi:10.4161/auto.25573.
- Wang, Y., Serricchio, M., Jauregui, M., Shanbhag, R., Stoltz, T., Di Paolo, C. T., et al. (2015). Deubiquitinating enzymes regulate PARK2-mediated mitophagy. *Autophagy* 11, 595–606. doi:10.1080/15548627.2015.1034408.
- Wang, Z., Zhu, W. G., and Xu, X. (2017). *Ubiquitin-like modifications in the DNA damage response*. Elsevier B.V. doi:10.1016/j.mrfmmm.2017.07.001.
- Waris, S., Wilce, M. C. J., and Wilce, J. A. (2014). RNA recognition and stress granule formation by TIA proteins. *Int. J. Mol. Sci.* 15, 23377–23388. doi:10.3390/ijms151223377.
- Watanabe, N., Madaule, P., Reid, T., Ishizaki, T., Watanabe, G., Kakizuka, A., et al. (1997). p140mDia, a mammalian homolog of *Drosophila* diaphanous, is a target protein for Rho small GTPase and is a ligand for profilin. *EMBO J.* doi:10.1093/emboj/16.11.3044.
- Wauer, T., and Komander, D. (2013). Structure of the human Parkin ligase domain in an autoinhibited state. *EMBO J.* 32, 2099–2112. doi:10.1038/emboj.2013.125.
- Wei, S. J., Williams, J. G., Dang, H., Darden, T. A., Betz, B. L., Humble, M. M., et al.

- (2008). Identification of a Specific Motif of the DSS1 Protein Required for Proteasome Interaction and p53 Protein Degradation. *J. Mol. Biol.* doi:10.1016/j.jmb.2008.08.044.
- Weidberg, H., Shvets, E., and Elazar, Z. (2011). Biogenesis and Cargo Selectivity of Autophagosomes. *Annu. Rev. Biochem.* 80, 125–156. doi:10.1146/annurev-biochem-052709-094552.
- Welchman, R. L., Gordon, C., and Mayer, R. J. (2005). Ubiquitin and ubiquitin-like proteins as multifunctional signals. *Nat. Rev. Mol. Cell Biol.* 6, 599–609. doi:10.1038/nrm1700.
- Wild, P., Farhan, H., McEwan, D. G., Wagner, S., Rogov, V. V., Brady, N. R., et al. (2011). Phosphorylation of the autophagy receptor optineurin restricts Salmonella growth. *Science (80-.)*. 333, 228–233. doi:10.1126/science.1205405.
- Wileman, T. (2013). Autophagy as a defence against intracellular pathogens. *Essays Biochem.* 55, 153–163. doi:10.1042/bse0550153.
- Wong, Y. C., and Holzbaur, E. L. F. (2014). Optineurin is an autophagy receptor for damaged mitochondria in parkin-mediated mitophagy that is disrupted by an ALS-linked mutation. *Proc. Natl. Acad. Sci.* 111, E4439–E4448. doi:10.1073/pnas.1405752111.
- Woods, N. T., Mesquita, R. D., Sweet, M., Carvalho, M. A., Li, X., Liu, Y., et al. (2012). Charting the landscape of tandem BRCT domain-mediated protein interactions. *Sci. Signal.* doi:10.1126/scisignal.2002255.
- Wooten, M. W., Geetha, T., Babu, J. R., Seibenhener, M. L., Peng, J., Cox, N., et al. (2008). Essential role of sequestosome 1/p62 in regulating accumulation of Lys63-ubiquitinated proteins. *J. Biol. Chem.* 283, 6783–6789. doi:10.1074/jbc.M709496200.
- Wu, W. K. K., Wu, Y. C., Yu, L., Li, Z. J., Sung, J. J. Y., and Cho, C. H. (2008). Induction of autophagy by proteasome inhibitor is associated with proliferative arrest in colon cancer cells. *Biochem. Biophys. Res. Commun.* 374, 258–263. doi:10.1016/j.bbrc.2008.07.031.
- Wyant, G. A., Abu-Remaileh, M., Frenkel, E. M., Laqtom, N. N., Dharamdasani, V., Lewis, C. A., et al. (2018). Nufip1 is a ribosome receptor for starvation-induced ribophagy. *Science (80-.)*. 360, 751–758. doi:10.1126/science.aar2663.
- Xia, P., Wang, S., Du, Y., Zhao, Z., Shi, L., Sun, L., et al. (2013). WASH inhibits autophagy through suppression of Beclin 1 ubiquitination. *EMBO J.* 32, 2685–

2696. doi:10.1038/emboj.2013.189.
- Xiong, X., Tao, R., DePinho, R. A., and Dong, X. C. (2012). The autophagy-related gene 14 (Atg14) is regulated by forkhead box O transcription factors and circadian rhythms and plays a critical role in hepatic autophagy and lipid metabolism. *J. Biol. Chem.* 287, 39107–39114. doi:10.1074/jbc.M112.412569.
- Xu, C., Fan, C. D., and Wang, X. (2015). Regulation of Mdm2 protein stability and the p53 response by NEDD4-1 E3 ligase. *Oncogene* 34, 342–350. doi:10.1038/onc.2013.557.
- Xu, C., Feng, K., Zhao, X., Huang, S., Cheng, Y., Qian, L., et al. (2014). Regulation of autophagy by E3 ubiquitin ligase RNF216 through BECN1 ubiquitination. *Autophagy* 10, 2239–2250. doi:10.4161/15548627.2014.981792.
- Xu, J., Wang, S., Viollet, B., and Zou, M. H. (2012). Regulation of the proteasome by AMPK in endothelial cells: The role of O-GlcNAc transferase (OGT). *PLoS One* 7. doi:10.1371/journal.pone.0036717.
- Xu, P., Das, M., Reilly, J., and Davis, R. J. (2011). JNK regulates FoxO-dependent autophagy in neurons. *Genes Dev.* 25, 310–322. doi:10.1101/gad.1984311.
- Yamano, K., and Youle, R. J. (2013). PINK1 is degraded through the N-end rule pathway. *Autophagy* 9, 1758–1769. doi:10.4161/auto.24633.
- Yamashita, S. ichi, Abe, K., Tatemichi, Y., and Fujiki, Y. (2014). The membrane peroxin PEX3 induces peroxisome-ubiquitination-linked pexophagy. *Autophagy* 10, 1549–1564. doi:10.4161/auto.29329.
- Yang, L., Tang, Z., Zhang, H., Kou, W., Lu, Z., Li, X., et al. (2013). PSMA7 directly interacts with NOD1 and regulates its function. *Cell. Physiol. Biochem.* doi:10.1159/000350113.
- Yao, T. P. (2010). The role of ubiquitin in autophagy-dependent protein aggregate processing. *Genes and Cancer* 1, 779–786. doi:10.1177/1947601910383277.
- Yao, T., Song, L., Jin, J., Cai, Y., Takahashi, H., Swanson, S. K., et al. (2008). Distinct Modes of Regulation of the Uch37 Deubiquitinating Enzyme in the Proteasome and in the Ino80 Chromatin-Remodeling Complex. *Mol. Cell.* doi:10.1016/j.molcel.2008.08.027.
- Yau, R., and Rape, M. (2016). The increasing complexity of the ubiquitin code. *Nat. Cell Biol.* 18, 579–586. doi:10.1038/ncb3358.
- Yi, P., Feng, Q., Amazit, L., Lonard, D. M., Tsai, S. Y., Tsai, M. J., et al. (2008). Atypical Protein Kinase C Regulates Dual Pathways for Degradation of the

- Oncogenic Coactivator SRC-3/AIB1. *Mol. Cell.* doi:10.1016/j.molcel.2007.12.030.
- Ying, H., Zheng, H., Scott, K., Wiedemeyer, R., Yan, H., Lim, C., et al. (2010). Mig-6 controls EGFR trafficking and suppresses gliomagenesis. *Proc. Natl. Acad. Sci.* doi:10.1073/pnas.0914930107.
- Yonashiro, R., Ishido, S., Kyo, S., Fukuda, T., Goto, E., Matsuki, Y., et al. (2006). A novel mitochondrial ubiquitin ligase plays a critical role in mitochondrial dynamics. *EMBO J.* 25, 3618–3626. doi:10.1038/sj.emboj.7601249.
- Yonekawa, T., Gamez, G., Kim, J., Choon Tan, A., Thorburn, J., Gump, J., et al. (2015). RIP1 negatively regulates basal autophagic flux through TFEB to control sensitivity to apoptosis. *EMBO Rep.* 16, 700–708. doi:10.15252/embr.
- Yoshii, S. R., Kishi, C., Ishihara, N., and Mizushima, N. (2011). Parkin mediates proteasome-dependent protein degradation and rupture of the outer mitochondrial membrane. *J. Biol. Chem.* 286, 19630–19640. doi:10.1074/jbc.M110.209338.
- Young, A. R. J. (2006). Starvation and ULK1-dependent cycling of mammalian Atg9 between the TGN and endosomes. *J. Cell Sci.* 119, 3888–3900. doi:10.1242/jcs.03172.
- Yousefi, S., Perozzo, R., Schmid, I., Ziemiecki, A., Schaffner, T., Scapozza, L., et al. (2006). Calpain-mediated cleavage of Atg5 switches autophagy to apoptosis. *Nat. Cell Biol.* doi:10.1038/ncb1482.
- Yu, L., Chen, Y., and Tooze, S. A. (2018). Autophagy pathway: Cellular and molecular mechanisms. *Autophagy.* doi:10.1080/15548627.2017.1378838.
- Yuan, F., Ma, Y., You, P., Lin, W., Lu, H., Yu, Y., et al. (2013). A novel role of proteasomal $\beta 1$ subunit in tumorigenesis. *Biosci. Rep.* doi:10.1042/BSR20130013.
- Yuan, G., Khan, S. A., Luo, W., Nanduri, J., Semenza, G. L., and Prabhakar, N. R. (2011). Hypoxia-inducible factor 1 mediates increased expression of NADPH oxidase-2 in response to intermittent hypoxia. *J. Cell. Physiol.* doi:10.1002/jcp.22640.
- Yun, J., Puri, R., Yang, H., Lizzio, M. A., Wu, C., Sheng, Z. H., et al. (2014). MUL1 acts in parallel to the PINK1/parkin pathway in regulating mitofusin and compensates for loss of PINK1/parkin. *Elife* 2014, 1–26. doi:10.7554/eLife.01958.001.
- Zhang, H., Bosch-Marce, M., Shimoda, L. A., Yee, S. T., Jin, H. B., Wesley, J. B., et al. (2008). Mitochondrial autophagy is an HIF-1-dependent adaptive metabolic response to hypoxia. *J. Biol. Chem.* 283, 10892–10903.

- doi:10.1074/jbc.M800102200.
- Zhang, J., Tripathi, D. N., Jing, J., Alexander, A., Kim, J., Powell, R. T., et al. (2015a). ATM functions at the peroxisome to induce pexophagy in response to ROS. *Nat. Cell Biol.* 17, 1259–1269. doi:10.1038/ncb3230.
- Zhang, T., Dong, K., Liang, W., Xu, D., Xia, H., Geng, J., et al. (2015b). G-protein Coupled Receptors Regulate Autophagy by ZBTB16-mediated Ubiquitination and Proteasomal Degradation of Adaptor Protein Atg14L. *Elife* 2015, 1–19. doi:10.7554/eLife.06734.
- Zhang, X., Bogunovic, D., Payelle-Brogard, B., Francois-Newton, V., Speer, S. D., Yuan, C., et al. (2015c). Human intracellular ISG15 prevents interferon- α/β over-amplification and auto-inflammation. *Nature*. doi:10.1038/nature13801.
- Zhang, X., and Qian, S.-B. (2011). Chaperone-mediated hierarchical control in targeting misfolded proteins to aggresomes. *Mol. Biol. Cell* 22, 3277–3288. doi:10.1091/mbc.E11-05-0388.
- Zhao, C., Denison, C., Huibregtse, J. M., Gygi, S., and Krug, R. M. (2005). Human ISG15 conjugation targets both IFN-induced and constitutively expressed proteins functioning in diverse cellular pathways. *Proc. Natl. Acad. Sci.* doi:10.1073/pnas.0504754102.
- Zhao, J., Brault, J. J., Schild, A., Cao, P., Sandri, M., Schiaffino, S., et al. (2007). FoxO3 Coordinately Activates Protein Degradation by the Autophagic/Lysosomal and Proteasomal Pathways in Atrophying Muscle Cells. *Cell Metab.* 6, 472–483. doi:10.1016/j.cmet.2007.11.004.
- Zhao, J., and Goldberg, A. L. (2016). Coordinate regulation of autophagy and the ubiquitin proteasome system by MTOR. *Autophagy* 12, 1967–1970. doi:10.1080/15548627.2016.1205770.
- Zhao, J., Zhai, B., Gygi, S. P., and Goldberg, A. L. (2015). mTOR inhibition activates overall protein degradation by the ubiquitin proteasome system as well as by autophagy. *Proc. Natl. Acad. Sci.* 112, 15790–15797. doi:10.1073/pnas.1521919112.
- Zheng, Y. T., Shahnazari, S., Brech, A., Lamark, T., Johansen, T., and Brumell, J. H. (2009). The Adaptor Protein p62/SQSTM1 Targets Invading Bacteria to the Autophagy Pathway. *J. Immunol.* 183, 5909–5916. doi:10.4049/jimmunol.0900441.
- Zhu, K., Dunner, K., and McConkey, D. J. (2010). Proteasome inhibitors activate

- autophagy as a cytoprotective response in human prostate cancer cells. *Oncogene*. doi:10.1038/onc.2009.343.
- Zhu, Y., Massen, S., Terenzio, M., Lang, V., Chen-Lindner, S., Eils, R., et al. (2013). Modulation of serines 17 and 24 in the LC3-interacting region of Bnip3 determines pro-survival mitophagy versus apoptosis. *J. Biol. Chem.* 288, 1099–1113. doi:10.1074/jbc.M112.399345.
- Abdelmohsen, K., Srikantan, S., Yang, X., Lal, A., Kim, H. H., Kuwano, Y., et al. (2009). Ubiquitin-mediated proteolysis of HuR by heat shock. *EMBO J.* doi:10.1038/emboj.2009.67.
- Aerbajinai, W., Giattina, M., Lee, Y. T., Raffeld, M., and Miller, J. L. (2003). The proapoptotic factor Nix is coexpressed with Bcl-xL during terminal erythroid differentiation. *Blood* 102, 712–717. doi:10.1182/blood-2002-11-3324.
- Altieri, D. C. (2010). Survivin and IAP proteins in cell-death mechanisms. *Biochem. J.* doi:10.1042/BJ20100814.
- Ambivero, C. T., Cilenti, L., Main, S., and Zervos, A. S. (2014). Mulan E3 ubiquitin ligase interacts with multiple E2 conjugating enzymes and participates in mitophagy by recruiting GABARAP. *Cell. Signal.* 26, 2921–2929. doi:10.1016/j.cellsig.2014.09.004.
- An, H., and Harper, J. W. (2018). Systematic analysis of ribophagy in human cells reveals bystander flux during selective autophagy. *Nat. Cell Biol.* 20, 135–143. doi:10.1038/s41556-017-0007-x.
- Antonioli, M., Albiero, F., Nazio, F., Vescovo, T., Perdomo, A. B., Corazzari, M., et al. (2014a). AMBRA1 interplay with cullin E3 Ubiquitin ligases regulates autophagy dynamics. *Dev. Cell* 31, 734–746. doi:10.1016/j.devcel.2014.11.013.
- Antonioli, M., Ciccocanti, F., Dengjel, J., and Fimia, G. M. (2017). “Methods to Study the BECN1 Interactome in the Course of Autophagic Responses,” in *Methods in Enzymology* doi:10.1016/bs.mie.2016.09.069.
- Antonioli, M., Di Rienzo, M., Piacentini, M., Fimia, G. M., Albiero, F., Nazio, F., et al. (2014b). AMBRA1 interplay with cullin E3 Ubiquitin ligases regulates autophagy dynamics. *Dev. Cell* 31, 734–746. doi:10.1016/j.devcel.2014.11.013.
- Apcher, G.-S., Maitland, J., Dawson, S., Sheppard, P., and Mayer, R. J. (2004). The alpha4 and alpha7 subunits and assembly of the 20S proteasome. *FEBS Lett.* doi:10.1016/j.febslet.2004.05.067.

- Apcher, G. S., Heink, S., Zantopf, D., Kloetzel, P. M., Schmid, H. P., Mayer, R. J., et al. (2003). Human immunodeficiency virus-1 Tat protein interacts with distinct proteasomal alpha and beta subunits. *FEBS Lett.* doi:S0014579303010251 [pii] ET - 2003/10/11.
- Arora, V., Cheung, H. H., Plenchette, S., Micali, O. C., Liston, P., and Korneluk, R. G. (2007). Degradation of survivin by the X-linked Inhibitor of Apoptosis (XIAP)-XAF1 complex. *J. Biol. Chem.* 282, 26202–26209. doi:10.1074/jbc.M700776200.
- Banning, A., Deubel, S., Kluth, D., Zhou, Z., and Brigelius-Flohe, R. (2005a). The GI-GPx Gene Is a Target for Nrf2. *Mol. Cell. Biol.* 25, 4914–4923. doi:10.1128/MCB.25.12.4914-4923.2005.
- Banning, A., Deubel, S., Kluth, D., Zhou, Z., and Brigelius-Flohe, R. (2005b). The GI-GPx Gene Is a Target for Nrf2. *Mol. Cell. Biol.* 25, 4914–4923. doi:10.1128/MCB.25.12.4914-4923.2005.
- Bansal, M., Moharir, S. C., Sailasree, S. P., Sirohi, K., Sudhakar, C., Sarathi, D. P., et al. (2018). Optineurin promotes autophagosome formation by recruiting the autophagy-related Atg12-5-16L1 complex to phagophores containing the Wipi2 protein. *J. Biol. Chem.* doi:10.1074/jbc.M117.801944.
- Behrends, C., and Harper, J. W. (2011). Constructing and decoding unconventional ubiquitin chains. *Nat. Struct. Mol. Biol.* 18, 520–528. doi:10.1038/nsmb.2066.
- Behrends, C., Sowa, M. E., Gygi, S. P., and Harper, J. W. (2010). Network organization of the human autophagy system. *Nature.* doi:10.1038/nature09204.
- Bellot, G., Garcia-Medina, R., Gounon, P., Chiche, J., Roux, D., Pouyssegur, J., et al. (2009). Hypoxia-Induced Autophagy Is Mediated through Hypoxia-Inducible Factor Induction of BNIP3 and BNIP3L via Their BH3 Domains. *Mol. Cell. Biol.* 29, 2570–2581. doi:10.1128/MCB.00166-09.
- Benanti, J. A. (2012). Coordination of cell growth and division by the ubiquitin-proteasome system. *Semin. Cell Dev. Biol.* 23, 492–498. doi:10.1016/j.semcdb.2012.04.005.
- Bennett, E. J., Rush, J., Gygi, S. P., and Harper, J. W. (2010). Dynamics of cullin-RING ubiquitin ligase network revealed by systematic quantitative proteomics. *Cell.* doi:10.1016/j.cell.2010.11.017.
- Bhat, K. P., Yan, S., Wang, C.-E., Li, S., and Li, X.-J. (2014). Differential ubiquitination and degradation of huntingtin fragments modulated by ubiquitin-protein ligase E3A. *Proc. Natl. Acad. Sci.* 111, 5706–5711.

doi:10.1073/pnas.1402215111.

- Bingol, B., Tea, J. S., Phu, L., Reichelt, M., Bakalarski, C. E., Song, Q., et al. (2014). The mitochondrial deubiquitinase USP30 opposes parkin-mediated mitophagy. *Nature* 510, 370–375. doi:10.1038/nature13418.
- Birgisdottir, Á. B., Lamark, T., Johansen, T., Alemu, E. A., Lamark, T., Torgersen, K. M., et al. (2013). The LIR motif - crucial for selective autophagy. *J. Cell Sci.* 126, 3237–47. doi:10.1242/jcs.126128.
- Blomen, V. A., Májek, P., Jae, L. T., Bigenzahn, J. W., Nieuwenhuis, J., Staring, J., et al. (2015). Gene essentiality and synthetic lethality in haploid human cells. *Science* (80-.). doi:10.1126/science.aac7557.
- Bloom, J., Peschiaroli, A., DeMartino, G., and Pagano, M. (2006). Modification of Cull1 regulates its association with proteasomal subunits. *Cell Div.* doi:10.1186/1747-1028-1-5.
- Bodemann, B. O., Orvedahl, A., Cheng, T., Ram, R. R., Ou, Y. H., Formstecher, E., et al. (2011). RalB and the exocyst mediate the cellular starvation response by direct activation of autophagosome assembly. *Cell.* doi:10.1016/j.cell.2010.12.018.
- Bogunovic, D., Byun, M., Durfee, L. A., Abhyankar, A., Sanal, O., Mansouri, D., et al. (2012). Mycobacterial disease and impaired IFN- γ immunity in humans with inherited ISG15 deficiency. *Science* (80-.). 337, 1684–1688. doi:10.1126/science.1224026.
- Boldt, K., Van Reeuwijk, J., Lu, Q., Koutroumpas, K., Nguyen, T. M. T., Texier, Y., et al. (2016). An organelle-specific protein landscape identifies novel diseases and molecular mechanisms. *Nat. Commun.* doi:10.1038/ncomms11491.
- Bousquet-Dubouch, M.-P., Baudalet, E., Guérin, F., Matondo, M., Uttenweiler-Joseph, S., Burlet-Schiltz, O., et al. (2009). Affinity Purification Strategy to Capture Human Endogenous Proteasome Complexes Diversity and to Identify Proteasome-interacting Proteins. *Mol. Cell. Proteomics.* doi:10.1074/mcp.M800193-MCP200.
- Bowman, C. J., Ayer, D. E., and Dynlacht, B. D. (2014). Foxk proteins repress the initiation of starvation-induced atrophy and autophagy programs. *Nat. Cell Biol.* 16, 1202–1214. doi:10.1038/ncb3062.
- Braschi, E., Zunino, R., and McBride, H. M. (2009). MAPL is a new mitochondrial SUMO E3 ligase that regulates mitochondrial fission. *EMBO Rep.* 10, 748–754. doi:10.1038/embor.2009.86.
- Buchan, J. R., Kolaitis, R. M., Taylor, J. P., and Parker, R. (2013). XEukaryotic stress

- granules are cleared by autophagy and Cdc48/VCP function. *Cell* 153, 1461–1474. doi:10.1016/j.cell.2013.05.037.
- Budanov, A. V, and Karin, M. (2009). The p53-regulated Sestrin gene products inhibit mTOR signaling. *October* 134, 451–460. doi:10.1016/j.cell.2008.06.028.
- Byron, A., Humphries, J. D., Craig, S. E., Knight, D., and Humphries, M. J. (2012). Proteomic analysis of $\alpha 4\beta 1$ integrin adhesion complexes reveals α -subunit-dependent protein recruitment. *Proteomics*. doi:10.1002/pmic.201100487.
- Carvalho, A. F., Pinto, M. P., Grou, C. P., Alencastre, I. S., Fransen, M., Sá-Miranda, C., et al. (2007). Ubiquitination of mammalian Pex5p, the peroxisomal import receptor. *J. Biol. Chem.* 282, 31267–31272. doi:10.1074/jbc.M706325200.
- Cassavaugh, J. M., Hale, S. A., Wellman, T. L., Howe, A. K., Wong, C., and Lounsbury, K. M. (2011). Negative regulation of HIF-1 α by an FBW7-mediated degradation pathway during hypoxia. *J. Cell. Biochem.* doi:10.1002/jcb.23321.
- Chen, C., Pore, N., Behrooz, A., Ismail-Beigi, F., and Maity, A. (2001). Regulation of glut1 mRNA by hypoxia-inducible factor-1: Interaction between H-ras and hypoxia. *J. Biol. Chem.* doi:10.1074/jbc.M010144200.
- Chen, D., Fan, W., Lu, Y., Ding, X., Chen, S., and Zhong, Q. (2012). A Mammalian Autophagosome Maturation Mechanism Mediated by TECPR1 and the Atg12-Atg5 Conjugate. *Mol. Cell.* doi:10.1016/j.molcel.2011.12.036.
- Chen, M., Chen, Z., Wang, Y., Tan, Z., Zhu, C., Li, Y., et al. (2016). Mitophagy receptor FUNDC1 regulates mitochondrial dynamics and mitophagy. *Autophagy* 12, 689–702. doi:10.1080/15548627.2016.1151580.
- Chen, Y., and Klionsky, D. J. (2011). The regulation of autophagy - unanswered questions. *J. Cell Sci.* 124, 161–170. doi:10.1242/jcs.064576.
- Chen, Y., Yang, L.-N., Cheng, L., Tu, S., Guo, S.-J., Le, H.-Y., et al. (2013). Bcl2-associated Athanogene 3 Interactome Analysis Reveals a New Role in Modulating Proteasome Activity. *Mol. Cell. Proteomics*. doi:10.1074/mcp.M112.025882.
- Chen, Z.-H., Cao, J.-F., Zhou, J.-S., Liu, H., Che, L.-Q., Mizumura, K., et al. (2014). Interaction of caveolin-1 with ATG12-ATG5 system suppresses autophagy in lung epithelial cells. *AJP Lung Cell. Mol. Physiol.* doi:10.1152/ajplung.00268.2013.
- Chen, Z., Liu, L., Cheng, Q., Li, Y., Wu, H., Zhang, W., et al. (2017). Mitochondrial E3 ligase MARCH5 regulates FUNDC1 to fine-tune hypoxic mitophagy. *EMBO Rep.* 18, 495–509. doi:10.15252/embr.201643309.
- Cho, S., Choi, Y. J., Kim, J. M., Jeong, S. T., Kim, J. H., Kim, S. H., et al. (2001).

- Binding and regulation of HIF-1 α by a subunit of the proteasome complex, PSMA7. *FEBS Lett.* doi:10.1016/S0014-5793(01)02499-1.
- Christianson, J. C., Olzmann, J. A., Shaler, T. A., Sowa, M. E., Bennett, E. J., Richter, C. M., et al. (2012). Defining human ERAD networks through an integrative mapping strategy. *Nat. Cell Biol.* doi:10.1038/ncb2383.
- Cianfanelli, V., De Zio, D., Di Bartolomeo, S., Nazio, F., Strappazzon, F., and Cecconi, F. (2015). Ambra1 at a glance. *J. Cell Sci.* 128, 2003–2008. doi:10.1242/jcs.168153.
- Ciani, B., Layfield, R., Cavey, J. R., Sheppard, P. W., and Searle, M. S. (2003). Structure of the ubiquitin-associated domain of p62 (SQSTM1) and implications for mutations that cause Paget's disease of bone. *J. Biol. Chem.* 278, 37409–37412. doi:10.1074/jbc.M307416200.
- Ciechanover, A. (2012). Intracellular protein degradation: From a vague idea through the lysosome and the ubiquitin-proteasome system and onto human diseases and drug targeting. *ASH Educ. B.* 2006. doi:10.1182/asheducation-2006.1.1.
- Clague, M. J., Heride, C., and Urbé, S. (2015). The demographics of the ubiquitin system. *Trends Cell Biol.* 25, 417–426. doi:10.1016/j.tcb.2015.03.002.
- Clausen, T. H., Lamark, T., Isakson, P., Finley, K., Larsen, K. B., Brech, A., et al. (2010). p62/SQSTM1 and ALFY interact to facilitate the formation of p62 bodies/ALIS and their degradation by autophagy. *Autophagy* 6, 330–344. doi:10.4161/auto.6.3.11226.
- Claverol, S., Burlet-Schiltz, O., Girbal-Neuhauser, E., Gairin, J. E., and Monsarrat, B. (2002). Mapping and Structural Dissection of Human 20 S Proteasome Using Proteomic Approaches. *Mol. Cell. Proteomics.* doi:10.1074/mcp.M200030-MCP200.
- Codogno, P., and Meijer, A. J. (2006). Atg5: More than an autophagy factor. *Nat. Cell Biol.* doi:10.1038/ncb1006-1045.
- Cohen-kaplan, V., Livneh, I., Avni, N., Fabre, B., Ziv, T., and Tae, Y. (2016). autophagy of the mammalian 26S proteasome. doi:10.1073/pnas.1615455113.
- Collins, C. A., De Mazière, A., Van Dijk, S., Carlsson, F., Klumperman, J., and Brown, E. J. (2009). Atg5-independent sequestration of ubiquitinated mycobacteria. *PLoS Pathog.* 5. doi:10.1371/journal.ppat.1000430.
- Collins, G. A., and Goldberg, A. L. (2017). The Logic of the 26S Proteasome. *Cell* 169, 792–806. doi:10.1016/j.cell.2017.04.023.

- Copetti, T., Bertoli, C., Dalla, E., Demarchi, F., and Schneider, C. (2009). p65/RelA Modulates BECN1 Transcription and Autophagy. *Mol. Cell. Biol.* 29, 2594–2608. doi:10.1128/MCB.01396-08.
- Cornelissen, T., Haddad, D., Wauters, F., Van Humbeeck, C., Mandemakers, W., Koentjoro, B., et al. (2014). The deubiquitinase USP15 antagonizes Parkin-mediated mitochondrial ubiquitination and mitophagy. *Hum. Mol. Genet.* 23, 5227–5242. doi:10.1093/hmg/ddu244.
- Crighton, D., Wilkinson, S., O’Prey, J., Syed, N., Smith, P., Harrison, P. R., et al. (2006). DRAM, a p53-Induced Modulator of Autophagy, Is Critical for Apoptosis. *Cell.* doi:10.1016/j.cell.2006.05.034.
- Cuervo, A. M., Palmer, A., Rivett, A. J., and Knecht, E. (1995). Degradation of Proteasomes by Lysosomes in Rat Liver. *Eur. J. Biochem.* 227, 792–800. doi:10.1111/j.1432-1033.1995.0792p.x.
- Dan, H. C., and Baldwin, A. S. (2008). Differential Involvement of I B Kinases and in Cytokine- and Insulin-Induced Mammalian Target of Rapamycin Activation Determined by Akt. *J. Immunol.* 180, 7582–7589. doi:10.4049/jimmunol.180.11.7582.
- Deas, E., Plun-Favreau, H., Gandhi, S., Desmond, H., Kjaer, S., Loh, S. H. Y., et al. (2011). PINK1 cleavage at position A103 by the mitochondrial protease PARL. *Hum. Mol. Genet.* 20, 867–879. doi:10.1093/hmg/ddq526.
- Delgado, M. E., Dyck, L., Laussmann, M. A., and Rehm, M. (2014). Modulation of apoptosis sensitivity through the interplay with autophagic and proteasomal degradation pathways. *Cell Death Dis.* 5, e1011-8. doi:10.1038/cddis.2013.520.
- Demishtein, A., Fraiberg, M., Berko, D., Tirosh, B., Elazar, Z., and Navon, A. (2017). SQSTM1 / p62-mediated autophagy compensates for loss of proteasome polyubiquitin recruiting capacity. 8627. doi:10.1080/15548627.2017.1356549.
- Dengjel, J., Akimov, V., Olsen, J. V, Bunkenborg, J., Mann, M., Blagoev, B., et al. (2007). Quantitative proteomic assessment of very early cellular signaling events. *Nat. Biotechnol.* doi:10.1038/nbt1301.
- Dengjel, J., Høyer-Hansen, M., Nielsen, M. O., Eisenberg, T., Harder, L. M., Schandorff, S., et al. (2012). Identification of Autophagosome-associated Proteins and Regulators by Quantitative Proteomic Analysis and Genetic Screens. *Mol. Cell. Proteomics.* doi:10.1074/mcp.M111.014035.
- Deosaran, E., Larsen, K. B., Hua, R., Sargent, G., Wang, Y., Kim, S., et al. (2013).

- NBR1 acts as an autophagy receptor for peroxisomes. *J. Cell Sci.* 126, 939–952. doi:10.1242/jcs.114819.
- Deribe, Y. L., Wild, P., Chandrashaker, A., Curak, J., Schmidt, M. H. H., Kalaidzidis, Y., et al. (2009). Regulation of epidermal growth factor receptor trafficking by lysine deacetylase hdac6. *Sci. Signal.* doi:10.1126/scisignal.2000576.
- Dikic, I. (2017). Proteasomal and Autophagic Degradation Systems. *Annu. Rev. Biochem.* 86, 193–224. doi:10.1146/annurev-biochem-061516-044908.
- Dikic, I., and Bremm, A. (2014). DUBs counteract parkin for efficient mitophagy. *EMBO J.* 33, 2442–3. doi:10.15252/embj.201490101.
- Ding, W.-X., Ni, H.-M., Li, M., Liao, Y., Chen, X., Stolz, D. B., et al. (2010). Nix is critical to two distinct phases of mitophagy: reactive oxygen species (ROS)-mediated autophagy induction and Parkin-ubiquitin-p62-mediated mitochondria priming. *J. Biol. Chem.* doi:10.1074/jbc.M110.119537.
- Djavaheri-Mergny, M., Amelotti, M., Mathieu, J., Besançon, F., Bauvy, C., Souquère, S., et al. (2006). NF- κ B activation represses tumor necrosis factor- α -induced autophagy. *J. Biol. Chem.* 281, 30373–30382. doi:10.1074/jbc.M602097200.
- Dong, J., Chen, W., Welford, A., and Wandinger-Ness, A. (2004). The proteasome α -subunit XAPC7 interacts specifically with Rab7 and late endosomes. *J. Biol. Chem.* doi:10.1074/jbc.M401022200.
- Dooley, H. C., Razi, M., Polson, H. E. J., Girardin, S. E., Wilson, M. I., and Tooze, S. A. (2014). WIPI2 Links LC3 Conjugation with PI3P, Autophagosome Formation, and Pathogen Clearance by Recruiting Atg12-5-16L1. *Mol. Cell.* doi:10.1016/j.molcel.2014.05.021.
- Drissi, R., Dubois, M.-L., Douziech, M., and Boisvert, F.-M. (2015). Quantitative Proteomics Reveals Dynamic Interactions of the Minichromosome Maintenance Complex (MCM) in the Cellular Response to Etoposide Induced DNA Damage. *Mol. Cell. Proteomics.* doi:10.1074/mcp.M115.048991.
- Du, H., Kim, S., Hur, Y.-S., Lee, M.-S., Lee, S.-H., and Cheon, C.-I. (2015). A cytosolic thioredoxin acts as a molecular chaperone for peroxisome matrix proteins as well as antioxidant in peroxisome. *Mol. Cells.* doi:10.14348/molcells.2015.2277.
- Durcan, T. M., and Fon, E. A. (2015). USP8 and PARK2/parkin-mediated mitophagy. *Autophagy* 11, 428–429. doi:10.1080/15548627.2015.1009794.
- Durcan, T. M., Tang, M. Y., Perusse, J. R., Dashti, E. A., Aguilera, M. A., McLelland,

- G.-L., et al. (2014). USP8 regulates mitophagy by removing K6-linked ubiquitin conjugates from parkin. *EMBO J.* 33, 2473–2491. doi:10.15252/embj.201489729.
- Dzierzak, E., and Philipsen, S. (2013). Erythropoiesis : Development and Differentiation. 1–16.
- Egan, D. F., Shackelford, D. B., Mihaylova, M. M., Gelino, S., Kohnz, R. A., Mair, W., et al. (2011). Phosphorylation of ULK1 (hATG1) by AMP-activated protein kinase connects energy sensing to mitophagy. *Science (80-)*. 331, 456–461. doi:10.1126/science.1196371.
- Elliott, P. R., Leske, D., Hrdinka, M., Bagola, K., Fiil, B. K., McLaughlin, S. H., et al. (2016). SPATA2 Links CYLD to LUBAC, Activates CYLD, and Controls LUBAC Signaling. *Mol. Cell*. doi:10.1016/j.molcel.2016.08.001.
- Emdal, K. B., Pedersen, A. K., Bekker-Jensen, D. B., Tsafou, K. P., Horn, H., Lindner, S., et al. (2015). Temporal proteomics of NGF-TrkA signaling identifies an inhibitory role for the E3 ligase Cbl-b in neuroblastoma cell differentiation. *Sci. Signal*. doi:10.1126/scisignal.2005769.
- Erbil, S., Oral, O., Mitou, G., Kig, C., Durmaz-Timucin, E., Guven-Maiorov, E., et al. (2016). RACK1 is an interaction partner of ATG5 and a novel regulator of autophagy. *J. Biol. Chem.* doi:10.1074/jbc.M115.708081.
- Ertych, N., Stolz, A., Valerius, O., Braus, G. H., and Bastians, H. (2016). *CHK2 – BRCA1* tumor-suppressor axis restrains oncogenic Aurora-A kinase to ensure proper mitotic microtubule assembly. *Proc. Natl. Acad. Sci.* doi:10.1073/pnas.1525129113.
- Esteban-Martínez, L., Sierra-Filardi, E., McGreal, R. S., Salazar-Roa, M., Mariño, G., Seco, E., et al. (2017). Programmed mitophagy is essential for the glycolytic switch during cell differentiation. *EMBO J.* 36, 1688–1706. doi:10.15252/embj.201695916.
- Ewing, R. M., Chu, P., Elisma, F., Li, H., Taylor, P., Climie, S., et al. (2007). Large-scale mapping of human protein-protein interactions by mass spectrometry. *Mol. Syst. Biol.* doi:10.1038/msb4100134.
- Fan, T., Huang, Z., Wang, W., Zhang, B., Xu, Y., Mao, Z., et al. (2018). Proteasome inhibition promotes autophagy and protects from endoplasmic reticulum stress in rat alveolar macrophages exposed to hypoxia-reoxygenation injury. 1–11. doi:10.1002/jcp.26516.
- Farny, N. G., Kedersha, N. L., and Silver, P. A. (2009). Metazoan stress granule

- assembly is mediated by P-eIF2a-dependent and -independent mechanisms. 1814–1821. doi:10.1261/rna.1684009.initiation.
- Feng, Y., Longo, D. L., and Ferris, D. K. (2001). Polo-like kinase interacts with proteasomes and regulates their activity. *Cell Growth Differ.*
- Feng, Z., Hu, W., De Stanchina, E., Teresky, A. K., Jin, S., Lowe, S., et al. (2007). The regulation of AMPK β 1, TSC2, and PTEN expression by p53: Stress, cell and tissue specificity, and the role of these gene products in modulating the IGF-1-AKT-mTOR pathways. *Cancer Res.* 67, 3043–3053. doi:10.1158/0008-5472.CAN-06-4149.
- Filimonenko, M., Isakson, P., Finley, K. D., Anderson, M., Jeong, H., Melia, T. J., et al. (2010). The Selective Macroautophagic Degradation of Aggregated Proteins Requires the PI3P-Binding Protein Alfy. *Mol. Cell* 38, 265–279. doi:10.1016/j.molcel.2010.04.007.
- Finley, D. (2009). Recognition and Processing of Ubiquitin-Protein Conjugates by the Proteasome. *Annu. Rev. Biochem.* doi:10.1146/annurev.biochem.78.081507.101607.
- Fiskin, E., Bionda, T., Dikic, I., and Behrends, C. (2016). Global Analysis of Host and Bacterial Ubiquitinome in Response to Salmonella Typhimurium Infection. *Mol. Cell* 62, 967–981. doi:10.1016/j.molcel.2016.04.015.
- Flugel, D., Gorlach, a, and Kietzmann, T. (2012a). GSK-3beta regulates cell growth, migration, and angiogenesis via Fbw7 and USP28-dependent degradation of HIF-1alpha. *Blood* 119, 1292–1301. doi:10.1182/blood-2011-08-375014 [pii]r10.1182/blood-2011-08-375014.
- Flugel, D., Gorlach, a, and Kietzmann, T. (2012b). GSK-3beta regulates cell growth, migration, and angiogenesis via Fbw7 and USP28-dependent degradation of HIF-1alpha. *Blood* 119, 1292–1301. doi:10.1182/blood-2011-08-375014 [pii]r10.1182/blood-2011-08-375014.
- Foster, M. W., Thompson, J. W., Forrester, M. T., Sha, Y., McMahon, T. J., Bowles, D. E., et al. (2013). Proteomic analysis of the NOS2 interactome in human airway epithelial cells. *Nitric Oxide.* doi:10.1016/j.niox.2013.02.079.
- Fracchiolla, D., Sawa-Makarska, J., Zens, B., de Ruiter, A., Zaffagnini, G., Brezovich, A., et al. (2016). Mechanism of cargo-directed Atg8 conjugation during selective autophagy. *Elife.* doi:10.7554/eLife.18544.
- Franco, L. H., Nair, V. R., Scharn, C. R., Xavier, R. J., Torrealba, J. R., Shiloh, M. U.,

- et al. (2017). The Ubiquitin Ligase Smurf1 Functions in Selective Autophagy of Mycobacterium tuberculosis and Anti-tuberculous Host Defense. *Cell Host Microbe*. doi:10.1016/j.chom.2016.11.002.
- Fricke, B., Heink, S., Steffen, J., Kloetzel, P. M., and Krüger, E. (2007). The proteasome maturation protein POMP facilitates major steps of 20S proteasome formation at the endoplasmic reticulum. *EMBO Rep*. doi:10.1038/sj.embor.7401091.
- Froment, C., Uttenweiler-Joseph, S., Bousquet-Dubouch, M. P., Matondo, M., Borges, J. P., Esmenjaud, C., et al. (2005). A quantitative proteomic approach using two-dimensional gel electrophoresis and isotope-coded affinity tag labeling for studying human 20S proteasome heterogeneity. in *Proteomics* doi:10.1002/pmic.200401281.
- Fu, M., St-Pierre, P., Shankar, J., Wang, P. T. C., Joshi, B., and Nabi, I. R. (2013). Regulation of mitophagy by the Gp78 E3 ubiquitin ligase. *Mol. Biol. Cell* 24, 1153–1162. doi:10.1091/mbc.E12-08-0607.
- Fu, W., Ma, Q., Chen, L., Li, P., Zhang, M., Ramamoorthy, S., et al. (2009). MDM2 acts downstream of p53 as an E3 ligase to promote FOXO ubiquitination and degradation. *J. Biol. Chem.* 284, 13987–14000. doi:10.1074/jbc.M901758200.
- Fuertes, G., Villarroya, A., and Knecht, E. (2003). Role of proteasomes in the degradation of short-lived proteins in human fibroblasts under various growth conditions. *Int. J. Biochem. Cell Biol.* 35, 651–664. doi:10.1016/S1357-2725(02)00382-5.
- Fujii, K., Kitabatake, M., Sakata, T., and Ohno, M. (2012). 40S subunit dissociation and proteasome-dependent RNA degradation in nonfunctional 25S rRNA decay. *EMBO J.* 31, 2579–2589. doi:10.1038/emboj.2012.85.
- Fujita, N., Morita, E., Itoh, T., Tanaka, A., Nakaoka, M., Osada, Y., et al. (2013). Recruitment of the autophagic machinery to endosomes during infection is mediated by ubiquitin. *J. Cell Biol.* 203, 115–128. doi:10.1083/jcb.201304188.
- Funderburk, S. F., Wang, Q. J., and Yue, Z. (2010). The Beclin 1-VPS34 complex - at the crossroads of autophagy and beyond. *Trends Cell Biol.* doi:10.1016/j.tcb.2010.03.002.
- Gamerding, M., Kaya, A. M., Wolfrum, U., Clement, A. M., and Behl, C. (2011). BAG3 mediates chaperone-based aggresome-targeting and selective autophagy of misfolded proteins. *EMBO Rep.* 12, 149–156. doi:10.1038/embor.2010.203.

- Gammoh, N., Florey, O., Overholtzer, M., and Jiang, X. (2013). Interaction between FIP200 and ATG16L1 distinguishes ULK1 complex-dependent and-independent autophagy. *Nat. Struct. Mol. Biol.* doi:10.1038/nsmb.2475.
- Gao, F., Chen, D., Si, J., Hu, Q., Qin, Z., Fang, M., et al. (2015). The mitochondrial protein BNIP3L is the substrate of PARK2 and mediates mitophagy in PINK1/PARK2 pathway. *Hum. Mol. Genet.* 24, 2528–2538. doi:10.1093/hmg/ddv017.
- Gao, Y., Lecker, S., Post, M. J., Hietaranta, A. J., Li, J., Volk, R., et al. (2000). Inhibition of ubiquitin-proteasome pathway-mediated I kappa B alpha degradation by a naturally occurring antibacterial peptide. *J. Clin. Invest.* doi:10.1172/JCI9826.
- Gao, Z., Gammoh, N., Wong, P. M., Erdjument-Bromage, H., Tempst, P., and Jiang, X. (2010). Processing of autophagic protein LC3 by the 20S proteasome. *Autophagy.* doi:10.4161/auto.6.1.10928.
- Garrett, H., Thompson, R., Harris, J. W., and Brody, J. P. (2004). Post-translationally modified S12, absent in transformed breast epithelial cells, is not associated with the 26S proteasome and is induced by proteasome inhibitor. *Int. J. Cancer.* doi:10.1002/ijc.20261.
- Ge, P., Zhang, J., Wang, X., Meng, F., Li, W., Luan, Y., et al. (2009). Inhibition of autophagy induced by proteasome inhibition increases cell death in human SHG-44 glioma cells. 1046–1052. doi:10.1038/aps.2009.71.
- Geisler, S., Holmström, K. M., Skujat, D., Fiesel, F. C., Rothfuss, O. C., Kahle, P. J., et al. (2010). PINK1/Parkin-mediated mitophagy is dependent on VDAC1 and p62/SQSTM1. *Nat. Cell Biol.* 12, 119–131. doi:10.1038/ncb2012.
- Giannone, R. J., McDonald, H. W., Hurst, G. B., Shen, R. F., Wang, Y., and Liu, Y. (2010). The protein network surrounding the human telomere repeat binding factors TRF1, TRF2, and POT1. *PLoS One.* doi:10.1371/journal.pone.0012407.
- Glotzer, M., Murray, A. W., and Kirschner, M. W. (1991). Cyclin is degraded by the ubiquitin pathway. *Nature* 349, 132–138. doi:10.1038/349132a0.
- Goodall, M. L., Fitzwalter, B. E., Zahedi, S., Wu, M., Rodriguez, D., Mulcahy-Levy, J. M., et al. (2016). The Autophagy Machinery Controls Cell Death Switching between Apoptosis and Necroptosis. *Dev. Cell.* doi:10.1016/j.devcel.2016.04.018.
- Griffin, T. A., Nandi, D., Cruz, M., Fehling, H. J., Kaer, L. V, Monaco, J. J., et al. (1998). Immunoproteasome assembly: cooperative incorporation of interferon gamma (IFN-gamma)-inducible subunits. *J. Exp. Med.* 187, 97–104.

doi:10.1084/jem.187.1.97.

- Groll, M., and Huber, R. (2003). Substrate access and processing by the 20S proteasome core particle. *Int. J. Biochem. Cell Biol.* 35, 606–616. doi:10.1016/S1357-2725(02)00390-4.
- Groll, M., and Huber, R. (2004). Inhibitors of the eukaryotic 20S proteasome core particle: A structural approach. *Biochim. Biophys. Acta - Mol. Cell Res.* 1695, 33–44. doi:10.1016/j.bbamcr.2004.09.025.
- Grou, C. P., Pinto, M. P., Mendes, A. V., Domingues, P., and Azevedo, J. E. (2015). The de novo synthesis of ubiquitin: Identification of deubiquitinases acting on ubiquitin precursors. *Sci. Rep.* 5, 1–16. doi:10.1038/srep12836.
- Gutierrez, M. G., Master, S. S., Singh, S. B., Taylor, G. A., Colombo, M. I., and Deretic, V. (2004). Autophagy is a defense mechanism inhibiting BCG and Mycobacterium tuberculosis survival in infected macrophages. *Cell* 119, 753–766. doi:10.1016/j.cell.2004.11.038.
- Hamazaki, J., Sasaki, K., Kawahara, H., Hisanaga, S. -i., Tanaka, K., and Murata, S. (2007). Rpn10-Mediated Degradation of Ubiquitinated Proteins Is Essential for Mouse Development. *Mol. Cell. Biol.* doi:10.1128/MCB.00509-07.
- Hanada, T., Noda, N. N., Satomi, Y., Ichimura, Y., Fujioka, Y., Takao, T., et al. (2007). The Atg12-Atg5 conjugate has a novel E3-like activity for protein lipidation in autophagy. *J. Biol. Chem.* 282, 37298–37302. doi:10.1074/jbc.C700195200.
- Hara, K., Yonezawa, K., Weng, Q. P., Kozlowski, M. T., Belham, C., and Avruch, J. (1998). Amino acid sufficiency and mTOR regulate p70 S6 kinase and eIF-4E BP1 through a common effector mechanism. *J. Biol. Chem.* doi:10.1074/jbc.273.23.14484.
- Hara, T., Nakamura, K., Matsui, M., Yamamoto, A., Nakahara, Y., Suzuki-Migishima, R., et al. (2006). Suppression of basal autophagy in neural cells causes neurodegenerative disease in mice. *Nature* 441, 885–889. doi:10.1038/nature04724.
- Hasson, S. A., Kane, L. A., Yamano, K., Huang, C. H., Sliter, D. A., Buehler, E., et al. (2013). High-content genome-wide RNAi screens identify regulators of parkin upstream of mitophagy. *Nature* 504, 291–295. doi:10.1038/nature12748.
- Havugimana, P. C., Hart, G. T., Nepusz, T., Yang, H., Turinsky, A. L., Li, Z., et al. (2012). A census of human soluble protein complexes. *Cell.* doi:10.1016/j.cell.2012.08.011.

- He, M., Zhou, Z., Shah, A. A., Zou, H., Tao, J., Chen, Q., et al. (2016). The emerging role of deubiquitinating enzymes in genomic integrity, diseases, and therapeutics. *Cell Biosci.* 6, 1–15. doi:10.1186/s13578-016-0127-1.
- Heath, R. J., Goel, G., Baxt, L. A., Rush, J. S., Mohanan, V., Paulus, G. L. C., et al. (2016). RNF166 Determines Recruitment of Adaptor Proteins during Antibacterial Autophagy. *Cell Rep.* doi:10.1016/j.celrep.2016.11.005.
- Hein, M. Y., Hubner, N. C., Poser, I., Cox, J., Nagaraj, N., Toyoda, Y., et al. (2015). A Human Interactome in Three Quantitative Dimensions Organized by Stoichiometries and Abundances. *Cell.* doi:10.1016/j.cell.2015.09.053.
- Heinemeyer, W., Ramos, P. C., and Dohmen, R. J. (2004). Ubiquitin-proteasome system. *Cell. Mol. Life Sci.* doi:10.1007/s00018-004-4130-z.
- Hendriks, I. A., D'Souza, R. C. J., Yang, B., Verlaan-De Vries, M., Mann, M., and Vertegaal, A. C. O. (2014). Uncovering global SUMOylation signaling networks in a site-specific manner. *Nat. Struct. Mol. Biol.* 21, 927–936. doi:10.1038/nsmb.2890.
- Hendriks, I. A., and Vertegaal, A. C. O. (2016). A comprehensive compilation of SUMO proteomics. *Nat. Rev. Mol. Cell Biol.* 17, 581–595. doi:10.1038/nrm.2016.81.
- Heo, J. M., Ordureau, A., Paulo, J. A., Rinehart, J., and Harper, J. W. (2015). The PINK1-PARKIN Mitochondrial Ubiquitylation Pathway Drives a Program of OPTN/NDP52 Recruitment and TBK1 Activation to Promote Mitophagy. *Mol. Cell* 60, 7–20. doi:10.1016/j.molcel.2015.08.016.
- Herhaus, L., and Dikic, I. (2015). Expanding the ubiquitin code through post-translational modification. *EMBO Rep.* 16, 1071–1083. doi:10.15252/embr.201540891.
- Hershko, A. (1983). Ubiquitin: Roles in protein modification and breakdown. *Cell.* doi:10.1016/0092-8674(83)90131-9.
- Hershko, A. (2005). The ubiquitin system for protein degradation and some of its roles in the control of the cell-division cycle (Nobel Lecture). *Angew. Chemie - Int. Ed.* doi:10.1002/anie.200501724.
- Hershko, A., and Ciechanover, A. (1998). The ubiquitin system. *Annu. Rev. Biochem.* doi:10.1146/annurev.biochem.67.1.425.
- Higgins, R., Gendron, J. M., Rising, L., Mak, R., Webb, K., Kaiser, S. E., et al. (2015). The Unfolded Protein Response Triggers Site-Specific Regulatory Ubiquitylation

- of 40S Ribosomal Proteins. *Mol. Cell* 59, 35–49.
doi:10.1016/j.molcel.2015.04.026.
- Hirano, Y., Hayashi, H., Iemura, S. ichiro, Hendil, K. B., Niwa, S. ichiro, Kishimoto, T., et al. (2006). Cooperation of Multiple Chaperones Required for the Assembly of Mammalian 20S Proteasomes. *Mol. Cell*. doi:10.1016/j.molcel.2006.11.015.
- Hochstrasser, M. (2009). Origin and function of ubiquitin-like proteins. *Nature* 458, 422–429. doi:10.1038/nature07958.
- Honda, S., Arakawa, S., Nishida, Y., Yamaguchi, H., Ishii, E., and Shimizu, S. (2014). Ulk1-mediated Atg5-independent macroautophagy mediates elimination of mitochondria from embryonic reticulocytes. *Nat. Commun.* 5, 1–13.
doi:10.1038/ncomms5004.
- Honsho, M., Yamashita, S. ichi, and Fujiki, Y. (2016). Peroxisome homeostasis: Mechanisms of division and selective degradation of peroxisomes in mammals. *Biochim. Biophys. Acta - Mol. Cell Res.* 1863, 984–991.
doi:10.1016/j.bbamcr.2015.09.032.
- Huang, H., Regan, K. M., Wang, F., Wang, D., Smith, D. I., van Deursen, J. M. A., et al. (2005). Skp2 inhibits FOXO1 in tumor suppression through ubiquitin-mediated degradation. *Proc. Natl. Acad. Sci.* 102, 1649–1654.
doi:10.1073/pnas.0406789102.
- Huang, H., and Tindall, D. J. (2011). Regulation of FOXO protein stability via ubiquitination and proteasome degradation. *Biochim. Biophys. Acta - Mol. Cell Res.* doi:10.1016/j.bbamcr.2011.01.007.
- Huang, L., Kinnucan, E., Wang, G., Beaudenon, S., Howley, P. M., Huibregtse, J. M., et al. (1999). Structure of an E6AP-UbcH7 complex: Insights into ubiquitination by the E2-E3 enzyme cascade. *Science (80-.)*. doi:10.1126/science.286.5443.1321.
- Huett, A., Heath, R. J., Begun, J., Sassi, S. O., Baxt, L. A., Vyas, J. M., et al. (2012). The LRR and RING domain protein LRSAM1 is an E3 ligase crucial for ubiquitin-dependent autophagy of intracellular salmonella typhimurium. *Cell Host Microbe* 12, 778–790. doi:10.1016/j.chom.2012.10.019.
- Humphries, J. D., Byron, A., Bass, M. D., Craig, S. E., Pinney, J. W., Knight, D., et al. (2009). Proteomic analysis of integrin-associated complexes identifies RCC2 as a dual regulator of Rac1 and Arf6. *Sci. Signal.* doi:10.1126/scisignal.2000396.
- Huttlin, E. L., Bruckner, R. J., Paulo, J. A., Cannon, J. R., Ting, L., Baltier, K., et al. (2017). Architecture of the human interactome defines protein communities and

- disease networks. *Nature*. doi:10.1038/nature22366.
- Huttlin, E. L., Ting, L., Bruckner, R. J., Gebreab, F., Gygi, M. P., Szpyt, J., et al. (2015). The BioPlex Network: A Systematic Exploration of the Human Interactome. *Cell*. doi:10.1016/j.cell.2015.06.043.
- Hwang, S. P., and Lee, D. H. (2017). Autophagy mediates SUMO-induced degradation of a polyglutamine protein ataxin-3. *Animal Cells Syst. (Seoul)*. 21, 169–176. doi:10.1080/19768354.2017.1330765.
- Ichimura, Y., Kumanomidou, T., Sou, Y. S., Mizushima, T., Ezaki, J., Ueno, T., et al. (2008). Structural basis for sorting mechanism of p62 in selective autophagy. *J. Biol. Chem.* 283, 22847–22857. doi:10.1074/jbc.M802182200.
- Iioka, H., Iemura, S. I., Natsume, T., and Kinoshita, N. (2007). Wnt signalling regulates paxillin ubiquitination essential for mesodermal cell motility. *Nat. Cell Biol.* doi:10.1038/ncb1607.
- Ikeda, K., Nakano, R., Uraoka, M., Nakagawa, Y., Koide, M., Katsume, A., et al. (2009a). Identification of ARIA regulating endothelial apoptosis and angiogenesis by modulating proteasomal degradation of cIAP-1 and cIAP-2. *Proc. Natl. Acad. Sci.* doi:10.1073/pnas.0806780106.
- Ikeda, Y., DeMartino, G. N., Brown, M. S., Lee, J. N., Goldstein, J. L., and Ye, J. (2009b). Regulated endoplasmic reticulum-associated degradation of a polytopic protein: p97 recruits proteasomes to Insig-1 before extraction from membranes. *J. Biol. Chem.* doi:10.1074/jbc.M109.044875.
- Ishii, K., Noda, M., Yagi, H., and Thammaporn, R. (2015). Disassembly of the self-assembled, double-ring structure of proteasome $\alpha 7$ homo-tetradecamer by $\alpha 6$. *Nat. Publ. Gr.* doi:10.1038/srep18167.
- Ishimura, R., Tanaka, K., and Komatsu, M. (2014). Dissection of the role of p62/Sqstm1 in activation of Nrf2 during xenophagy. *FEBS Lett.* 588, 822–828. doi:10.1016/j.febslet.2014.01.045.
- Ito, C., Saito, Y., Nozawa, T., Fujii, S., Sawa, T., Inoue, H., et al. (2013). Endogenous nitrated nucleotide is a key mediator of autophagy and innate defense against bacteria. *Mol. Cell* 52, 794–804. doi:10.1016/j.molcel.2013.10.024.
- Itoh, T., Fujita, N., Kanno, E., Yamamoto, A., Yoshimori, T., and Fukuda, M. (2008). Golgi-resident small GTPase Rab33B interacts with Atg16L and modulates autophagosome formation. *Mol. Biol. Cell*. doi:10.1091/mbc.E07-12-1231.
- Iwata, A., Riley, B. E., Johnston, J. A., and Kopito, R. R. (2005). HDAC6 and

- microtubules are required for autophagic degradation of aggregated Huntingtin. *J. Biol. Chem.* 280, 40282–40292. doi:10.1074/jbc.M508786200.
- Jaakkola, P., Jaakkola, P., Mole, D. R., Tian, Y., Kriegsheim, A. Von, Hebestreit, H. F., et al. (2014). Targeting of HIF- α to the von Hippel – Lindau Ubiquitylation Complex by O₂-Regulated Prolyl Hydroxylation. 468. doi:10.1126/science.1059796.
- Jager, S. (2004). Role for Rab7 in maturation of late autophagic vacuoles. *J. Cell Sci.* 117, 4837–4848. doi:10.1242/jcs.01370.
- Jain, A., Lamark, T., Sjøttem, E., Larsen, K. B., Awuh, J. A., Øvervatn, A., et al. (2010). p62/SQSTM1 is a target gene for transcription factor NRF2 and creates a positive feedback loop by inducing antioxidant response element-driven gene transcription. *J. Biol. Chem.* 285, 22576–22591. doi:10.1074/jbc.M110.118976.
- Jana, N. R., Dikshit, P., Goswami, A., Kotliarova, S., Murata, S., Tanaka, K., et al. (2005). Co-chaperone CHIP associates with expanded polyglutamine protein and promotes their degradation by proteasomes. *J. Biol. Chem.* 280, 11635–11640. doi:10.1074/jbc.M412042200.
- Jayarapu, K., and Griffin, T. A. (2004). Protein-protein interactions among human 20S proteasome subunits and proteasomelin. *Biochem. Biophys. Res. Commun.* doi:10.1016/j.bbrc.2003.12.119.
- Jayarapu, K., and Griffin, T. A. (2007). Differential intra-proteasome interactions involving standard and immunosubunits. *Biochem. Biophys. Res. Commun.* doi:10.1016/j.bbrc.2007.05.011.
- Jia, Y., Song, T., Wei, C., Ni, C., Zheng, Z., Xu, Q., et al. (2009). Negative Regulation of MAVS-Mediated Innate Immune Response by PSMA7. *J. Immunol.* doi:10.4049/jimmunol.0901646.
- Jiang, L., Hara-kuge, S., Yamashita, S., and Fujiki, Y. (2015a). Peroxin Pex14p is the key component for coordinated autophagic degradation of mammalian peroxisomes by direct binding to LC3-II. 36–49. doi:10.1111/gtc.12198.
- Jiang, S., Park, D. W., Gao, Y., Ravi, S., Darley-Usmar, V., Abraham, E., et al. (2015b). Participation of proteasome-ubiquitin protein degradation in autophagy and the activation of AMP-activated protein kinase. *Cell. Signal.* doi:10.1016/j.cellsig.2015.02.024.
- Jin, S. M., Lazarou, M., Wang, C., Kane, L. A., Narendra, D. P., and Youle, R. J. (2010). Mitochondrial membrane potential regulates PINK1 import and proteolytic

- destabilization by PARL. *J. Cell Biol.* 191, 933–942. doi:10.1083/jcb.201008084.
- Jin, S., Tian, S., Chen, Y., Zhang, C., Xie, W., Xia, X., et al. (2016). USP19 modulates autophagy and antiviral immune responses by deubiquitinating Beclin-1. *EMBO J.* 35, 866–880. doi:10.15252/emboj.201593596.
- Johnston, J. A., Ward, C. L., and Kopito, R. R. (2012). A Cellular Response to Misfolded Proteins Aggregates : *Cell* 143, 1883–1898. doi:10.1083/jcb.143.7.1883.
- Ju, J. S., Miller, S. E., Hanson, P. I., and Weihl, C. C. (2008). Impaired protein aggregate handling and clearance underlie the pathogenesis of p97/VCP-associated disease. *J. Biol. Chem.* 283, 30289–30299. doi:10.1074/jbc.M805517200.
- Juenemann, K., Schipper-Krom, S., Wiemhoefer, A., Kloss, A., Sanz, A. S., and Reits, E. A. J. (2013). Expanded polyglutamine-containing N-terminal huntingtin fragments are entirely degraded by mammalian proteasomes. *J. Biol. Chem.* 288, 27068–27084. doi:10.1074/jbc.M113.486076.
- Kabeya, Y. (2004). LC3, GABARAP and GATE16 localize to autophagosomal membrane depending on form-II formation. *J. Cell Sci.* 117, 2805–2812. doi:10.1242/jcs.01131.
- Kane, L. A., Lazarou, M., Fogel, A. I., Li, Y., Yamano, K., Sarraf, S. A., et al. (2014). PINK1 phosphorylates ubiquitin to activate parkin E3 ubiquitin ligase activity. *J. Cell Biol.* 205, 143–153. doi:10.1083/jcb.201402104.
- Kang, Y.-A., Sanalkumar, R., O’Geen, H., Linnemann, A. K., Chang, C.-J., Bouhassira, E. E., et al. (2012). Autophagy Driven by a Master Regulator of Hematopoiesis. *Mol. Cell Biol.* 32, 226–239. doi:10.1128/MCB.06166-11.
- Kato, S., Ding, J., Pisch, E., Jhala, U. S., and Du, K. (2008). COP1 functions as a FoxO1 ubiquitin E3 ligase to regulate FoxO1-mediated gene expression. *J. Biol. Chem.* 283, 35464–35473. doi:10.1074/jbc.M801011200.
- Kaushik, S., and Cuervo, A. M. (2018). The coming of age of chaperone-mediated autophagy. *Nat. Rev. Mol. Cell Biol.* 2018. doi:10.1038/s41580-018-0001-6.
- Kawaguchi, Y., Kovacs, J. J., McLaurin, A., Vance, J. M., Ito, A., and Yao, T. P. (2003). The deacetylase HDAC6 regulates aggresome formation and cell viability in response to misfolded protein stress. *Cell* 115, 727–738. doi:10.1016/S0092-8674(03)00939-5.
- Kazlauskaitė, A., Kondapalli, C., Gourlay, R., Campbell, D. G., Ritorto, M. S., Hofmann, K., et al. (2014). Parkin is activated by PINK1-dependent

- phosphorylation of ubiquitin at Ser⁶⁵. *Biochem. J.* 460, 127–141.
doi:10.1042/BJ20140334.
- Kedersha, N., Cho, M. R., Li, W., Yacono, P. W., Chen, S., Gilks, N., et al. (2000). Dynamic shuttling of TIA-1 accompanies the recruitment of mRNA to mammalian stress granules. *J. Cell Biol.* 151, 1257–1268. doi:10.1083/jcb.151.6.1257.
- Kedersha, N., Panas, M. D., Achorn, C. A., Lyons, S., Tisdale, S., Hickman, T., et al. (2016). G3BP-Caprin1-USP10 complexes mediate stress granule condensation and associate with 40S subunits. *J. Cell Biol.* 212, 845–860.
doi:10.1083/jcb.201508028.
- Kedersha, N., Stoecklin, G., Ayodele, M., Yacono, P., Lykke-Andersen, J., Fitzler, M. J., et al. (2005). Stress granules and processing bodies are dynamically linked sites of mRNP remodeling. *J. Cell Biol.* doi:10.1083/jcb.200502088.
- Kenzelmann Broz, D., Mello, S. S., Biegging, K. T., Jiang, D., Dusek, R. L., Brady, C. A., et al. (2013). Global genomic profiling reveals an extensive p53-regulated autophagy program contributing to key p53 responses. *Genes Dev.*
doi:10.1101/gad.212282.112.
- Kırlı, K., Karaca, S., Dehne, H. J., Samwer, M., Pan, K. T., Lenz, C., et al. (2015). A deep proteomics perspective on CRM1-mediated nuclear export and nucleocytoplasmic partitioning. *Elife*. doi:10.7554/eLife.11466.
- Kim, J. H., Hong, S. B., Lee, J. K., Han, S., Roh, K. H., Lee, K. E., et al. (2015). Insights into autophagosome maturation revealed by the structures of ATG5 with its interacting partners. *Autophagy*. doi:10.4161/15548627.2014.984276.
- Kim, J. W., Tchernyshyov, I., Semenza, G. L., and Dang, C. V. (2006). HIF-1-mediated expression of pyruvate dehydrogenase kinase: A metabolic switch required for cellular adaptation to hypoxia. *Cell Metab.* doi:10.1016/j.cmet.2006.02.002.
- Kim, P. K., Hailey, D. W., Mullen, R. T., and Lippincott-Schwartz, J. (2008). Ubiquitin signals autophagic degradation of cytosolic proteins and peroxisomes. *Proc. Natl. Acad. Sci.* 105, 20567–20574. doi:10.1073/pnas.0810611105.
- Kirisako, T., Ichimura, Y., Okada, H., Kabeya, Y., Mizushima, N., Yoshimori, T., et al. (2000). The reversible modification regulates the membrane-binding state of Apg8/Aut7 essential for autophagy and the cytoplasm to vacuole targeting pathway. *J. Cell Biol.* 151, 263–275. doi:10.1083/jcb.151.2.263.
- Kirkegaard, K., Taylor, M. P., and Jackson, W. T. (2004). Cellular autophagy: Surrender, avoidance and subversion by microorganisms. *Nat. Rev. Microbiol.*

doi:10.1038/nrmicro865.

- Kirkin, V., McEwan, D. G., Novak, I., and Dikic, I. (2009). A Role for Ubiquitin in Selective Autophagy. *Mol. Cell* 34, 259–269. doi:10.1016/j.molcel.2009.04.026.
- Klionsky, D. J. (2007). Autophagy: From phenomenology to molecular understanding in less than a decade. *Nat. Rev. Mol. Cell Biol.* doi:10.1038/nrm2245.
- Kobayashi, A., Kang, M., Okawa, H., Zenke, Y., Chiba, T., Igarashi, K., et al. (2004). Oxidative Stress Sensor Keap1 Functions as an Adaptor for Cul3-Based E3 Ligase To Regulate Proteasomal Degradation of Nrf2 Oxidative Stress Sensor Keap1 Functions as an Adaptor for Cul3-Based E3 Ligase To Regulate Proteasomal Degradation of Nrf2. *Mol. Cell. Biol.* 24, 7130–7139. doi:10.1128/MCB.24.16.7130.
- Kobayashi, E. H., Suzuki, T., Funayama, R., Nagashima, T., Hayashi, M., Sekine, H., et al. (2016). Nrf2 suppresses macrophage inflammatory response by blocking proinflammatory cytokine transcription. *Nat. Commun.* 7, 1–14. doi:10.1038/ncomms11624.
- Koch, H. B., Zhang, R., Verdoodt, B., Bailey, A., Zhang, C. D., Yates, J. R., et al. (2007). Large-scale identification of c-MYC-associated proteins using a combined TAP/MudPIT approach. *Cell Cycle*. doi:10.4161/cc.6.2.3742.
- Koh, M. Y., Darnay, B. G., and Powis, G. (2008). Hypoxia-Associated Factor, a Novel E3-Ubiquitin Ligase, Binds and Ubiquitinates Hypoxia-Inducible Factor 1 , Leading to Its Oxygen-Independent Degradation. *Mol. Cell. Biol.* doi:10.1128/MCB.00773-08.
- Komander, D., Clague, M. J., and Urbé, S. (2009). Breaking the chains: Structure and function of the deubiquitinases. *Nat. Rev. Mol. Cell Biol.* 10, 550–563. doi:10.1038/nrm2731.
- Komatsu, M., Kurokawa, H., Waguri, S., Taguchi, K., Kobayashi, A., Ichimura, Y., et al. (2010). The selective autophagy substrate p62 activates the stress responsive transcription factor Nrf2 through inactivation of Keap1. *Nat. Cell Biol.* doi:10.1038/ncb2021.
- Komatsu, M., Waguri, S., Chiba, T., Murata, S., Iwata, J. I., Tanida, I., et al. (2006). Loss of autophagy in the central nervous system causes neurodegeneration in mice. *Nature*. doi:10.1038/nature04723.
- Komatsu, M., Waguri, S., Koike, M., Sou, Y. shin, Ueno, T., Hara, T., et al. (2007). Homeostatic Levels of p62 Control Cytoplasmic Inclusion Body Formation in

- Autophagy-Deficient Mice. *Cell* 131, 1149–1163. doi:10.1016/j.cell.2007.10.035.
- Komatsu, M., Waguri, S., Ueno, T., Iwata, J., Murata, S., Tanida, I., et al. (2005). Impairment of starvation-induced and constitutive autophagy in Atg7-deficient mice. *J. Cell Biol.* doi:10.1083/jcb.200412022.
- Kondapalli, C., Kazlauskaite, A., Zhang, N., Woodroof, H. I., Campbell, D. G., Gourlay, R., et al. (2012). PINK1 is activated by mitochondrial membrane potential depolarization and stimulates Parkin E3 ligase activity by phosphorylating Serine 65. *Open Biol.* 2, 120080–120080. doi:10.1098/rsob.120080.
- Kopito, R. R. (2000). Aggresomes, inclusion bodies and protein aggregation. *Trends Cell Biol.* 10, 524–530. doi:10.1016/S0962-8924(00)01852-3.
- Korac, J., Schaeffer, V., Kovacevic, I., Clement, A. M., Jungblut, B., Behl, C., et al. (2013). Ubiquitin-independent function of optineurin in autophagic clearance of protein aggregates. *J. Cell Sci.* 126, 580–592. doi:10.1242/jcs.114926.
- Korolchuk, V. I., Mansilla, A., Menzies, F. M., and Rubinsztein, D. C. (2009a). Autophagy Inhibition Compromises Degradation of Ubiquitin-Proteasome Pathway Substrates. *Mol. Cell* 33, 517–527. doi:10.1016/j.molcel.2009.01.021.
- Korolchuk, V. I., Mansilla, A., Menzies, F. M., and Rubinsztein, D. C. (2009b). Autophagy Inhibition Compromises Degradation of Ubiquitin-Proteasome Pathway Substrates. *Mol. Cell* 33, 517–527. doi:10.1016/j.molcel.2009.01.021.
- Korolchuk, V. I., Menzies, F. M., and Rubinsztein, D. C. (2009c). A novel link between autophagy and the ubiquitin-proteasome system. *Autophagy*. doi:10.4161/auto.8840.
- Korolchuk, V. I., Menzies, F. M., and Rubinsztein, D. C. (2010). Mechanisms of cross-talk between the ubiquitin-proteasome and autophagy-lysosome systems. *FEBS Lett.* 584, 1393–1398. doi:10.1016/j.febslet.2009.12.047.
- Koyano, F., Okatsu, K., Kosako, H., Tamura, Y., Go, E., Kimura, M., et al. (2014). Ubiquitin is phosphorylated by PINK1 to activate parkin. *Nature* 510, 162–166. doi:10.1038/nature13392.
- Kraft, C., Deplazes, A., Sohrmann, M., and Peter, M. (2008). Mature ribosomes are selectively degraded upon starvation by an autophagy pathway requiring the Ubp3p/Bre5p ubiquitin protease. *Nat. Cell Biol.* 10, 602–610. doi:10.1038/ncb1723.
- Kraft, C., and Peter, M. (2008). Is the Rsp5 ubiquitin ligase involved in the regulation of

- ribophagy? *Autophagy* 4, 838–840. doi:10.4161/auto.6603.
- Kravtsova-ivantsiv, Y., Ciechanover, A., Kravtsova-ivantsiv, Y., and Ciechanover, A. (2015). The ubiquitin-proteasome system and activation of NF- κ B : involvement of the ubiquitin ligase KPC1 in p105 processing and tumor suppression The ubiquitin-proteasome system and activation of NF- κ B : involvement of the ubiquitin ligase KPC1 in p105 proc. 3556. doi:10.1080/23723556.2015.1054552.
- Kristensen, A. R., Gsponer, J., and Foster, L. J. (2012). A high-throughput approach for measuring temporal changes in the interactome. *Nat. Methods*. doi:10.1038/nmeth.2131.
- Kroemer, G., Mariño, G., and Levine, B. (2010). Autophagy and the Integrated Stress Response. *Mol. Cell* 40, 280–293. doi:10.1016/j.molcel.2010.09.023.
- Kuchay, S., Duan, S., Schenkein, E., Peschiaroli, A., Saraf, A., Florens, L., et al. (2013). FBXL2- and PTPL1-mediated degradation of p110-free p85 β regulatory subunit controls the PI(3)K signalling cascade. *Nat. Cell Biol.* doi:10.1038/ncb2731.
- Kulikov, R., Letienne, J., Kaur, M., Grossman, S. R., Arts, J., and Blattner, C. (2010). Mdm2 facilitates the association of p53 with the proteasome. *Proc. Natl. Acad. Sci.* doi:10.1073/pnas.0911716107.
- Kundu, M., Lindsten, T., Yang, C. Y., Wu, J., Zhao, F., Zhang, J., et al. (2008). Ulk1 plays a critical role in the autophagic clearance of mitochondria and ribosomes during reticulocyte maturation. *Blood* 112, 1493–1502. doi:10.1182/blood-2008-02-137398.
- Kwon, Y. T., and Ciechanover, A. (2017). The Ubiquitin Code in the Ubiquitin-Proteasome System and Autophagy. *Trends Biochem. Sci.* 42, 873–886. doi:10.1016/j.tibs.2017.09.002.
- Kyrychenko, V. O., Nagibin, V. S., Tumanovska, L. V., Pashevin, D. O., Gurianova, V. L., Moibenko, A. A., et al. (2013). Knockdown of PSMB7 induces autophagy in cardiomyocyte cultures: Possible role in endoplasmic reticulum stress. *Pathobiology* 81, 8–14. doi:10.1159/000350704.
- Lamark, T., and Johansen, T. (2012). Aggrephagy: Selective disposal of protein aggregates by macroautophagy. *Int. J. Cell Biol.* 2012. doi:10.1155/2012/736905.
- Lamb, C. A., Yoshimori, T., and Tooze, S. A. (2013). The autophagosome: Origins unknown, biogenesis complex. *Nat. Rev. Mol. Cell Biol.* 14, 759–774. doi:10.1038/nrm3696.
- Lander, G. C., Estrin, E., Matyskiela, M. E., Bashore, C., Nogales, E., and Martin, A.

- (2012). Complete subunit architecture of the proteasome regulatory particle. *Nature* 482, 186–191. doi:10.1038/nature10774.
- Law, K. B., Bronte-tinkew, D., Pietro, E. Di, Snowden, A., Jones, O., Moser, A., et al. (2017). The peroxisomal AAA ATPase complex prevents pexophagy and development of peroxisome biogenesis disorders. *Autophagy* 13, 868–884. doi:10.1080/15548627.2017.1291470.
- Lazarou, M., Jin, S. M., Kane, L. A., and Youle, R. J. (2012). Role of PINK1 Binding to the TOM Complex and Alternate Intracellular Membranes in Recruitment and Activation of the E3 Ligase Parkin. *Dev. Cell* 22, 320–333. doi:10.1016/j.devcel.2011.12.014.
- Lazarou, M., Sliter, D. A., Kane, L. A., Sarraf, S. A., Wang, C., Burman, J. L., et al. (2015). The ubiquitin kinase PINK1 recruits autophagy receptors to induce mitophagy. *Nature* 524, 309–314. doi:10.1038/nature14893.
- Lee, D. F., Kuo, H. P., Chen, C. Te, Hsu, J. M., Chou, C. K., Wei, Y., et al. (2007). IKK β Suppression of TSC1 Links Inflammation and Tumor Angiogenesis via the mTOR Pathway. *Cell* 130, 440–455. doi:10.1016/j.cell.2007.05.058.
- Lee, I. H., Cao, L., Mostoslavsky, R., Lombard, D. B., Liu, J., Bruns, N. E., et al. (2008). A role for the NAD-dependent deacetylase Sirt1 in the regulation of autophagy. *Proc. Natl. Acad. Sci.* doi:10.1073/pnas.0712145105.
- Lee, J. H., Elly, C., Park, Y., Lee, J. H., Elly, C., Park, Y., et al. (2015). Inducible Factor-1 a to Maintain Regulatory T Cell Stability and Suppressive Capacity Article E3 Ubiquitin Ligase VHL Regulates Hypoxia-Inducible Factor-1 a to Maintain Regulatory T Cell Stability and Suppressive Capacity. *Immunity* 42, 1062–1074. doi:10.1016/j.immuni.2015.05.016.
- Lee, J. J., Sanchez-Martinez, A., Zarate, A. M., Benincá, C., Mayor, U., Clague, M. J., et al. (2018). Basal mitophagy is widespread in *Drosophila* but minimally affected by loss of Pink1 or parkin. *J. Cell Biol.*, jcb.201801044. doi:10.1083/jcb.201801044.
- Lee, J. Y., Koga, H., Kawaguchi, Y., Tang, W., Wong, E., Gao, Y. S., et al. (2010). HDAC6 controls autophagosome maturation essential for ubiquitin-selective quality-control autophagy. *EMBO J.* 29, 969–980. doi:10.1038/emboj.2009.405.
- Lee, M. J., Lee, B.-H., Hanna, J., King, R. W., and Finley, D. (2011). Trimming of Ubiquitin Chains by Proteasome-associated Deubiquitinating Enzymes. *Mol. Cell. Proteomics* 10, R110.003871. doi:10.1074/mcp.R110.003871.

- Lee, M. Y., Sumpter, R., Zou, Z., Sirasanagandla, S., Wei, Y., Mishra, P., et al. (2017). Peroxisomal protein PEX13 functions in selective autophagy. *EMBO Rep.* doi:10.15252/embr.201642443.
- Lemasters, J. J. (2005). John j. lemasters. 8, 3–5.
- Li, D., Dong, Q., Tao, Q., Gu, J., Cui, Y., Jiang, X., et al. (2015). c-Abl regulates proteasome abundance by controlling the ubiquitin-proteasomal degradation of PSMA7 subunit. *Cell Rep.* doi:10.1016/j.celrep.2014.12.044.
- Li, D., and Sewer, M. B. (2010). RhoA and DIAPH1 mediate adrenocorticotropin-stimulated cortisol biosynthesis by regulating mitochondrial trafficking. *Endocrinology.* doi:10.1210/en.2010-0044.
- Li, N., Zhang, Z., Zhang, W., and Wei, Q. (2011). Calcineurin B subunit interacts with proteasome subunit alpha type 7 and represses hypoxia-inducible factor-1 α activity via the proteasome pathway. *Biochem. Biophys. Res. Commun.* doi:10.1016/j.bbrc.2011.01.055.
- Li, Q., Chen, P., Zeng, Z., Liang, F., Song, Y., Xiong, F., et al. (2016). Yeast two-hybrid screening identified WDR77 as a novel interacting partner of TSC22D2. *Tumor Biol.* doi:10.1007/s13277-016-5113-z.
- Li, S., Wandel, M. P., Li, F., Liu, Z., He, C., Wu, J., et al. (2013). Sterical hindrance promotes selectivity of the autophagy cargo receptor NDP52 for the danger receptor galectin-8 in antibacterial autophagy. *Sci. Signal.* 6, 1–7. doi:10.1126/scisignal.2003730.
- Li, W. W., Li, J., and Bao, J. K. (2012). Microautophagy: Lesser-known self-eating. *Cell. Mol. Life Sci.* 69, 1125–1136. doi:10.1007/s00018-011-0865-5.
- Li, Z., Na, X., Wang, D., Schoen, S. R., Messing, E. M., and Wu, G. (2002a). Ubiquitination of a novel deubiquitinating enzyme requires direct binding to von Hippel-Lindau tumor suppressor protein. *J. Biol. Chem.* 277, 4656–4662. doi:10.1074/jbc.M108269200.
- Li, Z., Wang, D., Na, X., Schoen, S. R., Messing, E. M., and Wu, G. (2002b). Identification of a deubiquitinating enzyme subfamily as substrates of the von Hippel-Lindau tumor suppressor. *Biochem. Biophys. Res. Commun.* doi:10.1016/S0006-291X(02)00534-X.
- Liggett, A., Crawford, L. J., Walker, B., Morris, T. C. M., and Irvine, A. E. (2010). Methods for measuring proteasome activity: Current limitations and future developments. *Leuk. Res.* doi:10.1016/j.leukres.2010.07.003.

- Lim, P. J., Danner, R., Liang, J., Doong, H., Harman, C., Srinivasan, D., et al. (2009). Ubiquilin and p97/VCP bind erasin, forming a complex involved in ERAD. *J. Cell Biol.* 187, 201–217. doi:10.1083/jcb.200903024.
- Lin, Q., Dai, Q., Meng, H., Sun, A., Wei, J., Peng, K., et al. (2017). The HECT E3 ubiquitin ligase NEDD4 interacts with and ubiquitylates SQSTM1 for inclusion body autophagy. doi:10.1242/jcs.207068.
- Ling, J., Kang, Y., Zhao, R., Xia, Q., Lee, D. F., Chang, Z., et al. (2012). Kras G12D-Induced IKK2/ β /NF- κ B Activation by IL-1 α and p62 Feedforward Loops Is Required for Development of Pancreatic Ductal Adenocarcinoma. *Cancer Cell* 21, 105–120. doi:10.1016/j.ccr.2011.12.006.
- Liu, J., Xia, H., Kim, M., Xu, L., Li, Y., Zhang, L., et al. (2011). Beclin1 controls the levels of p53 by regulating the deubiquitination activity of USP10 and USP13. *Cell* 147, 223–234. doi:10.1016/j.cell.2011.08.037.
- Liu, X., Huang, W., Li, C., Li, P., Yuan, J., Li, X., et al. (2006). Interaction between c-Abl and Arg Tyrosine Kinases and Proteasome Subunit PSMA7 Regulates Proteasome Degradation. *Mol. Cell.* doi:10.1016/j.molcel.2006.04.007.
- Liu, Z., Chen, P., Gao, H., Gu, Y., Yang, J., Peng, H., et al. (2014). Ubiquitylation of Autophagy Receptor Optineurin by HACE1 Activates Selective Autophagy for Tumor Suppression. *Cancer Cell* 26, 106–120. doi:10.1016/j.ccr.2014.05.015.
- Lobato-Márquez, D., and Mostowy, S. (2017). *Salmonella* ubiquitination: ARIH1 enters the fray. *EMBO Rep.* 18, 1476–1477. doi:10.15252/embr.201744672.
- Long, J., Gallagher, T. R. A., Cavey, J. R., Sheppard, P. W., Ralston, S. H., Layfield, R., et al. (2008). Ubiquitin recognition by the ubiquitin-associated domain of p62 involves a novel conformational switch. *J. Biol. Chem.* 283, 5427–5440. doi:10.1074/jbc.M704973200.
- Lu, K., Psakhye, I., and Jentsch, S. (2014). Autophagic clearance of PolyQ proteins mediated by ubiquitin-Atg8 adaptors of the conserved CUET protein family. *Cell* 158, 549–563. doi:10.1016/j.cell.2014.05.048.
- Lu, L., Hu, S., Wei, R., Qiu, X., Lu, K., Fu, Y., et al. (2013). The HECT type ubiquitin ligase NEDL2 is degraded by anaphase-promoting complex/cyclosome (APC/C)-Cdh1, and its tight regulation maintains the metaphase to anaphase transition. *J. Biol. Chem.* doi:10.1074/jbc.M113.472076.
- Mammucari, C., Milan, G., Romanello, V., Masiero, E., Rudolf, R., Del Piccolo, P., et al. (2007). FoxO3 Controls Autophagy in Skeletal Muscle In Vivo. *Cell Metab.* 6,

- 458–471. doi:10.1016/j.cmet.2007.11.001.
- Manzanillo, P. S., Ayres, J. S., Watson, R. O., Collins, A. C., Souza, G., Rae, C. S., et al. (2013). The ubiquitin ligase parkin mediates resistance to intracellular pathogens. *Nature* 501, 512–516. doi:10.1038/nature12566.
- Mao, J., Xia, Q., Liu, C., Ying, Z., Wang, H., and Wang, G. (2017). A critical role of Hrd1 in the regulation of optineurin degradation and aggresome formation. *Hum. Mol. Genet.* 26, 1877–1889. doi:10.1093/hmg/ddx096.
- Marshall, R. S., Li, F., Gemperline, D. C., Book, A. J., and Vierstra, R. D. (2015). Autophagic Degradation of the 26S Proteasome Is Mediated by the Dual ATG8/Ubiquitin Receptor RPN10 in Arabidopsis. *Mol. Cell* 58, 1053–1066. doi:10.1016/j.molcel.2015.04.023.
- Matsumoto, M., Hatakeyama, S., Oyamada, K., Oda, Y., Nishimura, T., and Nakayama, K. I. (2005). Large-scale analysis of the human ubiquitin-related proteome. *Proteomics*. doi:10.1002/pmic.200401280.
- Matsushita, M., Suzuki, N. N., Obara, K., Fujioka, Y., Ohsumi, Y., and Inagaki, F. (2007). Structure of Atg5-Atg16, a complex essential for autophagy. *J. Biol. Chem.* doi:10.1074/jbc.M609876200.
- Matthias, P., Yoshida, M., and Khochbin, S. (2008). HDAC6 a new cellular stress surveillance factor. *Cell Cycle* 7, 7–10. doi:10.4161/cc.7.1.5186.
- Mauthe, M., Jacob, A., Freiburger, S., Hentschel, K., Stierhof, Y. D., Codogno, P., et al. (2011). Resveratrol-mediated autophagy requires WIPI-1-regulated LC3 lipidation in the absence of induced phagophore formation. *Autophagy* 7, 1448–1461. doi:10.4161/auto.7.12.17802.
- Mazroui, R., Di Marco, S., Kaufman, R. J., and Gallouzi, I.-E. (2007). Inhibition of the Ubiquitin-Proteasome System Induces Stress Granule Formation. *Mol. Biol. Cell.* doi:10.1091/mbc.E06.
- Mehrpour, M., Esclatine, A., Beau, I., and Codogno, P. (2010). Overview of macroautophagy regulation in mammalian cells. *Cell Res.* 20, 748–762. doi:10.1038/cr.2010.82.
- Meier, F., Abeywardana, T., Dhall, A., Marotta, N. P., Varkey, J., Langen, R., et al. (2012). Semisynthetic, site-specific ubiquitin modification of α -synuclein reveals differential effects on aggregation. *J. Am. Chem. Soc.* 134, 5468–5471. doi:10.1021/ja300094r.
- Menzies, F. M., Garcia-Arencibia, M., Imarisio, S., O’Sullivan, N. C., Ricketts, T.,

- Kent, B. A., et al. (2015). Calpain inhibition mediates autophagy-dependent protection against polyglutamine toxicity. *Cell Death Differ.* 22, 433–444. doi:10.1038/cdd.2014.151.
- Mishra, A., Godavarthi, S. K., Maheshwari, M., Goswami, A., and Jana, N. R. (2009). The ubiquitin ligase E6-AP is induced and recruited to aggresomes in response to proteasome inhibition and may be involved in the ubiquitination of Hsp70-bound misfolded proteins. *J. Biol. Chem.* 284, 10537–10545. doi:10.1074/jbc.M806804200.
- Mizushima, N. (2018). A brief history of autophagy from cell biology to physiology and disease. *Nat. Cell Biol.* doi:10.1038/s41556-018-0092-5.
- Morimoto, D., Walinda, E., Fukada, H., Sou, Y. S., Kageyama, S., Hoshino, M., et al. (2015). The unexpected role of polyubiquitin chains in the formation of fibrillar aggregates. *Nat. Commun.* 6, 1–10. doi:10.1038/ncomms7116.
- Moscat, J., and Diaz-Meco, M. T. (2009). p62 at the Crossroads of Autophagy, Apoptosis, and Cancer. *Cell* 137, 1001–1004. doi:10.1016/j.cell.2009.05.023.
- Nakagawa, T., Shirane, M., Lemura, S. I., Natsume, T., and Nakayama, K. I. (2007). Anchoring of the 26S proteasome to the organellar membrane by FKBP38. *Genes to Cells.* doi:10.1111/j.1365-2443.2007.01086.x.
- Nakamura, N., Kimura, Y., Tokuda, M., Honda, S., and Hirose, S. (2006). MARCH-V is a novel mitofusin 2- and Drp1-binding protein able to change mitochondrial morphology. *EMBO Rep.* 7, 1019–1022. doi:10.1038/sj.embor.7400790.
- Nakashima, H., Nguyen, T., Goins, W. F., and Chiocca, E. A. (2015). Interferon-stimulated gene 15 (ISG15) and ISG15-linked proteins can associate with members of the selective autophagic process, histone deacetylase 6 (HDAC6) and SQSTM1/p62. *J. Biol. Chem.* 290, 1485–1495. doi:10.1074/jbc.M114.593871.
- Nakatogawa, H., Ichimura, Y., and Ohsumi, Y. (2007). Atg8, a Ubiquitin-like Protein Required for Autophagosome Formation, Mediates Membrane Tethering and Hemifusion. *Cell* 130, 165–178. doi:10.1016/j.cell.2007.05.021.
- Nakayama, K., Frew, I. J., Hagensen, M., Skals, M., Habelhah, H., Bhoumik, A., et al. (2004). Siah2 regulates stability of prolyl-hydroxylases, controls HIF1 α abundance, and modulates physiological responses to hypoxia. *Cell* 117, 941–952. doi:10.1016/j.cell.2004.06.001.
- Nandi, D., Woodward, E., Ginsburg, D. B., and Monaco, J. J. (1997). Intermediates in the formation of mouse 20S proteasomes: Implications for the assembly of

- precursor β subunits. *EMBO J.* doi:10.1093/emboj/16.17.5363.
- Narendra, D. P., Kane, L. A., Hauser, D. N., Fearnley, I. M., and Youle, R. J. (2010). p62/SQSTM1 is required for Parkin-induced mitochondrial clustering but not mitophagy; VDAC1 is dispensable for both. *Autophagy* 6, 1090–1106. doi:10.4161/auto.6.8.13426.
- Narendra, D., Tanaka, A., Suen, D. F., and Youle, R. J. (2008). Parkin is recruited selectively to impaired mitochondria and promotes their autophagy. *J. Cell Biol.* 183, 795–803. doi:10.1083/jcb.200809125.
- Nazio, F., Strappazon, F., Antonioli, M., Bielli, P., Cianfanelli, V., Bordi, M., et al. (2013). mTOR inhibits autophagy by controlling ULK1 ubiquitylation, self-association and function through AMBRA1 and TRAF6. *Nat. Cell Biol.* 15, 406–416. doi:10.1038/ncb2708.
- Nezis, I. P., Simonsen, A., Sagona, A. P., Finley, K., Gaumer, S., Contamine, D., et al. (2008). Ref(2)P, the *Drosophila melanogaster* homologue of mammalian p62, is required for the formation of protein aggregates in adult brain. *J. Cell Biol.* 180, 1065–1071. doi:10.1083/jcb.200711108.
- Nie, J., Xie, P., Liu, L., Xing, G., Chang, Z., Yin, Y., et al. (2010). Smad ubiquitylation regulatory factor 1/2 (Smurf1/2) promotes p53 degradation by stabilizing the E3 ligase MDM2. *J. Biol. Chem.* 285, 22818–22830. doi:10.1074/jbc.M110.126920.
- Noad, J., Von Der Malsburg, A., Pathe, C., Michel, M. A., Komander, D., and Randow, F. (2017). LUBAC-synthesized linear ubiquitin chains restrict cytosol-invading bacteria by activating autophagy and NF- κ B. *Nat. Microbiol.* doi:10.1038/nmicrobiol.2017.63.
- Norman, J. A., and Shiekhhattar, R. (2006). Analysis of Nedd8-associated polypeptides: A model for deciphering the pathway for ubiquitin-like modifications. *Biochemistry.* doi:10.1021/bi052435a.
- Novak, I., Kirkin, V., McEwan, D. G., Zhang, J., Wild, P., Rozenknop, A., et al. (2010). Nix is a selective autophagy receptor for mitochondrial clearance. *EMBO Rep.* 11, 45–51. doi:10.1038/embor.2009.256.
- Ogawa, M., Yoshimori, T., Suzuki, T., Sagara, H., Mizushima, N., and Sasakawa, C. (2005). Escape of intracellular *Shigella* from autophagy. *Science (80-)*. 307, 727–731. doi:10.1126/science.1106036.
- Ohh, M., Park, C. W., Ivan, M., Hoffman, M. A., Kim, T., Huang, L. E., et al. (2000). Ubiquitination of hypoxia-inducible factor requires direct binding to the β -domain

- of the von Hippel – Lindau protein. *2*, 423–427.
- Ohsumi, Y., and Mizushima, N. (2004). Two ubiquitin-like conjugation systems essential for autophagy. *Semin. Cell Dev. Biol.* doi:10.1016/j.semcdb.2003.12.004.
- Okamoto, K., Kondo-Okamoto, N., and Ohsumi, Y. (2009). Mitochondria-Anchored Receptor Atg32 Mediates Degradation of Mitochondria via Selective Autophagy. *Dev. Cell* 17, 87–97. doi:10.1016/j.devcel.2009.06.013.
- Okatsu, K., Saisho, K., Shimanuki, M., Nakada, K., Shitara, H., Sou, Y. S., et al. (2010). P62/SQSTM1 cooperates with Parkin for perinuclear clustering of depolarized mitochondria. *Genes to Cells* 15, 887–900. doi:10.1111/j.1365-2443.2010.01426.x.
- Okerlund, N. D., Schneider, K., Leal-Ortiz, S., Montenegro-Venegas, C., Kim, S. A., Garner, L. C., et al. (2018). Erratum: Bassoon Controls Presynaptic Autophagy through Atg5 (*Neuron* (2017) 93(4) (897–913.e7)(S0896627317300508)(10.1016/j.neuron.2017.01.026)). *Neuron*. doi:10.1016/j.neuron.2018.01.010.
- Okumoto, K., Misono, S., Miyata, N., Matsumoto, Y., Mukai, S., and Fujiki, Y. (2011). Cysteine ubiquitination of PTS1 receptor Pex5p regulates Pex5p recycling. *Traffic* 12, 1067–1083. doi:10.1111/j.1600-0854.2011.01217.x.
- Oláh, J., Vincze, O., Virók, D., Simon, D., Bozsó, Z., Tokési, N., et al. (2011). Interactions of pathological hallmark proteins: Tubulin polymerization promoting protein/p25, β -amyloid, and α -synuclein. *J. Biol. Chem.* doi:10.1074/jbc.M111.243907.
- Olzmann, J. A., Li, A., Chudaev, M. V., Chen, J., Perez, F. A., Palmiter, R. D., et al. (2007). Parkin-mediated K63-linked polyubiquitination targets misfolded DJ-1 to aggresomes via binding to HDAC6. *J. Cell Biol.* 178, 1025–1038. doi:10.1083/jcb.200611128.
- Orian, A., Gonen, H., Bercovich, B., Fajerman, I., Eytan, E., Israe, A., et al. (2000). SCF b -TrCP ubiquitin ligase-mediated processing of NF- k B p105 requires phosphorylation of its C-terminus by I k B kinase. 19.
- Ossareh-Nazari, B., Bonizec, M., Cohen, M., Dokudovskaya, S., Delalande, F., Schaeffer, C., et al. (2010). Cdc48 and Ufd3, new partners of the ubiquitin protease Ubp3, are required for ribophagy. *EMBO Rep.* 11, 548–554. doi:10.1038/embor.2010.74.
- Ossareh-Nazari, B., Niño, C. A., Bengtson, M. H., Lee, J. W., Joazeiro, C. A. P., and

- Dargemont, C. (2014). Ubiquitylation by the Ltn1 E3 ligase protects 60S ribosomes from starvation-induced selective autophagy. *J. Cell Biol.* 204, 909–917. doi:10.1083/jcb.201308139.
- Otomo, C., Metlagel, Z., Takaesu, G., and Otomo, T. (2013). Structure of the human ATG12~ATG5 conjugate required for LC3 lipidation in autophagy. *Nat. Struct. Mol. Biol.* doi:10.1038/nsmb.2431.
- Palikaras, K., Lionaki, E., and Tavernarakis, N. (2015). Coordination of mitophagy and mitochondrial biogenesis during ageing in *C. elegans*. *Nature* 521, 525–528. doi:10.1038/nature14300.
- Pan, J. A., Sun, Y., Jiang, Y. P., Bott, A. J., Jaber, N., Dou, Z., et al. (2016). TRIM21 Ubiquitylates SQSTM1/p62 and Suppresses Protein Sequestration to Regulate Redox Homeostasis. *Mol. Cell* 61, 720–733. doi:10.1016/j.molcel.2016.02.007.
- Pankiv, S., Clausen, T. H., Lamark, T., Brech, A., Bruun, J. A., Outzen, H., et al. (2007). p62/SQSTM1 binds directly to Atg8/LC3 to facilitate degradation of ubiquitinated protein aggregates by autophagy*[S]. *J. Biol. Chem.* 282, 24131–24145. doi:10.1074/jbc.M702824200.
- Paul, S., Kashyap, A. K., Jia, W., He, Y. W., and Schaefer, B. C. (2012). Selective Autophagy of the Adaptor Protein Bcl10 Modulates T Cell Receptor Activation of NF- κ B. *Immunity*. doi:10.1016/j.immuni.2012.04.008.
- Peth, A., Besche, H. C., and Goldberg, A. L. (2009). Ubiquitinated Proteins Activate the Proteasome by Binding to Usp14/Ubp6, which Causes 20S Gate Opening. *Mol. Cell* 36, 794–804. doi:10.1016/j.molcel.2009.11.015.
- Petroski, M. D., and Deshaies, R. J. (2005). Function and regulation of cullin-RING ubiquitin ligases. *Nat. Rev. Mol. Cell Biol.* 6, 9–20. doi:10.1038/nrm1547.
- Pichler, A., Fatouros, C., Lee, H., and Eisenhardt, N. (2017). SUMO conjugation - A mechanistic view. *Biomol. Concepts* 8, 13–36. doi:10.1515/bmc-2016-0030.
- Pickart, C. M., and Eddins, M. J. (2004). Ubiquitin: Structures, functions, mechanisms. *Biochim. Biophys. Acta - Mol. Cell Res.* 1695, 55–72. doi:10.1016/j.bbamcr.2004.09.019.
- Pinto-Fernandez, A., and Kessler, B. M. (2016). DUBbing cancer: Deubiquitylating enzymes involved in epigenetics, DNA damage and the cell cycle as therapeutic targets. *Front. Genet.* 7, 1–13. doi:10.3389/fgene.2016.00133.
- Platta, H. W., Abrahamsen, H., Thoresen, S. B., and Stenmark, H. (2012). Nedd4-dependent lysine-11-linked polyubiquitination of the tumour suppressor Beclin 1.

- Biochem. J.* 441, 399–406. doi:10.1042/BJ20111424.
- Platta, H. W., El Magraoui, F., Baumer, B. E., Schlee, D., Girzalsky, W., and Erdmann, R. (2009). Pex2 and Pex12 Function as Protein-Ubiquitin Ligases in Peroxisomal Protein Import. *Mol. Cell. Biol.* 29, 5505–5516. doi:10.1128/MCB.00388-09.
- Protter, D. S. W., and Parker, R. (2016). Principles and Properties of Stress Granules. *Trends Cell Biol.* 26, 668–679. doi:10.1016/j.tcb.2016.05.004.
- Pyo, J. O., Jang, M. H., Kwon, Y. K., Lee, H. J., Jun, J. Il, Woo, H. N., et al. (2005). Essential roles of Atg5 and FADD in autophagic cell death: Dissection of autophagic cell death into vacuole formation and cell death. *J. Biol. Chem.* doi:10.1074/jbc.M413934200.
- Qing, G., Yan, P., Qu, Z., Liu, H., and Xiao, G. (2007). Hsp90 regulates processing of NF- κ B p100 involving protection of NF- κ B-inducing kinase (NIK) from autophagy-mediated degradation. *Cell Res.* 17, 520–530. doi:10.1038/cr.2007.47.
- Qiu, Y., Hofmann, K., Coats, J. E., Schulman, B. A., and Kaiser, S. E. (2013). Binding to E1 and E3 is mutually exclusive for the human autophagy E2 Atg3. *Protein Sci.* doi:10.1002/pro.2381.
- Randow, F., and Youle, R. J. (2014). Self and nonself: How autophagy targets mitochondria and bacteria. *Cell Host Microbe* 15, 403–411. doi:10.1016/j.chom.2014.03.012.
- Ravikumar, B., Moreau, K., Jahreiss, L., Puri, C., and Rubinsztein, D. C. (2010). Plasma membrane contributes to the formation of pre-autophagosomal structures. *Nat. Cell Biol.* doi:10.1038/ncb2078.
- Reichard, J. F., Motz, G. T., and Puga, A. (2007). Heme oxygenase-1 induction by NRF2 requires inactivation of the transcriptional repressor BACH1. *Nucleic Acids Res.* 35, 7074–7086. doi:10.1093/nar/gkm638.
- Reineke, L. C., and Lloyd, R. E. (2013). Diversion of stress granules and P-bodies during viral infection. *Virology.* doi:10.1016/j.virol.2012.11.017.
- Renna, M., Jimenez-Sanchez, M., Sarkar, S., and Rubinsztein, D. C. (2010). Chemical inducers of autophagy that enhance the clearance of mutant proteins in neurodegenerative diseases. *J. Biol. Chem.* 285, 11061–11067. doi:10.1074/jbc.R109.072181.
- Richter, B., Sliter, D. A., Herhaus, L., Stolz, A., Wang, C., Beli, P., et al. (2016). Phosphorylation of OPTN by TBK1 enhances its binding to Ub chains and promotes selective autophagy of damaged mitochondria. *Proc. Natl. Acad. Sci.*

- 113, 4039–4044. doi:10.1073/pnas.1523926113.
- Riley, B. E., Kaiser, S. E., Shaler, T. A., Ng, A. C. Y., Hara, T., Hipp, M. S., et al. (2010). Ubiquitin accumulation in autophagy-deficient mice is dependent on the Nrf2-mediated stress response pathway: A potential role for protein aggregation in autophagic substrate selection. *J. Cell Biol.* 191, 537–552. doi:10.1083/jcb.201005012.
- Rogov, V., Dötsch, V., Johansen, T., and Kirkin, V. (2014). Interactions between Autophagy Receptors and Ubiquitin-like Proteins Form the Molecular Basis for Selective Autophagy. *Mol. Cell* 53, 167–178. doi:10.1016/j.molcel.2013.12.014.
- Rolland, T., Taşan, M., Charlotiaux, B., Pevzner, S. J., Zhong, Q., Sahni, N., et al. (2014). A proteome-scale map of the human interactome network. *Cell.* doi:10.1016/j.cell.2014.10.050.
- Sakowski, E. T., Koster, S., Portal Celhay, C., Park, H. S., Shrestha, E., Hetzenecker, S. E., et al. (2015). Ubiquilin 1 Promotes IFN- γ -Induced Xenophagy of *Mycobacterium tuberculosis*. *PLoS Pathog.* 11, 1–18. doi:10.1371/journal.ppat.1005076.
- Sanchez, A. M. J., Csibi, A., Raibon, A., Cornille, K., Gay, S., Bernardi, H., et al. (2012). AMPK promotes skeletal muscle autophagy through activation of forkhead FoxO3a and interaction with Ulk1. *J. Cell. Biochem.* 113, 695–710. doi:10.1002/jcb.23399.
- Sandoval, H., Thiagarajan, P., Dasgupta, S. K., Schumacher, A., Prchal, J. T., Chen, M., et al. (2008). Essential role for Nix in autophagic maturation of erythroid cells. *Nature* 454, 232–235. doi:10.1038/nature07006.
- Sang, L., Miller, J. J., Corbit, K. C., Giles, R. H., Brauer, M. J., Otto, E. A., et al. (2011). Mapping the NPHP-JBTS-MKS protein network reveals ciliopathy disease genes and pathways. *Cell.* doi:10.1016/j.cell.2011.04.019.
- Sargent, G., Zutphen, T. Van, Shatseva, T., Zhang, L., Giovanni, V. Di, Bandsma, R., et al. (2016). PEX2 is the E3 ubiquitin ligase required for pexophagy during starvation. 214. doi:10.1083/jcb.201511034.
- Sarraf, S. A., Raman, M., Guarani-Pereira, V., Sowa, M. E., Huttlin, E. L., Gygi, S. P., et al. (2013). Landscape of the PARKIN-dependent ubiquitylome in response to mitochondrial depolarization. *Nature* 496, 372–376. doi:10.1038/nature12043.
- Sasaki, M., Sukegawa, J., Miyosawa, K., Yanagisawa, T., Ohkubo, S., and Nakahata, N. (2007). Low expression of cell-surface thromboxane A2 receptor beta-isoform

- through the negative regulation of its membrane traffic by proteasomes.
Prostaglandins Other Lipid Mediat. doi:10.1016/j.prostaglandins.2006.12.001.
- Scanlon, T. C., Gottlieb, B., Durcan, T. M., Fon, E. A., Beitel, L. K., and Trifiro, M. A. (2009). Isolation of human proteasomes and putative proteasome-interacting proteins using a novel affinity chromatography method. *Exp. Cell Res.* doi:10.1016/j.yexcr.2008.10.027.
- Schell-Steven, A., Stein, K., Amoros, M., Landgraf, C., Volkmer-Engert, R., Rottensteiner, H., et al. (2005). Identification of a novel, intraperoxisomal pex14-binding site in pex13: association of pex13 with the docking complex is essential for peroxisomal matrix protein import. *Mol. Cell. Biol.* doi:10.1128/MCB.25.8.3007-3018.2005.
- Schrader, J., Henneberg, F., Mata, R. A., Tittmann, K., Schneider, T. R., Stark, H., et al. (2016). The inhibition mechanism of human 20S proteasomes enables next-generation inhibitor design. *Science (80-.)*. doi:10.1126/science.aaf8993.
- Schwartz, A. L., and Ciechanover, A. (2009). Targeting Proteins for Destruction by the Ubiquitin System: Implications for Human Pathobiology. *Annu. Rev. Pharmacol. Toxicol.* doi:10.1146/annurev.pharmtox.051208.165340.
- Schweers, R. L., Zhang, J., Randall, M. S., Loyd, M. R., Li, W., Dorsey, F. C., et al. (2007). NIX is required for programmed mitochondrial clearance during reticulocyte maturation. *Proc. Natl. Acad. Sci. U. S. A.* 104, 19500–5. doi:10.1073/pnas.0708818104.
- Sdek, P., Ying, H., Chang, D. L. F., Qiu, W., Zheng, H., Touitou, R., et al. (2005). MDM2 promotes proteasome-dependent ubiquitin-independent degradation of retinoblastoma protein. *Mol. Cell.* doi:10.1016/j.molcel.2005.10.017.
- Seguin, S. J., Morelli, F. F., Vinet, J., Amore, D., De Biasi, S., Poletti, A., et al. (2014). Inhibition of autophagy, lysosome and VCP function impairs stress granule assembly. *Cell Death Differ.* 21, 1838–1851. doi:10.1038/cdd.2014.103.
- Selimovic, D., Porzig, B. B. O. W., El-Khattouti, A., Badura, H. E., Ahmad, M., Ghanjati, F., et al. (2013). Bortezomib/proteasome inhibitor triggers both apoptosis and autophagy-dependent pathways in melanoma cells. *Cell. Signal.* 25, 308–318. doi:10.1016/j.cellsig.2012.10.004.
- Sengupta, S., Peterson, T. R., and Sabatini, D. M. (2010). Regulation of the mTOR Complex 1 Pathway by Nutrients, Growth Factors, and Stress. *Mol. Cell* 40, 310–322. doi:10.1016/j.molcel.2010.09.026.

- Sha, Z., Schnell, H. M., Ruoff, K., and Goldberg, A. (2018). Rapid induction of p62 and GABARAPL1 upon proteasome inhibition promotes survival before autophagy activation. *J. Cell Biol.* doi:10.1083/jcb.201708168.
- Shaid, S., Brandts, C. H., Serve, H., and Dikic, I. (2013). Ubiquitination and selective autophagy. *Cell Death Differ.* 20, 21–30. doi:10.1038/cdd.2012.72.
- Shen, H., Korutla, L., Champtiaux, N., Toda, S., LaLumiere, R., Vallone, J., et al. (2007). NAC1 Regulates the Recruitment of the Proteasome Complex into Dendritic Spines. *J. Neurosci.* doi:10.1523/JNEUROSCI.1571-07.2007.
- Shi, C. S., and Kehrl, J. H. (2010). TRAF6 and A20 regulate lysine 63-linked ubiquitination of Beclin-1 to control TLR4-induced Autophagy. *Sci. Signal.* 3, 1–10. doi:10.1126/scisignal.2000751.
- Shiba-Fukushima, K., Arano, T., Matsumoto, G., Inoshita, T., Yoshida, S., Ishihama, Y., et al. (2014). Phosphorylation of Mitochondrial Polyubiquitin by PINK1 Promotes Parkin Mitochondrial Tethering. *PLoS Genet.* 10. doi:10.1371/journal.pgen.1004861.
- Shiba-Fukushima, K., Imai, Y., Yoshida, S., Ishihama, Y., Kanao, T., Sato, S., et al. (2012). PINK1-mediated phosphorylation of the Parkin ubiquitin-like domain primes mitochondrial translocation of Parkin and regulates mitophagy. *Sci. Rep.* 2, 1–8. doi:10.1038/srep01002.
- Shloush, J., Vlassov, J. E., Engson, I., Duan, S., Saridakis, V., Dhe-paganon, S., et al. (2011). Structural and functional comparison of the RING domains of two p53 E3 ligases, Mdm2 and Pirh2. *J. Biol. Chem.* 286, 4796–4808. doi:10.1074/jbc.M110.157669.
- Shpilka, T., Weidberg, H., Pietrokovski, S., and Elazar, Z. (2011). Atg8: An autophagy-related ubiquitin-like protein family. *Genome Biol.* 12. doi:10.1186/gb-2011-12-7-226.
- Smith, D. M., Chang, S. C., Park, S., Finley, D., Cheng, Y., and Goldberg, A. L. (2007). Docking of the Proteasomal ATPases' Carboxyl Termini in the 20S Proteasome's α Ring Opens the Gate for Substrate Entry. *Mol. Cell* 27, 731–744. doi:10.1016/j.molcel.2007.06.033.
- Sowter, H. M., Ratcliffe, P. J., Watson, P., Greenberg, A. H., and Harris, A. L. (2001). HIF-1-dependent regulation of hypoxic induction of the cell death factors BNIP3 and NIX in human tumors. *Cancer Res.* 61, 6669–6673. doi:10.1158/0008-5472.can-04-4130.

- Spinnenhirn, V., Farhan, H., Basler, M., Aichem, A., Cnaan, A., and Groettrup, M. (2014). The ubiquitin-like modifier FAT10 decorates autophagy-targeted Salmonella and contributes to Salmonella resistance in mice. *J. Cell Sci.* 127, 4883–4893. doi:10.1242/jcs.152371.
- Sriramachandran, A. M., and Dohmen, R. J. (2014). SUMO-targeted ubiquitin ligases. *Biochim. Biophys. Acta - Mol. Cell Res.* 1843, 75–85. doi:10.1016/j.bbamcr.2013.08.022.
- Stitt, T. N., Drujan, D., Clarke, B. A., Panaro, F., Timofeyeva, Y., Kline, W. O., et al. (2004). The IGF-1/PI3K/Akt pathway prevents expression of muscle atrophy-induced ubiquitin ligases by inhibiting FOXO transcription factors. *Mol. Cell* 14, 395–403. doi:10.1016/S1097-2765(04)00211-4.
- Stolz, A., Ernst, A., and Dikic, I. (2014). Cargo recognition and trafficking in selective autophagy. *Nat. Cell Biol.* 16, 495–501. doi:10.1038/ncb2979.
- Strappazon, F., and Cecconi, F. (2015). AMBRA1-induced mitophagy: A new mechanism to cope with cancer? *Mol. Cell. Oncol.* 2, e975647. doi:10.4161/23723556.2014.975647.
- Strappazon, F., Nazio, F., Corrado, M., Cianfanelli, V., Romagnoli, A., Fimia, G. M., et al. (2015). AMBRA1 is able to induce mitophagy via LC3 binding, regardless of PARKIN and p62/SQSTM1. *Cell Death Differ.* 22, 419–432. doi:10.1038/cdd.2014.139.
- Sun, A., Li, C., Chen, R., Huang, Y., Chen, Q., Cui, X., et al. (2016). GSK-3 β controls autophagy by modulating LKB1-AMPK pathway in prostate cancer cells. *Prostate.* doi:10.1002/pros.23106.
- Sun, A., Wei, J., Childress, C., Shaw, J. H., Peng, K., Shao, G., et al. (2017). The E3 ubiquitin ligase NEDD4 is an LC3-interactive protein and regulates autophagy. *Autophagy* 13, 522–537. doi:10.1080/15548627.2016.1268301.
- Suraweera, A., Münch, C., Hanssum, A., and Bertolotti, A. (2012). Failure of amino acid homeostasis causes cell death following proteasome inhibition. *Mol. Cell* 48, 242–253. doi:10.1016/j.molcel.2012.08.003.
- Susmita Kaushik and Ana Maria Cuervo (2013). NIH Public Access. 22, 407–417. doi:10.1016/j.tcb.2012.05.006.Chaperone-mediated.
- Suvorova, E. S., Lucas, O., Weisend, C. M., Rollins, M. C. F., Merrill, G. F., Capecchi, M. R., et al. (2009). Cytoprotective Nrf2 pathway is induced in chronically Txnrd 1-deficient hepatocytes. *PLoS One* 4. doi:10.1371/journal.pone.0006158.

- Svendsen, J. M., Smogorzewska, A., Sowa, M. E., O'Connell, B. C., Gygi, S. P., Elledge, S. J., et al. (2009). Mammalian BTBD12/SLX4 Assembles A Holliday Junction Resolvase and Is Required for DNA Repair. *Cell* 138, 63–77. doi:10.1016/j.cell.2009.06.030.
- Szargel, R., Shani, V., Elghani, F. A., Mekies, L. N., Liani, E., Rott, R., et al. (2015). The PINK1, synphilin-1 and SIAH-1 complex constitutes a novel mitophagy pathway. *Hum. Mol. Genet.* 25, 3476–3490. doi:10.1093/hmg/ddw189.
- Takaesu, G., Kobayashi, T., and Yoshimura, A. (2012). TGF β -activated kinase 1 (TAK1)-binding proteins (TAB) 2 and 3 negatively regulate autophagy. *J. Biochem.* doi:10.1093/jb/mvr123.
- Tan, J. M. M., Wong, E. S. P., Dawson, V. L., Dawson, T. M., and Lim, K. L. (2008). Lysine 63-linked polyubiquitin potentially partners with p62 to promote the clearance of protein inclusions by autophagy. *Autophagy* 4, 251–253. doi:10.4161/auto.5444.
- Tanaka, Y., Guhde, G., Suter, A., Eskelinen, E. L., Hartmann, D., Lüllmann-Rauch, R., et al. (2000). Accumulation of autophagic vacuoles and cardiomyopathy LAMP-2-deficient mice. *Nature* 406, 902–906. doi:10.1038/35022595.
- Tandle, A. T., Calvani, M., Uranchimeg, B., Zahavi, D., Melillo, G., and Libutti, S. K. (2009). Endothelial monocyte activating polypeptide-II modulates endothelial cell responses by degrading hypoxia-inducible factor-1 α through interaction with PSMA7, a component of the proteasome. *Exp. Cell Res.* doi:10.1016/j.yexcr.2009.03.021.
- Tang, B., Cai, J., Sun, L., Li, Y., Qu, J., Snider, B. J., et al. (2014). Proteasome inhibitors activate autophagy involving inhibition of PI3K-Akt-mTOR pathway as an anti-oxidation defense in human RPE cells. *PLoS One* 9, 3–10. doi:10.1371/journal.pone.0103364.
- Tanida, I., Ueno, T., and Kominami, E. (2004). Human light chain 3/MAP1LC3B Is cleaved at its carboxyl-terminal Met 121 to expose Gly120 for lipidation and targeting to autophagosomal membranes. *J. Biol. Chem.* 279, 47704–47710. doi:10.1074/jbc.M407016200.
- Tannous, P., Zhu, H., Nemchenko, A., Berry, J. M., Johnstone, J. L., Shelton, J. M., et al. (2008). Intracellular protein aggregation is a proximal trigger of cardiomyocyte autophagy. *Circulation* 117, 3070–3078. doi:10.1161/CIRCULATIONAHA.107.763870.

- Tasdemir, E., Maiuri, M. C., Galluzzi, L., Vitale, I., Djavaheri-Mergny, M., D'Amelio, M., et al. (2008a). Regulation of autophagy by cytoplasmic p53. *Nat. Cell Biol.* 10, 676–687. doi:10.1038/ncb1730.
- Tasdemir, E., Maiuri, M. C., Morselli, E., Criollo, A., D'Amelio, M., Djavaheri-Mergny, M., et al. (2008b). A dual role of p53 in the control of autophagy. *Autophagy*. doi:10.4161/auto.6486.
- Tattoli, I., Sorbara, M. T., Vuckovic, D., Ling, A., Soares, F., Carneiro, L. A. M., et al. (2012). Amino acid starvation induced by invasive bacterial pathogens triggers an innate host defense program. *Cell Host Microbe* 11, 563–575. doi:10.1016/j.chom.2012.04.012.
- Tattoli, I., Sorbara, M. T., Yang, C., Tooze, S. A., Philpott, D. J., and Girardin, S. E. (2013). Listeria phospholipases subvert host autophagic defenses by stalling pre-autophagosomal structures. *EMBO J.* 32, 3066–3078. doi:10.1038/emboj.2013.234.
- Thompson, J. W., Nagel, J., Hoving, S., Gerrits, B., Bauer, A., Thomas, J. R., et al. (2014). Quantitative Lys- ϵ -Gly-Gly (diGly) proteomics coupled with inducible RNAi reveals ubiquitin-mediated proteolysis of DNA damage-inducible transcript 4 (DDIT4) by the E3 Ligase HUWE1. *J. Biol. Chem.* doi:10.1074/jbc.M114.573352.
- Thurston, T. L. M. (2009). The tbk1 adaptor and autophagy receptor ndp52 restricts the proliferation of ubiquitin-coated bacteria. *Nat. Immunol.* 10, 1215–1222. doi:10.1038/ni.1800.
- Till, A., Lakhani, R., Burnett, S. F., and Subramani, S. (2012). Pexophagy: The selective degradation of peroxisomes. *Int. J. Cell Biol.* 2012. doi:10.1155/2012/512721.
- Tipler, C. P., Hutchon, S. P., Hendil, K., Tanaka, K., Fishel, S., and Mayer, R. J. (1997). Purification and characterization of 26S proteasomes from human and mouse spermatozoa. *Mol. Hum. Reprod.* doi:10.1093/molehr/3.12.1053.
- Tomkinson, B., and Lindås, A. C. (2005). Tripeptidyl-peptidase II: A multi-purpose peptidase. *Int. J. Biochem. Cell Biol.* 37, 1933–1937. doi:10.1016/j.biocel.2005.02.009.
- Tourrière, H., Chebli, K., Zekri, L., Courselaud, B., Blanchard, J. M., Bertrand, E., et al. (2003). The RasGAP-associated endoribonuclease G3BP assembles stress granules. *J. Cell Biol.* doi:10.1083/jcb.200212128.

- Tracy, K., Dibling, B. C., Spike, B. T., Knabb, J. R., Schumacker, P., and Macleod, K. F. (2007). BNIP3 Is an RB/E2F Target Gene Required for Hypoxia-Induced Autophagy. *Mol. Cell. Biol.* 27, 6229–6242. doi:10.1128/MCB.02246-06.
- Trempe, J. F., Sauvé, V., Grenier, K., Seirafi, M., Tang, M. Y., Meñade, M., et al. (2013). Structure of parkin reveals mechanisms for ubiquitin ligase activation. *Science (80-.)*. 340, 1451–1455. doi:10.1126/science.1237908.
- Tripathi, D. N., Zhang, J., Jing, J., Dere, R., and Lyn, C. (2016). A new role for ATM in selective autophagy of peroxisomes (pexophagy). *Autophagy* 12, 711–712. doi:10.1080/15548627.2015.1123375.
- Turcu Francisca E. Reyes, Ventii Karen H., W. K. D. (2010). NIH Public Access. *Annu Rev Biochem*, 363–397. doi:10.1146/annurev.biochem.78.082307.091526.Regulation.
- Van Humbeeck, C., Cornelissen, T., Hofkens, H., Mandemakers, W., Gevaert, K., De Strooper, B., et al. (2011). Parkin Interacts with Ambra1 to Induce Mitophagy. *J. Neurosci.* 31, 10249–10261. doi:10.1523/JNEUROSCI.1917-11.2011.
- Varjosalo, M., Keskitalo, S., VanDrogen, A., Nurkkala, H., Vichalkovski, A., Aebersold, R., et al. (2013). The Protein Interaction Landscape of the Human CMGC Kinase Group. *Cell Rep.* doi:10.1016/j.celrep.2013.03.027.
- Verma, R., Oania, R. S., Kolawa, N. J., and Deshaies, R. J. (2013). Cdc48/p97 promotes degradation of aberrant nascent polypeptides bound to the ribosome. *Elife* 2013, 1–17. doi:10.7554/eLife.00308.
- Vijay-Kumar, S., Bugg, C. E., Wilkinson, K. D., Vierstra, R. D., Hatfield, P. M., and Cook, W. J. (1987). Comparison of the three-dimensional structures of human, yeast, and oat ubiquitin. *J. Biol. Chem.*
- Vinayagam, A., Stelzl, U., Foulle, R., Plassmann, S., Zenkner, M., Timm, J., et al. (2011). A directed protein interaction network for investigating intracellular signal transduction. *Sci. Signal.* doi:10.1126/scisignal.2001699.
- Walter, K. M., Schönenberger, M. J., Trötz Müller, M., Horn, M., Elsässer, H. P., Moser, A. B., et al. (2014). Hif-2 α Promotes degradation of mammalian peroxisomes by selective autophagy. *Cell Metab.* 20, 882–897. doi:10.1016/j.cmet.2014.09.017.
- Wan, C., Borgeson, B., Phanse, S., Tu, F., Drew, K., Clark, G., et al. (2015). Panorama of ancient metazoan macromolecular complexes. *Nature*. doi:10.1038/nature14877.
- Wandel, M. P., Pathe, C., Werner, E. I., Ellison, C. J., Boyle, K. B., von der Malsburg,

- A., et al. (2017). GBPs Inhibit Motility of *Shigella flexneri* but Are Targeted for Degradation by the Bacterial Ubiquitin Ligase IpaH9.8. *Cell Host Microbe* 22, 507–518.e5. doi:10.1016/j.chom.2017.09.007.
- Wanders, R. J. A., Waterham, H. R., and Ferdinandusse, S. (2016). Metabolic Interplay between Peroxisomes and Other Subcellular Organelles Including Mitochondria and the Endoplasmic Reticulum. *Front. Cell Dev. Biol.* 3, 1–15. doi:10.3389/fcell.2015.00083.
- Wang, J., Huo, K., Ma, L., Tang, L., Li, D., Huang, X., et al. (2011). Toward an understanding of the protein interaction network of the human liver. *Mol. Syst. Biol.* doi:10.1038/msb.2011.67.
- Wang, W., and Subramani, S. (2017). Role of PEX5 ubiquitination in maintaining peroxisome dynamics and homeostasis. 4101. doi:10.1080/15384101.2017.1376149.
- Wang, X., Chen, C. F., Baker, P. R., Chen, P. L., Kaiser, P., and Huang, L. (2007). Mass spectrometric characterization of the affinity-purified human 26S proteasome complex. *Biochemistry*. doi:10.1021/bi061994u.
- Wang, X. J., Yu, J., Wong, S. H., Cheng, A. S., Chan, F. K., Ng, S. S., et al. (2013). A novel crosstalk between two major protein degradation systems. *Autophagy* 9, 1500–1508. doi:10.4161/auto.25573.
- Wang, Y., Serricchio, M., Jauregui, M., Shanbhag, R., Stoltz, T., Di Paolo, C. T., et al. (2015). Deubiquitinating enzymes regulate PARK2-mediated mitophagy. *Autophagy* 11, 595–606. doi:10.1080/15548627.2015.1034408.
- Wang, Z., Zhu, W. G., and Xu, X. (2017). *Ubiquitin-like modifications in the DNA damage response*. Elsevier B.V. doi:10.1016/j.mrfmmm.2017.07.001.
- Waris, S., Wilce, M. C. J., and Wilce, J. A. (2014). RNA recognition and stress granule formation by TIA proteins. *Int. J. Mol. Sci.* 15, 23377–23388. doi:10.3390/ijms151223377.
- Watanabe, N., Madaule, P., Reid, T., Ishizaki, T., Watanabe, G., Kakizuka, A., et al. (1997). p140mDia, a mammalian homolog of *Drosophila* diaphanous, is a target protein for Rho small GTPase and is a ligand for profilin. *EMBO J.* doi:10.1093/emboj/16.11.3044.
- Wauer, T., and Komander, D. (2013). Structure of the human Parkin ligase domain in an autoinhibited state. *EMBO J.* 32, 2099–2112. doi:10.1038/emboj.2013.125.
- Wei, S. J., Williams, J. G., Dang, H., Darden, T. A., Betz, B. L., Humble, M. M., et al.

- (2008). Identification of a Specific Motif of the DSS1 Protein Required for Proteasome Interaction and p53 Protein Degradation. *J. Mol. Biol.* doi:10.1016/j.jmb.2008.08.044.
- Weidberg, H., Shvets, E., and Elazar, Z. (2011). Biogenesis and Cargo Selectivity of Autophagosomes. *Annu. Rev. Biochem.* 80, 125–156. doi:10.1146/annurev-biochem-052709-094552.
- Welchman, R. L., Gordon, C., and Mayer, R. J. (2005). Ubiquitin and ubiquitin-like proteins as multifunctional signals. *Nat. Rev. Mol. Cell Biol.* 6, 599–609. doi:10.1038/nrm1700.
- Wild, P., Farhan, H., McEwan, D. G., Wagner, S., Rogov, V. V., Brady, N. R., et al. (2011). Phosphorylation of the autophagy receptor optineurin restricts Salmonella growth. *Science (80-)*. 333, 228–233. doi:10.1126/science.1205405.
- Wileman, T. (2013). Autophagy as a defence against intracellular pathogens. *Essays Biochem.* 55, 153–163. doi:10.1042/bse0550153.
- Wong, Y. C., and Holzbaur, E. L. F. (2014). Optineurin is an autophagy receptor for damaged mitochondria in parkin-mediated mitophagy that is disrupted by an ALS-linked mutation. *Proc. Natl. Acad. Sci.* 111, E4439–E4448. doi:10.1073/pnas.1405752111.
- Woods, N. T., Mesquita, R. D., Sweet, M., Carvalho, M. A., Li, X., Liu, Y., et al. (2012). Charting the landscape of tandem BRCT domain-mediated protein interactions. *Sci. Signal.* doi:10.1126/scisignal.2002255.
- Wooten, M. W., Geetha, T., Babu, J. R., Seibenhener, M. L., Peng, J., Cox, N., et al. (2008). Essential role of sequestosome 1/p62 in regulating accumulation of Lys63-ubiquitinated proteins. *J. Biol. Chem.* 283, 6783–6789. doi:10.1074/jbc.M709496200.
- Wu, W. K. K., Wu, Y. C., Yu, L., Li, Z. J., Sung, J. J. Y., and Cho, C. H. (2008). Induction of autophagy by proteasome inhibitor is associated with proliferative arrest in colon cancer cells. *Biochem. Biophys. Res. Commun.* 374, 258–263. doi:10.1016/j.bbrc.2008.07.031.
- Wyant, G. A., Abu-Remaileh, M., Frenkel, E. M., Laqtom, N. N., Dharamdasani, V., Lewis, C. A., et al. (2018). Nufip1 is a ribosome receptor for starvation-induced ribophagy. *Science (80-)*. 360, 751–758. doi:10.1126/science.aar2663.
- Xia, P., Wang, S., Du, Y., Zhao, Z., Shi, L., Sun, L., et al. (2013). WASH inhibits autophagy through suppression of Beclin 1 ubiquitination. *EMBO J.* 32, 2685–

2696. doi:10.1038/emboj.2013.189.
- Xiong, X., Tao, R., DePinho, R. A., and Dong, X. C. (2012). The autophagy-related gene 14 (Atg14) is regulated by forkhead box O transcription factors and circadian rhythms and plays a critical role in hepatic autophagy and lipid metabolism. *J. Biol. Chem.* 287, 39107–39114. doi:10.1074/jbc.M112.412569.
- Xu, C., Fan, C. D., and Wang, X. (2015). Regulation of Mdm2 protein stability and the p53 response by NEDD4-1 E3 ligase. *Oncogene* 34, 342–350. doi:10.1038/onc.2013.557.
- Xu, C., Feng, K., Zhao, X., Huang, S., Cheng, Y., Qian, L., et al. (2014). Regulation of autophagy by E3 ubiquitin ligase RNF216 through BECN1 ubiquitination. *Autophagy* 10, 2239–2250. doi:10.4161/15548627.2014.981792.
- Xu, J., Wang, S., Viollet, B., and Zou, M. H. (2012). Regulation of the proteasome by AMPK in endothelial cells: The role of O-GlcNAc transferase (OGT). *PLoS One* 7. doi:10.1371/journal.pone.0036717.
- Xu, P., Das, M., Reilly, J., and Davis, R. J. (2011). JNK regulates FoxO-dependent autophagy in neurons. *Genes Dev.* 25, 310–322. doi:10.1101/gad.1984311.
- Yamano, K., and Youle, R. J. (2013). PINK1 is degraded through the N-end rule pathway. *Autophagy* 9, 1758–1769. doi:10.4161/auto.24633.
- Yamashita, S. ichi, Abe, K., Tatemichi, Y., and Fujiki, Y. (2014). The membrane peroxin PEX3 induces peroxisome-ubiquitination-linked pexophagy. *Autophagy* 10, 1549–1564. doi:10.4161/auto.29329.
- Yang, L., Tang, Z., Zhang, H., Kou, W., Lu, Z., Li, X., et al. (2013). PSMA7 directly interacts with NOD1 and regulates its function. *Cell. Physiol. Biochem.* doi:10.1159/000350113.
- Yao, T. P. (2010). The role of ubiquitin in autophagy-dependent protein aggregate processing. *Genes and Cancer* 1, 779–786. doi:10.1177/1947601910383277.
- Yao, T., Song, L., Jin, J., Cai, Y., Takahashi, H., Swanson, S. K., et al. (2008). Distinct Modes of Regulation of the Uch37 Deubiquitinating Enzyme in the Proteasome and in the Ino80 Chromatin-Remodeling Complex. *Mol. Cell.* doi:10.1016/j.molcel.2008.08.027.
- Yau, R., and Rape, M. (2016). The increasing complexity of the ubiquitin code. *Nat. Cell Biol.* 18, 579–586. doi:10.1038/ncb3358.
- Yi, P., Feng, Q., Amazit, L., Lonard, D. M., Tsai, S. Y., Tsai, M. J., et al. (2008). Atypical Protein Kinase C Regulates Dual Pathways for Degradation of the

- Oncogenic Coactivator SRC-3/AIB1. *Mol. Cell.* doi:10.1016/j.molcel.2007.12.030.
- Ying, H., Zheng, H., Scott, K., Wiedemeyer, R., Yan, H., Lim, C., et al. (2010). Mig-6 controls EGFR trafficking and suppresses gliomagenesis. *Proc. Natl. Acad. Sci.* doi:10.1073/pnas.0914930107.
- Yonashiro, R., Ishido, S., Kyo, S., Fukuda, T., Goto, E., Matsuki, Y., et al. (2006). A novel mitochondrial ubiquitin ligase plays a critical role in mitochondrial dynamics. *EMBO J.* 25, 3618–3626. doi:10.1038/sj.emboj.7601249.
- Yonekawa, T., Gamez, G., Kim, J., Choon Tan, A., Thorburn, J., Gump, J., et al. (2015). RIP1 negatively regulates basal autophagic flux through TFEB to control sensitivity to apoptosis. *EMBO Rep.* 16, 700–708. doi:10.15252/embr.
- Yoshii, S. R., Kishi, C., Ishihara, N., and Mizushima, N. (2011). Parkin mediates proteasome-dependent protein degradation and rupture of the outer mitochondrial membrane. *J. Biol. Chem.* 286, 19630–19640. doi:10.1074/jbc.M110.209338.
- Young, A. R. J. (2006). Starvation and ULK1-dependent cycling of mammalian Atg9 between the TGN and endosomes. *J. Cell Sci.* 119, 3888–3900. doi:10.1242/jcs.03172.
- Yousefi, S., Perozzo, R., Schmid, I., Ziemiecki, A., Schaffner, T., Scapozza, L., et al. (2006). Calpain-mediated cleavage of Atg5 switches autophagy to apoptosis. *Nat. Cell Biol.* doi:10.1038/ncb1482.
- Yu, L., Chen, Y., and Tooze, S. A. (2018). Autophagy pathway: Cellular and molecular mechanisms. *Autophagy.* doi:10.1080/15548627.2017.1378838.
- Yuan, F., Ma, Y., You, P., Lin, W., Lu, H., Yu, Y., et al. (2013). A novel role of proteasomal $\beta 1$ subunit in tumorigenesis. *Biosci. Rep.* doi:10.1042/BSR20130013.
- Yuan, G., Khan, S. A., Luo, W., Nanduri, J., Semenza, G. L., and Prabhakar, N. R. (2011). Hypoxia-inducible factor 1 mediates increased expression of NADPH oxidase-2 in response to intermittent hypoxia. *J. Cell. Physiol.* doi:10.1002/jcp.22640.
- Yun, J., Puri, R., Yang, H., Lizzio, M. A., Wu, C., Sheng, Z. H., et al. (2014). MUL1 acts in parallel to the PINK1/parkin pathway in regulating mitofusin and compensates for loss of PINK1/parkin. *Elife* 2014, 1–26. doi:10.7554/eLife.01958.001.
- Zhang, H., Bosch-Marce, M., Shimoda, L. A., Yee, S. T., Jin, H. B., Wesley, J. B., et al. (2008). Mitochondrial autophagy is an HIF-1-dependent adaptive metabolic response to hypoxia. *J. Biol. Chem.* 283, 10892–10903.

- doi:10.1074/jbc.M800102200.
- Zhang, J., Tripathi, D. N., Jing, J., Alexander, A., Kim, J., Powell, R. T., et al. (2015a). ATM functions at the peroxisome to induce pexophagy in response to ROS. *Nat. Cell Biol.* 17, 1259–1269. doi:10.1038/ncb3230.
- Zhang, T., Dong, K., Liang, W., Xu, D., Xia, H., Geng, J., et al. (2015b). G-protein Coupled Receptors Regulate Autophagy by ZBTB16-mediated Ubiquitination and Proteasomal Degradation of Adaptor Protein Atg14L. *Elife* 2015, 1–19. doi:10.7554/eLife.06734.
- Zhang, X., Bogunovic, D., Payelle-Brogard, B., Francois-Newton, V., Speer, S. D., Yuan, C., et al. (2015c). Human intracellular ISG15 prevents interferon- α/β over-amplification and auto-inflammation. *Nature*. doi:10.1038/nature13801.
- Zhang, X., and Qian, S.-B. (2011). Chaperone-mediated hierarchical control in targeting misfolded proteins to aggresomes. *Mol. Biol. Cell* 22, 3277–3288. doi:10.1091/mbc.E11-05-0388.
- Zhao, C., Denison, C., Huibregtse, J. M., Gygi, S., and Krug, R. M. (2005). Human ISG15 conjugation targets both IFN-induced and constitutively expressed proteins functioning in diverse cellular pathways. *Proc. Natl. Acad. Sci.* doi:10.1073/pnas.0504754102.
- Zhao, J., Brault, J. J., Schild, A., Cao, P., Sandri, M., Schiaffino, S., et al. (2007). FoxO3 Coordinately Activates Protein Degradation by the Autophagic/Lysosomal and Proteasomal Pathways in Atrophying Muscle Cells. *Cell Metab.* 6, 472–483. doi:10.1016/j.cmet.2007.11.004.
- Zhao, J., and Goldberg, A. L. (2016). Coordinate regulation of autophagy and the ubiquitin proteasome system by MTOR. *Autophagy* 12, 1967–1970. doi:10.1080/15548627.2016.1205770.
- Zhao, J., Zhai, B., Gygi, S. P., and Goldberg, A. L. (2015). mTOR inhibition activates overall protein degradation by the ubiquitin proteasome system as well as by autophagy. *Proc. Natl. Acad. Sci.* 112, 15790–15797. doi:10.1073/pnas.1521919112.
- Zheng, Y. T., Shahnazari, S., Brech, A., Lamark, T., Johansen, T., and Brumell, J. H. (2009). The Adaptor Protein p62/SQSTM1 Targets Invading Bacteria to the Autophagy Pathway. *J. Immunol.* 183, 5909–5916. doi:10.4049/jimmunol.0900441.
- Zhu, K., Dunner, K., and McConkey, D. J. (2010). Proteasome inhibitors activate

autophagy as a cytoprotective response in human prostate cancer cells. *Oncogene*.
doi:10.1038/onc.2009.343.

Zhu, Y., Massen, S., Terenzio, M., Lang, V., Chen-Lindner, S., Eils, R., et al. (2013).
Modulation of serines 17 and 24 in the LC3-interacting region of Bnip3 determines
pro-survival mitophagy versus apoptosis. *J. Biol. Chem.* 288, 1099–1113.
doi:10.1074/jbc.M112.399345.

APPENDIX A

MATERIAL LIST

Name of Material/ Equipment	Company	Catalog Number
Acrylamide/Bis-Acrylamide Solution	Sigma	A3574
Alexa fluor 546 phalloidin	Molecular Probes	A22283
Anti mouse IgG, HRP conjugated	Jackson Immuno.	115035003
Anti-Mouse IgG Alexa Fluor 488	Invitrogen	A11001
Anti-rabbit IgG HRP conjugated	Jackson Immuno.	1110305144
Anti-Rabbit IgG Alexa Fluor 568	Invitrogen	A11011
ATG5 Antibody	Sigma	A0856
Bradford Solution	Sigma	6916
Bromophenol blue	Appllichem	A3640.0005
BSA	Sigma	A4503
CCCP	Sigma	C2759
Coumeric Acid	Sigma	C9008
Coverslides	Jena Bioscience	CSL-103
DIAPH1 Antibody	Millipore	AB3888
DMEM (high glucose)	PAN Biotech	P04-03500
DMSO	Sigma	VWRSAD2650
EBSS	Biological Industries	BI02-010-1A
Fetal bovine serum (FBS)	Biowest	S1810-500
Flag Antibody	Sigma	F3165
Flag M2 Beads	Sigma	A2220
Glutaraldehyde	Sigma	G5882
Glycerol	Appllichem	A4453
Hemocytometer	Sigma	Z359629-1EA
Hydrogen Peroxide	Merck	K35522500604
L-glutamine	Biological Industries	BI03-020-1B
Luminol	Fluka	9253
MFN2 Antibody	Sigma	M6444
MG132	Enzo Life Sciences	BML-PI102-0005
MOPS	Sigma	M1254
Nitocellulose membrane	GE Healthcare	A10083108
Non-Fat milk	Appllichem	A0830
Non-targeting SiRNA	Dharmacon	D-0011210-02-20
NP-40	Appllichem	A16694.0250
P62 Antibody	Abnova	H00008878-M01

Paraformaldehyde (PFA)	Sigma	15812-7
Parkin Antibody	Santa Cruz Biotechnology	Sc-32282
PBS	PAN Biotech	P04-36500
Penicillin/streptomycin solution	Biological Industries	03-031-1B
Phenol red	Sigma	114537-5G
PhosphoSer65-Ub Antibody	Millipore	ABS1513
PINK1 Antibody	Novus	NB100-493
Poly-L-Lysine	Sigma	P8920
Protease inhibitor	Sigma	P8340
Protein A-Agarose Beads	Santa Cruz Biotechnology	Sc-2001
Protein G-Agarose Beads	Santa Cruz Biotechnology	Sc-2002
PSMA7 Antibody	Enzo Life Sciences	PW 8120
PSMB5 Antibody	Enzo Life Sciences	PW 8895
Rapamycin	Sigma	R0395
Saponin	Sigma	84510
SiRNA DIAPH1	Dharmacon	M-010347-02-0005 5
SiRNA PSMA7	Dharmacon	M-004209-00-0005
SiRNA PSMB5	Dharmacon	M-004522-00-0005
Slides	Isolab	I.075.02.005
Sodium Azide	Riedel de Haen	13412
Sodium Chloride	Appllichem	A9242.5000
Sodium deoxycholate	Sigma	30970
Sodium dodecyl sulphate (SDS)	Biochemika	A2572
Sodium orthovanadate	Sigma	450243
Staurosporine	Sigma	S5921
Sucrose	Sigma	S0389
TIM23 Antibody	BD	VWRSAD2650
TOM40 Antibody	Santa Cruz Biotechnology	Sc-11414
Torin	Tocris	4247
Triton-X	Appllichem	4975
Trizma Base	Sigma	T1503
Trypan Blue	Sigma	A4503
Trypsin EDTA Solution A	Biological Industries	BI03-050-1A
Tween 20	Sigma	P5927
Ubiquitin (P4D1)	Santa Cruz Biotechnology	Sc-8017
VDAC1 Antibody	Millipore	AB10527
X-ray Films	Fujifilm	47410 19289
β -Actin Antibody	Sigma	A5441
β -Mercaptoethanol	Appllichem	A1108.0250

APPENDIX B

SEQUENCE ANALYSIS OF CLONE 47-PSMA7 OBTAINED FROM Y2H SCREENING

APPENDIX B.1 Clone 47 PSMA7

(Retrieved from SE thesis)

>101305-M4-101251 sequence exported from 47-475.ab1

TTTCCCCATTCTNTTNNNCCCAGATCGAGACCCGCAGGTTACTTAGTTGCTT
ATTAGNCTGCTTGGGTGGTCATATGCCCTTGGAGGCCCGGGGATCCGAATT
CGCGGCCGCGTCGACCTTAACTATACTGACGAAGCCATTGAAACAGATGAT
CTGACCATTAAGCTGGTGATCAAGGCACTCCTGGAAGTGGTTCAATCAGGT
GGCAAAAACATTGAACTTGCTGTCATGAGGCGAGATCAATCCCTCAAGATT
TTAAATCCTGAAGAAATTGAGAAGTATGTTGCTGAAATTGAAAAAGAAAA
GAAGAAAACGAAAAGAAGAAACAAAAGAAAGCATCATGATGAATAAAATG
TCTTTGCTTGTAATTTTTAAATTCATATCAATCATGGATGAGTCTCGATGTGT
AGGCCTTTCCATTCCATTTATTCACACTGAGTGTCTACAATAAACTTCCGT
ATTTTTAAAAAAAAAAAAAAAAAACCCTCAAAAATTTTTAAATCCAAAAC
CGGAAAACCCCTCAATTTCTTTAAA

Color code:

HA Vector EcoR1 Linker Xho1 start of matching nucleotides

TAC CCA TAC GAT GTT CCA GAT TAC GCT AGC TTG GGT GGT CAT ATG GCC
ATG GAG GCC CCG GGG ATC CGA ATTCGC GGC GTC GAC CTCGAG

APPENDIX C

PUBLICATIONS

Publication List

Kocaturk NM.* and Gozuacik D. Otofaji ve Nörodejeneratif Hastalıklar (Autophagy and Neurodegenerative Diseases). *Turkiye Klinikleri J. Pharmacol-Special Topics* 2017;5(1):11-20.

Erbil-Bilir S., **Kocaturk NM.***, Yayli M., Gozuacik D. Study of Protein-Protein Interactions in Autophagy Research. *J. Vis. Exp.* (127), e55881, DOI:10.3791/55881 (2017).

Bayraktar O., Oral O.*, **Kocaturk NM.***, Akkoc,Y., Eberhart K., Kosar A., Gozuacik D. IBMPFD disease-causing mutant VCP/p97 proteins are targets of autophagic - lysosomal degradation. *Plos One*, (2016), 11(10): e0164864. DOI: 10.1371/journal.pone.0164864.

Kocaturk NM.* and Gozuacik D., Crosstalk Between Autophagy and the Ubiquitin-Proteasome System. *Front. Cell Dev. Biol.* (2018) (*In revision, invited review*).

Ozbey A., Karimzadehkhoei M., **Kocaturk NM.***, Erbil-Bilir S., Kutlu O., Gozuacik D., and Kosar A. Inertial Focusing of Cancer Cells in Curvilinear Microchannels. *Sens Actuators B Chem.* (2018) (*Submitted*).

Kocaturk NM.*, Eberhart K., Dengjel J., Sezerman OU. and Gozuacik D. Novel protein complexes containing autophagy and ubiquitin proteasome system components play a role in the autophagic clearance of mitochondria. (2018) (*manuscript in preparation*).

Kocaturk, NM.*, Erbil-Bilir S., Dengjel, J., Sezerman, OU., and Gozuacik, D. Description of a Novel Mega Complex in Autophagy Regulation. (*Manuscript in preparation*).

Kig C., **Kocaturk NM.***, Akkoc Y., Kutlu O. and Gozuacik D. Autophagy as a molecular target for cancer treatment. *Eur J Pharmacol.* (2018) (*in preparartion, invited review*).

Kig C., **Kocaturk NM.***, Erbil-Bilir S., Kutlu O. and Gozuacik D. PKC δ and Autophagy Mediate Survival of Neural Cells During Reperfusion. (*Manuscript in preparation*).

Conference Papers

Kocaturk NM.*, Eberhart K., Gozuacik D. A novel regulator of mitophagy is a putative autophagy-UPS coordinator protein. *Turkish Journal of Biochemistry*, 2016, 41(S4) page:184, e-ISSN 1303-829X p-ISSN 0250-4685, DOI: <https://doi.org/10.1515/tjb-2016-s511>.

Bayraktar O., Oral O.*, **Kocaturk NM.***, Eberhart K., Kosar A., Gozuacik D. Autophagy Targets An IBMPFD-Related VCP/P97 Mutant Protein. *Turkish Journal of Biochemistry*, 2016, 41(S4) page:185, e-ISSN 1303-829X p-ISSN 0250-4685, DOI: <https://doi.org/10.1515/tjb-2016-s511>.

Bayraktar O., Oral O.*, **Kocaturk NM.***, Akkoc Y., Eberhart K., Kosar A., Gozuacik D. IBMPFD Disease-Causing Mutant VCP/p97 Proteins are targets of Autophagic-Lysosomal Degradation. XV.National Congress of Medical Biology and Genetics.

Poster Presentations

Kocaturk M.N., Eberhart K. and Gozuacik D. Coordinatory Role of a Putative Autophagy-UPS Protein in the Maintenance of Mitochondrial Clearance. Autophagy: From Molecular Principles to Human Diseases. Cavtat-Dubrovnik, Croatia, December 25-29, 2017.

Kocaturk M.N., Eberhart K. and Gozuacik D. A novel regulator of mitophagy is a putative autophagy-UPS coordinator protein. The 24th Jerusalem School in Life Sciences on: Frontiers in Cell Biology. Givat Ram, Jerusalem, Israel, December 11-15,2016.

Kocaturk M.N., Eberhart K. and Gozuacik D. A novel regulator of mitophagy is a putative autophagy-UPS coordinator protein. 7th Autophagy and UPS Workshop, Clermont-Ferrand, France, April 6-8,2016.

Kocaturk M.N., Eberhart K. and Gozuacik D. A novel regulator of mitophagy is a putative autophagy-UPS coordinator protein. Autophagic Membrane Trafficking and Dynamics in Ageing and Disease, Freiburg-Germany, January 28-31, 2016.

Kocaturk M.N., Eberhart K. and Gozuacik D. A novel regulator of mitophagy is a putative autophagy-UPS coordinator protein. 1st International Cell Death Research Congress Izmir, Turkey, 4-7 May 2016.

Bayraktar O., Oral O.*, **Kocaturk NM.***, Eberhart K., Kosar A., Gozuacik D. Autophagy Targets An IBMPFD-Related VCP/P97 Mutant Protein. 1st International Cell Death Research Congress Izmir, Turkey, 4-7 May 2016.

Bayraktar O., Oral O.*, **Kocaturk NM.***, Eberhart K., Kosar A., Gozuacik D. IBMPFD Disease-Causing Mutant VCP/p97 Proteins are targets of Autophagic-Lysosomal Degradation. XV.National Congress of Medical Biology and Genetics, Oludeniz-Fethiye, Turkey, 26-29 Oct 2017.

Awards

2017: Biomedicine and Molecular Biosciences COST Action BM1307. “In vivo analysis of ubiquitylation and SUMOylation” training school, Research Fellow, 2017. **REF:** COST-TS-ECOST-TRAINING_SCHOOL-BM1307-040917-087135.

2017: Biomedicine and Molecular Biosciences COST Action BM1307 PROTEOSTASIS Short-Term Scientific Missions, Research Fellow, 2017. **REF:** ECOST-STSM-BM1307-270217-083289.

2016: British Council and TUBITAK, Newton-Katip Celebi Fund, Researcher Links Programe Cellular Imaging Techniques Workshop, Grant holder, Izmir-Turkey, April 55-29, 2016.

2014: Turkish Academy of Sciences, TUBITAK-BIDEB 2229, FEBS Advanced Lecture Course 360 Degree Lysosome, Kusadası-Aydın, Turkey 23-28 October, 2014.

2012-2017: TUBITAK BIDEB 2211-A, Gradutae Scholarship.